Order Number 9518328

Separation process for the recovery of desalted water and chemical products from indigenous saline water resources

Ibrahim, Ahmed Aidid, Ph.D.

King Fahd University of Petroleum and Minerals (Saudi Arabia), 1993

U·M·I
300 N. Zeeb Rd.
Ann Arbor, MI 48106

Separation Process for the Recovery of Desalted Water and Chemical Products from Indigenous Saline Water Resources

BY

Ahmed Aidid Ibrahim

A Thesis Presented to the

FACULTY OF THE COLLEGE OF GRADUATE STUDIES

KING FAHD UNIVERSITY OF PETROLEUM & MINERALS

DHAHRAN, SAUDI ARABIA

In Partial Fulfillment of the

Requirements for the Degree of

DOCTOR OF PHILOSOPHY

In

CHEMICAL ENGINEERING

November, 1993

KING FAHD UNIVERSITY OF PETROLEUM AND MINERALS
DHAHRAN 31261,SAUDI ARABIA.

COLLEGE OF GRADUATE STUDIES

This dissertation, written by **AHMED AIDID IBRAHIM** under the direction of his Dissertation Advisor and approved by his Dissertation Committee, has been presented to and accepted by the Dean of the College of Graduate Studies, in partial fulfillment of the requirements for the degree of

DOCTOR OF PHILOSOPHY IN CHEMICAL ENGINEERING

Dissertation Committee

Dr. H.K. Abdel-Aal
Chairman

Dr. Mazen A. Shalabi
Co-Chairman

Dr. D.F. Fairbanks
Member

Dr. Dulaihan K. Al-Harbi
Member

Dr. M.S. Hussain
Member

Dr. Dulaihan K. Al-Harbi
Chairman
Department of Chemical Engineering

Dr. Ala H. Al-Rabeh
Dean
College of Graduate Studies

Date : 22.2.94

كلية الدراسات العليا
COLLEGE OF GRADUATE STUDIES

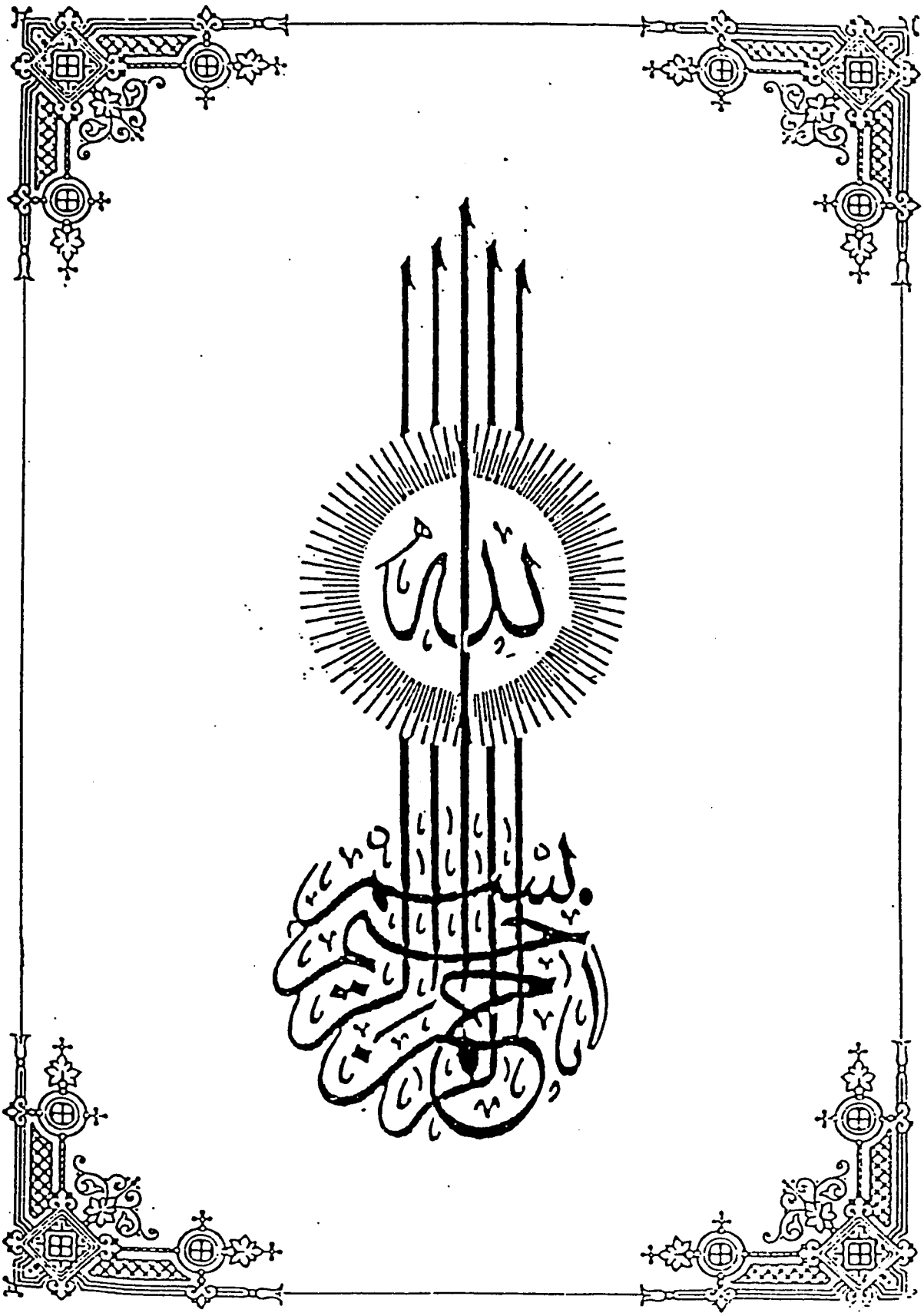

DEDICATED TO

My Parents/Sisters/Brothers/Relatives

My Spouse (Fatuma Sh. Mohamud)

My Children (Maryam & Zakariyah Ahmed)

ACKNOWLEDGEMENTS

Praise and gratitude be to Allah Almighty, with whose gracious help it was possible to accomplish this work.

Acknowledgment and thanks are due to King Fahd University of Petroleum and Minerals for providing all facilities and financial assistance.

I wish to express my deepest gratitude and sincere appreciation to my dissertation committee chairman Prof. H.K. Abdel Aal for his valuable guidance and encouragement throughout the course of my studies.

I am also grateful to Dr. Mazen A. Shalabi, my dissertation committee co-chairman for his support and co-operation throughout the course of my studies. I would like also to thank Prof. D.F. Fairbanks and Prof. M.S. Hussain (Chemistry Dept.) for their constructive comments and helpful suggestions.

I would like to thank Dr. D.K. Al-Harbi, Chairman of Chemical Engineering Department and member of my dissertation committee for his co-operation and support during my research work. I would also like to thank all the faculty members in the Department of Chemical Engineering for their co-operation.

I am thankful to Chemical Engineering workshop technicians Mr. John Chapman, Mr. Mahdi Al-Saffar, Mr. Ibrahim Al-Salem and Mr. Carpeso

Romeo., for their co-operation and help during the experimental work. I am grateful to our secretaries, Mr. Riasat Khan and Mr. Tasudduq Husain, Mr. Ali Hamid, for their co-operation.

I would like to offer very special thanks to CHE. laboratory technicians: the late Mr. Wagih Hossam Eldeen, Mr. Mariano Gica, Mr. Sayed Kamal, Mr. Bashir Ahmed, Mr. Ahmad Ullah and Mr. Essam Al-Deeb (Civil-Engineering), for their extensive assistance and co-operation during the experimental work.

Also, very special thanks to the KFUPM Research Institute, CAL/MCL Section, for their excellent work and co-operation for the analysis of liquid samples.

I would like to thank all colleagues and friends who made my stay at the university a memorable and valuable experience.

Especial thanks are extended to my friends Mr. Abdulsalam Mohamed Ahmed, Mr. Mohamed Hussein Issa, Mr. Hassan Mohamed Hassan, and Mr. Mohamed Ali Moallim, who were very helpful in many aspects of this research.

Lastly, but by no means the least, I am obliged to offer my indebtedness and sincere appreciation to my parents, family, relatives and friends, for their love, moral support, prayers, encouragement, patience and understanding.

TABLE OF CONTENTS

LIST OF TABLES

LIST OF FIGURES

DISSERTATION ABSTRACT

Full Name : **Ahmed Aidid Ibrahim**

Title of Study : **Separation Process for the Recovery of Desalted water and Chemical Products from Indigenous Saline-Water Resources**

Major Field : **Chemical Engineering**

Date of Degree : **November, 1993**

A modified Solvay process was experimentally carried out for the separation of sodium chloride salt from highly saline indigineous water resources. The technical viability of the process as a non-conventional approach to desalination was investigated. The proposed process utilizes a series of chemical reactions involving the conversion of both Na^{+} and Cl^{-} into $NaHCO_3$ that precipitates under experimental conditions and NH_4Cl which can be separated by crystallization respectively. Synthetic saline and sabkha waters were used.

The effects of relevant parameters on the conversion (such as temperature, initial concentrations of NH_3 and $NaCl$, and $NH_3/NaCl$ ratio), were studied. The optimum values of operating temperature and pH range are found to be 22 $^{\circ}C$. and 8 - 10, respectively. A higher concentration of NH_3 enhances the separation, while a higher concentration of $NaCl$ reduces the conversions, and an optimum value for the ratio of $NH_3/NaCl$ is found to be 1.2. The maximum conversions obtained were 82.2 % and 66.7 % for the synthetic saline and the sabkha waters, respectively.

Hydrodynamic parameters of the bubble column (reactor), in which carbonation of an ammmoniated brine occurs, are reported. These include: interfacial area, mass transfer coefficient, gas holdup and mixing efficiency.

The absorption process was shown to be an instantaneous diffusion-controlled chemical reaction. A mathematical model involving the formulation of an algorithm to find the values of unreacted ammonia and unconverted sodium chloride in water is presented using the concept of mass balance and the fundamentals of chemical reactions.

The free energy of formation of terminal chemical products is utilized to drive the reactions, and the total Gibbs free energy for the conversion of $NaCl$ solution of 20 % by weight into $NaHCO_3$ and NH_4Cl has a value of -85.4kJ/kg.

DOCTOR OF PHILOSOPHY DEGREE
KING FAHD UNIVERSITY OF PETROLEUM AND MINERALS
Dhahran, Suadi Arabia

ملخص بحث

الاسم بالكامل : أحمد عيديد ابراهيم .
مسمى البحث : عملية الفصل لاسترداد الماء غير المالح والمنتجات الكيميائية من مصادر المياه المالحة .
التخصص العام : الهندسة الكيميائية .
تاريخ الدرجة : نوفمبر ١٩٩٣م .

تم تنفيذ خطوات سولفاي المطورة لفصل ملح كلوريد الصوديوم من مصادر مياه عالية الملوحة وتم فحص القدرة التكنولوجية للعملية على أساس أنها طريقة غير تقليدية للتحلية . وقد تطلبت الاجراءات المقترحة سلسلة من التفاعلات الكيميائية بما في ذلك تحويل كل من الـ +Na و - Cl إلى $NaHCO_3$ وكذلك NH_4Cl التي يمكن فصلها عن طريق البلورة بالترتيب . وتم أيضا استعمال الملح الصناعي ومياه السبخة المالحة .

وتمت دراسة آثار الأبعاد المرتبطة بذلك على التحويل مثل درجة الحرارة وتركيزات NH_3 ، NaCl ونسبة $NH_3/NaCl$ وتبين أن القيمة القصوى للحرارة هي ٢٢ سنتغريد وبالنسبة لمعدل PH فهو ٨ - ١٠ . والتركيز العالي لـ NH_3 يعزز من عملية الفصل ، حين أن التركيز العالي لـ NaCl يخفض من عملية التحويل وأعلى درجة تحول توصلنا إليها كانت ٢ر٨٢٪ بالنسبة للملح الصناعي و ٧ر٦٦٪ بالنسبة لمياه السبخة .

وهناك تقرير شمل الأبعاد الهايدروديناميكية للمُعامل . وأتضح أن عملية الامتصاص كانت في شكل تفاعل كيميائي بانتشار وقتي . وتم أيضا تقديم نموذج رياضي يتضمن عمل الغوريتم لايجاد قيمة الأمونيا وكلوريد الصوديوم في المياه باستخدام مفهوم التوازن الكتلي وأسس التفاعلات الكيميائية .

وتم أيضا استعمال المنتجات الكيميائية الخالية من تراكيب الطاقة لدعم التفاعل وتحويل محلول NaCl بمعدل ٢٠٪ بالوزن إلى $NaHCO_3$ و NH_4Cl بقيمة ٤ر٨٥ كجم .

درجة الدكتوراة
جامعة الملك فهد للبترول والمعادن
الظهران - المملكة العربية السعودية

Chapter 1

INTRODUCTION

1.1. Background on the proposed separation process:

Naturally occurring processes are often inherently mixing processes. This has led to the reverse procedure of separation processes, which become one of the most challenging categories of the chemical engineering problems. Separation processes may be defined as those operations that transform a mixture of substances into two or more products that differ from each other in composition (Faith, 1975). The process of separation is difficult to achieve because it is the opposite of mixing, a process favored by the second law of thermodynamics. Consequently, separations often account for major production costs in chemical and petrochemical industries.

Three basic criteria of separation are defined on the basis whether the separation is the result of :

(a) Phase change; mass transfer or diffusional operations (which is achieved by energy separating agent (ESA), or mass separating agent (MSA).

(b) Difference in rate; membrane separation (rate controlled) or

(c) Difference in physical properties (with no change in phase); mechanical separation.

The principal basis for a choice in any case is the cost. Occasionally other factors influence the choice of the method, for instance: the simplicity in the operations, the availability of data, the extent of knowledge, and favorable previous experience.

Applying the above criteria for the conversion of saline water into fresh water, several separation techniques have been industrially established. Multistage Flash Distillation (MSF) uses thermal energy as an energy separating agent to generate a phase change; Reverse Osmosis utilizes the application of pressure above osmotic pressure to force pure water through a semi permeable membrane, while in Electrodialysis (ED) separation takes place through a selective membrane under the influence of electric field. A mass separating agent could be used, on the other hand, such as separation by Extraction, or Hydrate formation. Other possible means of desalting water (i.e to remove undesirable salts) is to use Chemical Precipitation or Ion exchange. However, the latter approach is not applicable to the desalting of highly saline water and is considered essentially as a polishing process for industrial waters.

The research work undertaken in this dissertation involves a dual-purpose separation process for the recovery of chemical products as well as desalted water from highly saline sources (coastal water, sabkha, and desalination blowdown). The separation approach utilizes a series of chemical reaction sequences involving the conversion of the sodium cation and the chloride anion into soda ash and

ammonium chloride respectively. Other valuable minerals could be separated as well. Ultimately, water free from salt (desalinated water) could be made available. Accordingly, by separating sodium cation (Na^{+})and chloride anion (Cl^{-}) through the proposed series of chemical reactions i.e staged chemical reactions, we are in effect desalting saline water in the absence of separating agents, (neither energy nor mass). Simply, the free energy of formation of the terminal chemical products (ΔG) has been utilized to drive the reaction at the required temperature levels.

This proposed staged chemical reaction sequences require highly saline water sources such as sabkha and coastal waters for the reaction to proceed. Thus the task of the research is not only the design of useful products, but to husband resources available in the kingdom of Saudi Arabia and deploy them for the need of its people .

Almost all the important processes for the absorption of CO_2 involve chemical reaction and it is therefore necessary to know how the nature and the rate of reaction influence the rate of absorption. The rate of absorption will be determined partly by the hydrodynamic conditions (flow rate, geometry of packing, physical properties of the liquid etc.) and partly by the physico-chemical properties of the system (solubility of CO_2 in the absorbent, diffusivity of dissolved CO_2 and of reactant in solution, kinetics of reactions occurring in solution, etc). The hydrodynamic factors can be adequately described by

the mass transfer coefficient and the effective interfacial area.

The core of the present system under study rests on the absorption of CO_2 into ammoniated brine solution. The enhanced absorption reaction of the gas in the liquid takes place in a contactor that will meet the requirements of the available reaction system. The Primary reaction happens between the absorbed CO_2 (Lewis acid) and the ammonia in the ammoniated brine that acts as chemical base to form carbamic acid i.e

$$CO_2 + NH_3 \rightarrow NH_2COOH \tag{1.1}$$

$$NH_3 + NH_2COOH \rightarrow NH_4^{+} + NH_2COO^{-} \tag{1.2}$$

The net result of these two reactions is the overall reaction.

$$CO_2 + 2\,NH_3 \rightarrow NH_2COO^{-} + NH_4^{+} \tag{1.3}$$

The rapid reaction, leading to the formation of ammonium carbamate, accompanies the absorption process and determines its rate. In the bulk of the solution the carbamate hydrolyzes comparatively slowly to bicarbonate.

$$NH_2COO^{-} + H_2O \rightarrow NH_3 + HOCOO^{-} \tag{1.4}$$

The bicarbonate ion is precipitated as sodium bicarbonate. The reaction is too slow to influence the rate of absorption directly. The absorber should be designed to provide a large volume of liquid and small volume of surface compared, to packed column or bubble-tray. This is to provide a sufficient holding-time for the secondary reaction.

The system described above involves both mass transfer and chemical reaction, therefore, consideration of both mentioned factors is important in an actual design. The NH_3 concentration and the purity of the CO_2 can influence the regimes responsible for the overall absorption rate. Mass transfer of CO_2 into highly carbonated ammoniated brine solution proceeds extremely slowly. The primary reaction that consumes the CO_2 is fast, and the system is diffusion controlled at higher carbonation time . Therefore, to obtain a higher yield from this system it is important to maximize the absorption of CO_2 and increase the rate of the secondary reaction. A bubble column contactor, where gas is dispersed through a relatively deep pool of liquid, is found to be a suitable choice for the aforementioned system.

In most cases mass transfer equipment is designed for a particular application and not purchased as such from a manufacturer. The goal of the designer is to arrive at a proper economic balance of investment and operating costs. The investment is roughly proportional to the rate of mass transfer. The rate of mass transfer depends on the nature of phase equilibria and is proportional to a mass transfer coefficient and the interfacial area as shown by the well known relationship:

$$r_A = K A \Delta C \qquad (1.5)$$

Large coefficients can be obtained by increasing turbulence, while the most effective way of reducing the equipment size is to provide a very large interfacial area.

Bubble columns are frequently used as absorbers and reactors because of their low cost, simplicity of operation, ability to handle solids and the ease with which the liquid residence time can be varied. On this ground, bubble columns are introduced to carry out the separation anticipated in this experimental investigation. However, back mixing in a bubble column is so significant to the extent that only one or two equilibrium stages can be provided in a column of reasonable height. In addition, the gas pressure drop is high for tall columns. The gas bubbles expand and do work on the liquid causing it to be mixed and agitated. This same energy is then dissipated by viscous shear as heat. Work energy is required for gas flow through the sparger, but this is relatively small. Most of the kinetic energy of the gas jets is probably dissipated as heat.

The choice, to use a bubble column as a suitable contactor was made on the basis of a thorough literature review. Although the construction of bubble columns is relatively easy, it is quite difficult to obtain the actual hydrodynamic properties. A considerable number of studies concerning the hydrodynamic parameters of bubble columns have been carried out, yet the literature survey suggests that the results of previous work should be used with some caution. That is, until present differences are resolved by a more extensive study, it

does not appear satisfactory merely to use reported values of gas hold up and interfacial area. Hydrodynamic parameters are experimentally determined for the proposed bubble columns.

1.2. Present Status of the Problem

The research study involves an experimental investigation of a modified Solvay process. A couple of staging reactions which are characterized by negative and hence favorable values of ΔG_o. The presented process is modified from classical Solvay Clusters as will be discussed concisely in the next chapter. The modification mainly lies on the type of the ammonia and the carbon dioxide feed sources needed in the process for the formations of ammonium carbonates.

Another feature of the modified process is the utilization of various new sources of saline waters such as sabkha, which will provide the sodium chloride that is to be transformed as result of the staging reactions. The major raw materials employed in this process are abundantly available in Saudi Arabia. The main products of this process are soda ash and water rich in fertile salts such as ammonium chloride. The ammonium chloride is an extremely effective nitrogenous fertilizer and its solution is suited well for irrigation systems. As an alternative instead of having the ammonia chloride in solution, it could be crystallized; i.e co-production process of soda ash and ammonium chloride.

1.3. Research Objectives:

The work undertaken in this research involves an experimental investigation and modification of what is known as the "Solvay" process. The design and the hydrodynamic properties of gas -liquid reactors are also investigated experimentally. The experimental work is coupled with a theoretical analysis and modelling of of the chemical reactions involved in the process. Thermodynamic and kinetic principles are applied throughout the course of analysis, particularly, in the computation of the energy of separation to compare it with minimum theoretical energy requirements.

To fulfil the objectives of this research study, extensive laboratory investigations were performed accordingly. The salient features of the research objectives may be listed as below, while the experimental techniques are described broadly in Chapter III.

1. To exploit new sources of highly saline waters, such as sabkha, coastal, and desalination-blowdown waters that can be used as a raw material for the proposed desalination process, and to determine their major chemical constituents.
2. To study the absorption process and the chemical reactions underlying the separation of NaCl from the brines in order to maximize the yield of chemical products and to minimize the salt content in the desalted waters.
3. To design and construct gas-liquid contactors (bubble columns) that can handle the chemical reactions involved in the process.

4. To construct and build a relatively novel experimental set-up for determining the non-adjustable parameters, such as gas hold-up, interfacial area, mass transfer, and the reaction involved in the gas liquid contactors.
5. To study the different feed sources for the separation process.
6. To study the salinity and concentration effects of the major constituents involved in the dual-purpose process.
7. To analyse theoretically the absorption and the reactions involved in the process.
8. To investigate the technical viability of the proposed dual-purpose separation process as a desalination method for handling these highly saline-water resources.
9. To compare the proposed process with conventional ones in terms of energy requirements. This experimental investigation will provide the engineering data and fundamentals that could permit the rational design of a dual-purpose separation process to produce desalted water along with chemical products.

Chapter 2

LITERATURE SURVEY

In this chapter, the present state of the art on separation techniques as applied to water desalination is first covered. Next, potential sources of highly saline water are identified. Finally, the basic operations of diffusion accompanied by chemical reactions, bubble columns, and their hydrodynamics and flow properties are reviewed.

2.1 Method of Separation of Saline Water

There are various terms in the literature used for describing a separation process that treats saline water to reduce the dissolved salt content to a desired level. Among these are: desalination, desalting, and desalinization. These three terms refer to the same process and represent the same meaning.

Saline water is water containing a significant amount of total dissolved solids (TDS), that constitutes a resource which can be treated by desalination to produce for instance, fresh water, potable water, and water usable for industrial or agricultural purposes. Most saline waters includes small quantities of organic materials and dissolved gases, but the majority of the dissolved materials are inorganic salts.

2.1.1 Classification of Water

For convenience in discussions of saline water treatment, water is divided into four classifications:

(i) Fresh water

(ii) Brackish water

(i) Sea water

(i) Brine: water remaining in a salt solution after some of pure water has been removed.

The extent of the salinity or total dissolved solids (TDS) expressed in parts per million (ppm) by weight is commonly used to classify the various types of water. Table 2.1 depicts some water classifications.

Table 2.1: Some Classifications of Water

Source	Salinity (ppm)
1. Potable Water	500 - 1000 with max. NaCl 250 ppm
2. Irrigation water	Max. 1000
3. Brackish water	1000 - 3500
4. Sea water	35000
5. Arabian Gulf water	45000
6. Brine	Variable Conc.

In the past, the only viable process for treating saline waters was desalination by distillation technique But the apparent simple heat transfer task could not be easily realized in practice because of the formation of scale and the corrosion behavior of sea water. For instance, the potential scale forming substances in seawater are present to the extent of only about 0.1% (Silver, 1982). Desalination involves the chemistry of water with dissolved salts and dissolved gases. The fundamental processing of these substances, and their effects, need certainly chemical engineering effort. These processes are concerned with the thermodynamics of separation from solution.

The energy which must be consumed to achieve such separation is determined by the physics and chemistry of the solution and by processes to which the solution is submitted, only careful application of these fundamentals can lead to improvements in the design of one process or indeed to alternative processes. The concept of desalting is not new (having being discussed and experimented with many years), however, a number of new processes are nearing commercial viability.

All current desalination methods fall into one of two main categories: Those that remove fresh water and leave behind a concentrated brine or those that remove the salt and leave the fresh water as a residue (Shreve, 1984). In either case, this will alleviate the need for desired water (Taubenblatt, 1982; Bushnak, 1990). Both approaches are being implemented in the kingdom of Saudi Arabia

(Al-Golaikah, 1984). Classification of saline water conversion processes is summarized in Table 2.2

Table 2.2: Classification of Saline-Water Conversion Process.

Processes that separate Salt from Solution	Processes that separate Water from Solution
1. Electrodialysis	1. Distillation or Evaporation
2. Adsorption	a. Multiple-effect longtube
3. Liquid Extraction	b. Multistage flash.
4. Ion Exchange	c. Vapor-compression
5. Controlled Diffusion	d. Humidification(Solar)
6. Biological System	2. Crystallization or Freezing
	a. Direct Freezing
	b. Indirect Freezing
	c. Hydrates Freezing
	3. Reverse Osmosis
	4. Solvent Extraction

The same processes may be reclassified according to the separating agents used: Heat or power consuming. This is shown next in Table 2.3.

Table 2.3: Classification of Conversion Process Based on the Type of Energy Consumption.

Heat Consuming	Power Consuming
1. Flash distillation	1. Vapor Compression Evaporation
a. Multistage Flash (MSF)	2. Freezing
2. Boiling	3. Electrodialysis
a. Submerged Tube	4. Reverse Osmosis
3.Evaporation	
a. Vapour inside Tube	
b. Vapour outside Tube	

The range of applicability of one process over the other is determined primarily by the salinity and the composition of feed water as shown in Figure 2.1. In practice, from thermodynamics one can readily determine that the work input required for an ideal reverse process producing a small amount of fresh water is about 2.8 kJ/kg. Different separation process of saline water require different energy inputs. Table 2.4 depicts some practical examples.

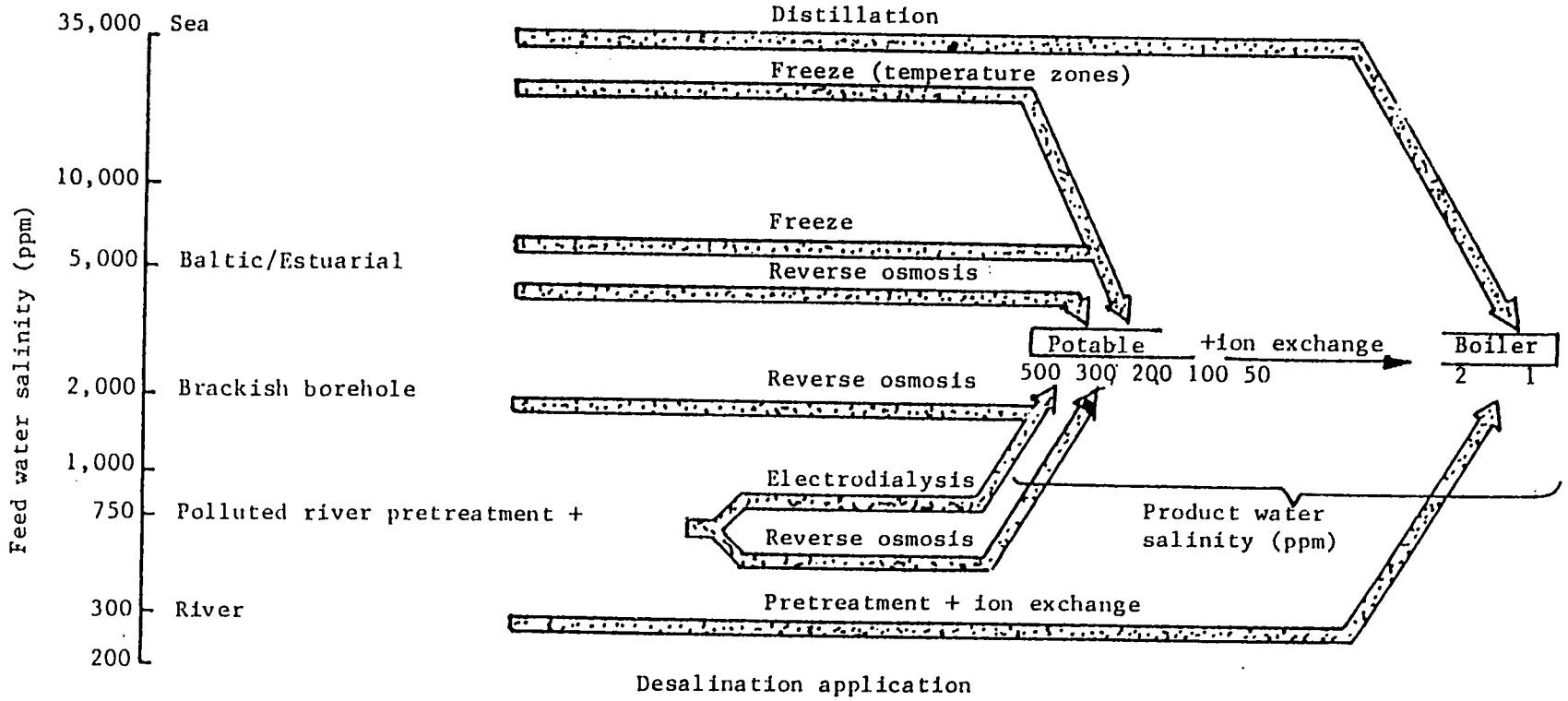

Figure: 2.1 Feed Water Salinity and Process Applicability

Table 2.4: Relative Primary Energy Consumption of Various Processes

Process	Energy in kJ/kG
1. Ideal reversible	2.8
2. Reverse Osmosis	50.0
3. Freezing	90.0
4. Distillation	
i). Msf dual purpose	100.0
ii). Msf single purpose	110.0
iii). Vapor compression	150.0

In some cases, disposal problems can affect the selection of the desalination process as well the overall viability of desalination as a water resources option. In fact , if one of the product streams is brine with a high level of total dissolved solids, it must be discharged somewhere. For facilities near the sea, disposal does not generally pose a problem, but it can be a serious for facilities inland. Improperly discharged brine can contaminate existing ground water or surface water due to its high salt content. It is generally too salty to be used for irrigation. The disposal options are very limited.

Many investigations in this field are engaged in overcoming the disposal problem. Therefore, nowadays research is directed to the extraction of minerals from desalination brine (Abdel Aal et al. 1990;

Al Mumtaz and Wagiall, 1983). This extraction represents a potentially important source of minerals. It is usually recommended for reducing fresh water production costs and minimizing waste disposal. In Saudi Arabia, the availability of large quantities of highly concentrated brine from desalination plants provides strong incentive for exploring the techno-economic feasibility of extracting minerals from the brine (Abdel Aal 1982, 1989). For instance, the recovery of magnesium chloride from sea water could be accomplished by employing any of the schemes demonstrated in the flow chart of Figure 2.2.

In the present study, the method adopted in treating saline water depends on a series of chemical reactions. Thus, we consider saline water conversion processes as:

a) physical or b) chemical. Figure 2.3 indicates the class type of the process conversions carried out in this work, while Figure 2.4 shows the overall layout and stages of the proposed process. The method proposed in this research utilizes highly saline sources of water for desalination. Under the present technological conditions, it is almost impossible to totally desalinate sea water which contains 3.5% by weight of salt.

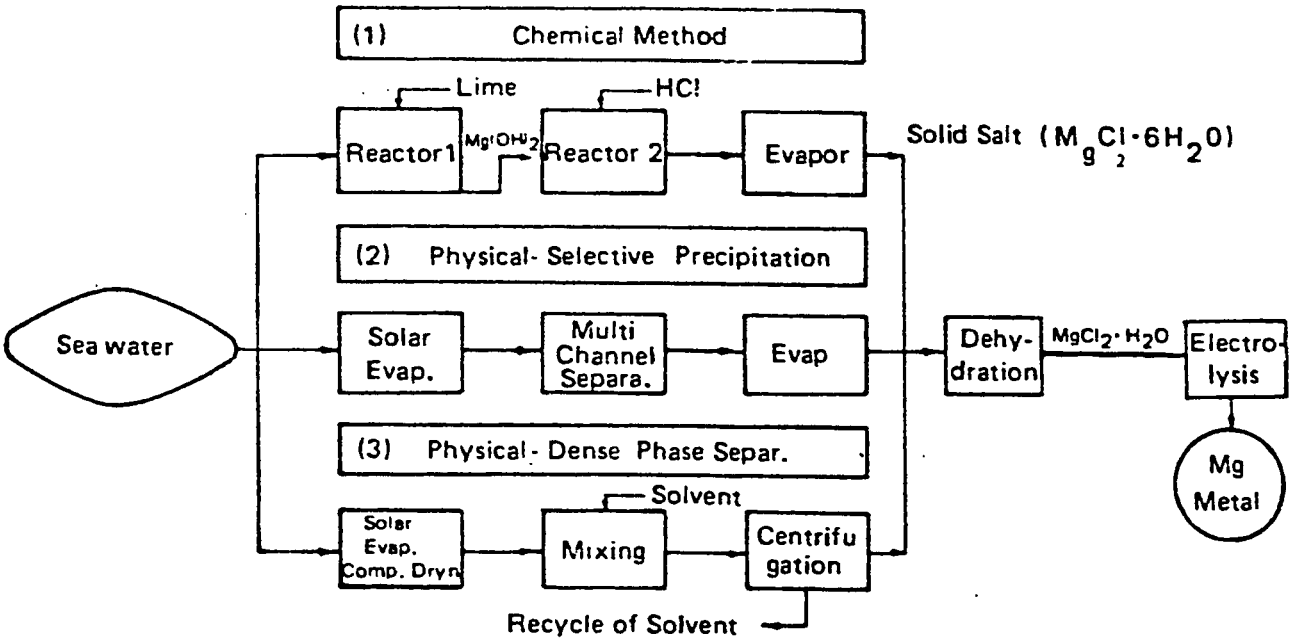

Figure: 2.2 Methods for Recovery of Magnesium Chloride from Sea Water (Abdel-AAL, 1989)

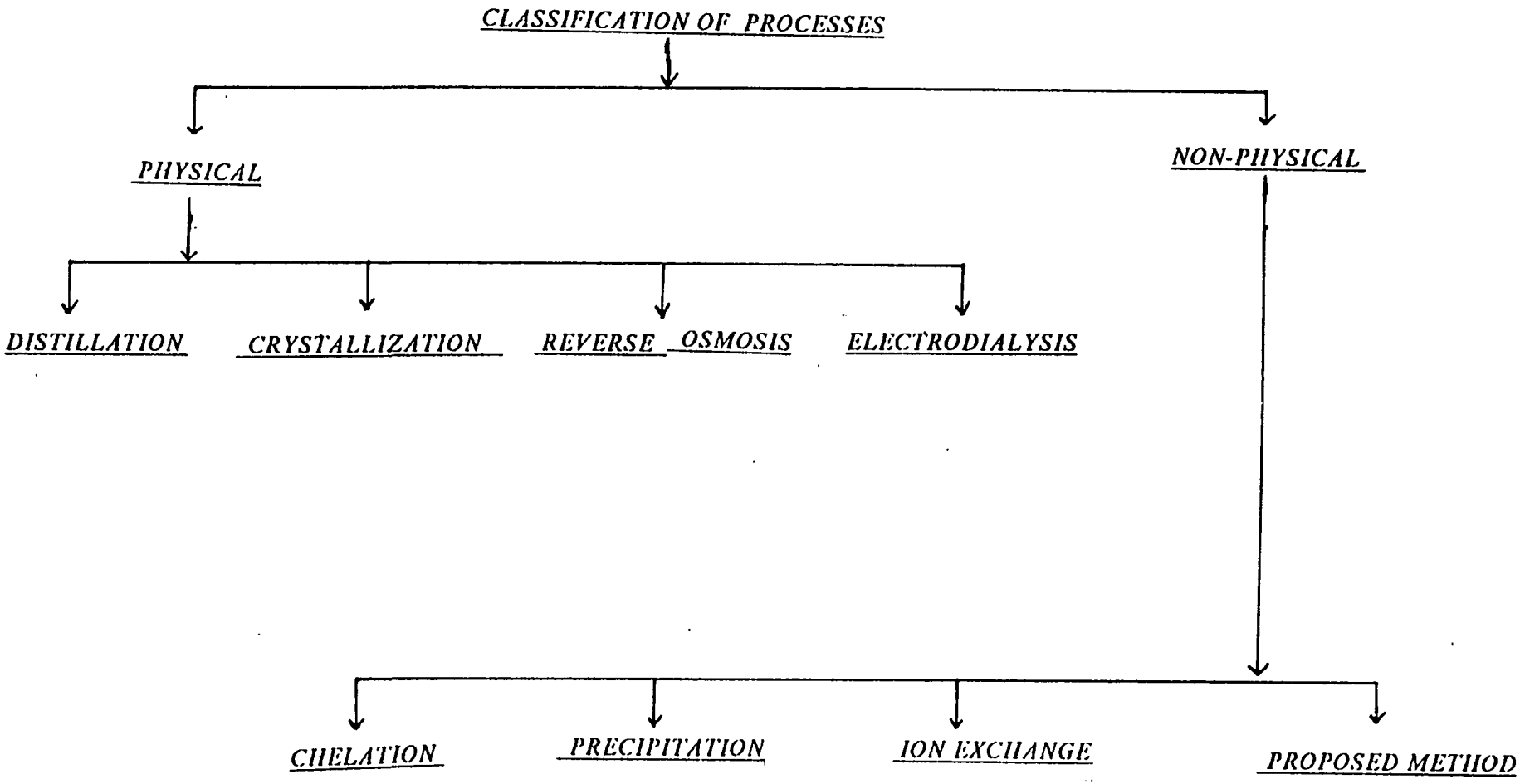

Figure: 2.3 Classifications of Conversion Processes

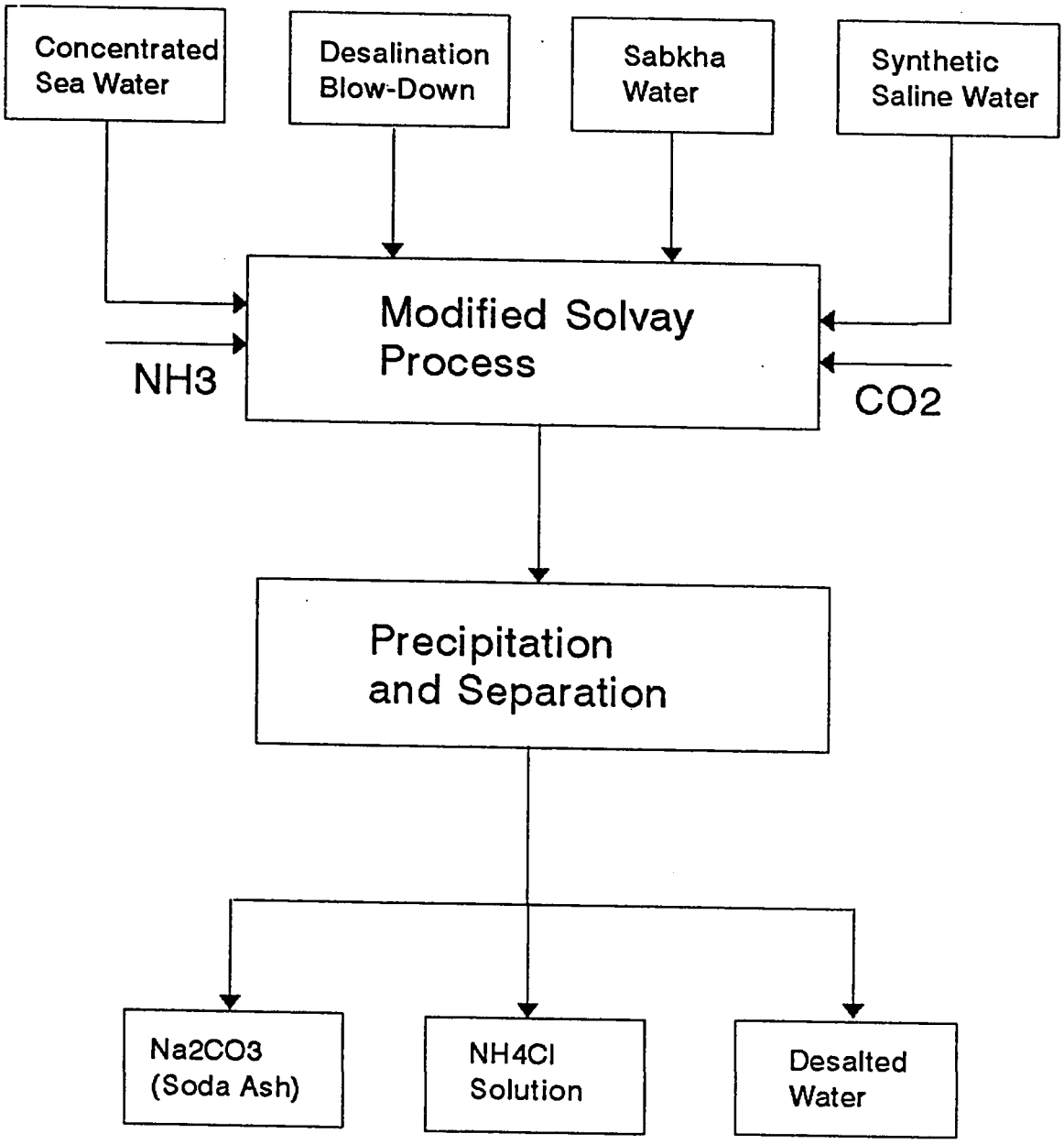

Figure: 2.4 Outline of Modified Solvay Process

2.1.2 Modified Solvay Process

The artificial soda industry originated in France. Nicolas Le Blanc (1742 - 1806) outlined a method of manufacture of soda, starting with common salt. This process laid the foundation of chemical technology of heavy chemicals. The development of the sulfuric acid industry, the production of hydrochloric acid and bleaching powder are on the other hand, a direct outcome of the Le Blanc process. Figure 2.5 shows the Le Blanc process.

The history of ammonia soda process dates back to 1811 when L. Fresnel conceived the idea of making soda from salt and ammonium carbonate. In 1837, John Thom attempted to make soda using the reaction between ammonium carbonate and salt. In the year 1838, H.G. Dyar and J. Hemming patented the treatment of brine with ammonium bicarbonate to precipitate sodium bicarbonate. In 1842, Canning patented the process of carbonation with gaseous carbon dioxide from the calcination of sodium bicarbonate. In the same year Chisholm patented the process for recovery of ammonia from the mother liquor by distillation with lime and absorption of ammonia gas in brine. In 1860, Ernest Solvay, independently discovered and developed to economic fruition a cluster of six chemical reactions which proceed rapidly under reasonable industrial operating conditions, (Hou, 1991). This process has for many years been the source of most of the soda, Na_2CO_3, produced in the world.

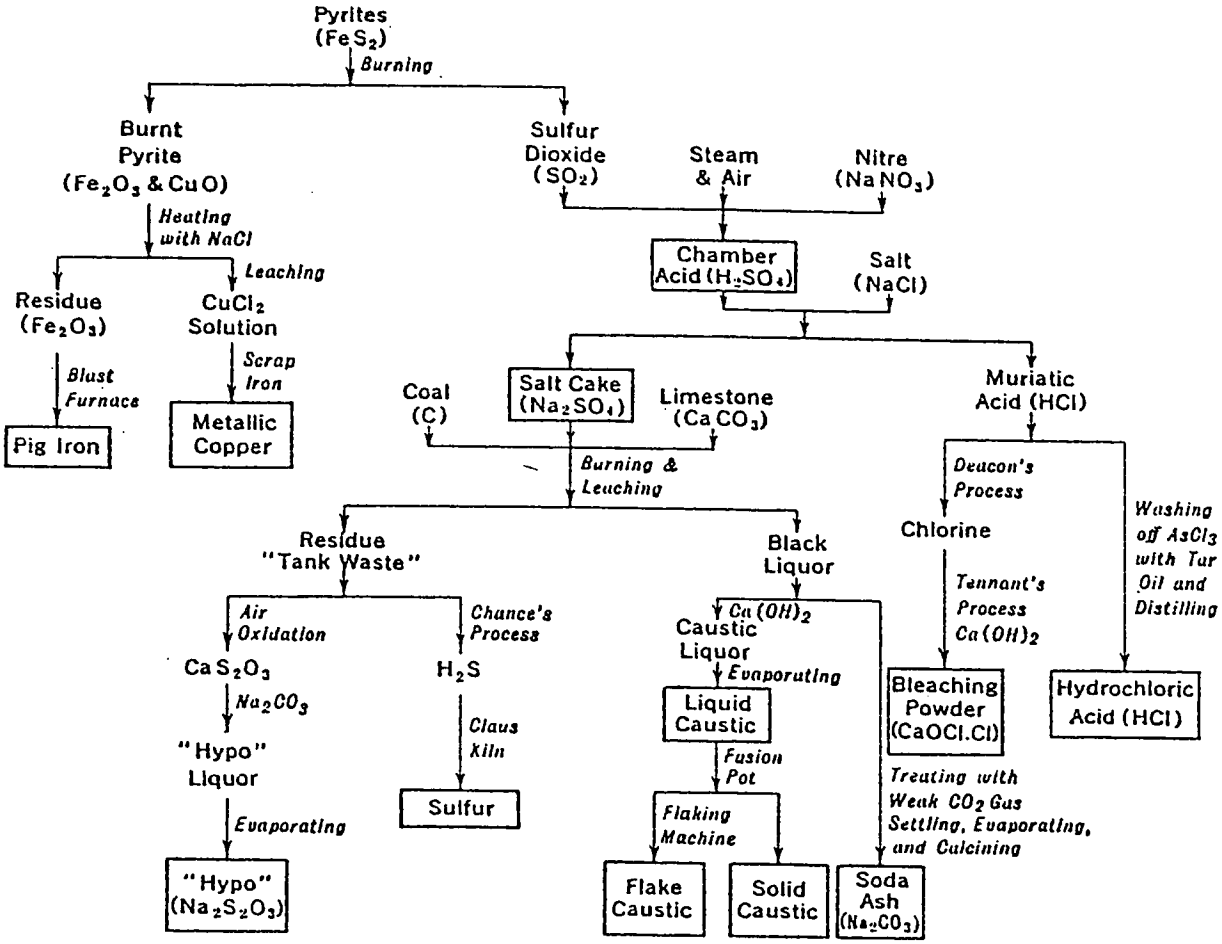

Figure 2.5 Diagram of Le Blanc Process (Hou, 1991)

The Solvay process is an excellent example of the recovery and recycle of materials so as to consume upon requirements for make up reactions. The process is considered as a major discovery in the history of processing. The Solvay process utilizes as feed:

(i) a sodium chloride rich brine (natural brine - dissolved rocks, or even concentrated seawater).

(ii) Limestone rock ($CaCO_3$)

The process centers on the reaction of ammonium bicarbonate with sodium chloride of this brine in concentrated aqueous solution. The least soluble compound ($NaHCO_3$) is caused to precipitate out of solution, is filtered and washed, and is then calcined to decompose it into sodium carbonate, with the release of carbon dioxide and water vapour. The main contribution of the Solvay process was to cause the ammonium bicarbonate to be formed in place in a highly concentrated brine solution by the successive absorptions of ammonia and then carbon dioxide into the solution. It was also economically necessary to provide to a high degree of recovery of ammonia for recycle, so as to minimize the need for fresh ammonia as feed.

The net result of these six reactions is the conversion of salt and limestone into calcium chloride and soda ash, a chemical reaction that does not occur directly under industrial conditions.

$$2\,NaCl + CaCO_3 = CaCl_2 + Na_2CO_3 \qquad \Delta G^{\circ}_{298} = 9600\ cal/gmole \qquad (2.1)$$

The cluster of reactions that yields this net result and the approximate temperatures at which they proceed as proposed by Solvay are :

$$CaCO_3 = CaO + CO_2 \qquad 1000^\circ C \tag{2.2}$$

$$CaO + H_2O = Ca(OH)_2 \qquad 100^\circ C \tag{2.3}$$

$$Ca(OH)_2 + 2\,NH_4Cl = CaCl_2 + 2\,NH_3 + 2\,H_2O \qquad 120^\circ C \tag{2.4}$$

$$2\,NH_3 + 2\,H_2O + 2\,CO_2 = 2\,NH_4HCO_3 \qquad 60^\circ C \tag{2.5}$$

$$2\,NH_4HCO_3 + 2\,NaCl = 2\,NaHCO_3 + 2\,NH_4Cl \qquad 60^\circ C \tag{2.6}$$

$$2\,NaHCO_3 = Na_2CO_3 + H_2O + CO_2 \qquad 200^\circ C \tag{2.7}$$

Table 2.5: shows the production/consumption analysis for the Solvay reactions, while Figure 2.6 depicts the schematic diagram of the classical Solvay process. Table 2.5 relates the reaction stoichiometry indicating that the Solvay process, when in reaction balance, consumes one mole of limestone and two moles of salt to produce one mole of soda ash and one mole of calcium chloride. The other materials are used for processing only to smooth chemical reaction routes, pulling the reactants easily to convert them to the products.

The sum of these reactions is the Solvay soda ash process, the classical example of replacement of infeasible reaction by a cluster of feasible chemical reactions involving the closed-cycle use of interme-

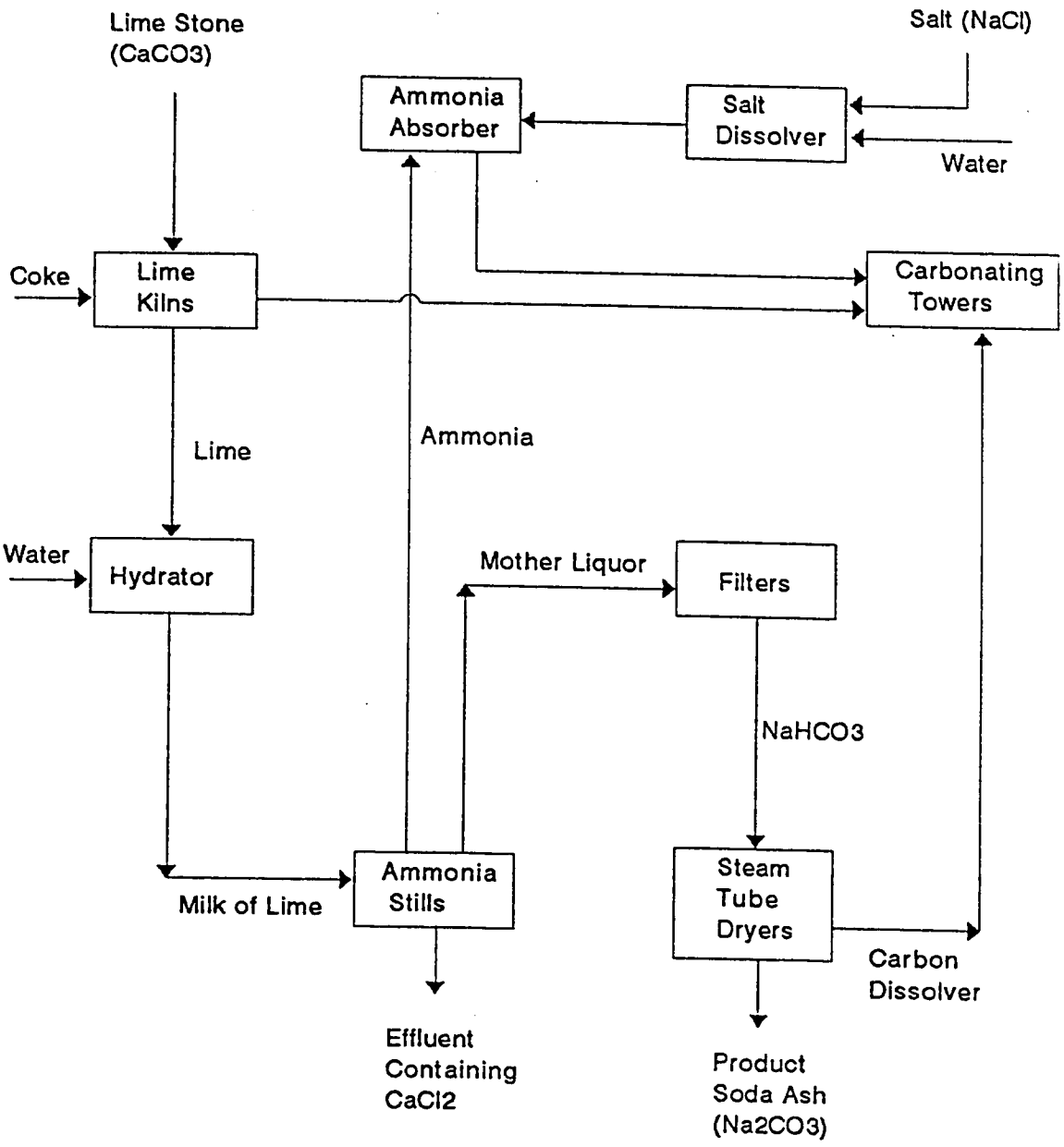

Figure: 2.6 Block Diagram of Solvay Process

Table 2.5 Production Consumption Analysis for Solvay Reaction Path

Reaction	$CaCO_3$	CaO	CO_2	H_2O	$Ca(OH)_2$	NH_4Cl	NH_3	$CaCl_2$	NH_4OH	$NaCl$	Na_2CO_3	$NaHCO_3$
1	-1	+1	+1									
2		-1		-1	+1							
3				+2	-1	-2	+2	+1				
4				-2			-2		+2			
5			-2			+2			-2	-2		+2
6			+1	+1							+1	-2
Net	-1	0	0	0	0	0	0	+1	0	-2	+1	0

diate chemicals. Similar Solvay clusters drive a score or more commercial processes including those which manufacture sulfuric acid, carbon tetrachloride, ethyl ether, isopropanol, aniline, hydrogen peroxide, ethylene glycol, butadiene, acetaldehyde, hydrogen cyanide, sodium thiosulfate, chlorine and vinyl acetate (Faith, 1975). There is now interest in the development of a Solvay clusters for the thermochemical splitting of water to obtain hydrogen (Chao, 1974) and for the mineral separation (Novak and Schuster, 1969). May and Rudd (1976) developed a theory of Solvay cluster synthesis that creates stoichiometrically consistent and thermodynamically feasible sets of reaction and that directs the search for superior clusters. They have shown that the development of thermodynamically feasible Solvay clusters is a problem in pattern recognition. Three factors that must be considered in the development of Solvay clusters are:

1. The stoichiometry reactions
2. The thermodynamic equilibrium.
3. The reaction kinetics.

One of the disadvantages of the original Solvay process is the low percentage utilization of raw salt (NaCl utilization rate = 70 %). This has a large effect on the manufacturing cost particularly when the salt is to be imported from distant countries. Various extensive efforts have been made to develop a new process enabling complete salt utilization.

These processes, like other commercial Solvay-cluster driven

reactions , are characterized by the fact that the intermediate chemicals and reactions seem to have little effect on the net reaction. Much of the production of NH_4Cl in Japan is tied to soda ash. Due to the shortage of salt there, the incentive is obvious for finding a way to use the Cl part of the salt molecule instead of wasting it in calcium chloride. This has been accomplished by coupling Japan's Solvay plant to ammonia units. Limestone is replaced with carbon dioxide for carbonation and ammonia is recovered as NH_4Cl instead of distilling it off. The recovery of ammonia is carried out by means of calcium hydroxide (a by product of the carbon dioxide generating lime kiln). The ammonium chloride is removed from the process and used for fertilizers.

In the conventional Solvay process, sodium carbonate is made from salt, fuel and limestone. Calcium chloride is a worthless by product and a serious pollutant. Later on consideration was given to a process modification which would eliminate the use of limestone and yield HCl as a by product. The technical feasibility of substituting reactive magnesia (together with HCl) by the hydrogen of magnesium chloride was also attempted. Appreciable tonnage of ammonium chloride made for fertilizer purposes are mainly used in India and the Far East.

Modern processes use a variety of raw materials and by-product reactions in the solid, liquid and vapour phases. NH_4Cl is popular

in the Far East as fertilizers for rice and some field crops. The reason for its popularity in this region is due to the fact that rice fungus, which reduces other fertilizers such as ammonium sulfate to toxic sulfides, does not affect ammonium chloride. In addition, when using in conjunction with calcium cyanamide and calcium silicate, ammonium chloride is of assistance in preventing plant disease. Another contributory factor is that ammonium chloride provides a useful outlet for surplus chloride or hydrochloric acid, which instead of being nuisance factor, helps to produce a fertilizer containing about 26% nitrogen.

Asahi Glass Co of Japan (Miyata, 1983), has succeeded in developing an ammonium-chloride and soda-ash co-production process in which ammonium chloride is crystallized after separating the sodium bicarbonate, and the mother liquor is recycled .

In the literature cited so far, not a single reference characterized the Solvay process as a separation method capable of producing desalted water along with the soda ash and ammonium chloride from a highly saline waters. It is towards this objective that the present work is aimed.

The process proposed in this work is different from the those cited above. It can be classified as a physico-chemical process in which NaCl is separated from the highly saline water. It utilizes the "Solvay" principles to manufacture soda ash from concentrated brine. These brines have to be saturated solutions, containing about 30 %

NaCl by weight.

2.2 Indigenous Saline Sources For Desalination (Sabkha)

There is no exact and unified definition for the word "Sabkha". The lack of agreement among geologists, sedimentologists and others, is due to the large number of designations given for various high water table situations available in the Middle East (Fookes, 1986). The word Sabkha appears in the literature with different spelling such as "Sabkhak, Sabkha, Sebkha, etc." There has been confusion in various usage of the term. Kinsman (1969) and Glennie (1970) gave a good explanation of Sabkha as the term is used in Saudi Arabia. Sabkhas are saline flats that are underlain by silt, clay and sand, and often incrusted with salt. They are equilibrium surface whose level is largely controlled by hydrological and climatic conditions (John et al., 1978).

Sabkha or saline-marsh materials, occur widely on the Arabian Penisula. They are generally of evaporite formation, either from sea invasion or from seepage of moisture from low-lying strata further inland. In both cases varying quantities of calcium carbonate, magnesium carbonate, calcium sulphate and calcium, magnesium and sodium chloride are found (Kinsman, 1969-1971; Bush, 1973; Hsu, 1969-73; Evans, 1969; Talor 1969; De Groot, 1969). There is a clear difference between salt pan (evaporatic pan) and sabkha as shown in Figure 2.7.

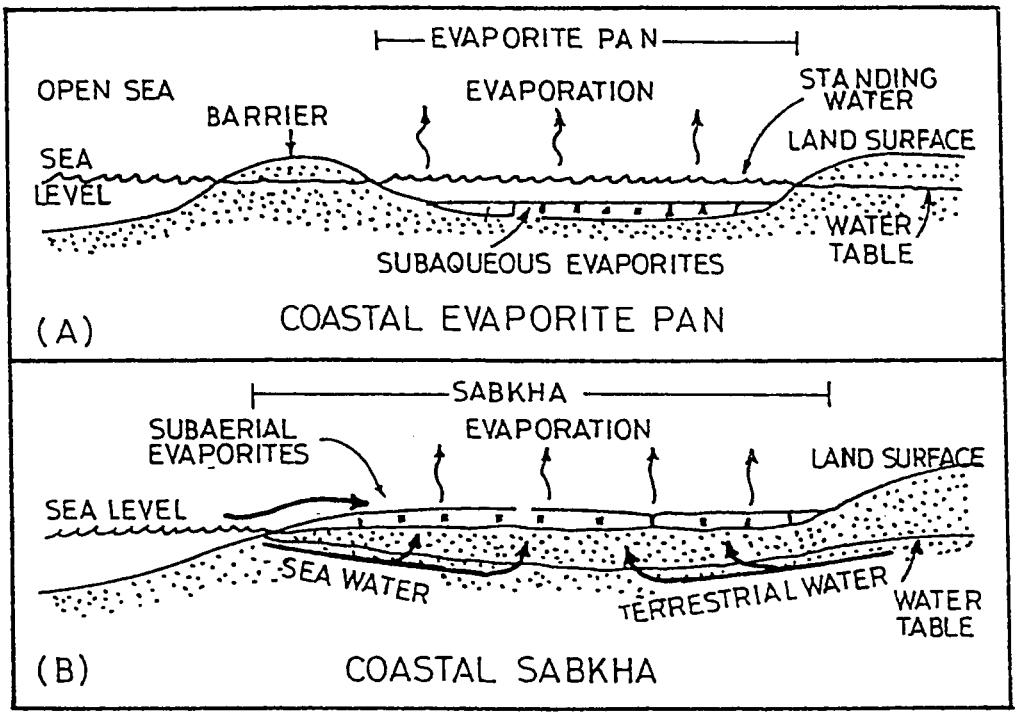

Figure: 2.7 **Diagrammatic Cross-Sections Illustrating the Difference between (a) a Coastal Evaporite Pan, and (b) a Coastal Sabkha (Renfro, 1974).**

Sabkhas are salt flats or salt-bearing soils which are composed mainly of carbonate granular soils in a sand-silt of varied density, composition, texture, and properties of evaporatic minerals. The Sabkha deposits are found to be of varying thickness, stratification and other geotechnical characteristics (Gazali, 1985). Sabkhas are equilibrium surfaces whose level is controlled by the local groundwater table. Sabkha can be easily distinguished from salt pan (an evaporatic basin) by its depositional interface which is subareal, whereas that of salt pan is subaqueous. In addition, the feed water of sabkha has a major lateral component of interstitial flow, while being concentrated by evaporation as shown in Figure 2.7. The mode of development and the profiles of sabkha in the coastal and inland areas are different as reported by Akili (1983).

2.2.1 Coastal Sabkha

The coastal plains generally lie above the high-tide level and slope gently seaward at approximately 0.4 m per Km (Evans et al., 1969). The coastal sabkha is described by Akili (1981) as supratidal surfaces which have developed as a result of sedimentation sequences that appear to have started several thousand years ago when Gulf waters transgressed over sand dunes that formed during the Pleistocene. This sea encroachment has resulted in the lagoons separated from the Gulf waters by barrier islands.

Figure 2.8 shows a generalized cross section of coastal sabkha from the Gulf waters to the inland margin were the sabkha plain may

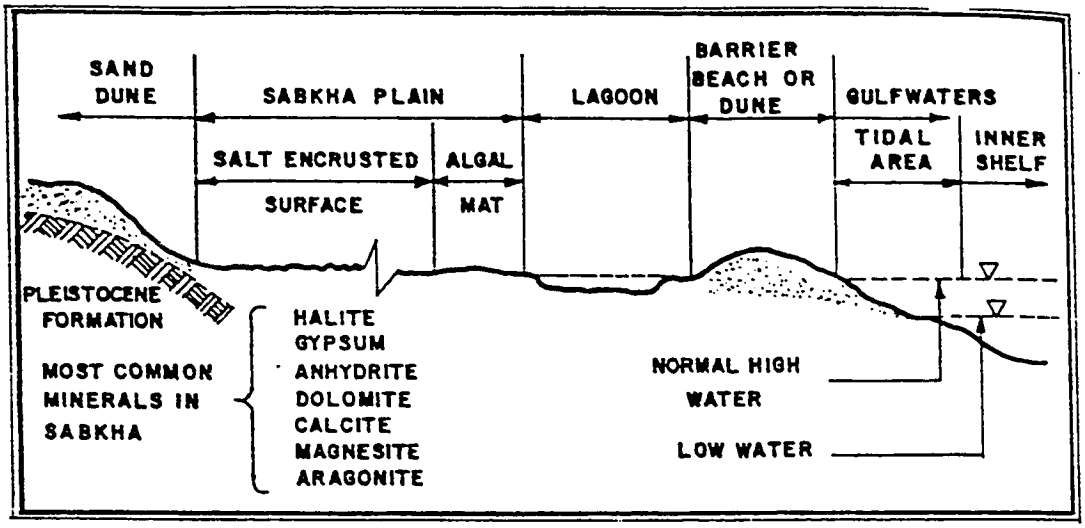

Figure: 2.8 Generalized Cross Section across a Coastal Sabkha with Typical Surface Features (Akili & Torrence, 1981).

abut sand dunes or rock outcrops. After this transgression and subsequent morphological changes, the depositional environment appears to have shifted from subaerial to subsequence causing extensive carbonate sedimentation in lagoons which led to gradual widening of sabkha plains and eventual progradation of the coastline.

As almost the whole spectrum of sedimentation in the Arabian Gulf is carbonate, the major constituent of the sabkha are calcite and aragonite (Shearman, 1966; Ellis, 1973: Akili, 1980). However, the carbonate content decreases as sabkhas grade landward. This is due to the closeness to the coasts. Sabkha development is likely to occur, when the prevailing weather is characterized by being very hot and arid with more evaporation than precipitation (Renfro, 1974).

An active sabkha is commonly seen when brine-saturated, porous and permeable sediments are capable of supplying sufficient amounts of water to keep balance with the amount of water being lost to the atmosphere by evaporation. An evaporite pan will be formed if the influx water exceeds the evaporation loss, while evaporite pan transforms to sabkha by either the increase in evaporation or reduction in the recharge. Because of the evaporative loss of water in the sabkha, a subsurface hydraulic gradient toward the sabkha is created by the induced flow of terrestrial groundwater and subsurface marine waters. Marine waters can also recharge the sabkha through floor of the lagoon which acts as barrier and hence separates it from the open sea (Kinsman, 1969; Friedman, 1972; Illing et al., 1965), or

during intermittent tide and storm induced flooding of the sabkha margin (Butler, 1969; 1970).

2.2.2 Inland Sabkha:

In the topographic depressions of hot deserts, the capillary fringe of the groundwater may reach the ground surface. Intermittent lakes may occur and evaporation may produce salt deposits analogous with those of the coastal sabkha. These areas are sometimes termed inland sabkhas though names such as playa and saline, as mentioned earlier, are more or often used, where groundwater is of greater importance than rain fall. The water in this environment comes from two sources: Periodic rainfall and groundwater (capillary rise and springs), and both sources bring soluble salt into the area.

Halite and Gypsum are important minerals in these evaporites and there is sometimes aerial zonation of the precipitation phases. The inland sabkha surface is much like that of the coastal sabkha with salt polygons again being characteristic, but the salts are often strongly influenced by local bed rock and therefore differ in composition from those related to marine coastal conditions.

2.2.3 Sabkha in Saudi Arabia:

In Saudi Arabia, Sabkha exists either along the coast of the Red Sea and the Arabian Gulf as coastal sabkha or inland as continental sabkha. The sabkha distribution in Saudi Arabia mainly occurs in the well populated cities along both the Red Sea and Arabian Gulf

Coasts. Figure 2.9 summaries the Sabkhas in the coastal plains of the Eastern province as described by Johnson et al., (1978). Along the western shores of Saudi Arabia, the coastal sabkhas also exists, as reported by Al-Amoudi, (1992); Ali and Hossain, (1988) at Obhor (21..B, 22) and al Lith, 250km South of Jeddah (Johnson et al., 1978) and Yanbu (Stipo, 1989). In the Southwestern Saudi Arabia, near the town of Jizan, coastal Sabkha is found to exist around a salt dome (Erol, 1989; Hodgson et al., 1989). Continental sabkhas are reported to exist in the north in the Wadi Al Sirhan (Smith, 1980). The ground water is also rich in salt and is usually less than one meter in depth.

The solubility of minerals in coastal water and groundwater are strongly affected by other phases present in rocks (Fookes, et al., 1985), by the presence of dissolved gases, such as carbon dioxide and by the pH of the water. Figure 2.10 depicts the concentrations of NaCl in Sabkha waters of various places. The NaCl concentration is about 30% by weight. Typical compositions of coastal and sabkha waters (Fookes, et al., 1985) is given in Table 2.6. These waters are characterized by a low content of calcium and a high content of magnesium, sulfate and, of course, sodium, potassium, and chloride, but are not normally saturated in these ions.

2.2.4 Geology of Sabkha:

The soil of the sabkha is described as heterogeneous and imperfect solid layers or unlayered sedimentological framework saturated

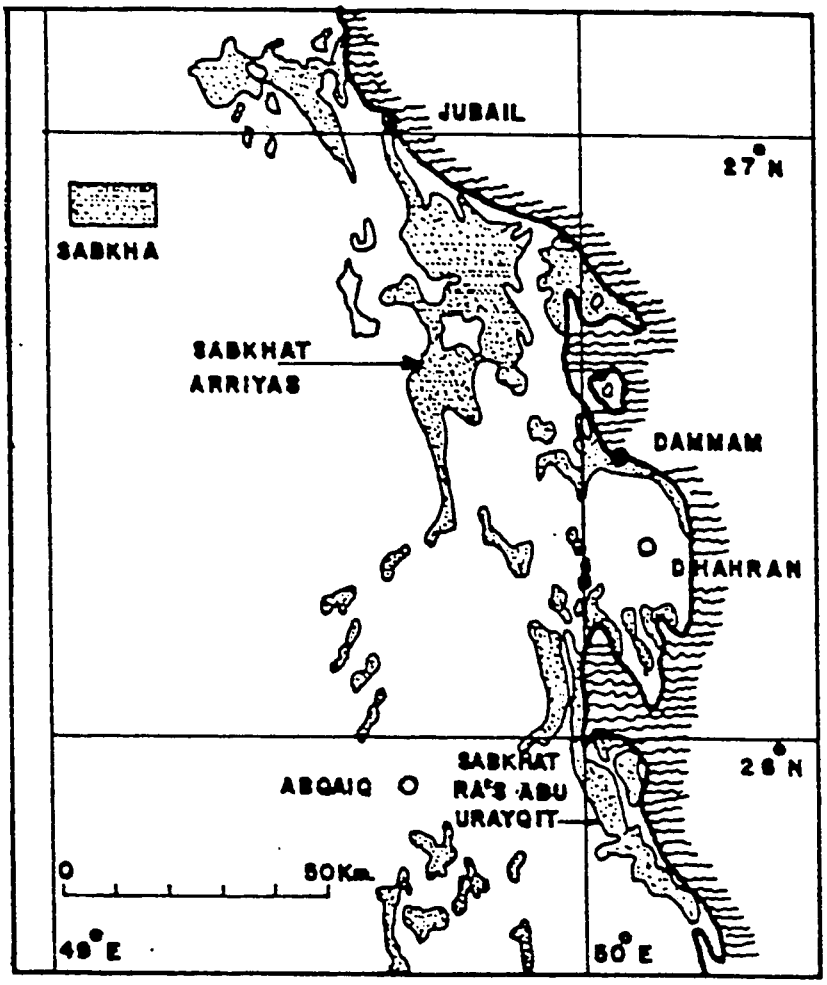

Figure: 2.9 Sabkha Flats Along the East Coast of Saudi Arabia (Johnson et al., 1978)

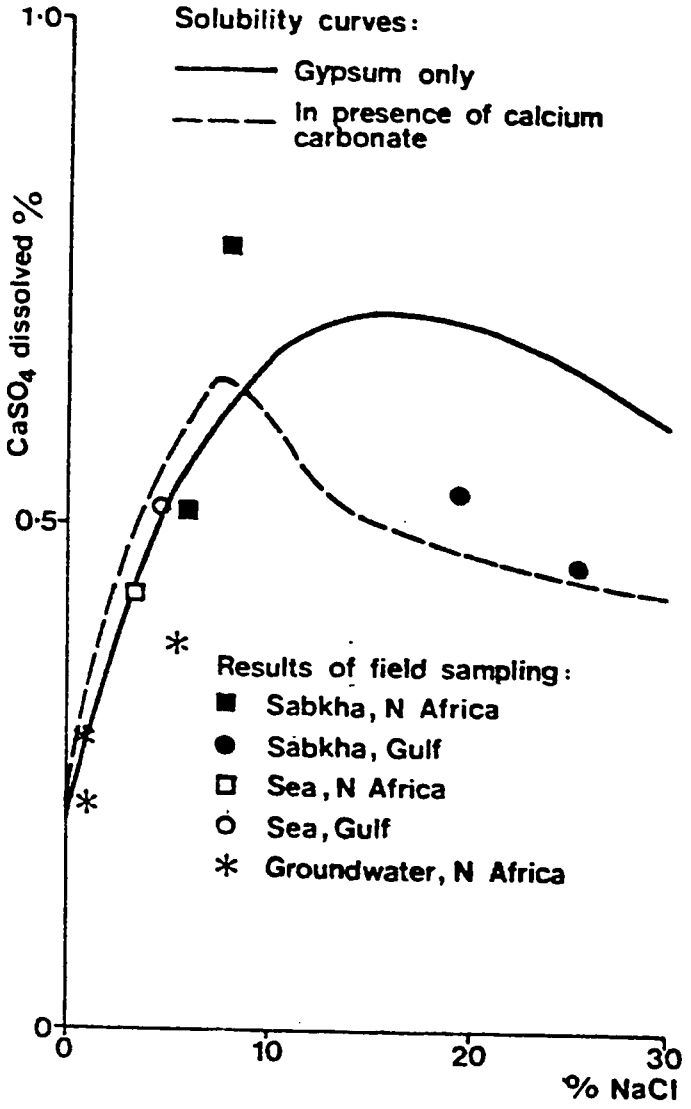

Figure 2.10 Solubility of Gypsum and NaCl in Saline Water(Fookes; et al. 1985).

with subsurface brine. The structure is often gritty, permeable and porous and untight, therefore prone to high rate of infiltration. The outer surface of sabkha soil is made of hydroscopic salts that rendes the surface crust slippery when it is wet (El-Naggar, 1988; Fookes, 1976).

Table 2.6 : Typical Experimental Chemical Compositions of Sea and Sabkha (Fookes, et al., 1985)

Sample location	Open sea	Coastal sea water Arabian Gulf	Sabkha
ppm			
Ca^{++}	420	420	1250
Mg^{++}	1320	1550	4000
Na^{+}	10700	20650	30000
K^{+}	380	660	1300
Cl^{-}	19300	35000	56600
SO_4^{--}	2700	3300	9950
HCO_3^{-}	75	170	150

The continuous reaction between the sediment framework and the brine produces new or modified sedimentary features and new minerals to the sabkha. These varying features and minerals are the main

description to sabkha deposits. The process reactions are quite slow and hence have geological rather than engineering significance, however, knowledge of the development of old sabkha will contribute considerably to the understanding of recent sabkha evolution. A "Sabkha cycle" is reported to exist (Wood and Wolf, 1969), with the featural changes being repeated.

A vast amount of research on sabkha soil was performed at Imperial College of the University of London, at Kiel, on the sabkhas of both Qatar and the United Arab Emirates. Some of this research work is recorded by (Bathurst, 1975) and (Purser, 1973).

2.2.5 Characteristic of Sabkha:

The general characteristic of sabkhas as described by different researchers may be summarized as follows:

1). Sabkha is commonly made of quartz sands and silts, which sometimes have small proportion of muds and clays. In addition to that, sabkha soils contain calcium sulphate and calcium carbonate. The carbonates work mainly as cementing agents of sabkha (Akili, 1981).

2). Sabkha is characterized by:

i). The presence of different compositions, shapes and sizes

ii). Highly saline groundwater tables.

iii). A relatively hard encrusted surface caused by encrustation and desiccation.

3). Some sabkha soils have gravel mixtures within their composition. The presence of these gravelly sediments is more common in the continental sabkha than in the coastal sabkha.

4). Sabkha soil is generally described as an unconsolidated, heterogeneous, layered sedimentological framework, bathed in highly concentrated, subsurface brine (Akili and Ahmed, 1983; Akili and Faletcher, 1978; Akili and Torrance, 1981).

5). The natural moisture content of the sabkha soil deposits ranges from 8 to 65%, so this large variation in the water content leads to large changes in density, consistency and strength (Iqbal and Sayed, 1981).

6). Sabkha has large changes in density, consistency and strength.

2.2.6 Advantages of Sabkha

The merit of the sabkha deposits were not well understood, however, it is becoming apparent that they could have advantages. In the Arabian Gulf, the exploitation of these resources has attracted many researchers and companies. For instance Sadaf, of Jubail in Saudi Arabia, obtains raw brine from a salt plant at Ar Riyas. The brine is used in the chlor-alkali plant. A uniform flow of high quality brine is fed to electrolytic diaphragm cells to produce hydrogen, chlorine, and caustic as shown in Figure 2.11. The annual and the daily use capacities are given in Table 2.7.

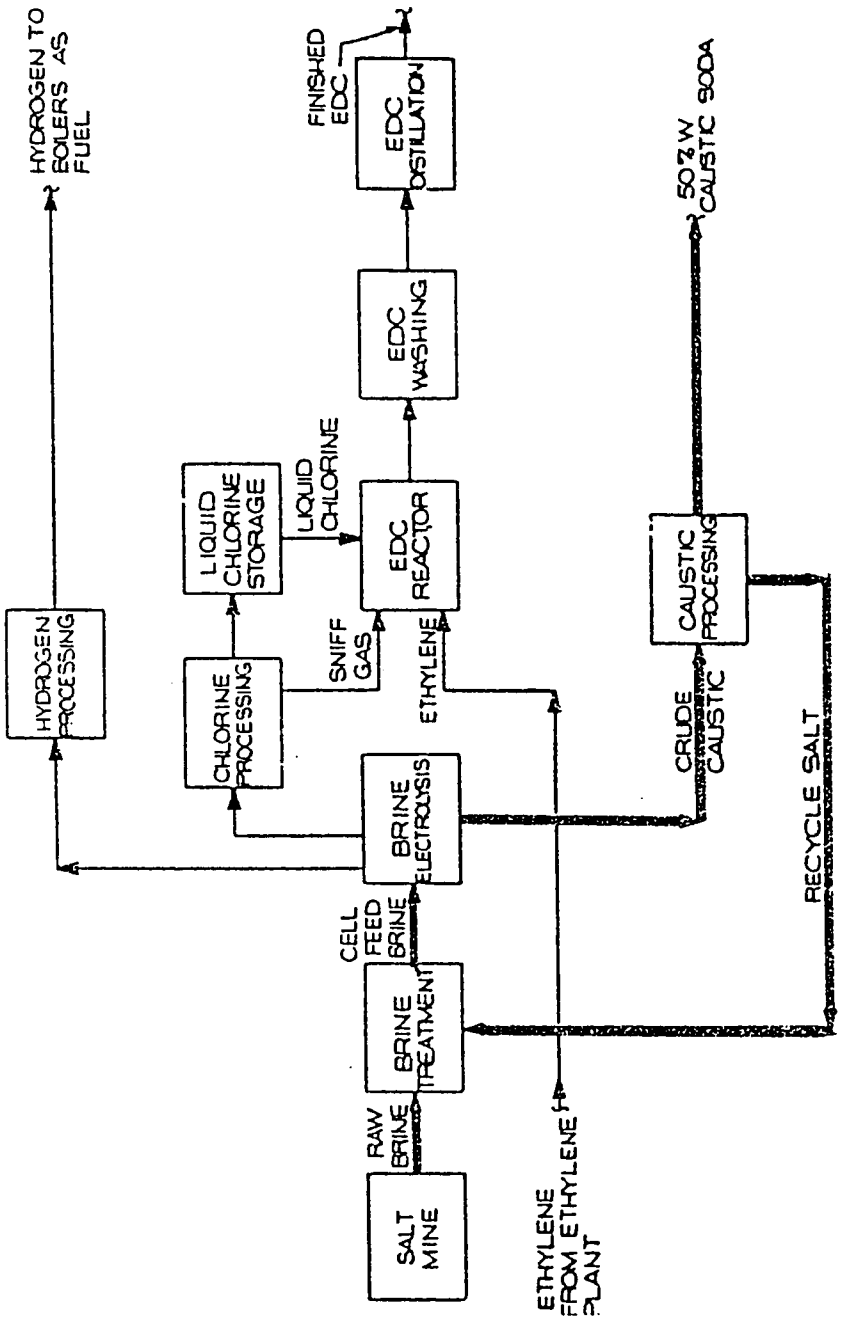

Figure 2.11 Block Flow Diagram: Salt / CA / EDC Plant (Sadaf-Jubail- 1991).

Table 2.7: Salt/CA/EDC Plants (Sadaf-Jubail-1991)

		Annual Capacity (in metric tonns)	Daily Capacity (in metric tonns)
Salt Plant	Salt	566,100	1,700
Chlor-Alkali Plant	Chlorine	333,000	1,000
	Hydrogen	9,880	29.6
	Caustic Soda	367,000	1,100
Ethylene Dichloride Plant	EDC	454,000	1,363

Though the study concerning the extent of the sabkha reserve is not yet disclosed, it is known that at Ar Riyas an area of at least sixty square kilometers is covered by this salt reserve. Portions of this area is allocated to Sadaf. Based on borings and site observation, the general stratigraphy consists of a surface layer, transition zone and main salt deposit. The surface layer is 0 - 0.5 meters of brown silt, sand, white clay , and NaCl crystals. Below this is a transition zone, consisting of alternating NaCl silt layers extending to an average depth of two meters below the surface. The transition zone grades into the main salt (NaCl) deposit, which averages 8.5 meters thick. Based on laboratory results, the NaCl quality of the transition zone ranges from 85 -95 % and the main deposit exceeds 95 % at each boring.

2.3 Mass Transfer with Chemical Reaction.

Chemical processes which incorporate diffusion usually involve chemical reactions. This is the case in the proposed separation process. Often diffusion and reaction occur in the same region, and the two rate phenomena are coupled so closely they have to be treated simultaneously. Simultaneous mass transfer and chemical reaction of soluble solution in two phase or three phase systems has considerable importance not only in the chemical process industries but also in biological processes (Doraiswamy and Sharma, 1981).

When a chemical reaction is used for separation purposes, it usually involves fast reactions. Examples of processes of industrial importance, where gas absorption is accompanied by chemical reaction are numerous. In two phase systems such as gas-liquid, the phenomena of mass transfer and chemical reaction will proceed as long as the two contacting phases are not at chemical equilibrium. The processes have two purposes:

1). The preparation of products like HNO_3, H_2SO_4 etc.

2). The removal of a component from a mixture of gases, as in the case CO_2 removal from synthesis gas.

The occurrence of chemical reaction has two distinct effects on the overall behavior of the system (Alper, 1979). The first one is, for the case of absorption, as follows. When a component is absorbed into the liquid phase, it is consumed by chemical reactions and therefore its concentration in the bulk of the liquid is decreased. This in turn implies that the driving force for additional absorption remains higher than it would be if no chemical reactions were taking place and the capacity of a unit volume of liquid for dissolving the gas can be greatly increased.

The second effect is at a given level of driving force, the actual rate of mass transfer may be significantly higher when chemical reactions are occurring than it would be in the absence of chemical reactions. The enhancement rate may be up to several orders of

magnitude, and may be so high as to reduce the mass-transfer resistance in the liquid phase to insignificance relative to the resistance in the gas phase. Table 2.8 shows some selected data (Sherwood et al., 1975) on the effect of increasing alkalinity of the solution on the mass transfer coefficient in a packed column. Notice that even very strongly alkaline solution give an appreciable resistance to the absorption of CO_2.

The enhancement factor can be obtained by using the classical hydrodynamic models of gas-liquid interface mass transfer available in the literature, such as film, penetration and surface renewal. These models give similar prediction for most of the cases, for fluid-fluid systems (Danckwerts, 1970), except in regard to the diffusivity of solute gas and of dissolved reactants on the rate of absorption.

Table 2.8 Absorption Coefficient for CO_2 in Various Solvents.

solvent	kga lb/h ft^3 atm
1. Water	0.05
2. 1N Na_2CO_3, 20% $NaHCO_3$	0.03
3. 3N Diethanol Amine, 50% CO_3	0.4
4. 2N NaOH, 15% Na_2CO_3	2.3
5. 2N KOH, 15% K_2CO_3	3.8
6. Perfect solvent, no liquid Resistance and having infinite chemical reactivity	24.0

The film model of Whitman (Danckwerts, 1970) assumes that, close to any fluid interface, therefore is a stagnant film of uniform thickness, δ, through which the transport process takes place by simple molecular diffusion alone. There is no convection in the film, while the rest of the fluid is kept uniform in composition by agitation. The model leads to an expression for the absorption rate:

$$N_A = D_A \frac{C_A^* - C_A^o}{\delta} \tag{2.8}$$

Where the mass transfer coefficient k_L is given by

$$k_L = \frac{D_A}{\delta} \tag{2.9}$$

The penetration theory, proposed by Higbie (1935) assumes that the liquid interface is made up of a variety of small elements, which are continuously brought up to interface from the bulk and returned later to the bulk by motion of the liquid phase itself. The surface elements were each assumed to stay at the surface for the same amount of time and were considered to be stagnant. Therefore, absorption occurs by unsteady molecular diffusion in the various elements of the liquid surface. The model gives the following expression:

$$N_A = 2 (C_A^* - C_A^\circ) \sqrt{\frac{D_A \Theta}{\pi}} \qquad (2.10)$$

where the mass transfer coefficient k_L is given

$$k_L = 2 \sqrt{\frac{D_A}{\pi \Theta}} \qquad (2.11)$$

The surface renewal model, proposed by Danckwerts (1975), is similar to the penetration theory of Higbie, except it rejects the hypothesis of equal life for all the surface elements of liquid. Instead, the model proposes that the chance of the element of surface being replaced with fresh liquid is independent of the length of time for which it has been exposed. This has led to a age-distribution function. The model gives:

$$k_L = \sqrt{D_A S} \qquad (2.12)$$

Where

S = the fraction of the area of surface which is replaced with fresh liquid in unit time.

any one of the described models of the gas absorption process can serve two functions. First, it can provide a basis for estimating physical absorption rates under different conditions. Second, the model may be employed to predict the effect of a chemical reaction on the rate of absorption. The interest in this study matches the latter case where the chemical reaction is concerned.

It appears fairly evident that the chemical reaction, which modifies the concentration profile near the interface, accordingly affects the mass transfer to the phase where the reaction takes place. If the dissolved gas reacts with the liquid or substance dissolved in it, then the differential equations which represent the phenomena of simultaneous diffusion and chemical reaction in the liquid phase may be written :

$$D_A \frac{\delta^2 C_A}{\delta x^2} = \frac{\delta C_A}{\delta t} + r(x,t) \qquad (2.13)$$

where r(x,t) is the rate per unit volume of liquid at which the reaction consumes the solute gas at time t and distance x below the surface. This rate will in general depend on the local concentration of the gas, and of any other solute with which it reacts. In deriving Equation 2.13 temperature, solubilities, diffusivities, reaction rate constant and other physico-chemical quantities, are supposed constant and uniform. Equation (2.13) simplifies in the case of the film model to :

$$D_A \frac{d^2 C_A}{dx^2} = r(x,t) \qquad (2.14)$$

In the consideration of a system in which only two reactants are involved, namely non-volatile liquid-phase reactant (B) and an absorbing solute component (A), the boundary conditions will be:

Film model :

$$x = 0; \qquad C_A = C_A^*; \qquad \frac{dC_B}{dx} = 0$$

$$x = \delta; \quad C_A = C_A^o, \quad C_B = C_B^o \qquad (2.15)$$

Penetration model :

$$t = 0, \quad x > 0; \quad C_A = C_A^o; \; C_B = C_B^o$$

$$x = 0; \quad \frac{\delta C_B}{\delta x} = 0, \quad C_A = C_A^* \qquad (2.16)$$

$$x \to \infty; \; C_B = C_B^o, \quad C_A = C_A^o$$

The solution of the original differential equation now depends on the rate expression as discussed below in 2.3.1 and 2.3.2.

2.3.1 Irreversible First Order Reaction

An irreversible first order reaction will take the rate of the form:

$$r = k_1 C_A \qquad (2.17)$$

equation(3.14), becomes :

$$D_A \frac{d^2 C_A}{dx^2} - k_1 C_A \qquad (2.18)$$

The solution of eq.(2.18) was obtained and the absorption was expressed as:

$$N_A = k_L \frac{\sqrt{M}}{\tanh\sqrt{M}} \left(C_A^* - \frac{C_A^\circ}{\cosh(\sqrt{M})} \right) \qquad (2.19)$$

The parameter M is the Hatta number, which is the measure of chemical reaction rate to diffusion rate, within the liquid phase,i.e.

$$M = \frac{k_1 D_A}{k_L^2} \qquad (2.20)$$

Since the flux without chemical reaction can be expressed:

$$N_A = k_L (C_A^* - C_A^\circ) \qquad (2.21)$$

The enhancement factor of mass transfer due to chemical reaction depends on the order of the reaction as well as its rate . In this case :

$$E_A = \frac{k_L \sqrt{M}}{\tanh\sqrt{M}} \frac{1}{k_L (C_A^* - C_A^\circ)} \left(C_A^* - \frac{C_A^\circ}{\cosh\sqrt{M}} \right) \qquad (2.22)$$

In fast reaction $C_A^\circ = 0$, then Eq.(2.22), reduces:

$$E_A = \frac{\sqrt{M}}{\tanh\sqrt{M}} \qquad (2.23)$$

When M < 0.3 , the reaction is slow and the enhancement factor is nearly unity, ($E_A \approx 1$), and there is practically no reaction in the film. The change caused in mass transfer by the chemical reaction

materializes only for M > 0.3 . When $\sqrt{M} >> 1$, $E_A \rightarrow \sqrt{M}$.

When the penetration model is applied, the solution obtained is (Danckwerts, 1951):

$$N_A = k_L C_A^* \sqrt{M} \left(\left(1 + \frac{\pi}{8M}\right) erf\left(\frac{2\sqrt{M}}{\pi}\right) + \frac{e^{4M/\pi}}{2\sqrt{M}} \right) \qquad (2.24)$$

With

$$E_A = \sqrt{M} \left(\left(1 + \frac{\pi}{8M}\right) erf\left(\frac{2\sqrt{M}}{\pi}\right) + \frac{e^{4M/\pi}}{2\sqrt{M}} \right) \qquad (2.25)$$

The surface renewal gives (Danckwerts, 1970) :

$$N_A = k_L C_A^* \sqrt{1 + M} \qquad (2.26)$$

with

$$E_A = \sqrt{1 + M} \qquad (2.27)$$

Both penetration and surface renewal models, show that $E_A \rightarrow \sqrt{M}$, *when* $\sqrt{M} >> 1$. Therefore, based on first order kinetics, the three models provide practically the same results in predicting the effects of chemical reaction, even though each considers a different picture of interface mass transfer and hydrodynamics.

2.3.2 Irreversible Second Order Reaction :

The pioneering work on this case was done by Van Krevelen and Hoftijzer in (1948) based on the film model. When a dissolved gas undergoes a second order reaction with a dissolved reactant B, the

governing differential equations, with rate of reaction

$$C_A + z C_B = y C_p \tag{2.28}$$

Where

z,y are stoichiometric coefficients

$r = k_2 C_A C_B$ are:

$$D_A \frac{\delta^2 C_A}{\delta x^2} = \frac{\delta C_A}{\delta t} + k_2 C_A C_B \tag{2.29}$$

$$D_B \frac{\delta^2 C_B}{\delta x^2} = \frac{\delta C_B}{\delta t} + z k_2 C_A C_B \tag{2.30}$$

with boundary conditions:

$$\begin{aligned} t = 0, \quad x > 0; \quad & C_A = C_A^o, \quad C_B = C_B^o \\ t = 0, \quad x = 0; \quad & \frac{\delta C_B}{\delta x} = 0, \quad C_A = C_A^* \\ t > 0, \quad x = \infty; \quad & C_B = C_B^o, \quad C_A = C_A^o \end{aligned} \tag{2.16}$$

These equations were solved numerically by Pearson (1963), and by Brian et al. (1961). The number of variables can be condensed by forming dimensionless groups. The enhancement factor obtained is similar to that of Van Krevelen and Hoftijzer who used the film model and assumed the zero bulk concentration of the solute.

$$E = \frac{\sqrt{M \frac{E_i - E}{E_i - 1}}}{\tanh \sqrt{M \frac{E_i - E}{E_i - 1}}} \tag{2.31}$$

And, therefore;

$$E_i = 1 + \frac{C_B D_B}{z D_A C_A^*} \qquad (2.32)$$

where E_i is the enhancement factor for instantaneous reaction. Figure 2.12 depicts the concentration profile near the interface for the irreversible instantaneous reaction. Eq.(2.31) is represented graphically in Figure 2.13.

Where

Ha = is the Hatta number

$$N_2 = 1/z * \frac{D_B^* C_B}{D_A^* C_A^*}$$

Some limiting types of behaviour can be identified in Figure 2.13. When $\sqrt{M} << 1$ then E = 1; the reaction is very slow and has negligible effect. When $\sqrt{M} >> E_i$, $E = E_i$, this happens in fast reactions, if the contact time is long or the concentration of reactant is small. The reactant is depleted in the neighborhood of the surface to the extent that rate of reaction is determined by diffusion alone. Hikita and Asai (1964) have shown that an approximate solution for the enhancement factor when a second-order irreversible reaction occurs is

$$E = (\gamma + \frac{\pi}{8\gamma}) erf(\frac{2\gamma}{\sqrt{\pi}}) + 0.5\, e^{-4\gamma^2/\pi} \qquad (2.33)$$

where

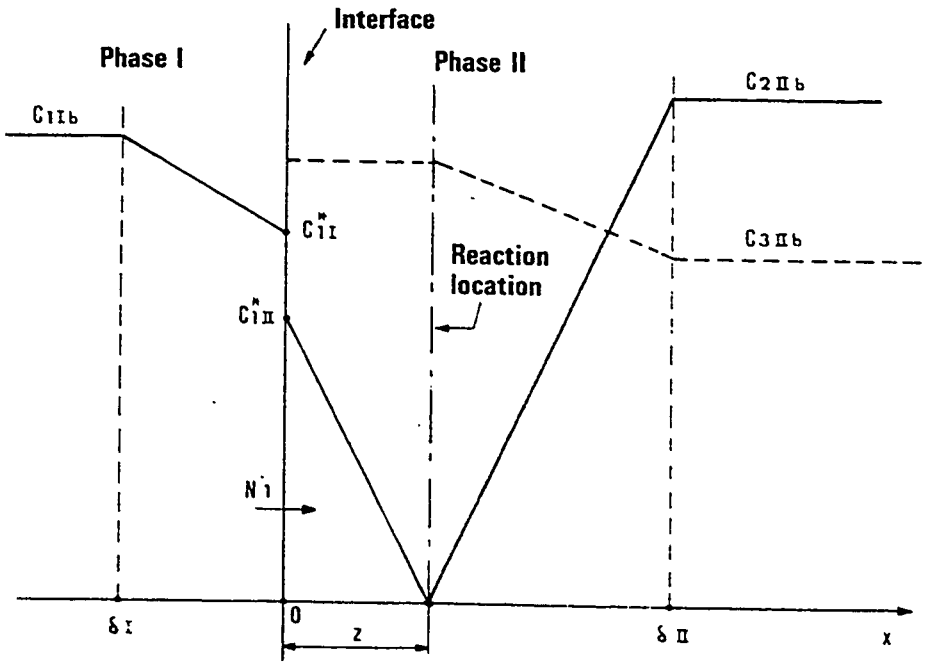

Figure 2.12 Concentration Profile Near the Interface for an Irreversible Instantaneous Reaction (Trambouze et al., 1988)

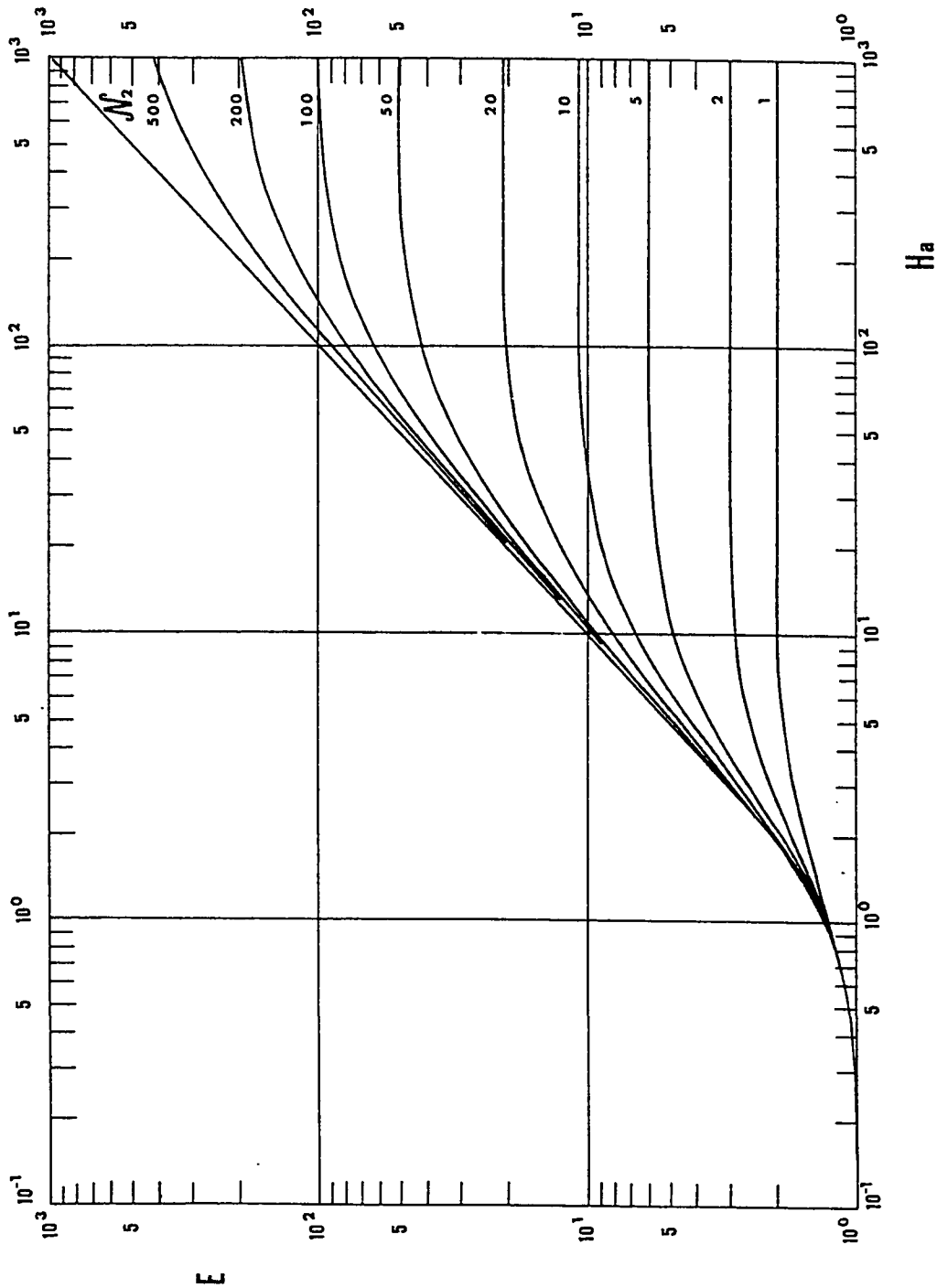

Figure 2.13 Enhancement Factor Versus Hatta Number and N_2 (Tramhouze et al., 1988)

$$\gamma = \sqrt{M \frac{E_i - E}{E_i - 1}} \qquad (2.34)$$

Decoursey (1974) developed an approximate solution using the surface renewal model:

$$E = \frac{M}{2(E_i - 1)} + \{\frac{M^2}{4(E_i - E)^2} + \frac{E_i M}{(E_i - 1)} + 1\}^{0.5} \qquad (2.35)$$

Matheron and Sandall (1978), solved the second order equation and have proposed that, for large values of E_i, E_i can be estimated as

$$E_i = \sqrt{\frac{D_A}{D_B}} + \frac{C_B}{z C_A^*} \sqrt{\frac{D_B}{D_A}} \qquad (2.36)$$

2.3.3 Instantaneous Reaction :

When the chemical reaction is extremely fast, molecules of the solute react with molecules of the reactant whenever both are present at the same point in the liquid. Chemical equilibrium therefore exists everywhere in the liquid phase and further increase of the reaction rate would have no effect . The rate of mass transfer is independent of chemical kinetics and depends only on factors affecting the physical mass transfer of reactants and reaction products. The enhancement factor can be very large in this regime, particularly when the concentration of reactant in the liquid is high.

According to Astarita et al.(1983), the enhancement factor for the instantaneous reaction regime can be on the order of (100-10000) and

above. The solution of the equations governing this case was given by Danckwerts (1950) and others, viz:

$$N_A = \frac{C_A^* \sqrt{\frac{D_A}{\pi t}}}{erf\left(\frac{\beta}{\sqrt{D_A}}\right)} \tag{2.37}$$

with

$$E_i = \frac{1}{erf\left(\frac{\beta}{\sqrt{D_A}}\right)} \tag{2.38}$$

and where

β is defined by

$$e^{\frac{\beta^2}{D_B}} erfc\left(\frac{\beta}{\sqrt{D_B}}\right) = \frac{B^\circ \sqrt{D_B}}{zC_A^* \sqrt{D_A}} e^{\frac{\beta^2}{D_A}} erf\left(\frac{\beta}{\sqrt{D_A}}\right) \tag{2.39}$$

The quantity E_i is the factor by which the reaction increases the amount absorbed in a given time, as compared to physical absorption.

2.4 Bubble Columns:

Bubble columns, where gas is dispersed through a relatively deep pool of liquid, are widely used in the chemical industry as absorbers, strippers and reactors. The gas phase which is discontinuous moves relative to the continuous phase. The continuous phase can be a liquid or a homogenous slurry.

Bubble columns can be multistage or single stage, continuous or batch and can be operated in two different modes: namely, concurrent (parallel) or counter-current (opposite) flow. Various types of bubble column reactors and their modifications are shown in Figure 2.14. Advantages of bubble columns outweigh their drawbacks, otherwise we wouldn't use them. The factors which favor the application of bubble columns compared to other multiphase contactors are:

1) Less maintenance is necessary due to the absence of moving parts (Mashelkar, 1970).
2) Simplicity of operation
3) Less floor space is occupied.
4) High heat transfer rates per unit volume of reactors can be achieved
5) High values of effective interfacial area and overall mass transfer coefficients can be obtained (Abraham and Sawant, 1990).
6) Liquid residence time can be varied easily
7) Ability to handle solids without any erosion or plugging problems
8) Slow reactions can be carried out due to high residence time

Considerable back mixing in both phases, bubble coalescence, and high pressure drop can be disadvantageous in some cases. Many modification, of bubble columns, such as bubble columns with downcomers, packed bubble columns with and without downcomer, and

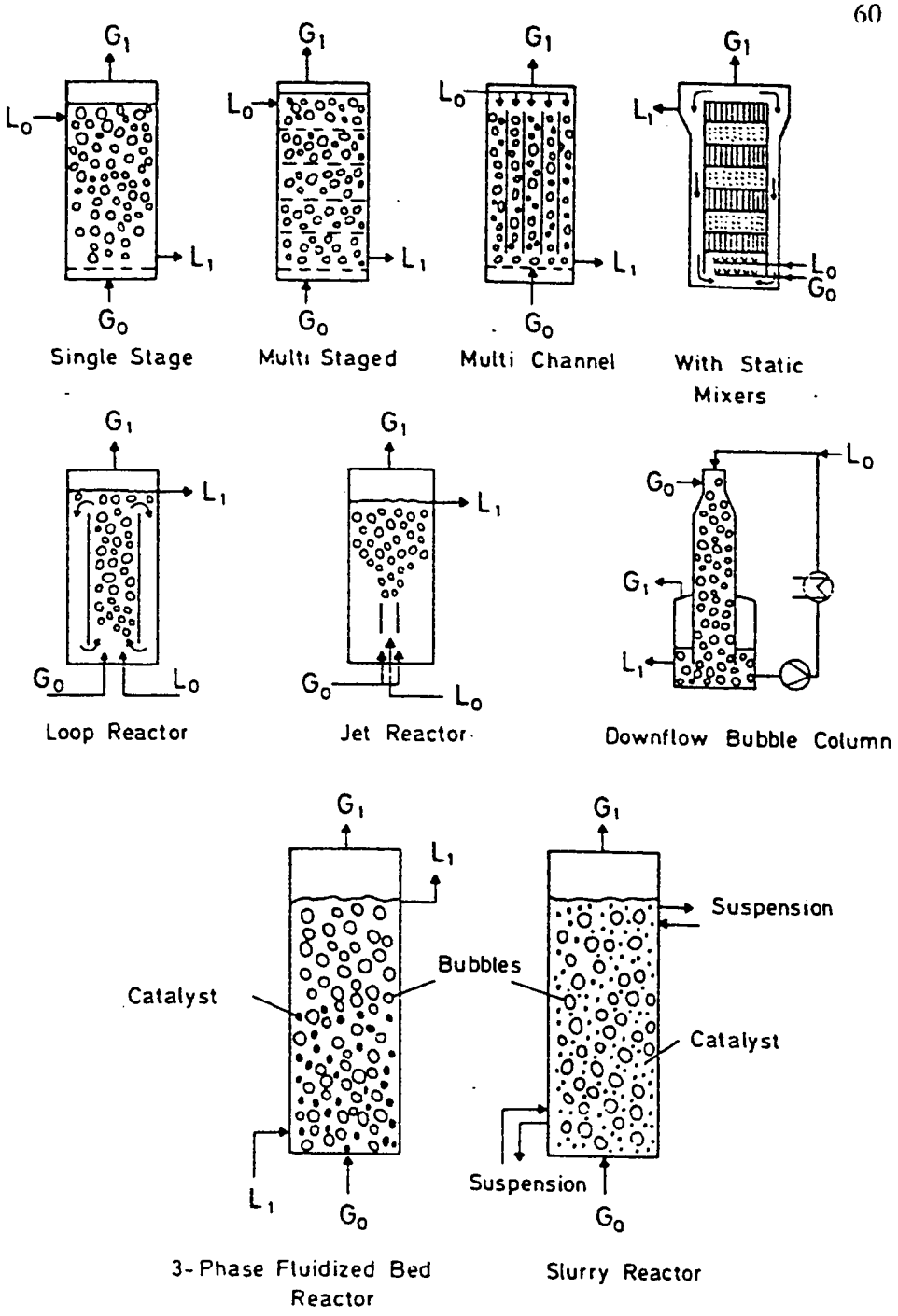

Figure: 2.14 Various Types of Bubble Column Reactors and Their Modifications.

sectionalised bubble columns, have been suggested to suit particular applications or certain specific processes.

Shah et al. (1978), have given a variety of examples of industrial importance where backmixing is undesirable. Loop reactors are used in the ICI pressure-cycle fermenter and its deep shaft modification (Hines, 1978). For certain reactions like air oxidation of inorganic and organic compounds, where gas component conversion is not necessary and low pressure drop is required, a horizontally sparged bubble column can be used (Joshi and Sharma, 1976). When complete gas phase conversion and hence long gas residence time is required, downflow bubble columns can be used (Herbrechtsmeier and Steiner, 1980). When low back mixing is required a sectionalised bubble column is preferred (Patil, 1983; Joshi, 1980; and Schuget et al., 1978).

2.4.1 Flow Regimes:

In bubble column reactors, flow regimes, bubble size distribution, and coalescence characteristics are important design parameters. The hydrodynamics, transport and mixing properties such as pressure drop, holdup of various phases, interfacial area between gas and liquid phases and interphase mass and heat transfer coefficients are greatly dependent on the prevailing flow regime. Many researchers such as (Govier Aziz, 1972; Wallis, 1969; Kawagoe et al., 1976; Miller, 1980; Lockett and Kirkpatrick, 1975; etc.) have suggested various criteria to classify the flow regimes.

The upward movement of bubble swarms is differentiated into three separate flow regimes. These regimes are encountered in order of increasing gas flow rate . Various flow regimes are schematically represented by Figure 2.15. The dependence of flow regime on column diameter and gas velocity can be approximated from Figure 2.16.

1) Quiescent Bubbling or Bubbly Flow : This regime is manifested by entirely uniformly sized bubbles with even radial distribution. If the superficial gas velocity is less than 5 cm./sec. (Fair, 1967), the bubbly flow regime occurs and the rise velocity of bubbles is in the interval 18-30 cm./sec. according to Levich (1962).

2) Churn Turbulent or Heterogeneous Regime : When the gas velocity increases, it comes to point where the homogenous gas- in-liquid dispersion cannot be maintained and therefore channelling and an unsteady flow pattern will prevail. The heterogeneous flow regime is characterized by broad bubbles moving with great rise velocities in the presence of small bubbles (Hills and Darton, 1976). The size of the large bubbles can increase up to a diameter of 15cm. They take the shape of spherical caps with a very flexible and mobile interface.

3) Slug Flow Regime: When very high gas flow rates are applied to small diameter column, large bubbles are formed and stabilized by the column wall . This leads to the formation of bubble slugs. These bubble slugs can be viewed in columns of diameters up to 15cm (Miller 1980).

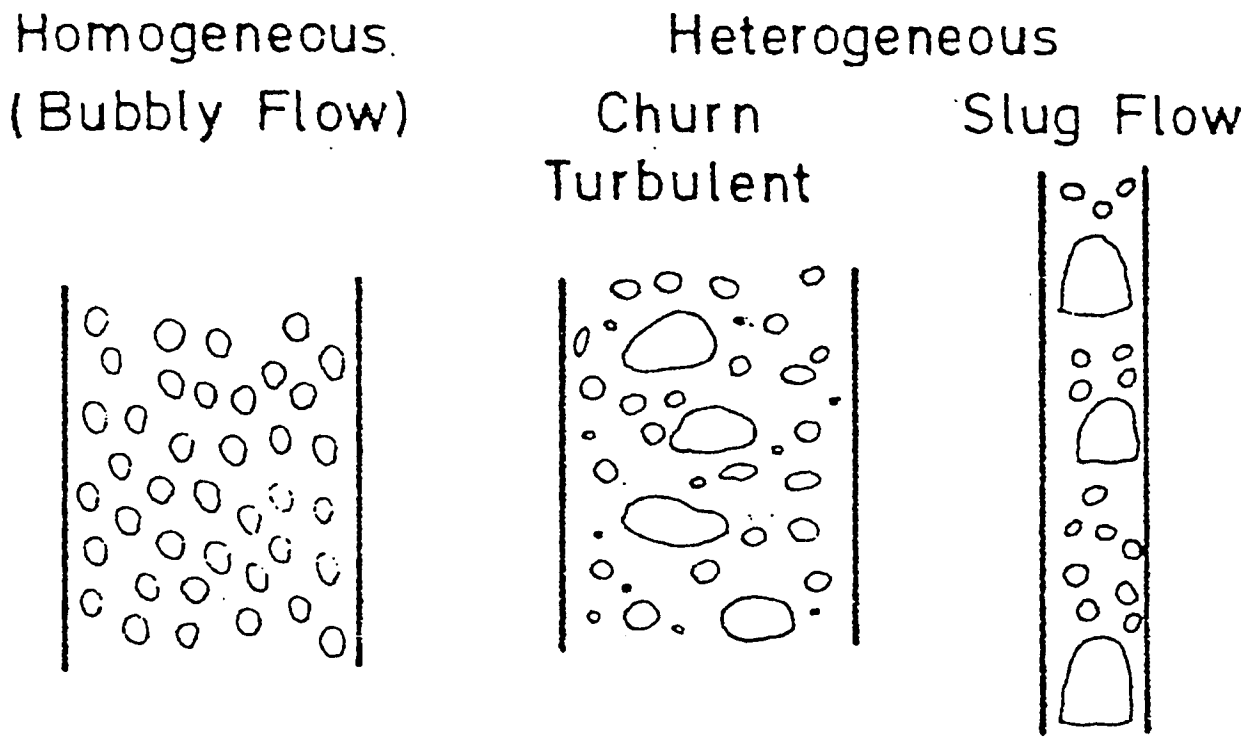

Figure 2.15 Schematic Representation of Flow Regimes Existing in Bubble Columns (Shah et al., 1982).

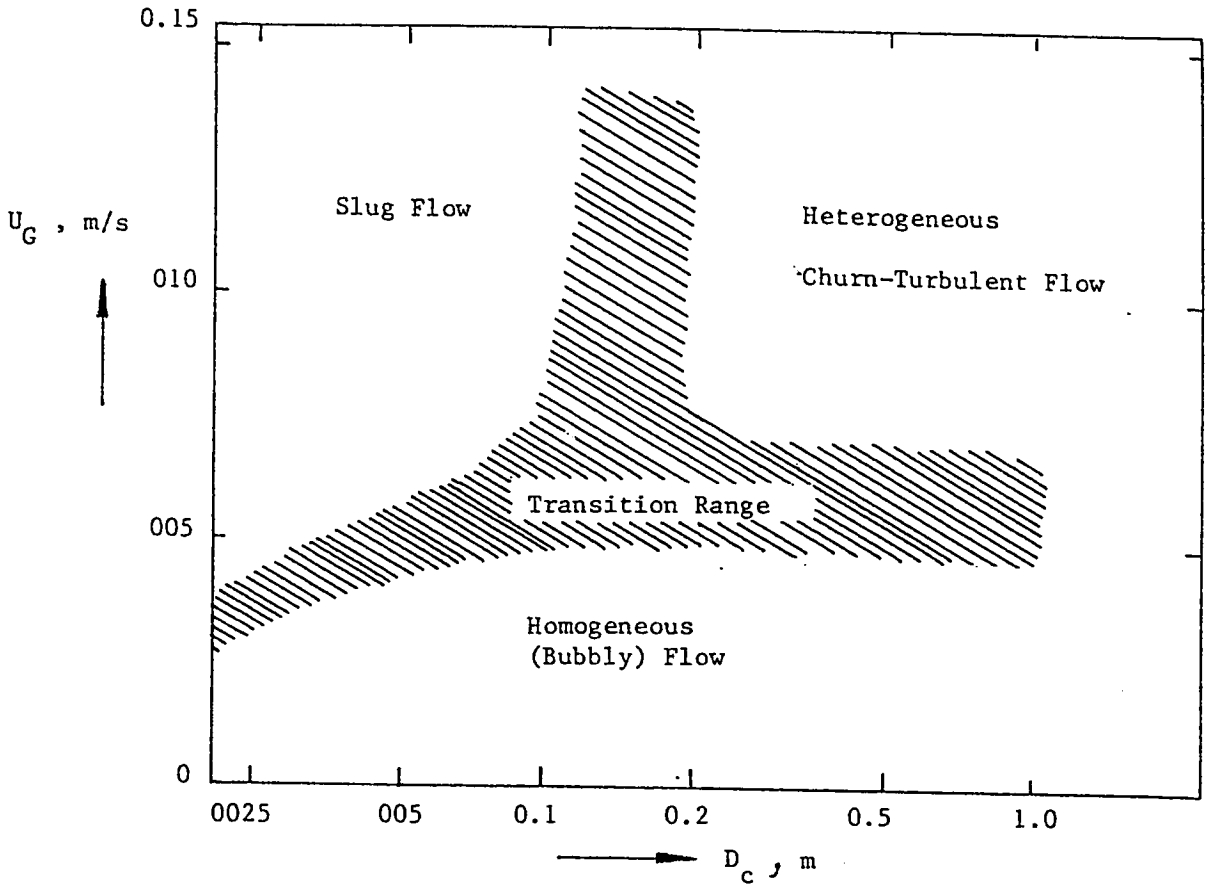

Figure 2.16 Dependence of Flow Regimes on Column Diameter and Gas Velocity (Shah et al., 1982).

The transition between the various flow regimes are affected by the type of sparger used, the liquid velocity and the physico-chemical properties of the liquid as reported by (Shah et al., 1982). For instance, slug flow can occur at low superficial gas velocity for highly viscous fluids (Schumpe, 1981). Anderson and Quinn (1970) have found that small traces of contaminants in the tap water can alter the transition between flow regimes.

Flow regimes have been determined by researchers either with the help of conductance probes or by visual observation, (Javdani et al., 1977; Oshinowo and Charles, 1974; and Barnea et al., 1980). The knowledge of the transition between the regimes is quite useful because the achievable conversion depends strongly on the flow regime (Deckwer and Schumpe, 1979; and Schumpe et al., 1979). That the heterogeneous regime is most commonly encountered in industrial bubble columns was suggested by Bach and Pilhofer (1978).

2.4.2 Hydrodynamics of Bubble Columns:

Gas holdup is one of the most important parameters characterizing the hydrodynamics of bubble columns. It can be defined as the percentage by volume of the gas in the two- or three-phase mixture in the column. The gas holdup has two main applications. On one hand, in the two phase systems, it gives the volume fraction of the phases present in the reactor and hence their residence time . On the other hand, the gas holdup in conjunction with the knowledge of mean

bubble diameter, allows the determination of interfacial area and thus can lead to estimation of the mass transfer rates between the gas and the liquid phases.

The gas holdup in bubbles column is closely related to the bubble rise velocity and gas superficial velocity. For low superficial gas velocities (homogenous flow), the gas holdup can be computed from

$$F = \frac{V_s}{V_{bs}} \tag{2.40}$$

Where

V_s = superficial velocity of the gas

V_{bs} = bubble rise velocity

It appears that it is necessary to know the bubble rise velocity V_{bs} if the gas holdup to be calculated. The bubble rise velocity is mainly dependent on bubble diameter. The gas holdup characteristics of bubble columns have been extensively studied, covering a wide range of column diameter, liquid height, and superficial gas and liquid velocity. A survey of published information indicated that there is a large variation of gas holdup values. These differences may be due to the following factors:

i) Different types of gas distributors and column sizes. It has been reported that smaller diameter columns (D < 7 to 15 cm.) show higher gas holdup and for diameters (D > 7 to 15 cm.) gas

holdup is not significantly affected by the column size at any specified superficial gas velocity (Miyauchi and Shyu, 1970; Katoetal., 1973; Akita and Yoshida, 1973; Hills, 1974; and Hikita et al., 1980).

ii) Surface active agents (adventitious impurities, maybe even the quality of water used by different investigators).

iii) The circulation of liquid induced by bubble cloud may have a significant effect on the gas holdup values.

The gas holdup depends mainly on superficial gas velocity, besides the physical properties of the liquid. The dependence of the gas holdup on the gas velocity is generally of the form :

$$E_g \alpha V_s^n \qquad (2.41)$$

The value of n depends on follow regime. For homogenous flow regime value of n varies from 0.7 to 1.2 (Reith et al. , 1980; Botton et al., 1978; Deckwer et al., 1980a). In the churn turbulent or transition flow the effect of V_s is less pronounced and the exponent n takes values from 0.4 to 0.7.

A large number of correlations for gas holdup have been proposed in the literature, however, the wide scatter in the reported data does not permit a single correlation. The presence of solids does not affect the gas holdup significantly (Ying et al, 1980a). The gas holdup and interfacial area have been observed to be proportional to the superficial velocity of the gas and independent of that of liquid (Gopal and

Sharma, 1983). The have been conflicting conclusion on effects of the fractional gas holdup. Bhaga et al. (1971) and Koetsier et al. (1976) concluded, after their study, that an increase in the gas density resulted in increasing gas holdup, while Akita and Yoshida (1973) and Shulman and Molstad (1950) found no effect of the nature of the gas.

Measurement Technique of Gas Holdup. Different researchers have applied different techniques for measuring the gas holdup:

i) Manometric Method

The gas holdup can be determined by measuring the static pressure at several points in the column. The value of the gas holdup is determined from the equation

$$E_g = 1 + (gc/lg)\, dp/dz \qquad (2.42)$$

where gc is the gravitational conversion factor and dp/dz is the slope of the curve representing the axial distribution of the static pressure in the column.

ii) Dynamic Gas Disengagement Method

The technique, first introduced by Sriram and Mann (1977), requires an accurate measurement of the rate at which the level of the gas-liquid dispersion drops once gas flow to the bubble column is shut off. The measured disengagement profile is then

used to estimate the holdup structure that existed in the dispersion prior to flow interruption. A videocamera and VCR unit are required to record the drop in the liquid level during the disengagement process. The dynamic gas disengagement technique has some limitations resulting from the assumption made, deficiencies in the data collection and analysis procedure, and from its dependence on corrections relating terminal bubble rise velocity to bubble size (Schumpe and Grund, 1989; Snehal et at., 1989).

iii). Direct Measurement of the Height.

The gas holdup can be obtained by directly measuring the height of dispersion or aerated liquid and that of clear liquid after stopping the gas flow (Yoshida and Akita, 1965; Abraham and Sawant, 1990). The average gas holdup is given by

$$E_g = \frac{H_d - H_c}{H_d} \qquad (2.43)$$

Since it is rather difficult to read distinctly the level of the dispersed liquid, the value of the gas holdup obtained thus probably involve a maximum error of about 10%. The gas holdup can be also determined directly by means of a liquid level indicator connected to the bubble. The liquid level in this indicator is found to be equal to the non-gassed dispersion height present in the column (Oyevaar et al., 1991).

Volumetric Mass Transfer Coefficient. In the selection and design of gas/liquid reactors, the volumetric mass transfer coefficient ($K_l a$) and

its dependence on the process conditions within the reactor are of paramount importance since mass transfer of a gaseous reactant into a liquid phase always constitutes the first step of any two-phase reaction. In many chemical processes mass transfer is the rate determining step. Therefore, the conversion depends only on the volumetric mass transfer coefficient and the driving concentration gradient of the reaction being observed.

The determination of the mass transfer coefficient is based either on physical or chemical methods. Both types of method need the setting-up of a concentration gradient for transferring a component from the interface into the bulk of liquid. In the physical methods the concentration gradient is produced either by stepwise variation of the gas phase concentration (dynamic method) or by continuous feeding into the reactor of liquid which has been partially depleted of the observed components (steady state method).

Physical methods can be employed for any material systems, however, very often the conditions necessary for the application of these methods are not satisfied. For example, the dynamic method requires the knowledge of the dynamic behavior of the gas and of the measuring probe (Keitel and Onken, 1981; Dunn and Einsele, 1975), while for the steady state method additional desorbing vessel must be provided for a continuous regeneration of the enrichment liquid.

In chemical methods, the gaseous component, being transferred into the liquid phase, is consumed by a chemical reaction. As long as

the chemical reaction is not accelerating, the rate of physical mass transfer, the volumetric mass transfer coefficient can be evaluated from the consumption of the reactants, when the driving concentration gradient is known.

Commonly employed chemical reactions are the oxidations of sodium sulfite to sulfate (Kato et al. 1973; Bottom et al., 1980), and the reaction of the carbon dioxide with alkali hydroxides (Sahay and Sharma, 1990; Abraham and Sawat, 1990) or aqueous ethonolamine (Danckwerts, 1979) or oxidation of hydrozine (Weiland et al., 1981).

Chemical methods have mainly being used for the determination of mass transfer performance of industrial gas/liquid reactors, however, the kinetics of the reactions involved have not yet been fully clarified. The main drawbacks of these methods arises from the fact that the physical properties of the liquid phase are entirely dependent on the reaction system. Most of the systems strongly inhibit coalescence and, as a result, depending on the type of reactor and gas sparger. The values of $K_l a$ determined using these methods are 1.5 to 7 times bigger than those in coalescing systems under the same conditions (Zlokarnik, 1979). Other chemical systems often used include air sodium diothionite. The values of volumetric mass transfer coefficient, $K_l a$, measured using air sodium diothionoite system in a continuous mode operation is higher then that obtained by using lean CO_2 buffer system in semi batch mode operation (Gopal and Sharma, 1983).

The mode of operation has very little effect on the values of $K_l a$ (Sharma and Mashelkar, 1968). Different systems will exhibit different dispersion characteristics. The literature survey reveals that different systems give different values of $K_l a$ (Kastenek, 1977), and values of $K_l a$ are not influenced by type and design of the sparging device, particularly, those which do not promote or do not prevent coalescence.

Akita and Yoshida (1974) correlation can be recommended as a conservative estimate applicable for less effective spargers. For highly viscous and non newtonian media, the correlation of Deckwer et al. (1981d) is applicable if slug flow prevails.

Interfacial Area. One of the objectives of the study involves the measurement of the interfacial area between the gas and the brine during the absorption process, which takes place in the bubble column. In most gas-liquid contacting equipment, the interfacial area available for mass and heat transfer is usually indeterminate.

The magnitude of the gas-liquid interfacial area is a considerable design criterion for gas-liquid reactors. This is true, in particular, if the chemical reaction in the liquid phase is fast in comparison with the rate of mass transfer. The influence of the interfacial area is less pronounced in the slow chemical reaction regime of absorption-reaction theory (Astarita, 1967; Danckwerts, 1970). The lack of knowledge of this important variable limits the analysis of many

processes. Among the common interfacial area determination methods include:

A) The techniques of light transmittance.

The interfacial area could be determined directly by using light transmission techniques (McDonough; Scott, 1958; Vermeulene et al., 1955) These techniques are available to determine bubble sizes.

1) Photographic techniques (Van Dierendonck et al., 1968; Towel et al., 1965), are used widely because of simplicity (Kobel et al., 1960; Akita and Yoshida, 1974; Schugerl et al., 1977; Burckhart and Deckwer, 1975; Quiker and Deckwer, 1981a). The Sauter mean dispersed phase diameter d_{ps} is measured photographically. Disadvantages of this technique are that only local values of the interfacial area are obtained, that it is time consuming and the dispersion may be disturbed by the sample fittings.

2) Other techniques involve light scattering, light reflection (Calderbank et al., 1960) and depolarization (Rodionow et al., 1969). In the light scattering technique a parallel beam of light with an intensity I_o is sent through the dispersion over a distance l and the remaining light intensity I is measured. The disadvantages of this technique are that only local values of interfacial area are obtained, that the measurement fittings may disturb the dispersion and that the method is limited to values

of interfacial area up to 600 m^{1} while values up to 2000 m^{1} are not uncommon in industrial reactors. The latter disadvantage can be overcome by modifications introduced by Landau et al. (1977).

3) In the past two decades, various optical and electrical probes have been developed to determine the bubble sizes (Pihofer and Miller, 1972, Burgess and Calderbank, 1975, Seizawa, et al.; 1975, Calderbank and Pereira, 1977, Koide, et al.; 1979). In past decade, a new dynamic bubble disengagement technique has been proposed to find out the bubble distribution (Sriram and Mann, 1977; Vermeer and Krishna, 1981). Though the original bubble size distributions obtained from various techniques differ markedly, the volume-to-surface mean bubble diameters d_{vs} (often called as Sauter mean diameter) evaluated consequently differ only slightly (Yamashita, et al.; 1979). For a non-reaction phase consisting of N spherical particles of different diameters d:

$$a = N\Pi\frac{d^2}{V} \tag{2.44}$$

and the volume of the dispersed phase is

$$V_g V = N\frac{\pi}{6}d^3 \tag{2.45}$$

Hence the specific contact area is

$$a = 6 \frac{E_g}{d_{vs}} \qquad (2.46)$$

where the sauter mean diameter of the particles, d_{vs} becomes:

$$d_{vs} = \frac{\sum d^3}{\sum d^2} \qquad (2.47)$$

This implies that a is inversely proportional to the average size of the dispersed particles. However, it should be pointed out that photographic, light scattering, electrical, and optical probe techniques give reliable results only in the homogeneous or bubbly flow regime; that is to say they are restricted to systems in which the dispersed phase is present as bubbles or drops. They fail in slug flow or in gas-liquid packed columns.

B) The Chemical Absorption Technique (Richard, et al; 1964, Danckwerts and Gillham, 1966).

This technique has been introduced by Westerterp (1963) and Yoshida and Yoshiharu (1963) and has found a wide application (Linek and Vacek, 1981, Sharma and Mashelkar, 1968, Linek, 1969) since then. The fundamental idea of this method is quite simple.

The absorption rates per unit interfacial area can be predicted from the theory of gas absorption accompanied by a chemical reaction if the kinetics of the reaction are known.

Consequently, interfacial areas can be computed from measurements of total absorption rates. When a component is transferred from non-reacting phase into reacting phase like *Gas→Liquid* in which it reacts, and is therefore chemically enhanced, according to

$$J_A a = k_L \varphi a C_{Ai} \tag{2.48}$$

Then the product $k_L\varphi$ is a function only of kinetics and is independent of k_L. The dimensionless parameter φ is defined as

$$\varphi = \delta\sqrt{\frac{k}{D_A}} \tag{2.49}$$

The physical meaning is that φ^2 equals to the ratio of the maximum conversion rate of A in the film per unit area interface and the maximum diffusional transport through the film in case of absence of reaction. Under these conditions a is straight forwardly obtainable from the observed conversion rate and kinetics, for instance, for a mixed tank reactor.

$$a = \frac{J_A a V_r}{k_L \varphi C_{Ai} V_r} = -\frac{\Phi_A}{k_L \varphi C_{Ai} V_r} \tag{2.50}$$

For kinetics of the type: A(gas) + zB(liq.) = Product, with rate

$$r = k_2 C_A C_B \text{ and } k_L\varphi = \sqrt{k_2 D_A C_B} \tag{2.51}$$

and we have to write :

$$a = -\frac{\Phi_A}{\sqrt{k_2 D_A \overline{C}_B} C_{Ai} V_r} \qquad (2.52)$$

In practice many complications may occur :

a) The reaction influences the area (Joosten and Danckwerts, 1973).

b) Gas phase resistance is not negligible .

c) The condition $2 < \varphi << E_{A\infty}$ is not fulfilled in a part of the reactor. Commonly employed chemical reactions are the absorption of CO_2 in hydroxide solution (Langlois, et al; 1954) and the absorption of oxygen in aqueous sodium sulfite solutions catalyzed by Co^{2+} (Reith and Beck, 1973). The latter system is sensitive to sulfite kinetics, the cobalt and the water quality while, possibly, an induction period before the reaction starts cannot be excluded (Sharma and Danckwerts, 1970).

The suitability of many of great number of gas-liquid reactions as model reactions has been discussed in length (Sridhara and Sharma, 1976). Table 2.9 gives a list of some convenient reaction systems . The interfacial area increases with gas rate as result of increase of the gas holdup (Gopal and Sharma, 1983). The superficial liquid velocity and the height to diameter ratio do not influence the values of interfacial areas (Sharma and Mashelkar, 1968; Towell et al., 1968). The sparger design is not of critical importance provided multinozzle gas spargers are used in in large diameter columns (Gopal

and Sharma, 1983).

Table 2.9 Expression Rate of Absorption for Various Systems

No.	System	m Order with respect to absorbent	n Order with respect to solute	Pseudo nth-order condition	Expression for rate of absorption	Expression for the effective interfacial area
1	1 (a) $NaOH-CO_2$ 1 (b) $KOH-CO_2$ 1 (c) $LiOH-CO_2$ 1 (d) $Ba(OH)_2-CO_2$ 1 (e) MEA-CO_2 1 (f) DEA-CO_2 1 (g) Na_2S-CO_2	1	1	$\frac{\sqrt{(D_L k_2[B])}}{k_L} < \frac{[B]}{2C^*}$	$R = C^*\sqrt{(D_L k_2[B])}$	$\frac{1}{K_G a} = \frac{1}{k_g a} + \frac{1}{(C^*\sqrt{(D_L k_2[B]_{av})}\, a}$
2	2 (a) $CuCl-O_2$ 2 (b) $CuCl-O_2$ (Neutral)	2	1	$\frac{\sqrt{(D_L k_2[B]^2)}}{k_L} < \frac{[B]}{2C^*}$	$R = C^*\sqrt{(D_L k_2[B]^2)}$	$a = \frac{\ln\left(\frac{[B]_i}{[B]_f}\right)}{4C^* l\sqrt{(D_L k_2)}}$
					$R = C^*\sqrt{(D_L k_2[B]^2 + k_L^2)}$	$a = \frac{\ln\left(\frac{[B]_i + \sqrt{([B]_i^2 + k_L^2/D_L k)}}{[B]_f + \sqrt{([B]_f^2 + k_L^2/D_L k)}}\right)}{4C^* l\sqrt{(Dk_2)}}$
3	Dithionite-O_2	1	0	$\frac{\sqrt{(2D_L k_1[B]/C^*)}}{k_L} < \frac{[B]}{2C^*}$	$R = \sqrt{(2C^* D_L k_1[B])}$	$a = \frac{2(\sqrt{([B]_i)} - \sqrt{([B]_f)})}{l\sqrt{(2C^* D_L k_1)}}$
4	Dithionite-O_2	2	0	$\frac{\sqrt{(2D_L k_2[B])^2/C^*)}}{k_L} < \frac{[B]}{2C^*}$	$R = \sqrt{(2C^* D_L k_2[B]^2)}$	$a = \frac{\ln\left(\frac{[B]_i}{[B]_f}\right)}{l\sqrt{(2C^* D_L k_2)}}$

Chapter III

EXPERIMENTAL APPARATUS AND PROCEDURE

3.1 Introduction

There are various types of laboratory devices that can be used for gas-liquid systems. However, the choice of one over the other is usually dependent on the nature of the gas and liquid, the hydrodynamic conditions such as physical properties of the liquid, flow rate of the fluid, geometry of packing and partly by the physical properties of the system such as diffusivity of dissolved gas and of reactant in solution, kinetics of reactions occurring in solution, and solubility of the gas, etc.

In the classical Solvay process, a bubble tray was used for carbonation of the ammoniated brine solution. The use of packed columns is not in any way possible due to precipitation of solid products that will definitely stick on the packing materials. This will bring about the choking of the column and the removal of attached solids on the packing is tedious and will require extra effort. The use of bubble column seems an excellent option. It combines the desired properties such as high holding time and easy handling of solid precipitates. Therefore, bubble columns are

more flexible and provide better contact between the gas and the liquid.

In this chapter, the apparatus, material used and experimental procedure are described. The chapter outlines in detail, the test methods implemented to achieve the objective of this investigation, and it consists of the following sections.

3.2 Description of the apparatus

3.3 Gas feed system

3.4 Thermocouples and pH meter

3.5 Gas flow meter and Liquid level indicator

3.6 Atomic absorption spectrometer

3.7 Total organic carbon analyzer

3.8 Experimental technique

3.9 Chemicals

Different types of experiments were performed. The parameters investigated and their ranges and levels are tabulated.

3.2 Description of the Apparatus :

An overall schematic flow diagram of the experimental set-up built for this study is shown in Figure 3.1. The set-up is composed of:

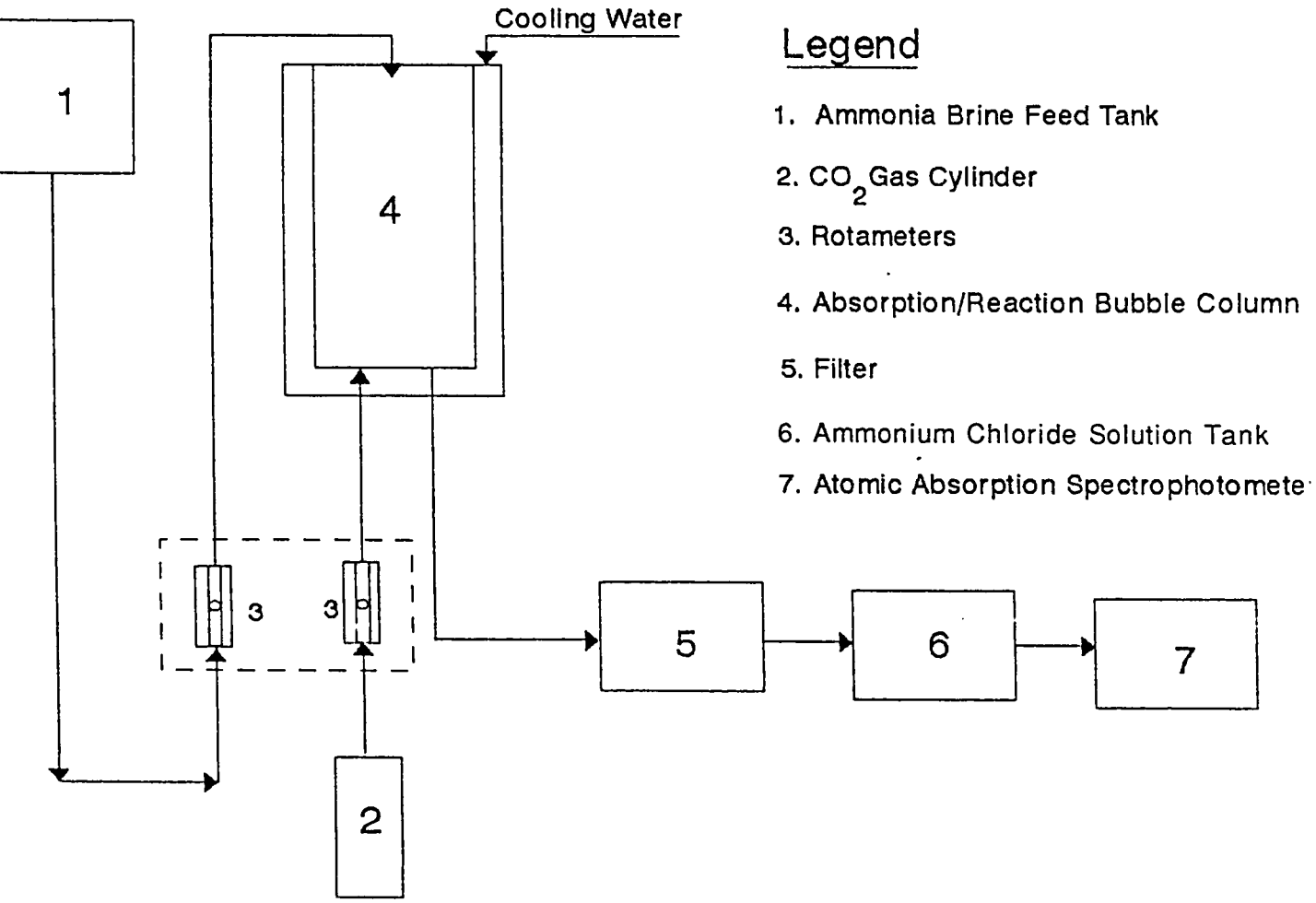

Figure 3.1 Schematic Diagram of Experimental Set-up

1) Ammonia brine feed tank

2) Gas supply system

3) Absorption/ Reaction bubble column

4) Filter

5) Ammonium chloride solution tank

6) Atomic absorption spectrometer

7) Temperature control system

8) Rotameters

3.2.1 Batch Gas Bubbler

A sketch of a batch gas bubbler is given in Figure 3.2. It consists of absorption glass vessel of about 40 cm high and an inside diameter of 5 cm, fitted with socket, inlet cone and a long inlet tube which passes almost to the bottom of absorption vessel. The carbon dioxide gas is fed to the solution through the inlet tube. Here the gas flows in the form of bubbles, the flow rate of the gas and the bubbles are sufficient to mix the solution thoroughly.

A volume of 100 ml of solution is always placed in the gas bubbler. To maintain the temperature of the solution in the gas bubbler, the set-up is placed in a water bath cylinder. The cylinder is also made of glass which serves as a jacket water. This laboratory appa-

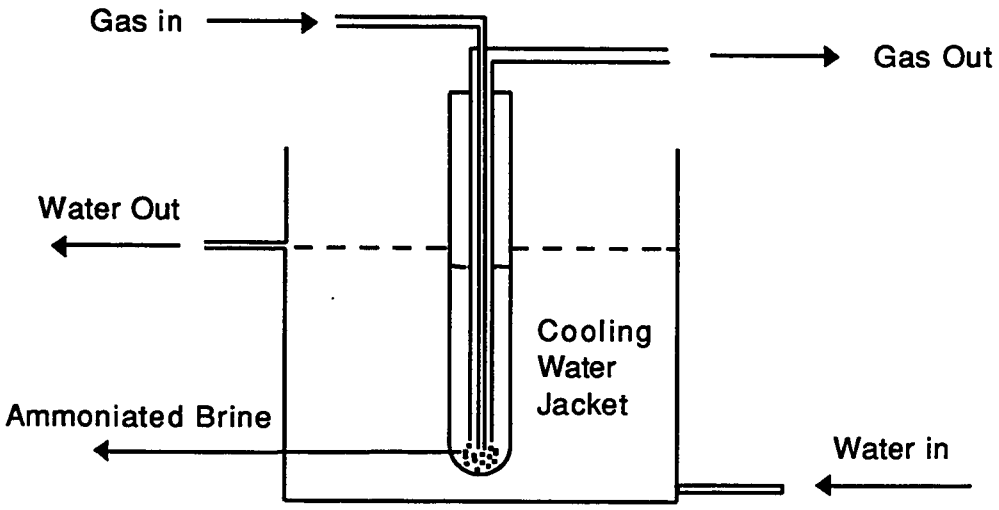

Figure 3.2. Sketch of the Batch Gas Bubbler.

ratus is operated continuously with respect to the carbon dioxide and in a batch mode with respect to the liquid. The unabsorbed gas is vented to the atmosphere. A flow rate of 2-3 l/min. was used in this operation.

3.2.2 Bubble Column (I)

A sketch of bubble column (I) is shown in Figure 3.3. The column is made of transparent plexiglass. The length of the column is 180 cm while the diameter is 8.9 cm. A liquid level indicator is attached to the column. Two orifices of 2.5 mm each are fitted at the base of the column. The carbon dioxide gas enters the column through these orifices. The operations of gas holdup carried out in this column, include deionized water and aqueous solution of various concentrations of NaCl and Sodium Sulfite.

The results of these experiments and some of their physical properties are given in appendix B. The effect of gas type and height to diameter ratio were determined. The constant values of gas holdup over the height of 30 cm have brought forward to the modification of the column height to reduce the solution volume.

3.2.3 Bubble Column (II)

A sketch of bubble column (II) is shown in Figure 3.4. This column is also made of transparent plexiglass cylinder. The length of the column is 40 cm while the diameter is 8.9 cm and also is operated in a batch wise mode. Two orifices of 2.5 mm each are fitted at the

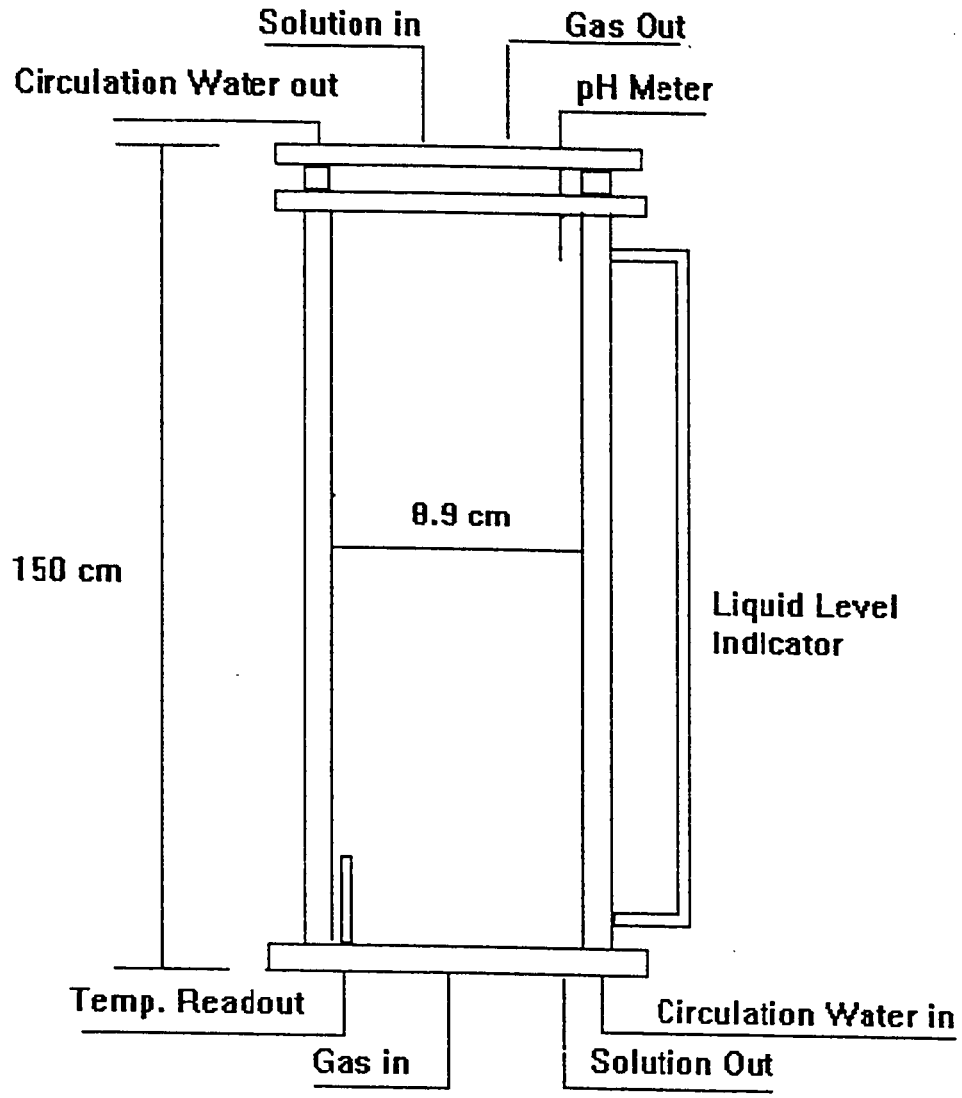

Figure: 3.3 Sketch of Bubble (I)

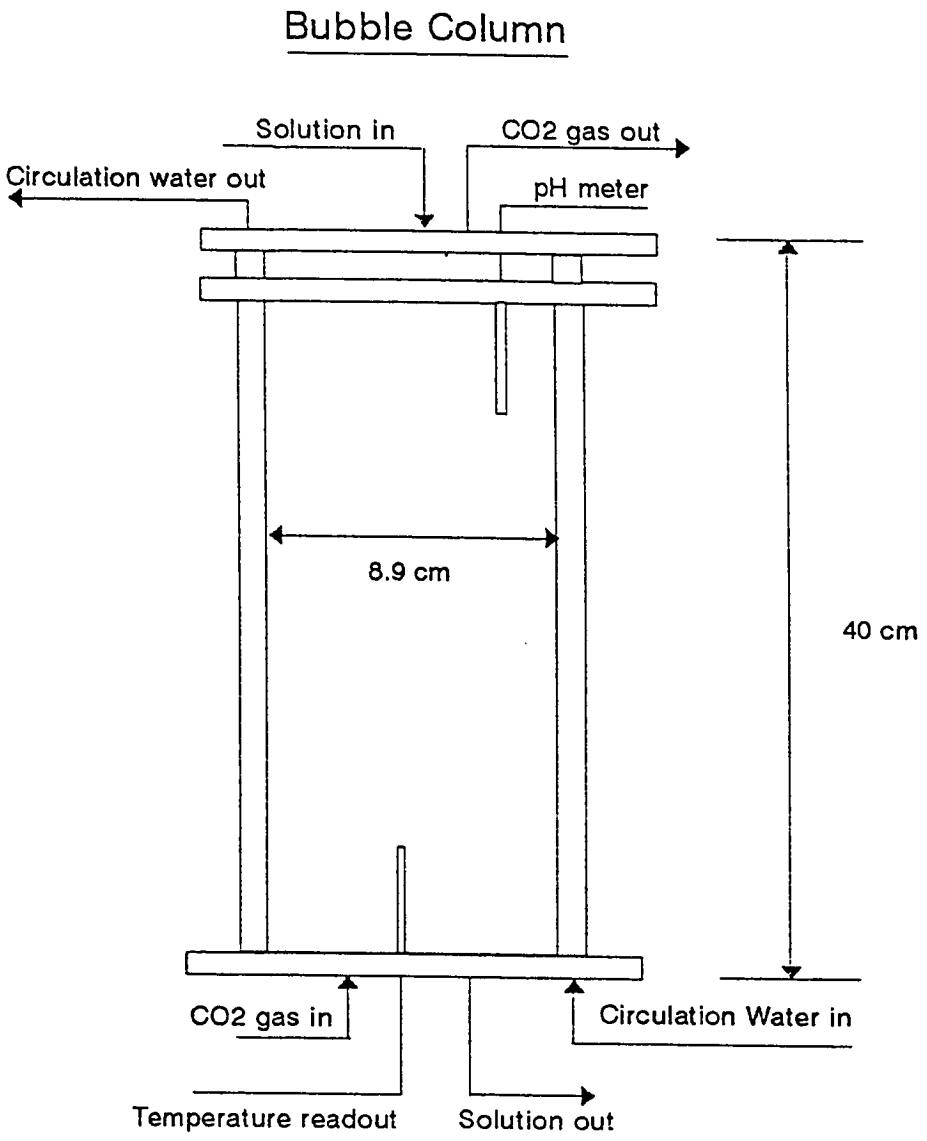

Figure: 3.4 Sketch of Bubble (II)

base of the column through the gas enters. The column (II) is similar to bubble column (I) described in previous paragraph except that column (II) is shorter and has additional design features, such as the temperature control and readout system and pH measurement devices.

3.3 Gas Feed System

The gas feed system consists of pure oxygen and pure carbon dioxide. The oxygen gas was used for the determination of the hydrodynamic parameters of the bubble column, while the carbon dioxide gas was used for the carbonation of the ammoniated brine. The cylinders are equipped with a pressure regulator and tygon tubing leading to the experimental set-up. The desired flow rate is adjusted by passing the gas through gas rotameters. The feed gas enters the solution via inlet glass tube in the case of batch gas bubbler. However, in the case of the bubble columns, the gas enters the solution via two orifices situated at the bottom of the columns.

3.4 Thermocouples and pH meter

A thermocouple of type K is inserted at the bottom of the bubble columns in order to measure the temperature of the solution at any instant. The leading wire is then connected to Omega type K readout, Model No. 650. The thermocouple is calibrated against a mercury thermometer. A digital pH meter, Fisher Accumet pH Meter, Model No. 805 Mp is used. The pH meter was initially calibrated before use

by means of standard buffer solutions.

3.5 Gas Flow Meter and Liquid Level Indicator

A gas flow meter is installed in all experimental assembly. The rotameters are calibrated before the experiment. The liquid level indicator is installed in bubble column (I). It is made of glass vessel of cylindrical shape and of a length of 100 cm and inside diameter of 0.8 cm. It is a common practice to measure the gas hold-up by comparing the dispersion height and the height when the gas flow is stopped. The liquid level indicator provides the height of clear liquid since the turbulence and mixing of the liquid due to the gas do not affect the liquid in it.

3.6 Atomic Absorption Spectrophotometer (AAS)

For accurate elemental analysis, Atomic Absorption Spectrophotometer (AAS) is indispensable. In this study, AAS model 3100 Perkin Elmer is used. The sketch of the unit and its accessories (powerful PC based data system with printer and automatic sampler model AS-90 Perkin Elmer) are given in Figure 3.5.

The main features of AAS unit include automatic selection of optimum operational parameters, large color video display which presents all the operational parameter and result of the analysis, wide variety of data processing functions and complete safety. The technique is based on the radiant absorption of atomic vapour. The source for generating the atomic vapour (gaseous free atoms for ions) from a

Figure 3.5 Model 3100 Atomic Absorption Spectrophotometer

Typical Installation

sample is a flame. The flame used was air-acetylene. The steps involved in the transformation of analyte atoms from solution to atomic species in the flame, are solution transport, nebulization, aerosol transport, desolvation, vaporization, equilibrium of vaporized species and atomic absorption measurement.

The analytical application of AAS generally involves obtaining the samples in an appropriate solution for measurement and calibrating the instrument properly. Calibration of the instrument in this study was performed by preparing standard solutions over the concentration range of interest and measuring the absorption of these under the same conditions at sample measurement. Sodium ion determination was performed by diluting the sample with deionized water and aspirating directly.

3.7 The Total Organic Carbon Analyzer

The Total Organic Carbon (TOC) analyzer is commonly used to quantify the carbon dioxide absorbed in a solution at any time. A sketch of the instrument is shown in Figure 3.6. The unit model is 915 TOC and provides rapid analysis of microsamples of aqueous solution for determinations. The analysis is based on conversion of sample of carbon into carbon dioxide for measurement by a non-dispersive infra-red analyzer.

The basic model 915 consists of two interconnected units: a sample-inject/furnace Module and a model 215B infrared analyzer, for a

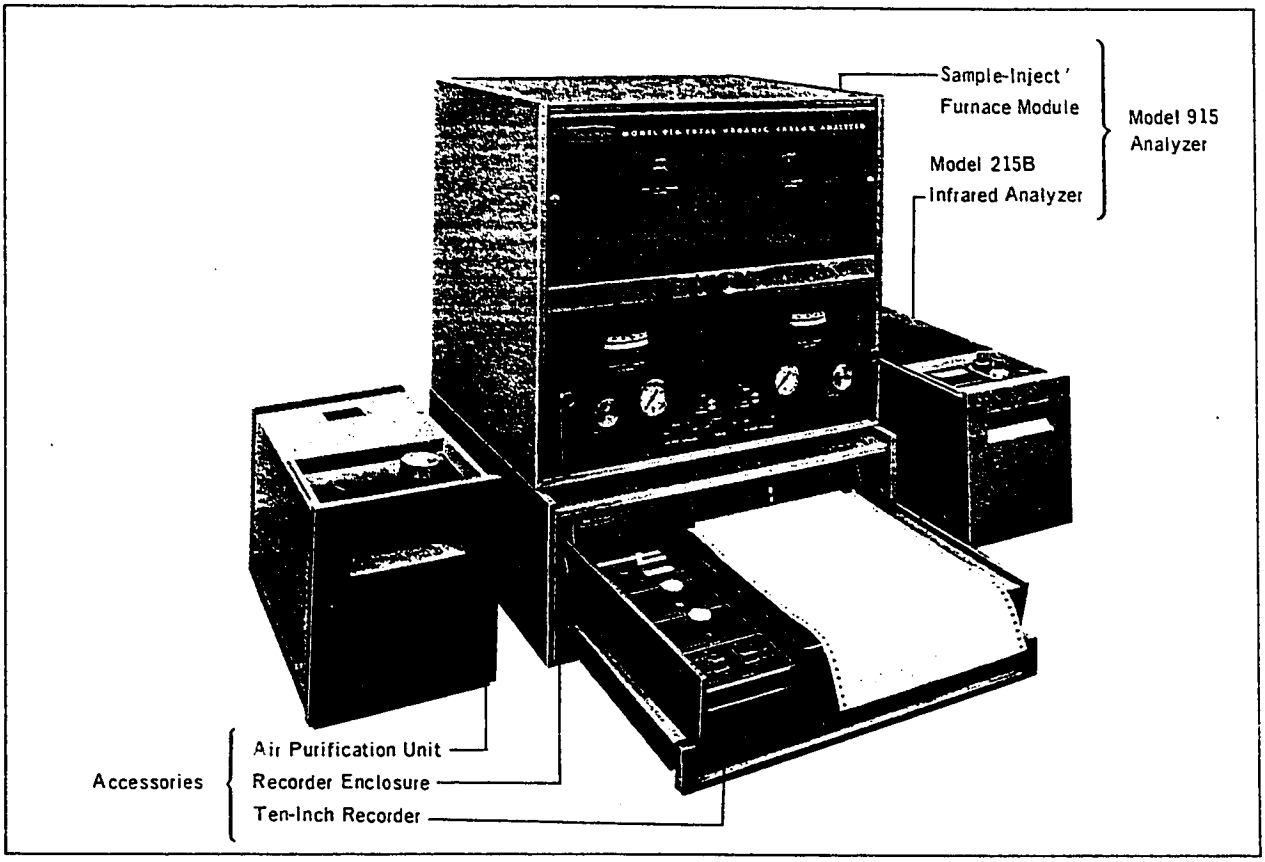

Figure: 3.6 Model 915 Total Organic Carbon Analyzer- Typical Installation

carrier-gas/oxidizer, the system requires a maximum of 300 cc/mm. of clear, pressurized, suitably regulated oxygen. Results of analysis are registered as peaks on a strip-chart recorder.

3.8 Chemicals

The chemicals used in this research at various stages comprise: NaCl, sodium sulfite, sodium thiosulfate, sodium hydroxide, ammonium hydroxide, hydrochloric acid, silver nitrate, cobalt sulfate catalyst, phenolphthalein, iodine, methyl orange and deionized water. All the were supplied from the local market and were of general purpose reagent type. The ammonium hydroxide solution supplied was of 28% by weight. The water used in all experiments was deionized in the Civil Engineering Environmental Laboratory. The gas cylinders were brought from a local supplier, Sigas, and had a purity of 99.5%. The standard solutions of sodium thiosulfate, sodium hydroxide, hydrochloric acid and iodine were brought from BDH chemicals Ltd. England through a local supplier. The sabkha samples were collected from a local source site.

3.9 Experimental Technique

First of all, the entire system was tested for any leaks. Rotameters were calibrated. The experimental technique can be divided into the following steps:

1. Preparation of highly saline waters
2. Preparation of ammoniated brine

3. Carbonation of ammoniated brine
4. Analysis of filtrates and precipitates
5. Hydrodynamic determination experiments
6. Quantification of carbon dioxide absorbed

3.9.1 Preparation of Highly Saline Waters

To prepare samples for experiments, it is required to have a saturated solution of sodium chloride. The preparation of a synthetic or sabkha saline water was performed by weighing the desired amount of pure sodium chloride or sabkha salt, respectively, and transferring it into a known volume flask. Deionized water is always used for dilution and to prepare solutions of desired concentration.

In the case of sabkha, the first phase of the study was to select a site in the Eastern Province, that represented a typical sabkha. Published literature was reviewed for selection of the potential site. Selected sites are located at King Fahd Military Hospital and Al-Hasa. These sites have a ground water table close to the surface, i.e less than 1 meter, as described in Chapter II.

Samples of the sabkha brine were taken for chemical analysis in order to compare the ionic phases at site with those quoted in the literature. Brine was collected in a clean plastic bottles that was rinsed with brine before taking the sample. Ionic phases determined were calcium, sodium, bicarbonate, magnesium, chloride and sulfate. Alkalinity and pH were also determined.

3.9.2 Preparation of Ammoniated Brine

The saturated brine of sodium chloride is ammoniated by mixing with the appropriate quantity of ammonium hydroxide solution to get the desired concentration of ammonia in the brine. The available aqueous ammonia solution is 28% by weight and density of 0.89 gr/ml. Prior to the mixing the concentration of ammonia solution in the bottle is determined by taking a sample volume and then adding an excess amount of HCl standard solution of a given molarity. The solution is titrated with standard sodium hydroxide solution of molarity equal to the HCl in the presence of phenolphthalein indicator. The additional volume of NaOH consumed leads to the actual concentration of ammonium hydroxide in the sample.

3.9.3 Carbonation of Ammoniated Brine

Once the ammoniated brine is obtained, it is then transferred to the absorption reaction vessel, which is operated at constant temperature, by circulation of a cooling water. The ammoniated brine of proper concentration in NaCl and ammonia is treated with pure carbon dioxide gas. The gas flow rate used is limited to 2-3 l/min. in the case of batch gas bubbler.

The carbonation is performed for a prespecified time period. The gas is then stopped and the solution is filtered. The experimental procedure is repeated with a higher carbonation time. Different concentrations of NaCl and ammonia were employed. In the case of the

bubble column, where the carbon dioxide gas enters the column via two orifices of 2.5mm diameter, frequent interruption of carbonation were experienced due to blocking of orifices by the precipitation of solids of sodium bicarbonate. To overcome this problem, the ammoniated solution free of salt was then transferred to the bubble column. The carbonation of the solution was then performed in a similar manner as that in the case of batch gas bubbler. The carbonated ammonia solution was then mixed with an already prepared saline water of known concentration. After a time the solution was filtered and the precipitates were removed.

The carbonation of the solution was performed at a rate of 11.8 l/min. The unabsorbed carbon dioxide was vented to the atmosphere.

3.9.4 Filtrate and Precipitate Analysis

This paragraph outlines the test methods that was implemented to achieve the objectives of this investigation. For each experimental run, analysis of filtrate or mother liquor and precipitate solids were performed. In the filtrate, the analysis of sodium ion, chloride ion, carbonates, ammonium chloride, alkalinity and pH were carried out. Analyses of the solid precipitates include chloride ion, sodium ion and carbonates.

Sodium Ion Analysis. The determination on sodium ion concentration present in either filtrate or precipitate solutions was obtained by

using atomic absorption spectrophotometer. In this analysis, a calibration curve is generated from standard solutions. The sample solutions of filtrate or precipitate are properly diluted with deionized water, so that their concentrations fall in the range of the calibration curve. The concentration values given by the atomic absorption spectrophotometer 3100 model are expressed in parts per million, with an accuracy of concentration of one mg/l.

Chloride Ion Analysis. The determination of chloride ion in the filtrate and precipitate samples was performed using the Mohr method. Suitable sample volumes with one ml of 5% potassium chromate indicator were prepared. Then the titration operation was accomplished against a wide background with standard silver nitrate, while agitating until the yellow of the suspension was converted to a reddish color.

Carbonate Analysis. The bicarbonate and carbonate ions determination were done by using the double-indicator titration method. Suitable sample solutions of filtrate and precipitate were titrated with standard hydrochloric acid , using phenolphthalein indicator that would produce a color change of pink to colorless when the sodium carbonate has been converted to sodium bicarbonate. Methyl orange would give a yellow color to the solution and the additional volume of acid required to change the color of the methyl orange would be that required to complete the reaction with the sodium bicarbonate formed from the sodium carbonate plus that required to react with the origi-

nal sodium bicarbonate.

Alkalinity. The alkalinity of properly prepared sample solutions was carried out by titrating with standard HCl solution, using methyl orange as the indicator. Titration operations were performed in Automatic Titrator Model Mettler DL 25.

Ammonium Chloride Determination. In the filtrate, the quantity of ammonium chloride is determined gravimetrically. A 10 ml volume of filtrate is transferred into a 150 ml evaporating dish. The solution is evaporated just to dryness over a steam bath, and is dried to a constant weight in an electric oven at 105 C. The contents of the dish is weighed, then ignited over a low gentle flame until all the ammonium chloride fumes disappear. The contents of the dish is cooled and weighed again. The contents of the first weighing can be taken as sodium chloride plus ammonium chloride and that of the second weighing as sodium chloride, so that the difference is ammonium chloride.

Carbon Dioxide Absorption. To determine the quantity of carbon dioxide absorbed in any experiment, a Total Organic Carbon Analyzer (Beckman, Model 915) was used. Inorganic carbon stock solution was prepared from anhydrous sodium carbonate and bicarbonate, using carbon-dioxide-free water. Standard solutions were prepared from the stock solution.

The calibration curve was generated by injecting 20 micro-liter standard solutions and measuring the peak heights. In this analysis a

suitable operating mode, sample volume, full scale span and setting of a gain control were taken. In this investigation, the zero adjust control of TOC machine was set at 9.58, Range to 2, the gain control to 5.36, the temperature to 150 $^{\circ}F$ and the oxygen flow rate to 100-150 ml per minute. Then the sample solutions were tested. If the sample value fell outside the range of the calibration curve, then the sample was further diluted with carbon-dioxide-free water, and the run was repeated.

3.9.5 Hydrodynamic Determinations

The experimental method can be divided into four phases.

1. Gas hold-up
2. Interfacial area
3. Mass transfer coefficient
4. Mixing efficiency

Gas Holdup. The measurement of the gas holdup was performed using deionized water and aqueous solutions of sodium chloride 3-30% by weight, sodium sulfite 0.8 molar, sodium hydroxide 1 molar. The bubble column was operated continuously with respect to the gas and batch wise with respect to the liquid. Gases employed in this phase were pure carbon dioxide, pure oxygen, and air.

In the measurement of the gas holdup, the flow rate of the gas ranged between 3.6 and 40 l/min., while the height of the solution tested in the column ranged from 30 to 100 cm. The measurements of

the gas flow rates at a constant temperature of 22 °C were determined by means of liquid-level indicator that was in connected to parallel to the bubble column. The liquid level in this indicator under gas sparging conditions was found to equal the height present in the column when no gas was being dispersed. The gas was fed from the nozzles after the flow rate was measured with rotameters. Each measurement was repeated three times.

The effect of temperature on the gas holdup was studied by varying the system temperature. The gas holdup was obtained by the ratio of the increased height of the liquid due to gasification to the height when the gas is stopped. In other words, it is the volumetric ratio defined by

$$\text{Gas Holdup} = \frac{H_d - H_c}{H_c} \qquad (3.1)$$

Where H_d is the height of the dispersed liquid, and H_c is the height of the clear liquid.

Interfacial Area Measurement. A chemical technique, based on the absorption of oxygen into sodium sulfite solutions catalyzed by cobalt ions, was used to measure the interfacial area. This sodium sulfite solution was of about 0.8 molar and contained 2×10^{-4} mole/l of cobalt sulfate. Pure oxygen was fed to the column after being metered. Operation was batch by batch with respect to the solution.

The decrease in the sulfite concentration with time was determined by analysing liquid samples taken at constant intervals. The analysis of the liquid samples was performed using iodometric titration. This was done by adding on the sample an excess amount of standard and acidified iodine solution. The sample was then titrated with standard thiosulfate.

$$I_2 + 2Na_2S_2O_3 \rightarrow 2NaI + Na_2S_4O_6 \qquad (3.2)$$

Starch indicator was added at the end point when the bulk of the iodine had been reduced. Temperature and pH of the system were maintained at the required conditions.

Mass Transfer Determination. The liquid mass-transfer coefficient was determined in the slow chemical reaction regime from the measurement of the absorption rate of pure oxygen in a sodium sulfite solution. The sodium sulfite solution was of an initial concentration of 0.8 molar. Absorption rates of oxygen were measured under the same experimental condition as the interfacial area determination, except for the cobalt sulfate catalyst concentration of 2×10^{5} mole/l.

The solubility of oxygen in sodium sulfite solution was estimated, using the Van Krevelen method on the assumption that the solubility of oxygen in sodium sulfite solution is equal to that in sodium sulfate solution of same normality. The correction of the interfacial concentration of oxygen in sodium sulfite is given in the appendix A.

Mixing Efficiency. Mixing efficiency is described here by two parameters: mixing time and circulation time. Mixing time is defined as the time between the beginning of the mixing operation and the moment when the fluid reaches a required degree of homogeneity (Ford et al. 1972). The discoloration technique using the iodine ammonium-thiosulfate reaction seems to be the most attractive; since it is easy to monitor and the chemicals used do not affect substantially the rheological properties of the liquid.

Mixing Time. Visual monitoring of a redox reaction between iodine and sodium thiosulfate was used for measuring the mixing time. One ml of 2 N iodine potassium-iodide solution and 20 ml of starch solution were added to the liquid, which turned deep blue. At t=0, 1.5 times the stoichiometric quantity of a normal (1 N) sodium thiosulfate was injected at the surface of the liquid. The mixing time was taken as the time necessary to obtain a complete discoloration except for small stagnant zones. Each experimental measurement was repeated four times and the average value recorded.

Circulation Time. The method used by Guerin et al. (1984) was employed and the circulation time was the time between two successive crossings of a particle, in the same direction through a chosen plane. The reference plane was the centre of the column and the particle used was a colored tracer bead of poly-styrene foam, of about 2 mm diameter, which became totally impregnated when immersed and thus reached close to the liquid density. The black

tracer particle was always clearly visible during the experiment. Each experiment included several measurements.

Chapter IV

INTERPRETATION OF EXPERIMENTAL RESULTS

In this research study, a series of reactions was employed to convert sodium and chloride ions in saline waters into sodium bicarbonate and ammonium chloride with the objective of developing a desalination process. In order to investigate the feasibility of the separation experimentally , bubble column reactors were used as suitable contactors.

The following experimental stages are identified:

4.1. Separation Using the Batch Gas Bubbler (B.G.B)

The gas bubbler has a wider mouth for gasification and hence the precipitates formed do not block the orifice completely. The following results were obtained with this unit using synthetic saline water of known sodium chloride concentration as a feed.

In this set of experiments, the effect of some operating parameters on the separation of sodium chloride from the feed water was

considered first.

4.1.1 Effect of the Operating Parameters

The optimum operating temperature for the separation of sodium chloride from saline water was sought. The effective removal of sodium chloride from a solution containing 2.5 molar ammonia and 4.3 molar sodium chloride, for one hour carbonation time at different temperatures, was studied.

In Figure 4.1, the results indicate that an operating temperature around 20 $^{\circ}C$ is most favorable. This is shown by the minimum sodium ion concentration in the filtrate. At a lower temperature, separation is less effective, probably because of poorer rates. Separation is less at higher temperatures probably because the absorption of carbon dioxide gas is less at increased temperature.

Secondly, the effect of the pH of the solution on the formation of carbonate, bicarbonate and the equilibrium between them were studied. This experiment was carried out using 3.5 molar ammonia solution, and no sodium chloride. The carbon dioxide gas was allowed to bubble until the formation of precipitates was visible. The analysis of these precipitates was carried out and showed the formation of ammonium carbonate exclusively.

The experiment was continued again by bubbling carbon dioxide

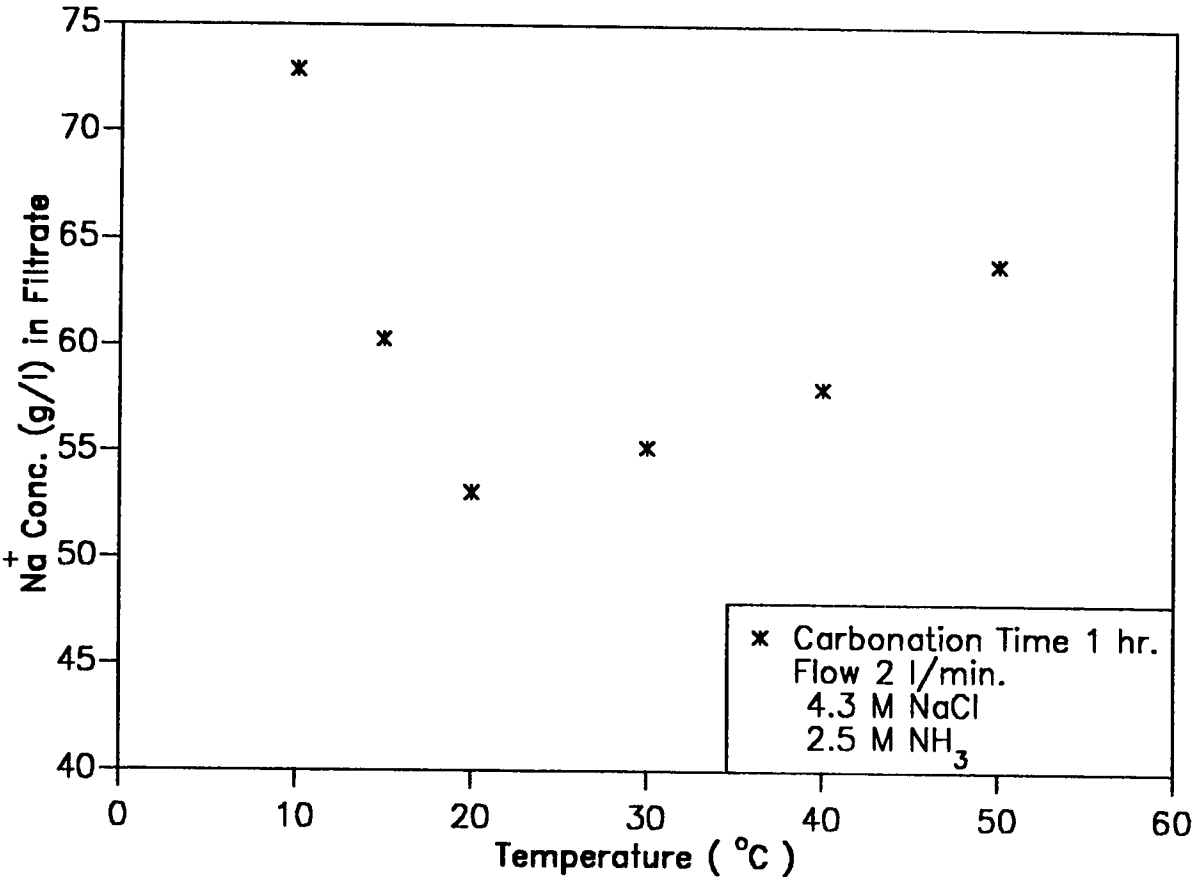

Figure 4.1 Effect of temperature on NaCl Removal

gas while a record of the time of carbonation was noted. Filtrates were obtained after different intervals and were analyzed to determine the ratio of carbonates to bicarbonates. The results were plotted in Figure 4.2, which shows that the ratio of ammonium carbonate to ammonium bicarbonate decreases as the carbonation time increases. This is in accordance with equilibrium relationship:

$$(NH_4)_2CO_3 + CO_2 + H_2O = 2\,NH_4HCO_3 \qquad (4.1)$$

The analysis of results indicated as well that the total moles of carbonate and bicarbonate remained unchanged, but transformation from one form to another takes place. Initially, the carbonate form is predominant, however, further carbonation leads to the formation of bicarbonates, and these increase with time as a result of the decrease of carbonates as given by the above reaction.

On the other hand, it is found that the pH value decreases with additional carbon dioxide gas, due to the acidity of the gas. Figures 4.3 and 4.4 are plots of changes of pH value with carbonation time, for separation of various concentrations of NaCl.

An appreciable change in value of pH from 12 to 9 is observed in the initial period of carbonation (up to 30 minutes). However, further carbonation time, brings only slight changes in pH value. It can be concluded that over the pH range of 8-10, the formation of bicarbonate is favorable. Outside this range (pH greater than 11), other chemical reactions take place (Cussler, 1984).

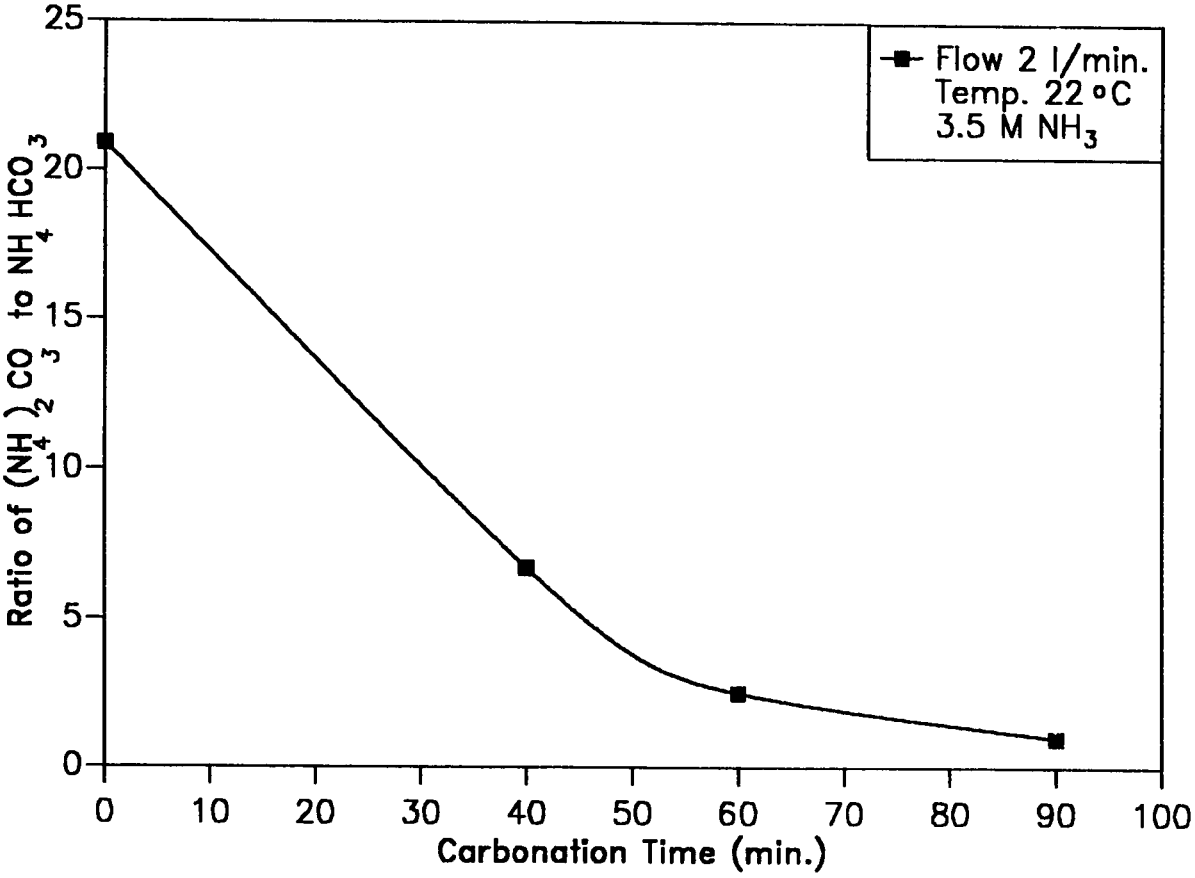

Figure 4.2 Equilibrium Conversion of $(NH_4)_2CO_3$ and NH_4HCO_3

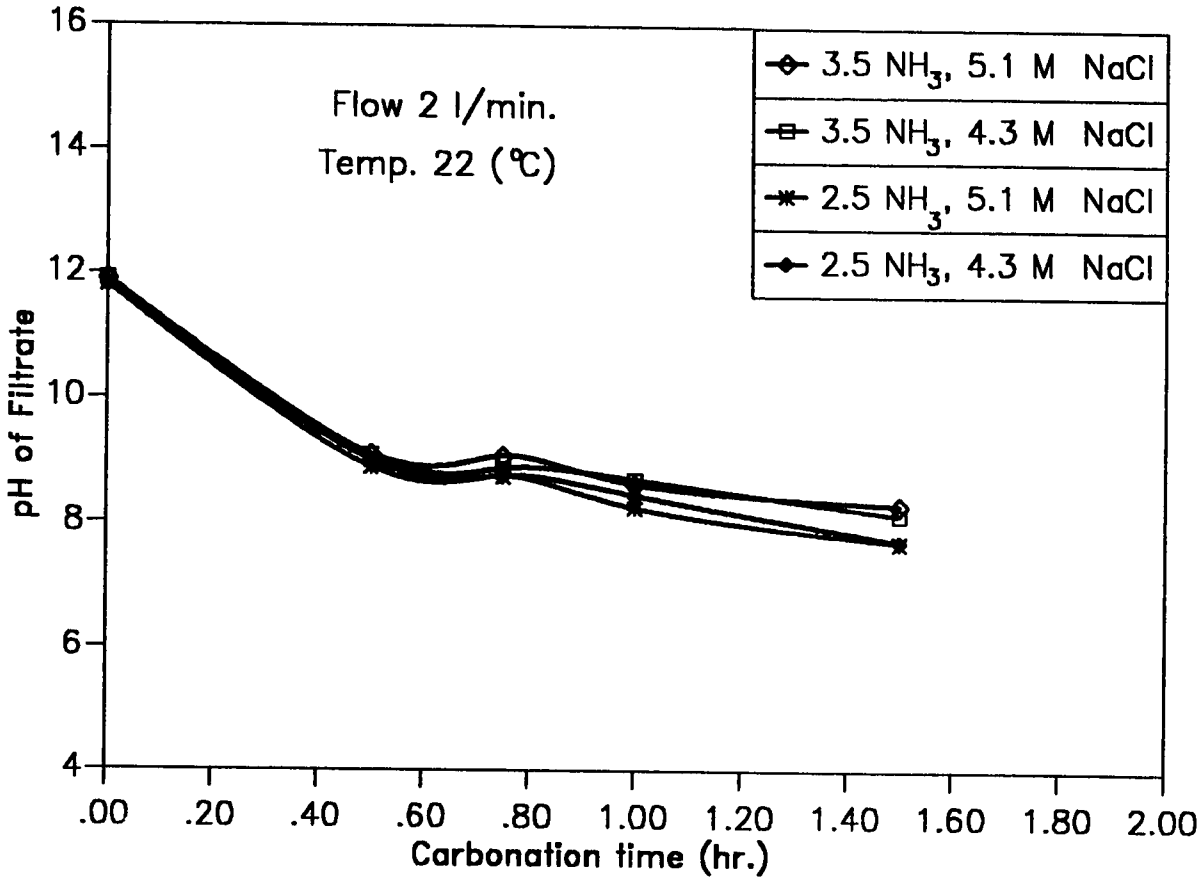

Figure 4.3 Effect of Carbonation on pH

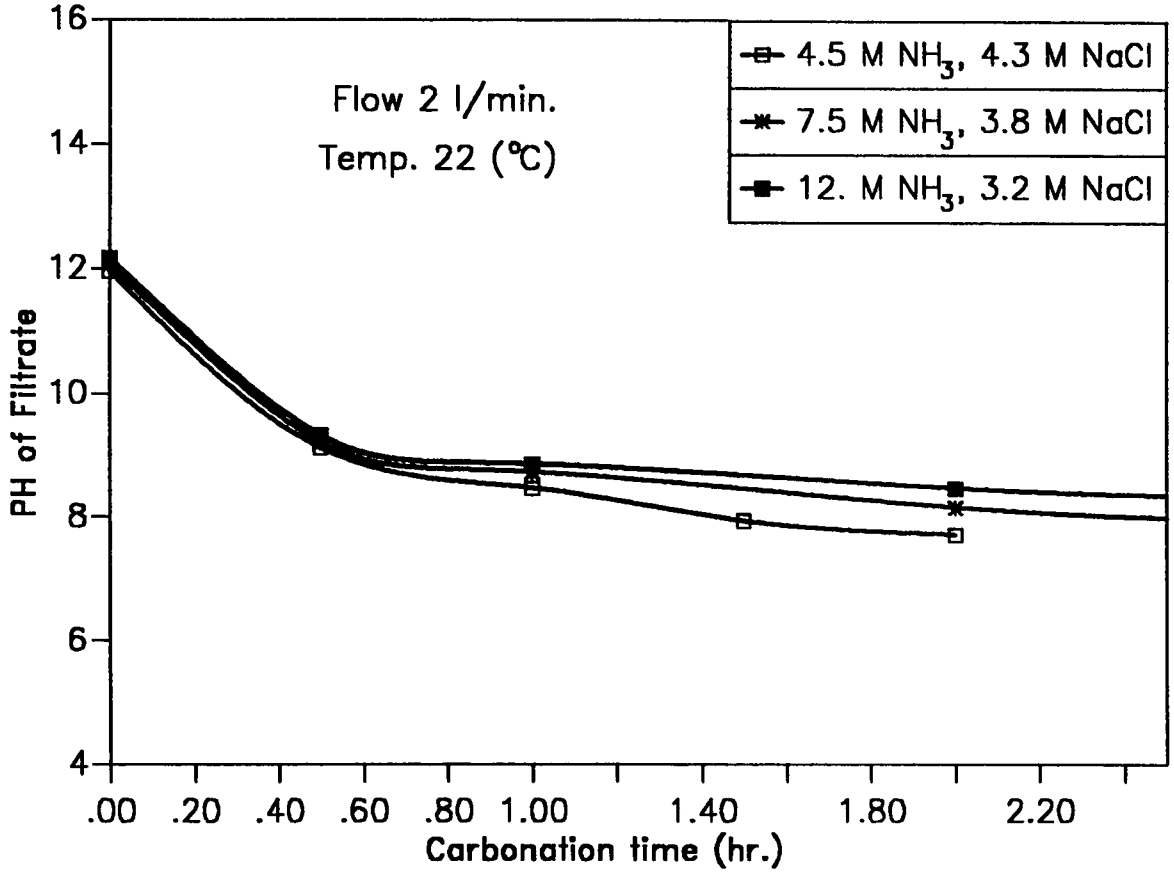

Figure 4.4 Effect of Carbonation on pH

Thirdly, the extent of absorption of carbon dioxide by ammoniated solution was investigated by measuring the rate of absorption of carbon dioxide in 2.5 molar ammonia, using the batch gas bubbler, with a flow rate of 2 liter per minute. Figure 4.5 depicts the result. The amount of carbon dioxide absorbed increases rapidly during the initial bubbling period, this is due to the higher driving force resulting from no carbon dioxide in the liquid phase; however, with increase in time, the rate of absorption of carbon dioxide diminishes.

From the stoichiometry of the reaction:

$$CO_2 + 2NH_3 = NH_2COO^- + NH_4^+ \qquad (4.2)$$

It can be seen that the maximum pick-up of CO_2 is limited to 0.5 moles of CO_2 per mole of ammonia if the carbamate ion formation is the only reaction. In general a CO_2 pick-up in excess of 0.5 moles is possible owing to the reversion of carbamates.

$$CO_2 + NH_2COO^- + H_2O = NH_4^+ + 2HCO_3^- \qquad (4.3)$$

Even if there is a driving force for carbamate reversion, the rate of reaction is, in general, extremely slow. Mass transfer of CO_2 into highly carbonated aqueous ammonia solution proceeds extremely slowly.

At this point we can summarize the above discussions as follows:

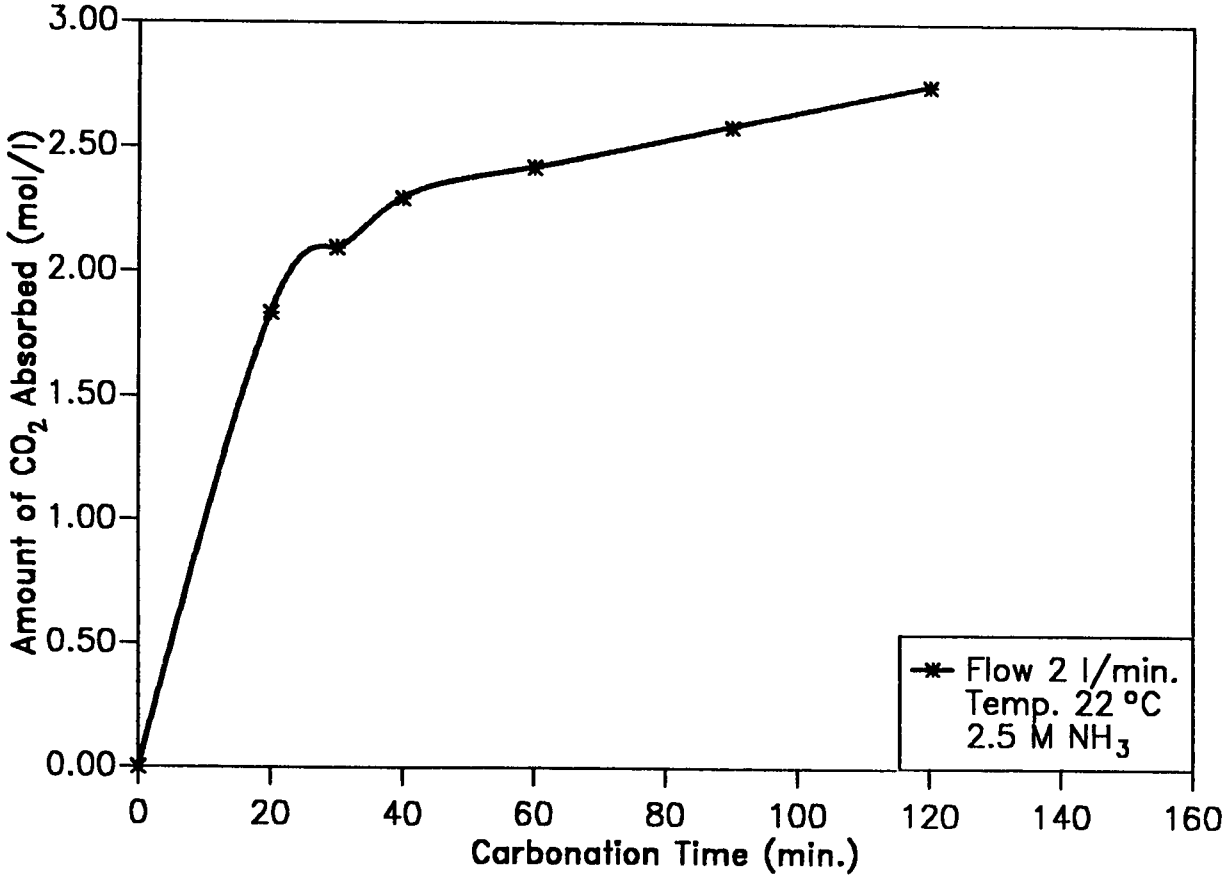

Figure 4.5 Quantitative Measurement of Total Gas Absorbed

a) The optimum operating temperature for absorption lies in the vicinity of 20 $^{\circ}C$.

b) The formation of bicarbonate is preceded by that of carbonate which transforms to bicarbonate when subjected to further carbonation.

c) The best range of pH for the precipitation process is found to be between pH (8 -10).

d) The measurement of the absorption of CO_2 indicated the need for a prolonged carbonation time.

4.1.2 Synthetic Saline Water (S.S.W)

The conversion rates of sodium and chloride ions for various conditions were studied, using laboratory synthetic saline water as feed. The carbonation of the ammoniated brine was carried out at specified conditions. Figures 4.6 and 4.7, show the results when 2.5 molar ammonia solution is carbonated at the rate of 2 litre per minute. Both figures indicate that the rate of sodium ion removal increases with carbonation time and tends towards a constant value.

The removal of sodium ion reported in Figure 4.6 is found to be 62.6%, while for the conditions given in Figure 4.7 is 56.8%. The difference in conversion for the two cases, is attributed to the difference in the initial salinity concentration. The higher the salinity, the lower the solubility of carbon dioxide in the ammoniated brine.

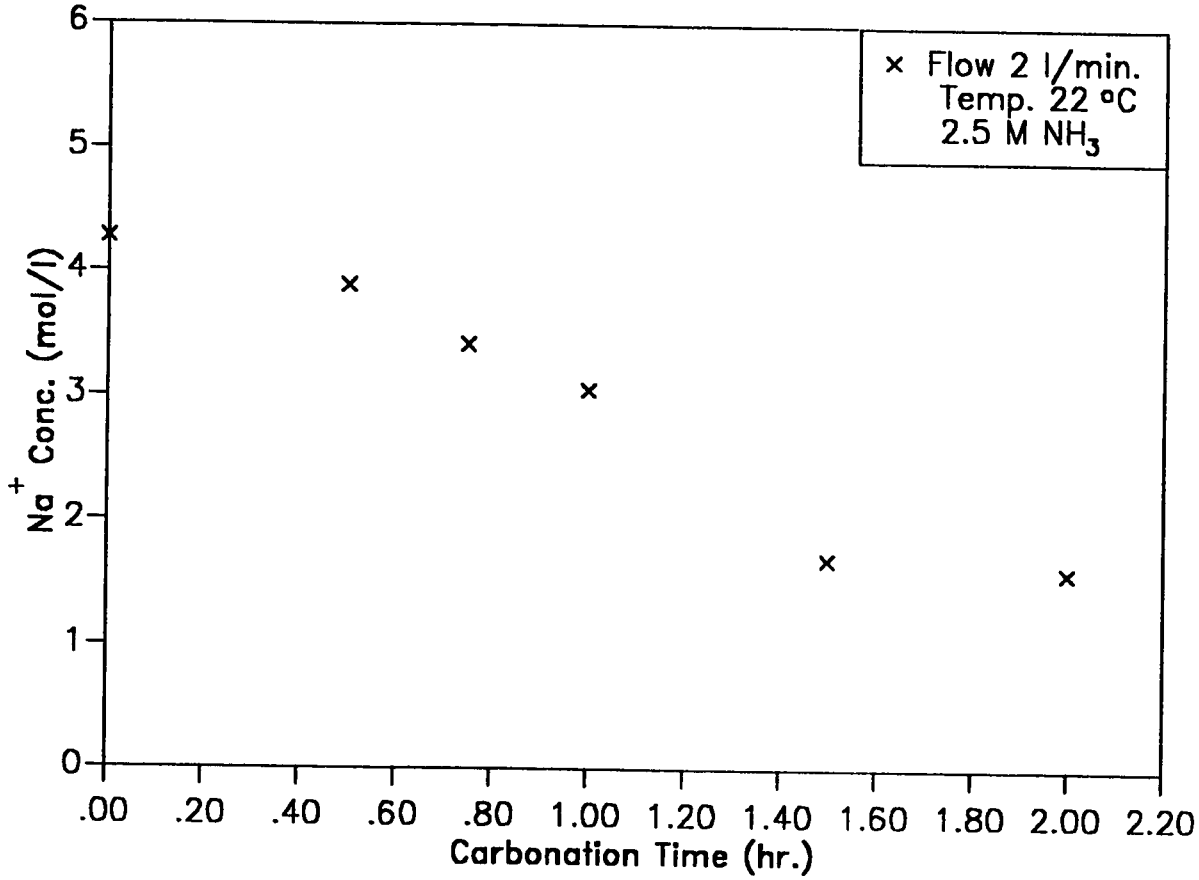

Figure 4.6 Effect of Carbonation on Na^+ Removal

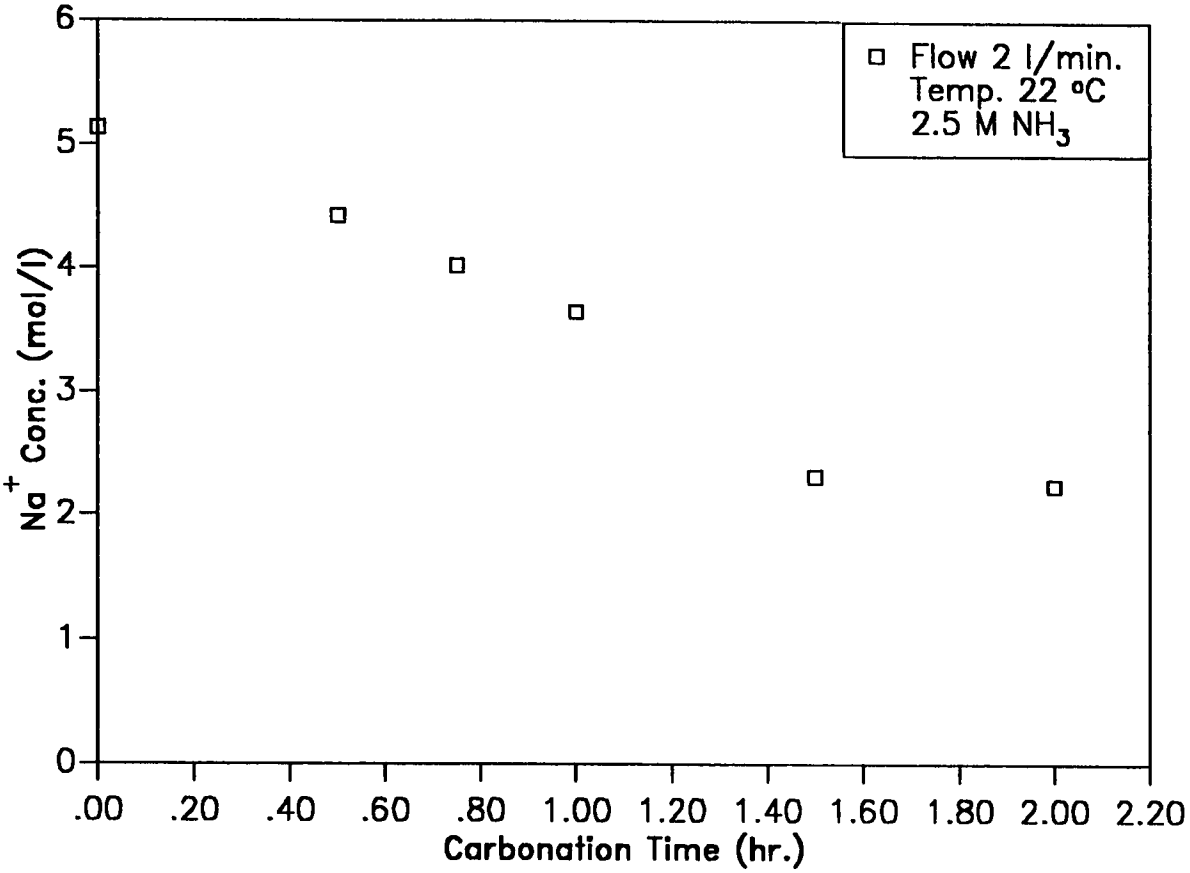

Figure 4.7 Effect of Carbonation on Na^+ Removal

When 3.5 molar ammonia solution is used, keeping other conditions same, the conversion of sodium ion is enhanced. This results mainly from the increase of ammonia concentration, and hence an increase of the amount of carbon dioxide able to form ammonium carbonates. A higher conversions of sodium ions 75.3 % is obtained for a feed of 4.3 mole per litre as shown in Figure 4.8, when compared with 67.8 % for a feed of a higher salt concentration, 5.1 mole per litre shown in Figure 4.9.

When the concentration of ammonia is increased to 4.5 molar, and the rate of flow of carbon dioxide is made 3 litre per minute, the conversion of saline water of 4.3 molar sodium chloride increases to 78.5%. This again confirms the fact that the conversion rate of carbon dioxide into ammonium carbonates increases with higher concentrations of ammonia. Figure 4.10 shows the case of 4.5 molar ammonia.

When the concentration was increased further to 7.5 and 12 molar, although the initial concentrations of NaCl were reduced in proportion to the increased molarity of the ammonia solution, the conversion rates increased to 82.2 and 81.4, respectively. Figures 4.11 and 4.12 show the results for those two cases of 7.5 molar and 12 molar ammonia respectively. The decrease in the percentage conversion of the sodium ion for the case of 12 molar ammonia solution is due to the initial salt content.

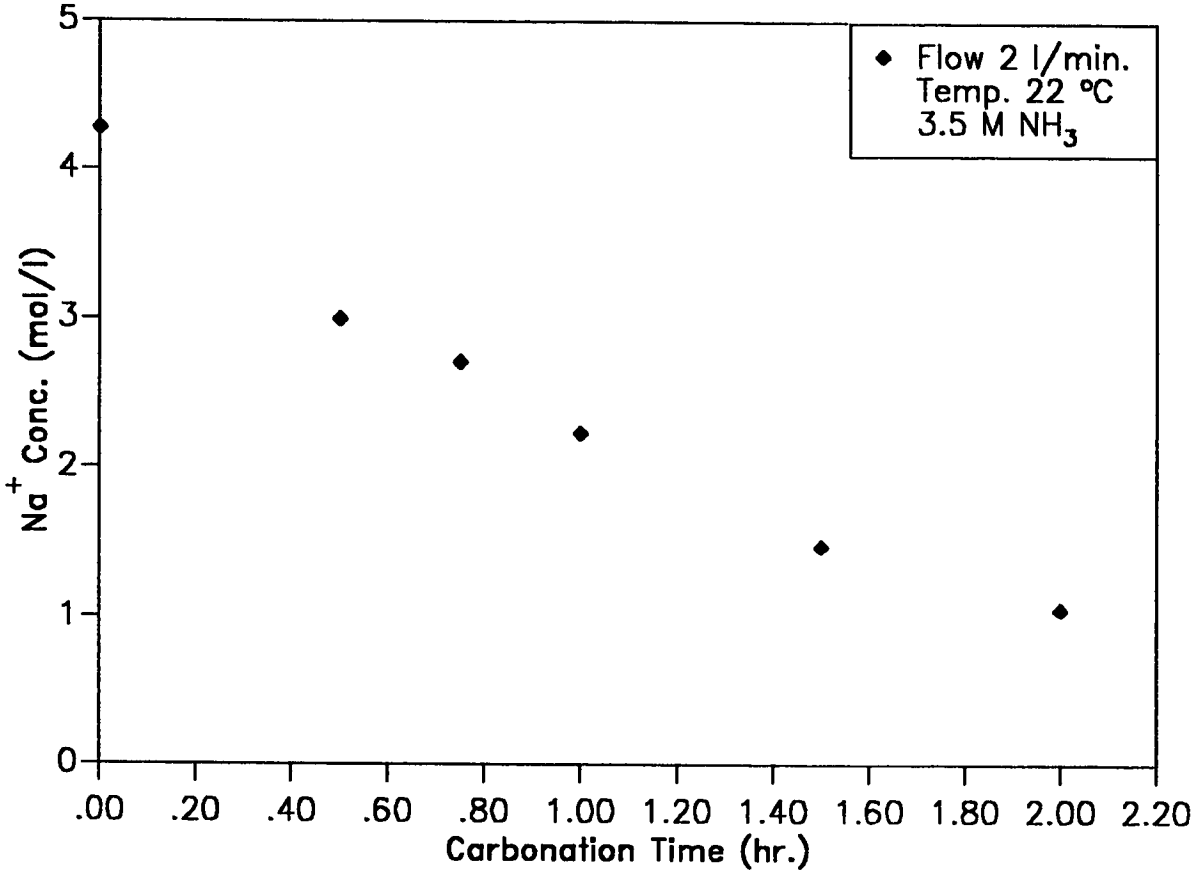

Figure 4.8 Effect of Carbonation on Na^+ Removal

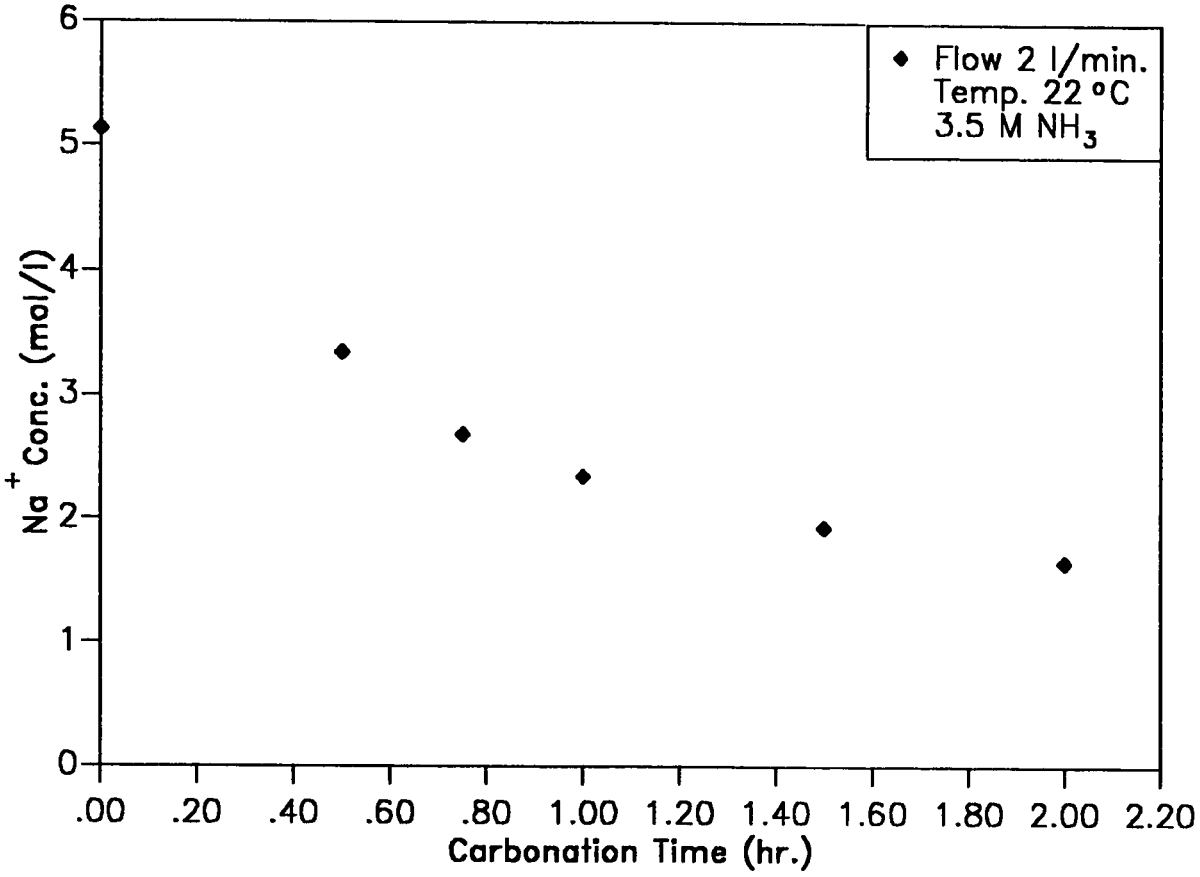

Figure 4.9 Effect of Carbonation on Na^+ Removal

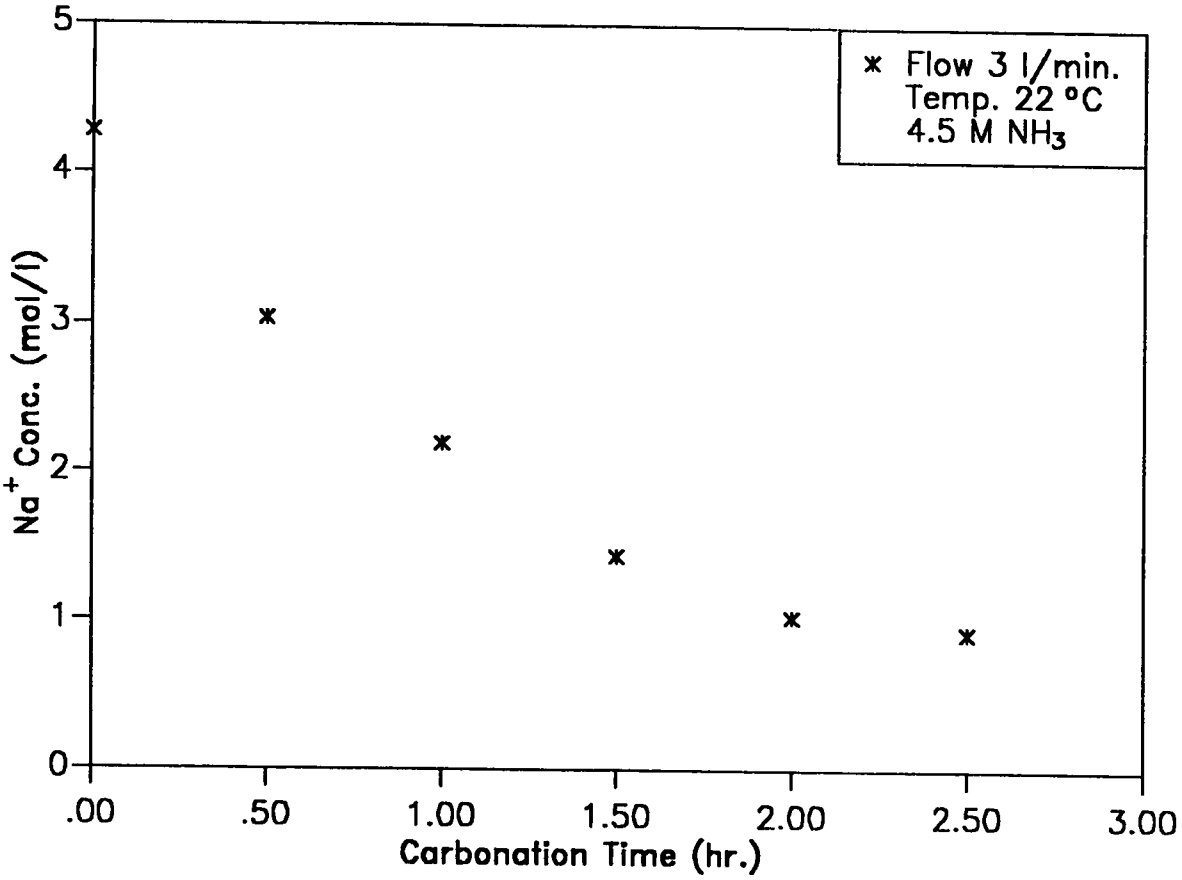

Figure 4.10 Effect of Carbonation on Na^+ Removal

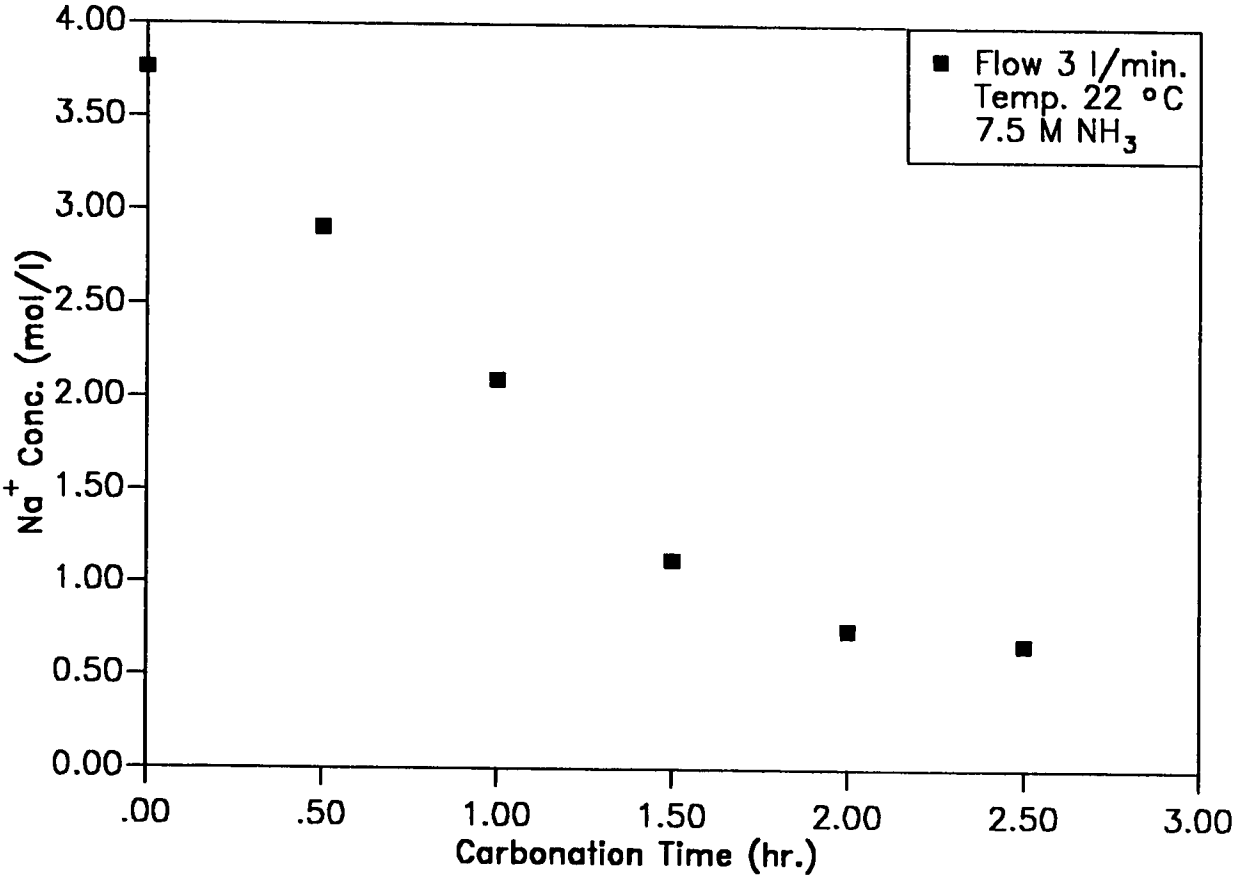

Figure 4.11 Effect of Carbonation on Na^+ Removal

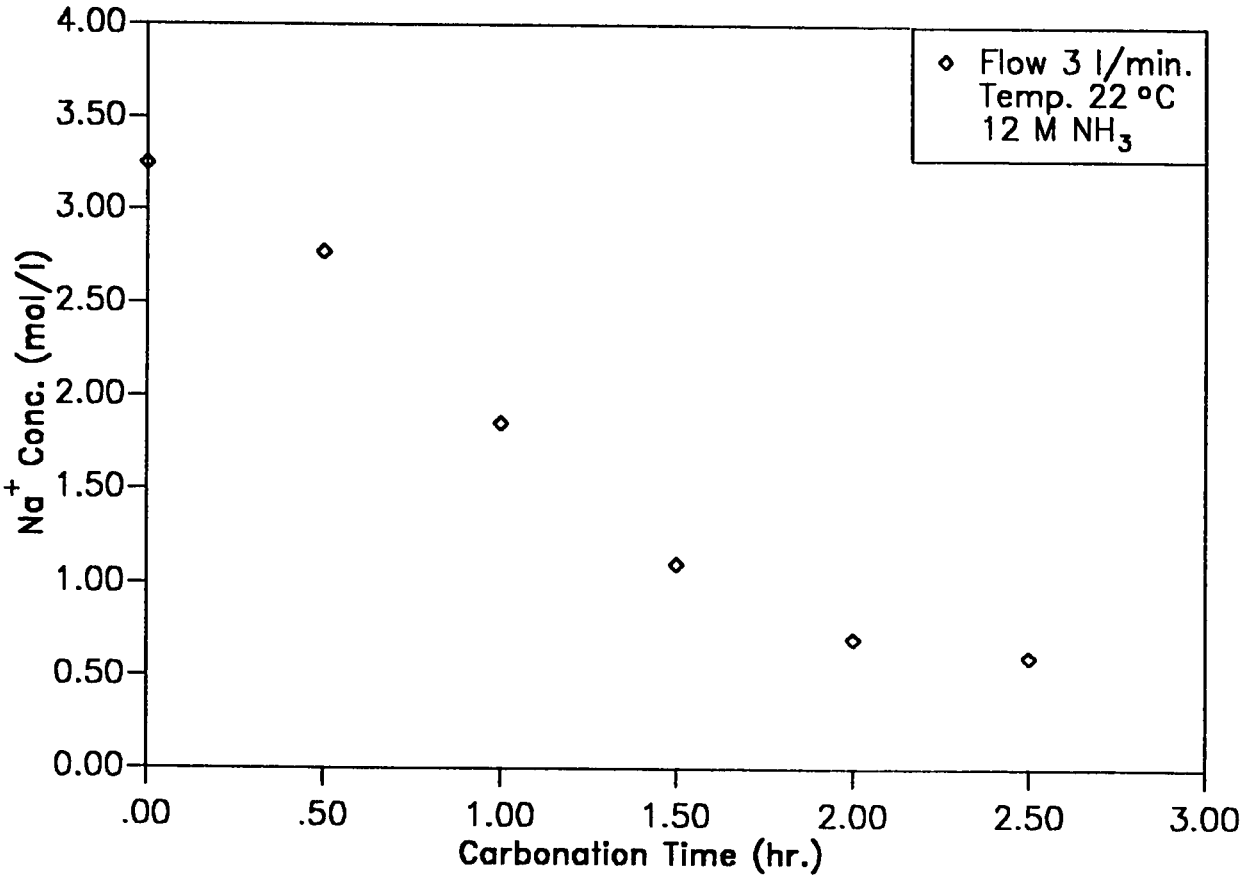

Figure 4.12 Effect of Carbonation on Na^+ Removal

Along with the formation of sodium carbonate, ammonium chloride comes as an additional product in the filtrate as a result of the reaction of ammonium and chloride ions. Figure 4.13 shows, the rate of formation of ammonium chloride as a function of carbonation time. The effect of ammonia concentration and the salinity of solution were considered as well in the experiment.

It can be concluded that for the same initial concentration of ammonia, ammonium chloride formation is higher the greater the sodium chloride salinity, while for same initial salinity, the formation is increased with the increase of ammonia concentration. Special consideration is given next to the effect of initial concentration.

4.1.3 Effect of the Initial Brine Concentration

The parameters that have considerable effects on the separation process include the strength of ammonia and the salinity of the brine. When solutions of equal salinity were prepared the following results were obtained:

Figure 4.14 compares the effect of two different initial salinities in solutions of same the ammonia concentration. The rate of conversion of sodium ion is higher when a less saline feed source is used. In other words the concentration of sodium ion in the filtrate is greater when a higher saline source is used with other conditions the same.

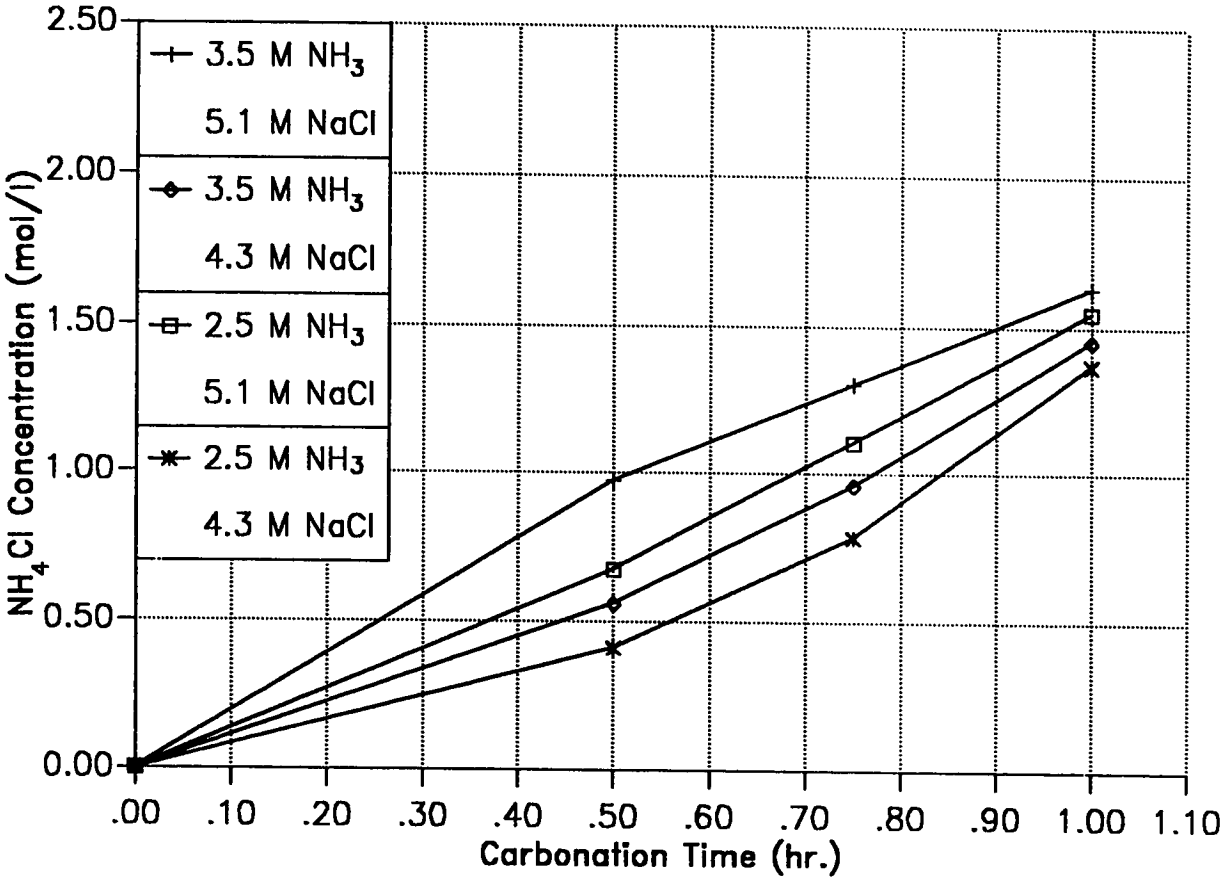

Figure 4.13 Rate of Formation of Ammonium Chloride

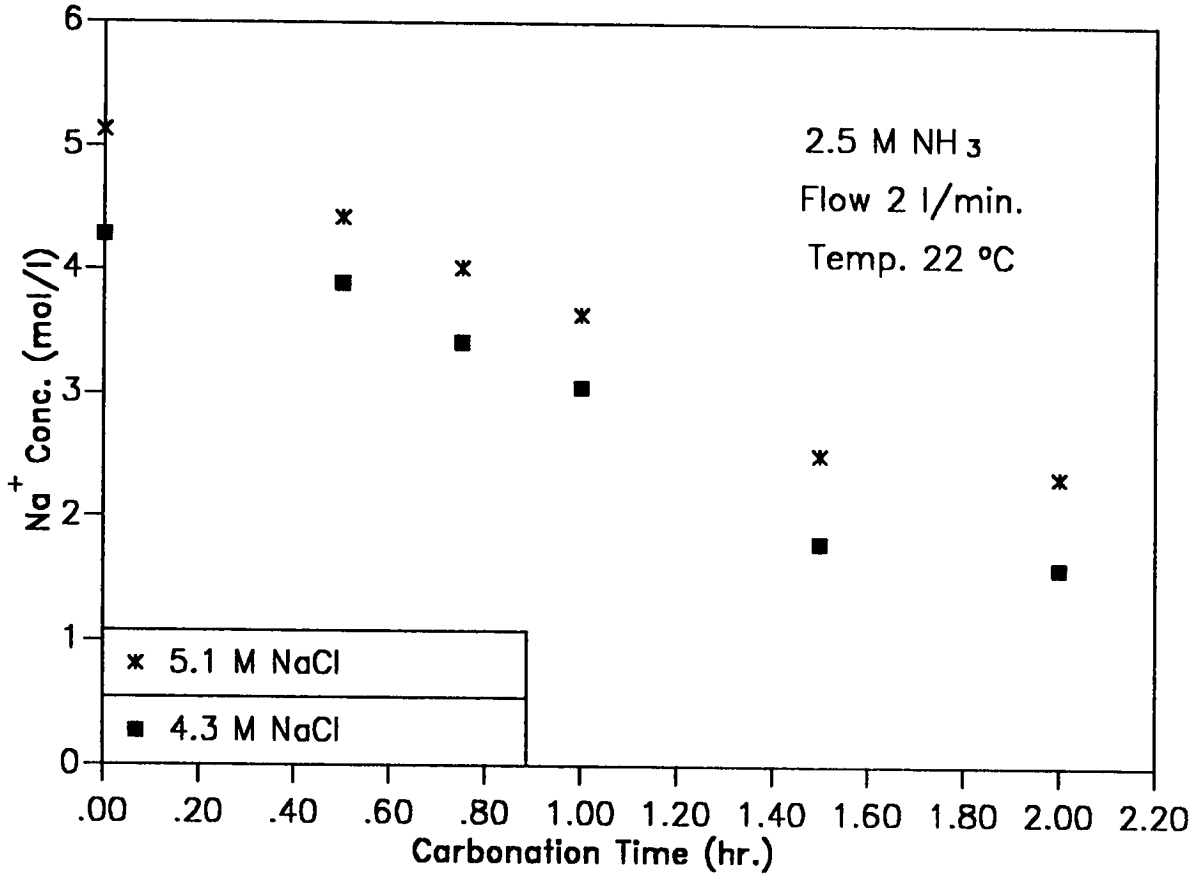

Figure 4.14 Effect of Initial salt on Na^+ Removal

Figure 4.15 demonstrates a similar dependence of the conversion of NaCl solution on the initial concentration of brine using a higher concentration of ammonia solution. (3.5 molar instead of 2.5 molar)

4.1.4 Effect of the Initial Ammonia Concentration

It is known that a substance which does not react with a solute, or form any complex ion with the solute, commonly decreases the solubility of that solute when such a substance is introduced into the solution. Therefore, the solubility of NaCl decreases with the increase of ammonia concentration. This in turn reduces the formation of sodium carbonates and bicarbonates.

In Figure 4.16 the effect of ammonia concentration on the sodium ion removal is depicted. The solubility of NaCl is reduced by the high concentration of ammonia. On the other hand, if a very high concentration of ammonia is employed then a large amount of ammonia is going to coprecipitate with sodium bicarbonate as ammonium carbonate exceeds its solubility product. This may be considered as a loss since it is not taking part in the conversion reaction of the salt.

Figure 4.17 shows the effect of the initial concentration of ammonia. Moreover, it indicates the need to adjust the initial salinity content of the solution with respect to the increased concentrations of ammonia, to obtain higher efficiency of NaCl conversion.

4.1.5 Effect of the Initial Concentration Ratio of $NH_3/NaCl$

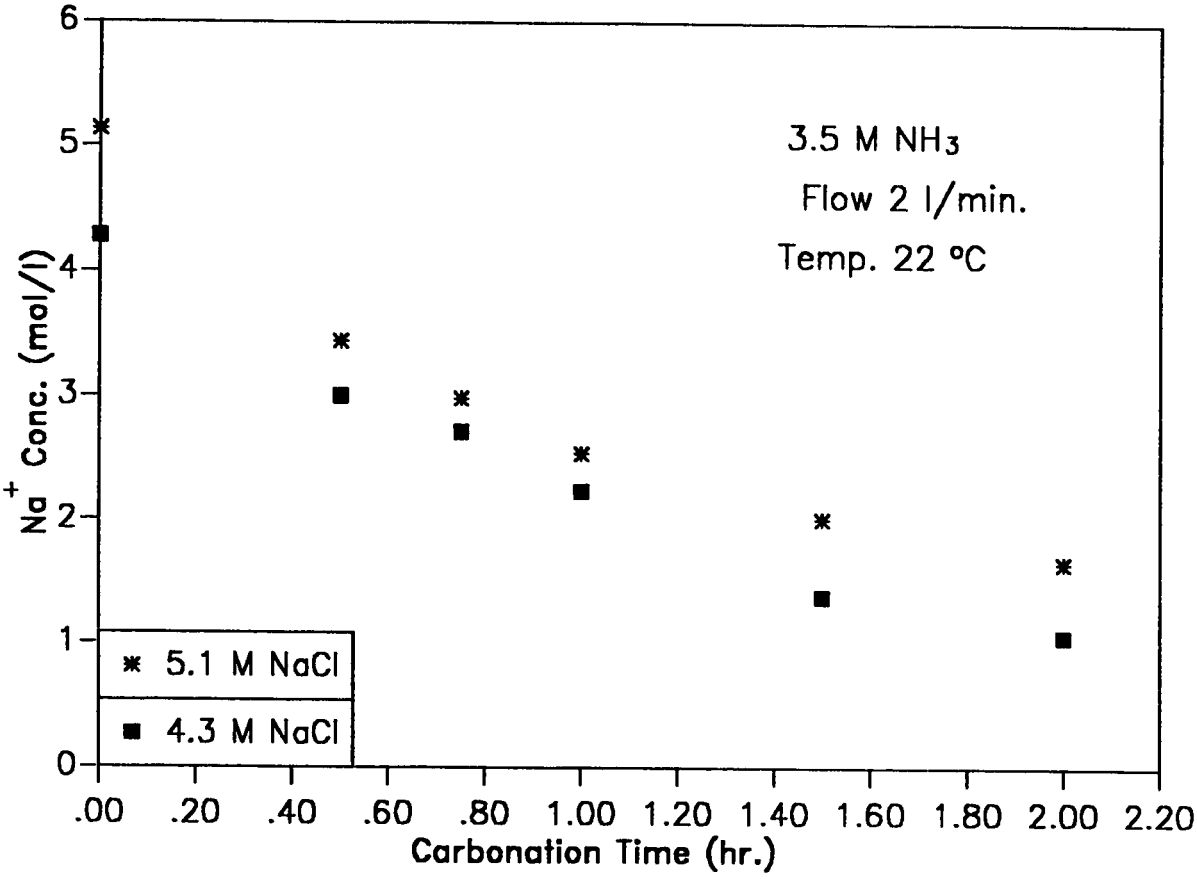

Figure 4.15 Effect of salt on Na^+ Removal

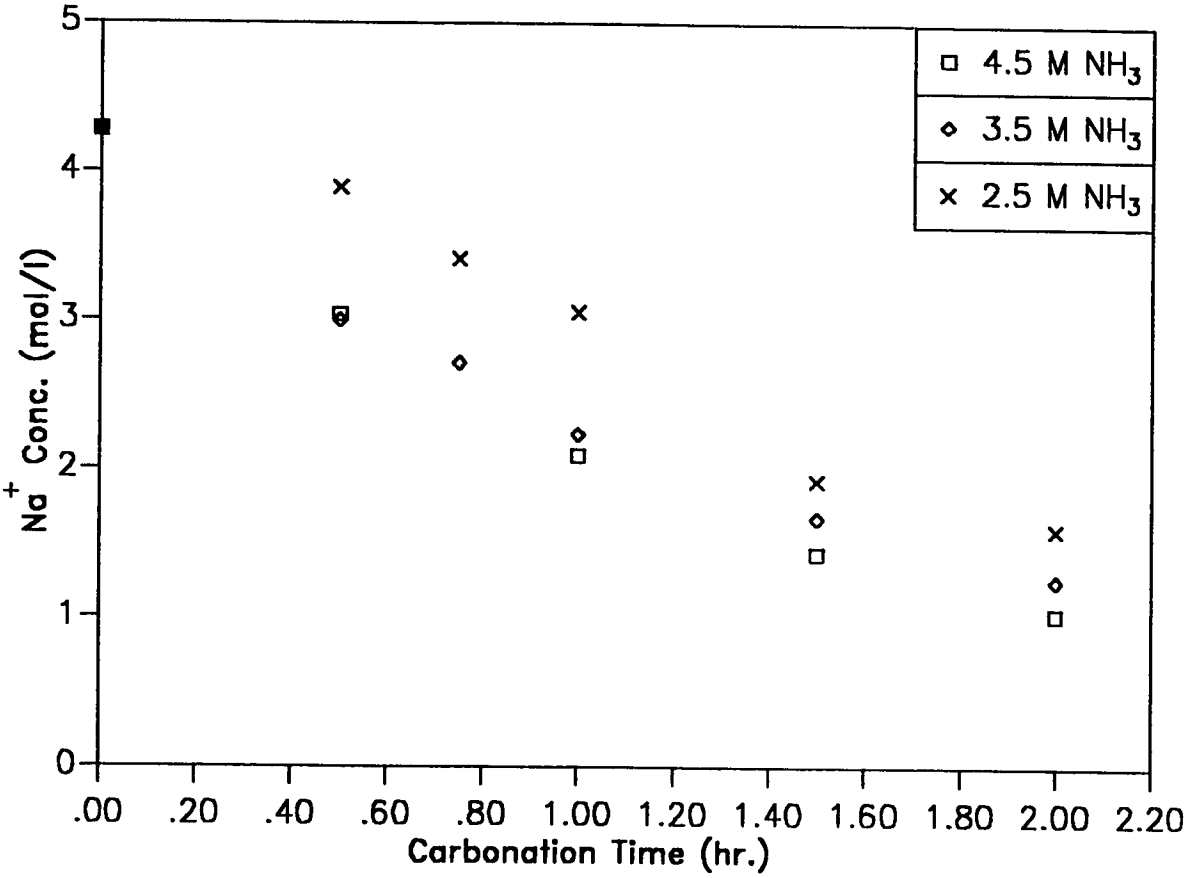

Figure 4.16 Effect of Initial NH_3 Concentration

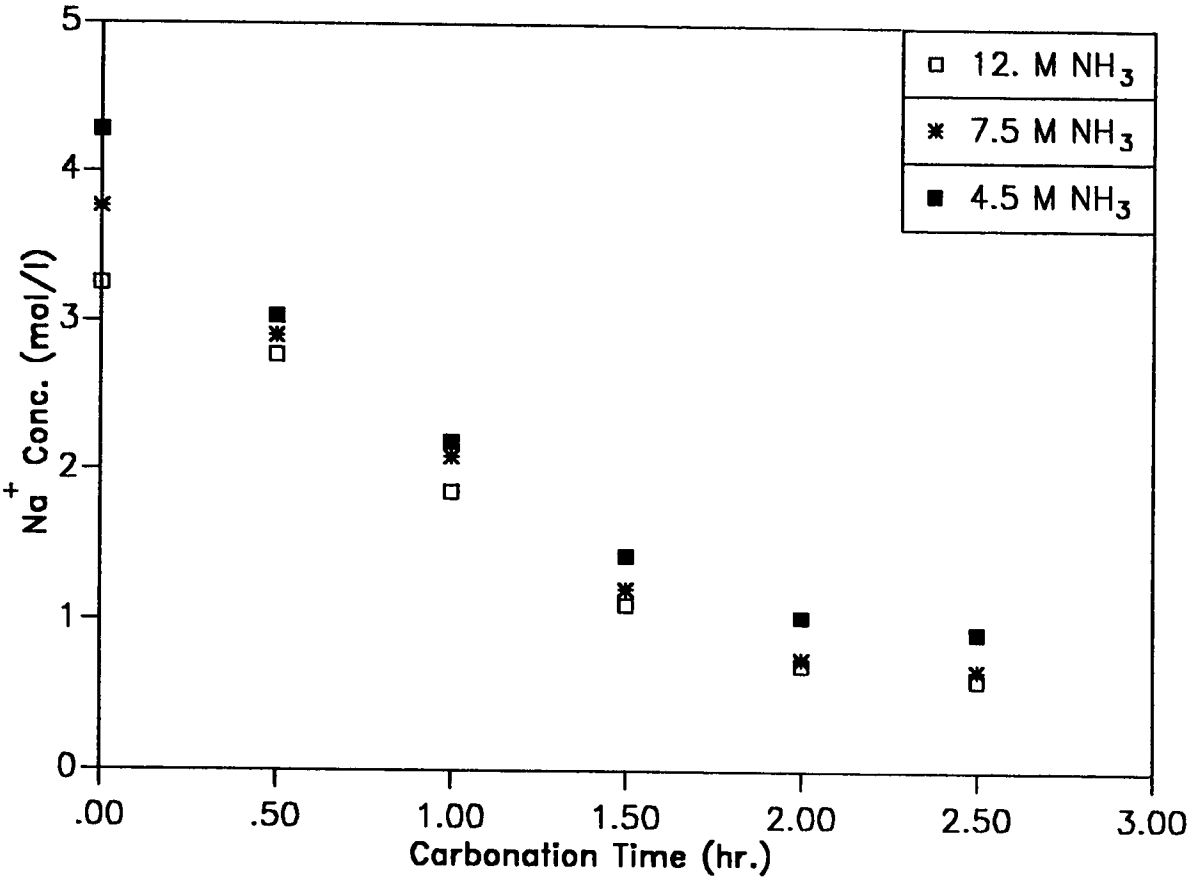

Figure 4.17 Effect of Ammonia Concentration

It was stated earlier that the reactions in this process require a saturated solution of NaCl to react with the carbonates of NH_3. However, the saturation concentration of NaCl is exclusively dependent on the properties and the characteristics of the solution, particularly, the concentrations of ammonia in the ammoniated brine. In theory, it is required to have equal strength of NH_3 and salinity (NaCl) as the stoichiometry of Equation (4.5) indicates.

$$CO_2 + NH_3 + H_2O \rightarrow NH_4HCO_3 \qquad (4.4)$$

$$NH_4HCO_3 + NaCl \rightarrow NaHCO_3 + NH_4Cl \qquad (4.5)$$

However, it is necessary to use higher amounts of NH_3 to compensate losses to evaporation or reaction with impurities in the feed.

It is found best economically to have a ratio of about 1.2 (Hou , 1991). If the ratio is too high, excessive amounts of ammonium bicarbonate were precipitate and leave without reacting with NaCl in solution, this is definitely uneconomical in the usage of the ammonia which is a relatively expensive chemical.

On the other hand, if the ratio is too low, then the conversion of sodium chloride will drop in the reactor and most of the NaCl salt will leave the reactor unchanged. This means there is insufficient ammonium bicarbonate to react with saturated NaCl solution. Therefore, this ratio affects directly the rate of salt decomposition, or conversion of NaCl into the required products, and utilization of ammonia.

It can be concluded that the ratio is vitally important to the overall yield and to the economic success of the process. It has been noticed that a very high efficiency in the utilization of ammonia is necessarily accompanied by a low efficiency in the conversion of the sodium chloride and vice versa. Since the case under study involves dual separation, the optimum efficiencies of NH_3 and NaCl consumption were not be as critical as in the case of the conventional Solvay process. However, the prime objective is to maximize the efficiency of conversion of NaCl to sodium bicarbonate which is separated as a precipitate.

Table 4.1 shows the effect of initial concentration ratio of NH_3 /NaCl, when synthetic saline water, having a concentration of ammonia that ranges between 2.5 M - 12 M, and sodium chloride solution of concentration ranges of 3.2 M - 4.2 M, was used in the batch gas bubbler, where carbonation time of two hours was considered. The table explicitly shows also the effect of the ratio of NH_3 /NaCl on the efficiency of Na^{+} conversion.

It is clear, that the conversion of Na^{+} is low at lower values of the ratio ($NH_3/NaCl$), less than unity, and increases with its increase towards unity. However, if the ratio becomes much greater than unity, the conversion efficiency will diminish again. This means the existence of suitable ratio or interval of ratios that is to be aimed for successful separation. This optimum ratio definitely occurs in the

Table 4.1 Effect of Concentration Ratio of NH3 /NaCl

Feed: Synthetic Saline Water
Flow: 2 l/min.
Temperature: 22 °C
Carbonation Time: 2 hr.
Contactor: B.G.Bubbler

NH_3 (M)	$NaCl$ (M)	$NH_3/NaCl$ (ratio)	% Conversion $[Na^+]$
2.5	5.1	0.5	56.5
2.5	4.3	0.6	62.6
3.5	5.1	0.7	67.8
3.5	4.3	0.8	75.3
4.5	4.3	1.0	76.0
7.5	3.8	2.0	80.2
12	3.5	3.7	78.4

vicinity of unity as referred to before.

It is noteworthy to mention that the presented percentage conversion of Na^{+} in the initial synthetic solution, is related to the utilization efficiency of NaCl only, and it does not compare the corresponding utilization efficiency of NH_3. This explains the fact that higher percentage conversions are obtained sometimes though the ratio might deviate substantially from unity. It should be remembered that a very high efficiency in the utilization of the salt is necessarily accompanied by a low efficiency in the consumption of ammonia and vice versa. The optimum ratio permits the proper utilization of these two principal raw materials in order to provide higher efficiencies.

Table 4.2 depicts a typical filtrate analysis, resulted from synthetic saline water treated in the batch gas bubbler. While Table 4.3 shows the corresponding precipitate analysis. Similar results for the case of sabkha feed are given in appendix C .

4.1.6 Sabkha Water Feed

A typical sabkha water was synthesized by dissolving 25 grams of sabkha salt. The main composition of the sabkha is provided in Table 4.4. This sabkha water was also used as feed to the batch gas bubbler. Different conditions were considered with sabkha feed.

In Figure 4.18 the effect of carbonation time on the sodium ion conversion is shown. The general trend is similar to the cases of

Table 4.2 Filtrate Analysis (Batch Gas Bubbler)

Feed: Synthetic Saline Water
Flow: 2 l/min.
Temperature: 22 °C

Ini. NH_3 M	Ini. NaCl g	Time hr	Flow l/min.	% CO_3^{--} wt	% HCO_3^- wt	% Cl^- wt	$T.A^*$ wt	NH_4Cl g/l	Filt. NaCl g/l	%Conversion
2.5M	30	1.5	2	---	2.7	15.1	18.7	57.3	13.5	54.9
2.5M	30	2	2	---	2.2	16	15.3	46.1	12.9	56.8
3.5M	25	1.5	2	2.1	4.0	14.	47.3	26.7	8.6	65.4
3.5M	25	2	2	0.5	4.8	14.1	38.5	26.3	6.2	75
4.5M	25	2.5	3	2.1	5.3	14.4	46.3	52.1	5.4	78.4

$T.A^*$ = Total Alkalinity

Ini = Initial

Filt. = Filtrate

Table 4.3 Precipitate Analysis (B.G.Bubbler)

Feed: Synthetic Saline Water
Flow: 2 l/min.
Temperature: 22 °C

Ini NH_3 M	Ini NaCl g	Carb Time hr	Flow Rate l/min.	% CO_3 wt	% HCO_3 wt	% Cl wt	ppt NaCl g
2.5M	30	1.5	2	11.5	50.3	15.1	18.1
2.5M	30	2	2	5.7	62.0	17.4	17.8
3.5M	25	1.5	2	64.3	---	17.7	14.3
3.5M	25	2	2	54.3	---	26.6	16
4.5M	25	2.5	3	8.3	38.3	11.4	20.5

Ini = Initial
ppt = Precipitate
Carb = Carbonation

Table 4.4 Chemical Composition of the Sabkha Salt used for this Study

Major Ions	Concentration (mg/g)
Sodium (Na^+)	362.0
Potassium (K^+)	3.0
Magnesium (Mg^{++})	4.0
Calcium (Ca^{++})	0.2
Chlorides (Cl^-)	615.2
Sulfates (SO_4^{--})	7.4

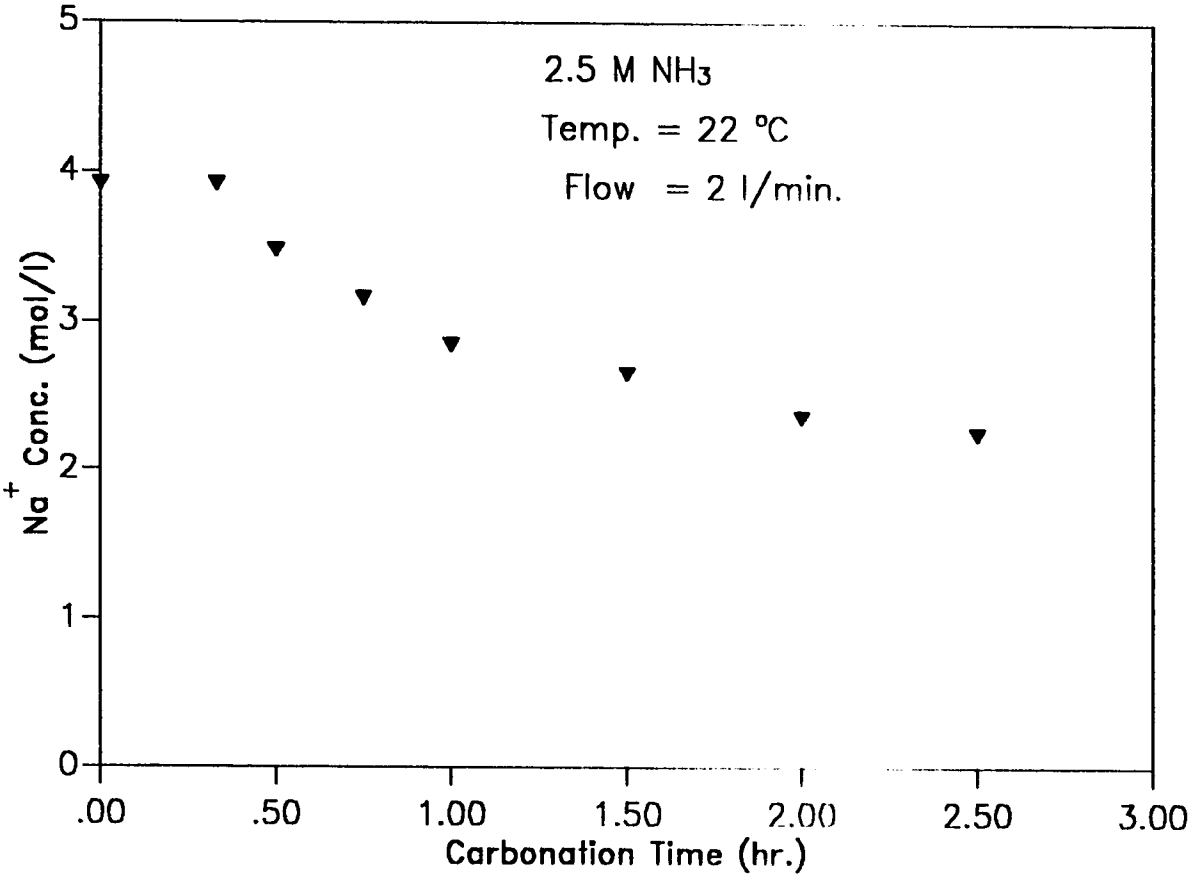

Figure 4.18 Reduction of Na^+ Concentration (Sabkha)

synthetic saline water. For this condition of 2.5 molar ammonia solution the conversion is 42.6%, while Figure 4.19 is for 3.5 molar ammonia and has a conversion of 58.0%. The increase of the conversion of sodium ion is due to the increase of ammonia concentration that favors the formation of ammonium bicarbonates.

Figures 4.20 and 4.21 are for 4.5 molar and 7.5 molar ammonia respectively keeping all the conditions the same except the concentration of ammonia. These two figures in turn emphasize the role of ammonia concentration in the overall efficiency. Indeed, the conversion has increased to 62.0% and to 66.8% respectively.

However, it important to compare the experimental results obtained from the batch gas bubbler when synthetic and sabkha waters were fed. It is apparent that the performance of the separation is higher when the synthetic saline water was used. This is due to the fact that synthetic water has pure NaCl, with practically no other elements or impurities.

The presence of other elements and impurities may somehow contribute to inhibition of absorption of CO_2, or consumption of NH_3 Such as the reactions of NH_3 with ions of Mg^{+2} and Ca^{+2} as in the case of sabkha feed.

$$Ca^{++} + (NH_4)_2CO_3 \rightarrow CaCO_3 + 2NH_4^{+} \qquad (4.6)$$

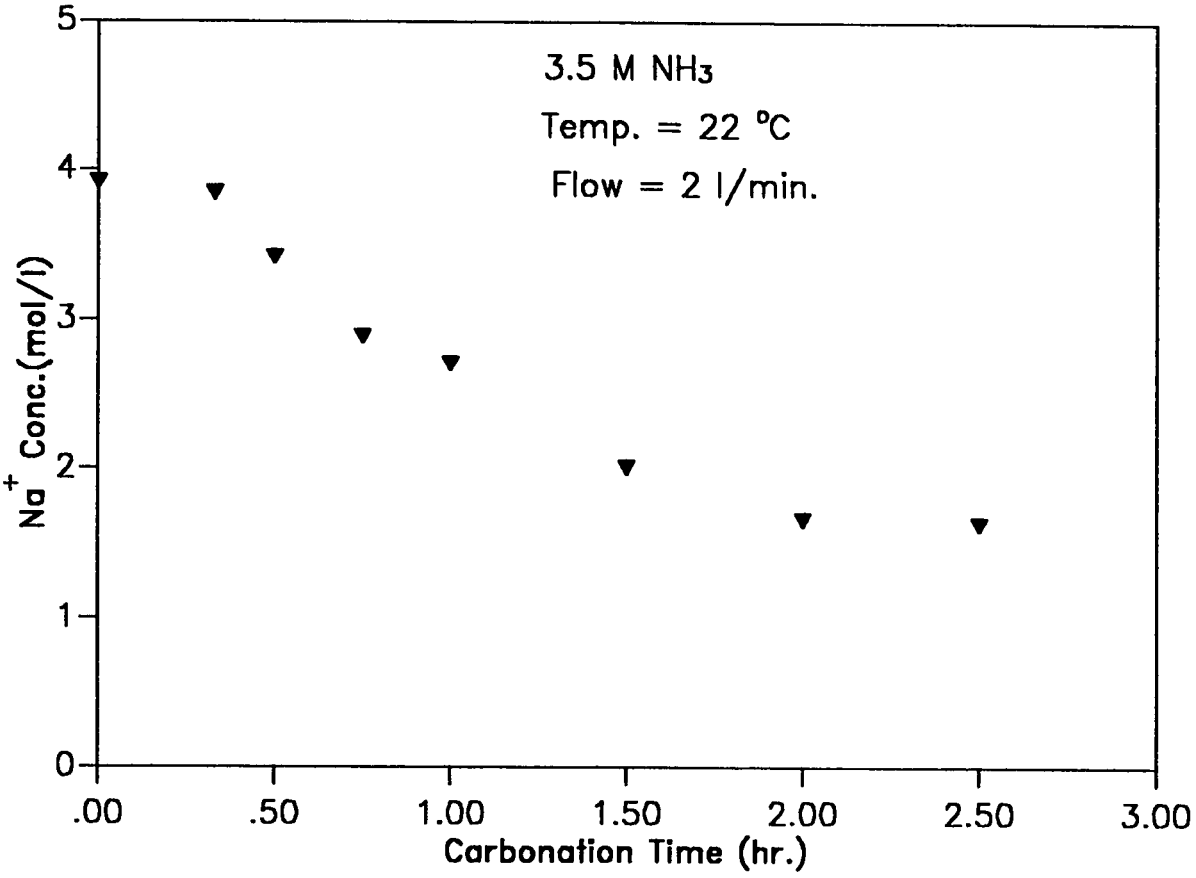

Figure 4.19 Reduction of Na^+ Concentration (Sabkha)

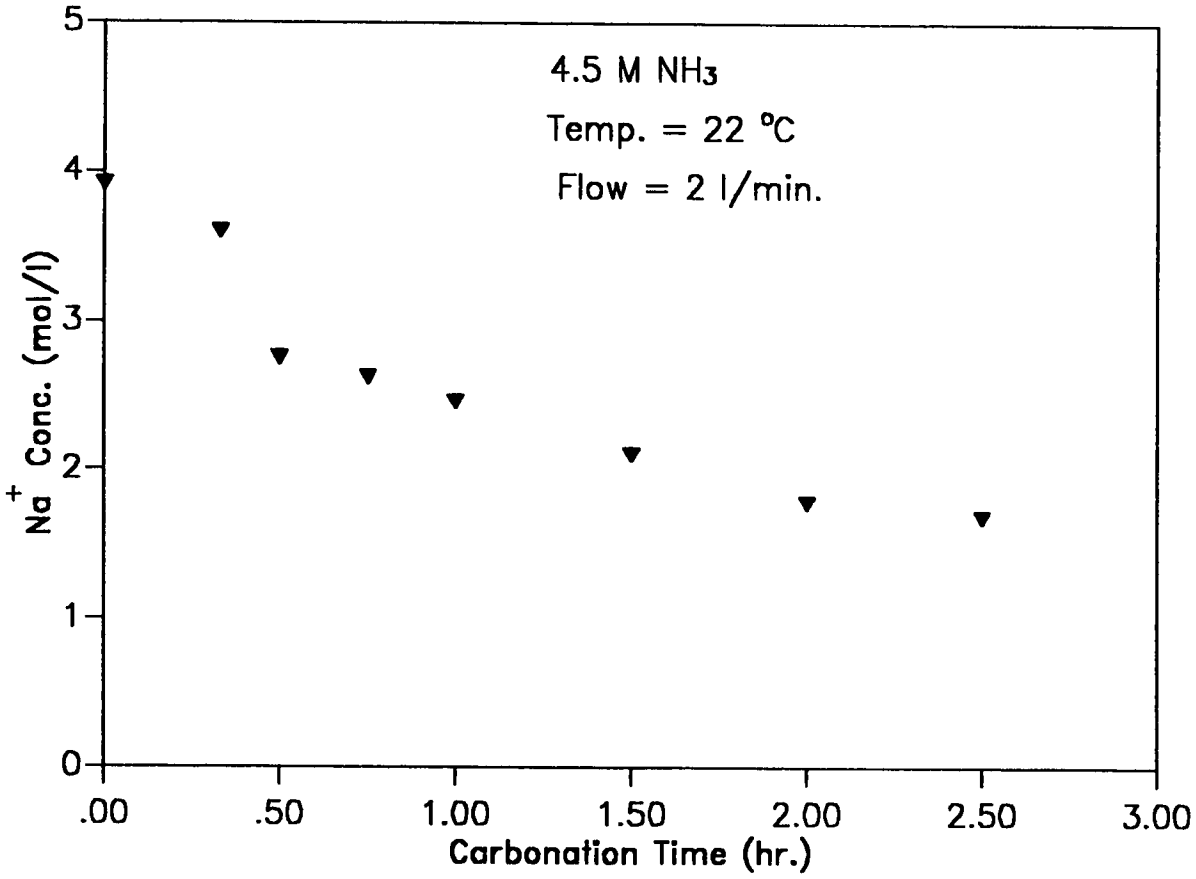

Figure 4.20 Reduction of Na^+ Concentration (Sabkha)

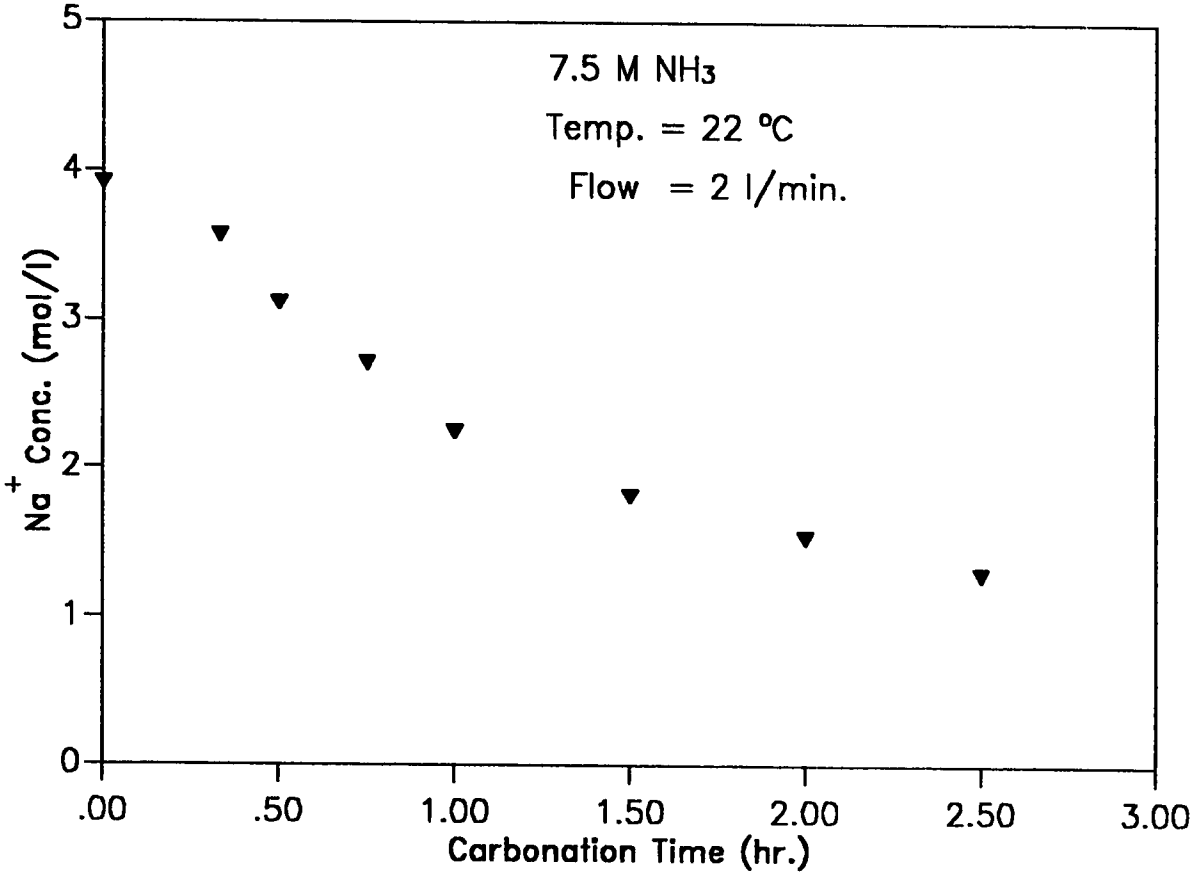

Figure 4.21 Reduction of Na^+ Concentration (Sabkha)

$$Mg^{++} + (NH_4)_2CO_3 \rightarrow MgCO_3 + 2NH_4^+ \quad (4.7)$$

$$MgCO_3 + (NH_4)_2CO_3 + 4H_2O \rightarrow MgCO_3.(NH_4)_2CO_3.4H_2O \quad (4.8)$$

$$Mg^{++} + 2NH_4OH \rightarrow Mg(OH)_2 + 2NH_4^+ \quad (4.9)$$

4.2 Separation Using the Bubble Column

This column is identical to the column used for hydrodynamic parameters except that it is shorter in length. The column is 8.9 cm inside diameter and 40 cm high. The column can handle large quantities of solution (2 liter). The are two orifices each of 2.5 mm situated at the bottom center. When this column was first employed, frequent interruptions of the gas flow were encountered due to the precipitates of sodium bicarbonate on the orifices.

The course of the experimental study was modified at this stage to reduce the aforementioned difficulty and to avoid frequent cleaning of the orifice. The modification introduced and followed afterwards for the rest of experimental studies in the bubble column, was to eliminate the addition of NaCl in the case of synthetic saline water or the sabkha salt in the sabkha water, before the carbonation is done. This means, the precipitate formation reaction of $NaHCO_3$, is to be

carried out in a separate vessel. Thus, the bubble column functions as a contactor between CO_2 gas and ammoniacal solution.

The main reactions that take place in the column are:

$$2NH_3 + CO_2 + H_2O$$

%=% (NH sub 4) sub 2 CO sub 3 (4.10)

$$(NH_4)_2CO_3 + H_2O + CO_2 = 2NH_4HCO_3 \quad (4.11)$$

In this case, precipitation will be observed only when the solubility products of ammonium carbonate and bicarbonate are exceeded. Figure 4.22 shows the solubility of pertinate salts in water. It is obvious from the figure that the sodium bicarbonate is the least soluble salt and that its removal will hinder or will retard the precipitation inside the column, unless the next less soluble component which is ammonium bicarbonate exceeds its solubility product.

At an operating temperature of 22 $^{\circ}C$, the most soluble salts are ammonium chloride and sodium chloride. The illustration of the experimental scheme is given in Figure 4.23.

To investigate the performance difference between the two experimental techniques of carbonation used for the batch gas bubbler and the bubble column, a test was carried out on the batch gas bubbler using synthetic saline water. The carbonation was done once on ammoniacal brine solution (presence of NaCl). While in the other case the carbonation was carried out with ammoniacal non-brine solution

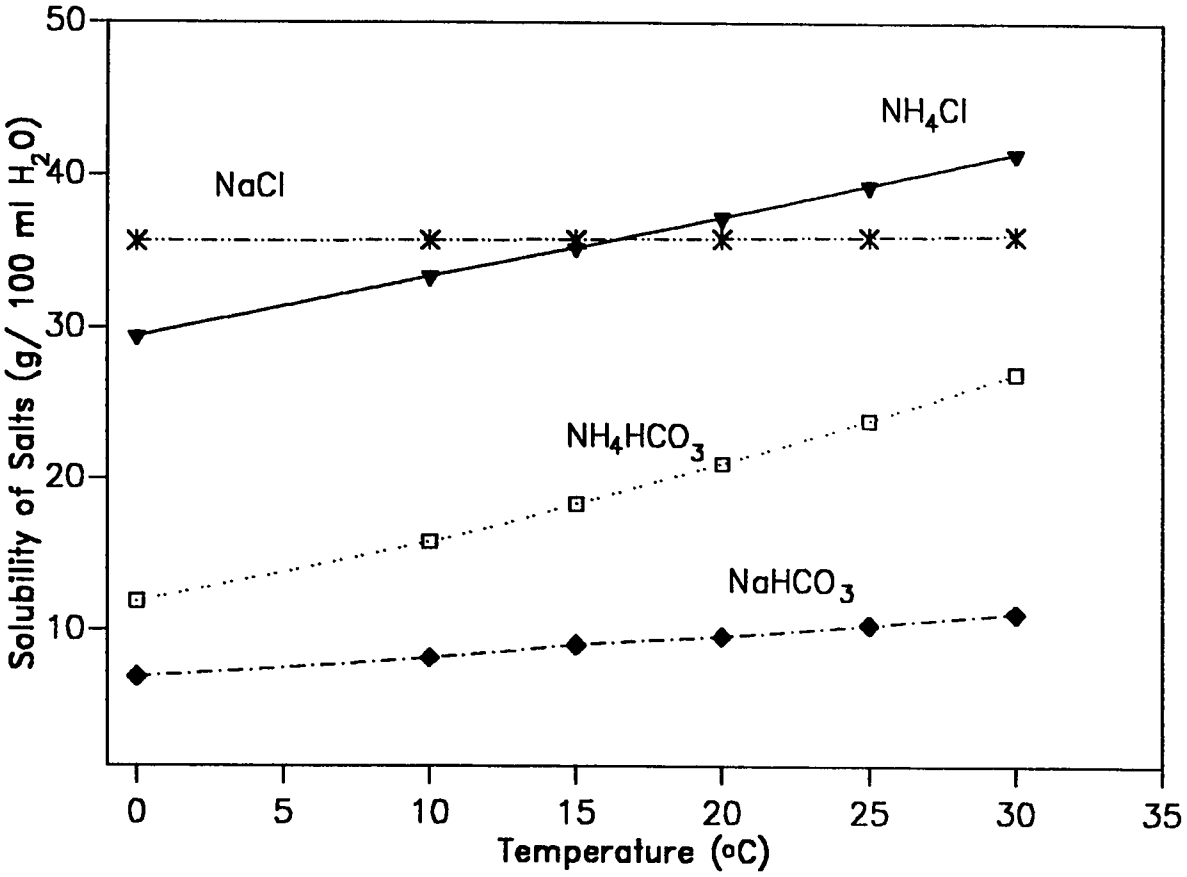

Figure 4.22 Solubility of Salts in Water

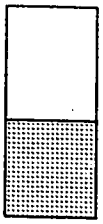

NH3 Solution

t = 0
Salt Content

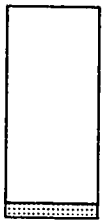

100 g
(a)

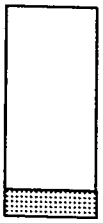

150 g
(b)

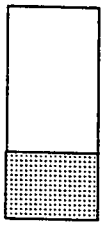

200 g
(c)

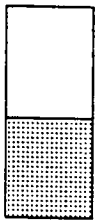

250g
(c)

t = 30 min.
Find Na+ remaining
after Filtration

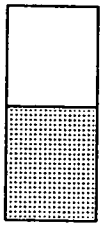

(a)

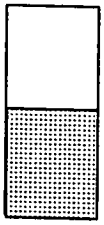

(b)

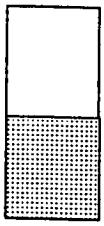

(c)

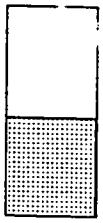

(c)

t = 1 hr
Find out Na+
Remaining after
Filtration

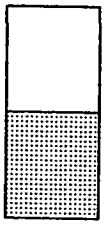

(a)

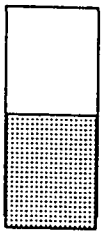

(b)

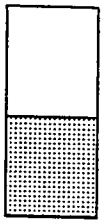

(c)

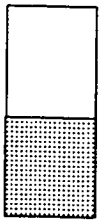

(c)

Figure 4.23 Schematic Diagram of the Modified Experimental Technique for the Bubble Column.

(absence of NaCl), and the precipitation reaction was done in a separate vessels.

Figure 4.24 depicts the sodium ion removal as the carbonation time increases, when a solution of 3.5 M ammonia is carbonated and the precipitation of 4.3 M NaCl is carried out in separate vessels. Figure 4.25 shows the comparison between the two schemes, when 3.5 M ammonia solution and 4.3 M NaCl are treated in the batch gas bubbler.

The result shows that the carbonation of ammoniacal brine solution, which permits all the reactions to occur inside the contactor is 10% better than the case which separates the precipitation reaction. This may be attributed to the fact that, when sodium bicarbonate precipitates the formation reaction of this $NaHCO_3$ will be enhanced by the shift of the reaction according to the law of mass action.

However, until the present difficulty of plugging of the orifices by precipitation is resolved by investigating different design features of the bubble column, the use of the second scheme as an alternative is worth considering. The difference in performance is evident for this specific condition.

The temperature time profile was studied under non-isothermal conditions for different flow rates of CO_2, under different ammonia concentration solutions in the column. This was carried out by stop-

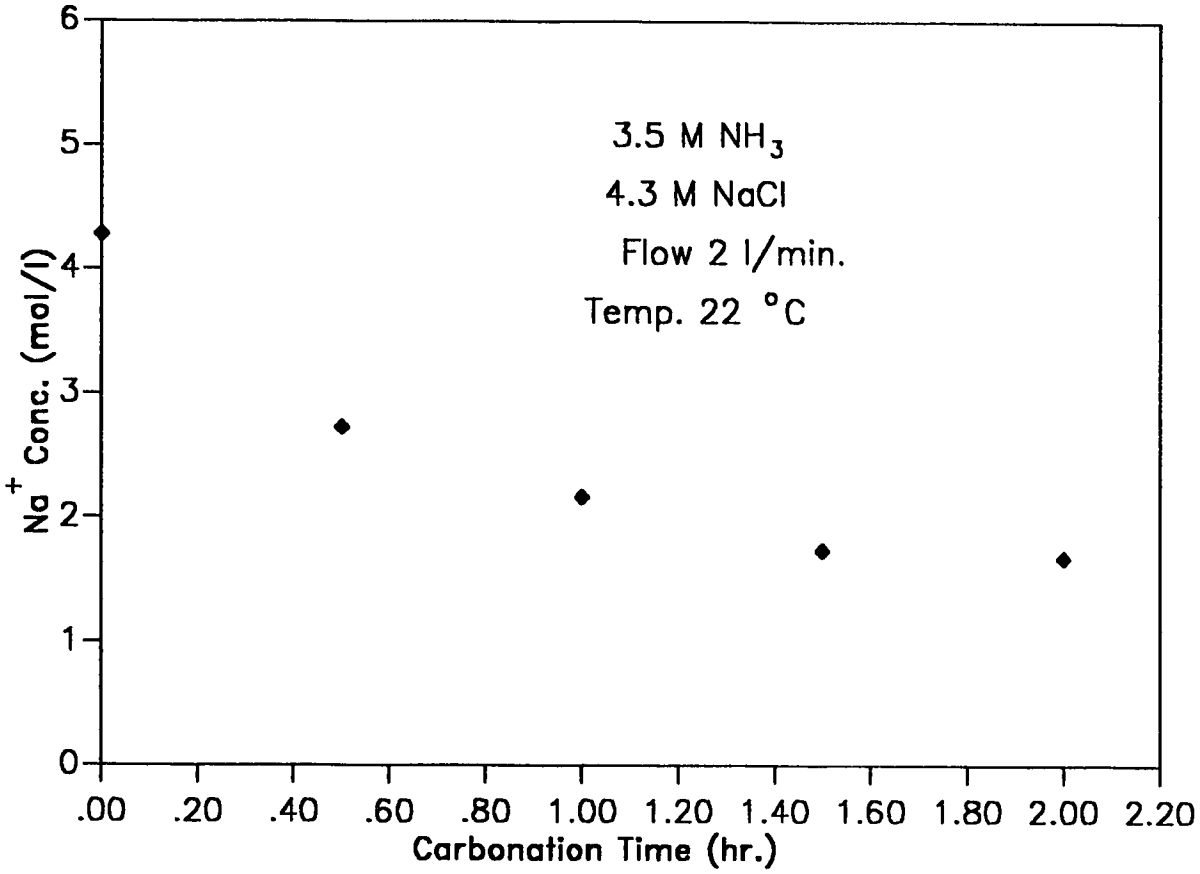

Figure 4.24 Effect of Carbonation on Na^+ Removal by the Modified Technique

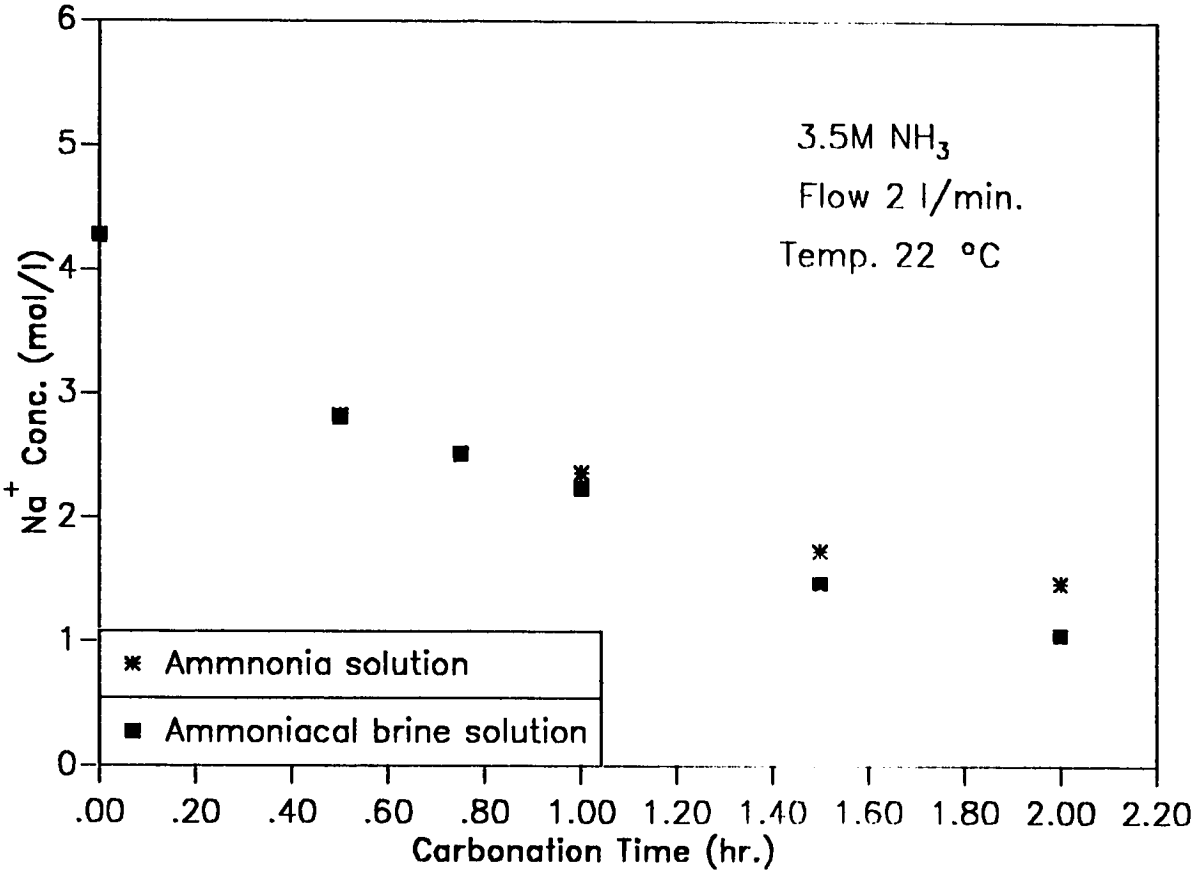

Figure 4.25 Comparison of the Two Exp. Schemes

ping the cooling water in the jacket. The result shows that the temperature/time profile passes through a maximum at about 20 minutes, regardless of the flow rate and the concentrations of the solution.

The temperature time profile is depicted in Figure 4.26. This is obtained when 2.5 M ammonia solution was carbonated at the rate of 9 l/min. Figures for other conditions are given in Appendix D.

To see the extent of CO_2 absorption in the bubble column which operates at the flow rate of 11.8 l/min. and at the temperature of 22 $^{\circ}C$, some experiments were carried out using 2.5 M, 3.5 M, and 4.5 M ammonia solutions. The result is given in Table 4.5 where the carbonation time involved reaches up to 1 hour.

Table 4.5 shows the amount of CO_2 absorbed increases with the increase of the initial concentration of NH_3, and the rate of absorption for any solution diminishes as the carbonation time increases, until the saturation of ammonium carbonates is reached, where any further mole of CO_2 absorbed will entail the removal of another mole of CO_2 from the solution by precipitation of ammonium carbonate.

4.2.1 Synthetic Saline Water Feed

Figures 4.27-4.31 show the results obtained when synthetic saline water was treated in the bubble column at carbonation rate of 11.8 l/min. The column capacity was 2 litres and the operating

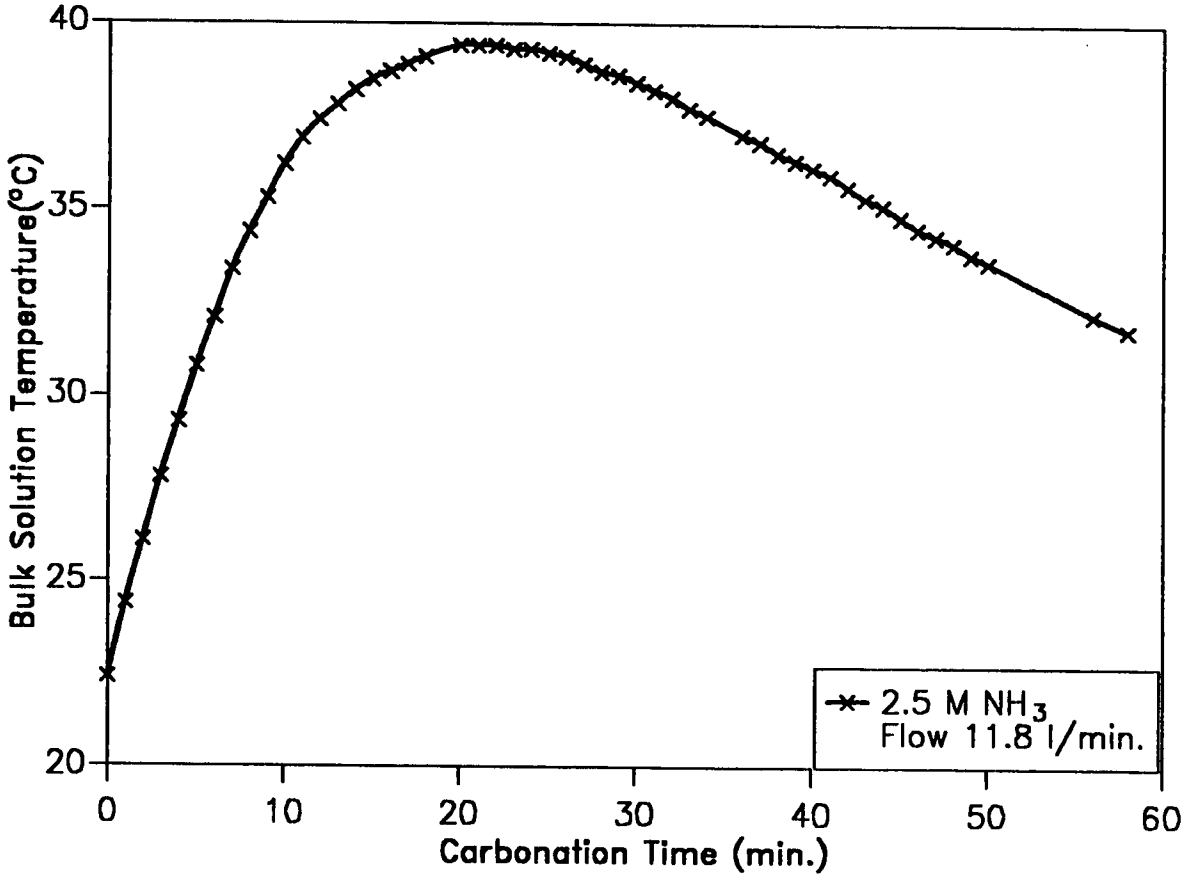

Figure 4.26 Temperature–Time Profile (B.Column)

Table 4.5 Extent of Absorption of CO_2 in Bubble Column

Flow: 11.8 l/min.
Temperature: 22 oC

NH_3 (M)	Absorbed CO_2 (Mole/l)	
	Time (hr) 0.5	Time (hr) 1.0
2.5	1.5833	2.0042
3.5	2.3958	2.5625
4.5	2.6875	2.8333

temperature was 22 °C. It can be concluded from this result that the precipitation of the sodium bicarbonate can be seen whenever the carbonation system provides a concentration of carbon dioxide of 1.5 mole per litre or above. The results in Figures 4.27 - 4.31 indicate that the conversion of Na^{+} increases with the increase of carbonation time. This same fact, was already found in the batch gas bubbler. Therefore, the performance of system and the efficiency of NaCl conversion are a function of the amount of CO_2 absorbed. Figure 4.27 is for 2.5 molar NH_3 solution, while Figures 4.28 and 4.29 are for higher ammonia concentrations, specifically 3.5 M and 4.5 M, respectively.

4.2.2 Effect of the Initial Brine Concentration

The concentration of NaCl that regulates the salinity of the solution is one of major factors that influences the process separation. This effect was seen in the case of batch gas bubbler when both types of feed water were used. Here, it also plays a great role by affecting the efficiency of separation.

Figure 4.27 depicts the effect of the salinity when a fixed ammonia solution of 2.5 M is used, while the concentration of NaCl varies from 100 to 250 gram per litre. The result shows that, when the initial concentration of salt goes up, the conversion of NaCl increases, and hence the efficiency of Na^{+} separation is directly proportional for this condition to the strength of salinity of the solution.

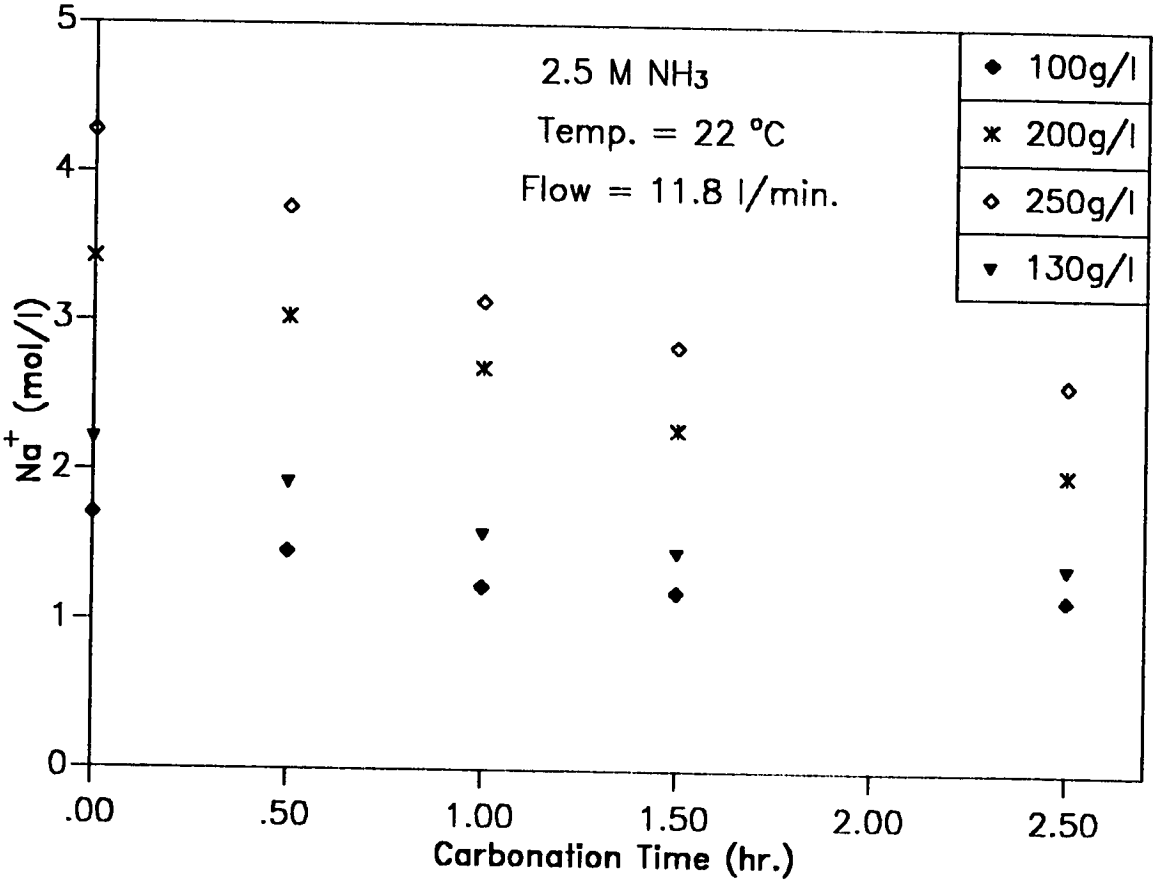

Figure 4.27 Effect of Salinity (B.C. & S.S.W)

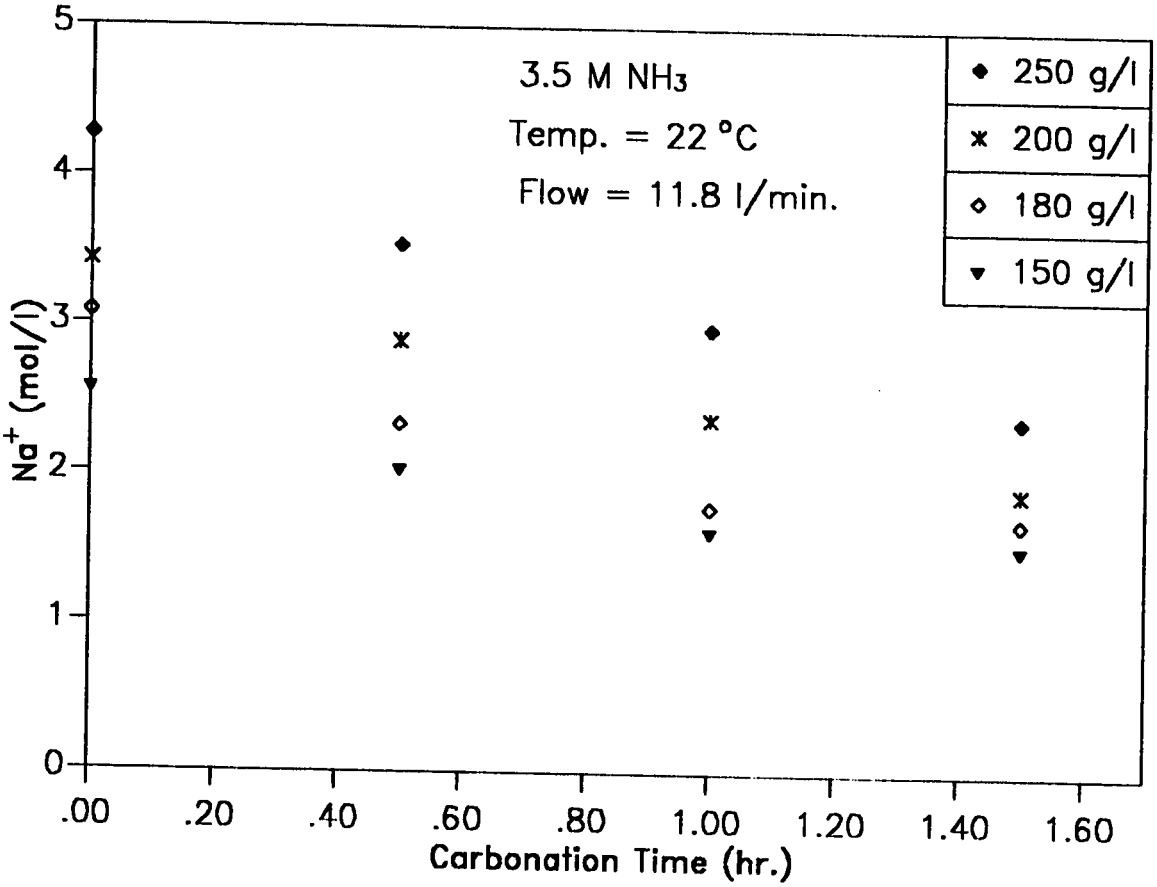

Figure 4.28 Effect of Salinity (B.C. & S.S.W)

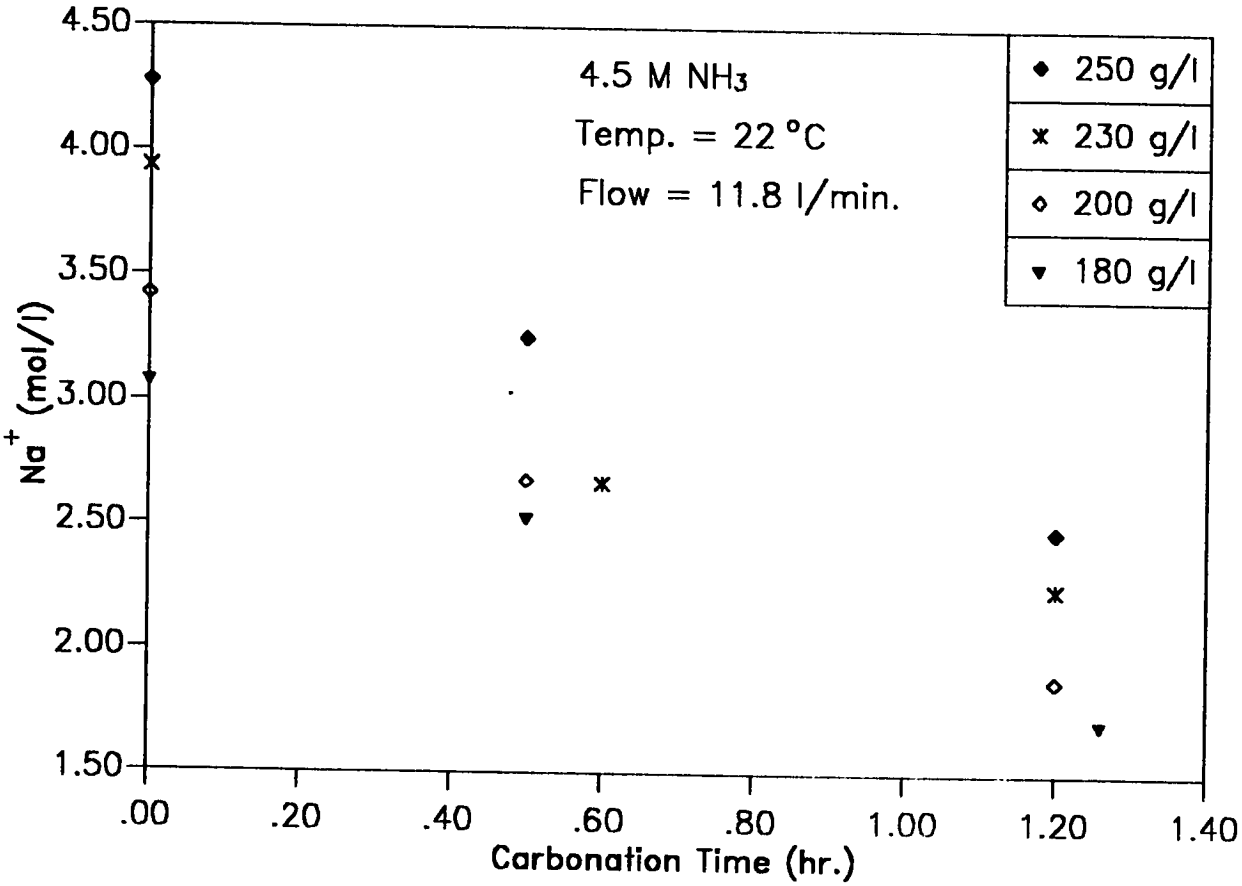

Figure 4.29 Effect of salinity (B.C. & S.S.W)

In Figure 4.28 the result is displayed when 3.5 M solution of ammonia was used. The efficiency of conversion of NaCl is almost the same for the range of salinity considered. Similar trends are also seen in Figure 4.29, where the ammonia concentration is now 4.5 M. Here the efficiencies obtained using different salinities are quite close to each other, therefore; there is not much effect.

4.2.3 Effect of the Initial Ammonia Concentration

The ammoniation of the brine is essential for the process reaction to form carbonates of ammonia. The concentration of NH_3 affects the solution properties and later the efficiency of NaCl conversion. For this specific study where the synthetic saline water was used as feed water to the bubble column, the effect of ammonia concentration is evident. Figures 4.30 and 4.31 show the effect of ammonia concentration on the conversion of Na^+ as a function of carbonation time. In fact, Figure 4.30 displays the result, when a constant salinity of 200 gram per litre of NaCl is used for 2.5 and 3.5 molar solutions of ammonia.

It is found, that the conversion efficiency of NaCl is higher when higher concentrations of NH_3 is used. This is because of the increase rate of absorption of CO_2 and subsequent increase in the rate of formation of $NaHCO_3$

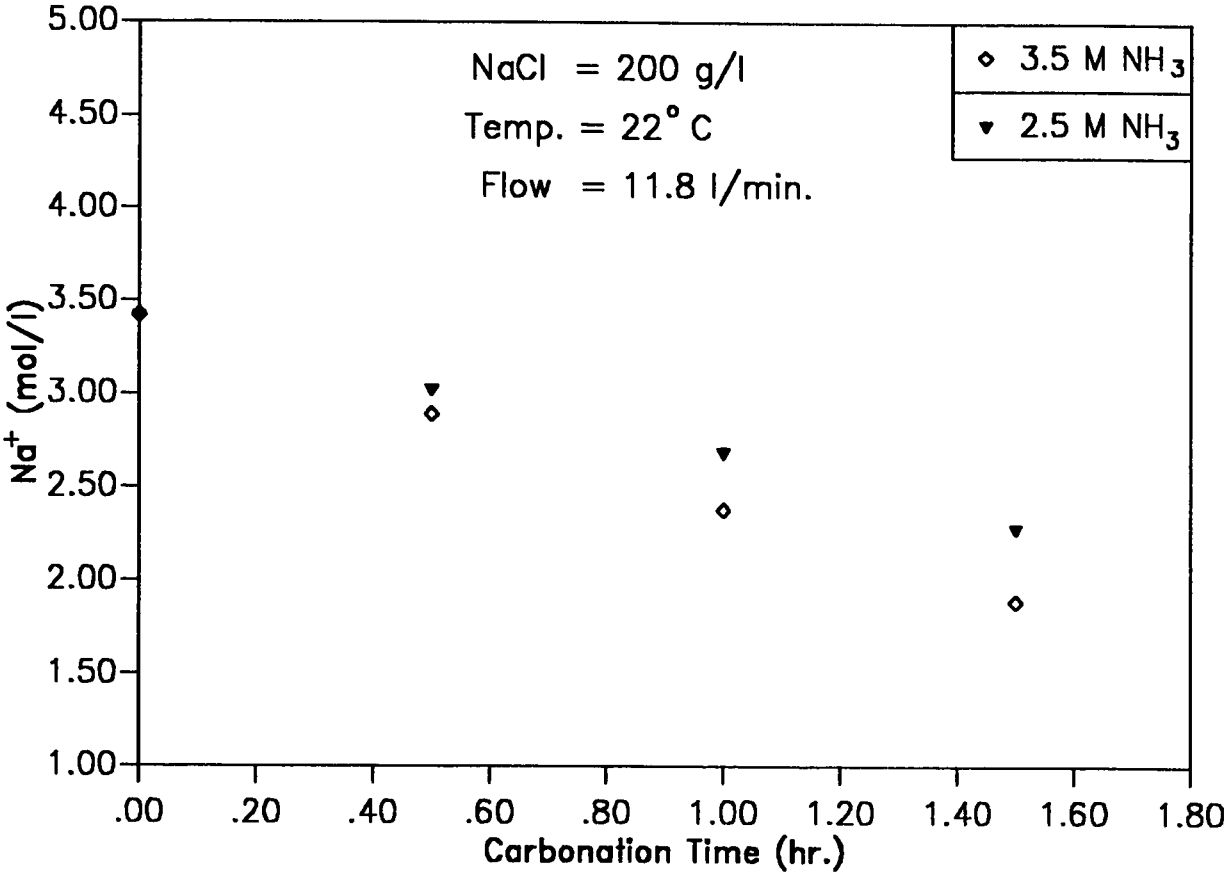

Figure 4.30 Effect of Ammonia Concentration (S.S.W & B.C.)

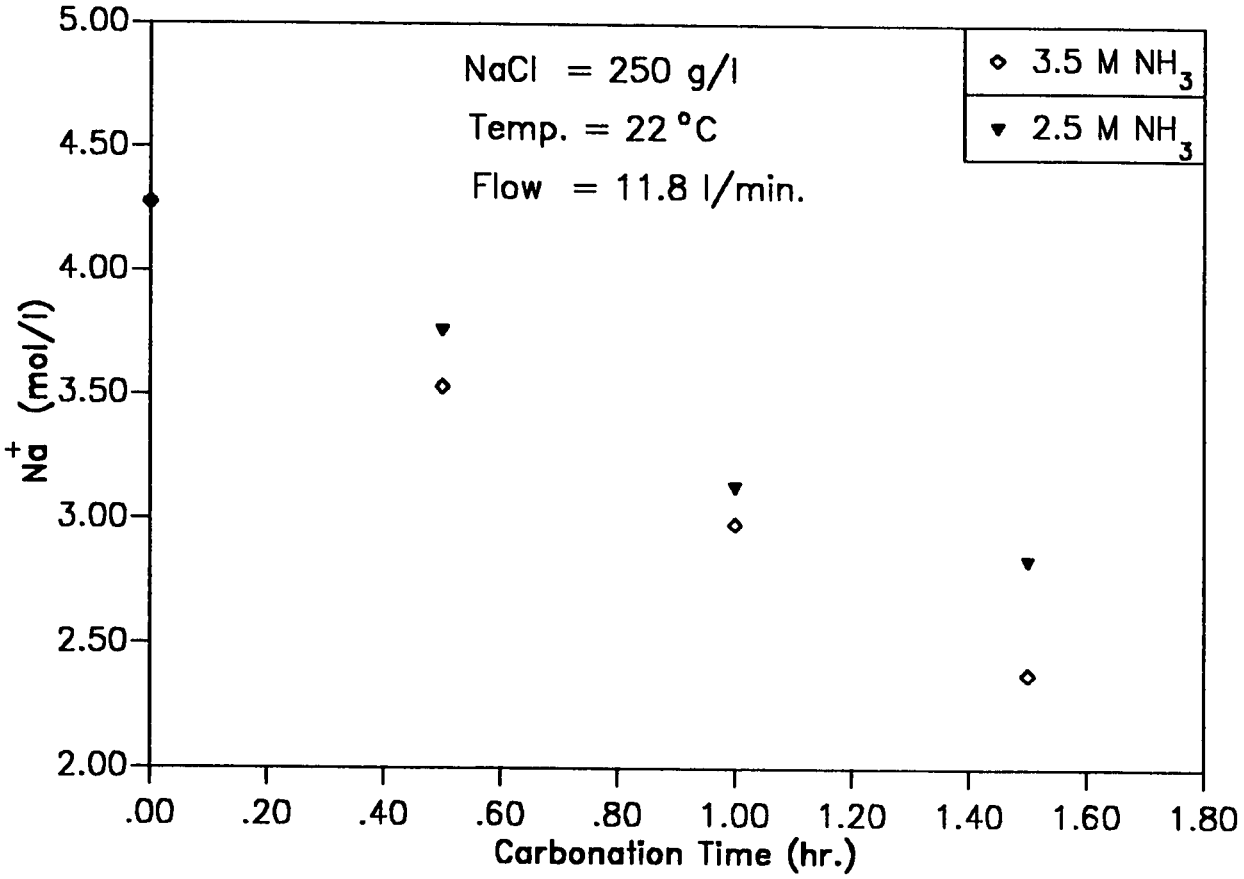

Figure 4.31 Effect of Ammonia Concentration (S.S.W & B.C.)

4.2.4 Effect of the Initial Concentration Ratio of $NH_3/NaCl$

The use of the knowledge of the important ratio of $NH_3/NaCl$ was shown in the case of the batch gas bubbler. Tables 4.6 - 4.8 depict the effect of $NH_3/NaCl$ on the percentage conversion of NaCl when the bubble column reactor was employed. Table 4.6 specifically shows for the case of 2.5 M NH_3 with carbonation time of 2.5 hr.

It is clear from Table 4.6 that the best conversion is obtained, when the ratio of $NH_3/NaCl$ is around 1, while Table 4.7 shows a similar result for 3.5 M NH_3 with 1.5 hr carbonation. This result shows the best ratio is 1.1 for the given condition, while the ratio of 0.8 represents the least percentage conversion on Na^+. Table 4.8 is for 4.5 M NH_3 with carbonation time limited to 1.2 hr. For this condition, the highest % conversion is obtained when the ratio $NH_3/NaCl$ is about 1.3.

4.2.5 Sabkha Water Feed

Preparation of sabkha feed is done exactly the same as the feed for the batch gas bubbler. The composition of sabkha salt is provided earlier in Table 4.4. Figures 4.32-4.34 depict the decrease of the sodium ion concentration with the carbonation time. Different salinity concentrations were employed.

Table 4.6 Effect of Concentration Ratio of NH_3/NaCl

Feed: Synthetic Saline Water
Flow: 11.8 li/min
Temperature: 22 °C
Carbonation Time: 2.5 hr.
contactor: Bubble Column

NH_3 (M)	NaCl (M)	NH_3/NaCl (ratio)	% Conversion [Na^+]
2.5	1.7	1.5	31.6
2.5	2.2	1.1	37.4
2.5	3.4	0.7	41.2
2.5	4.3	0.6	39.1

Table 4-7: Effect of Concentration Ratio of NH_3/NaCl

Feed: Synthetic Saline Water
Flow: 11.8 li/min
Temperature: 22 °C
Carbonation Time: 1.5 hr.
Contactor: Bubble Column

NH_3 (M)	NaCl (M)	NH_3/NaCl (ratio)	% Conversion [Na⁺]
3.5	2.6	1.4	40.8
3.5	3.1	1.1	45.1
3.5	3.4	1.0	44.7
3.5	4.3	0.8	44.4

Table 4-8: Effect of Concentration Ratio of NH_3/NaCl

Feed: Synthetic Saline Water
Flow: 11.8 li/min
Temperature: 22 oC
Carbonation Time: 1.2 hr.
Contactor: Bubble Column

NH_3 (M)	NaCl (M)	NH_3/NaCl (ratio)	% Conversion [Na⁺]
4.5	3.1	1.5	44.6
4.5	3.4	1.3	45.0
4.5	3.9	1.1	42.8
4.5	4.3	1.0	42.1

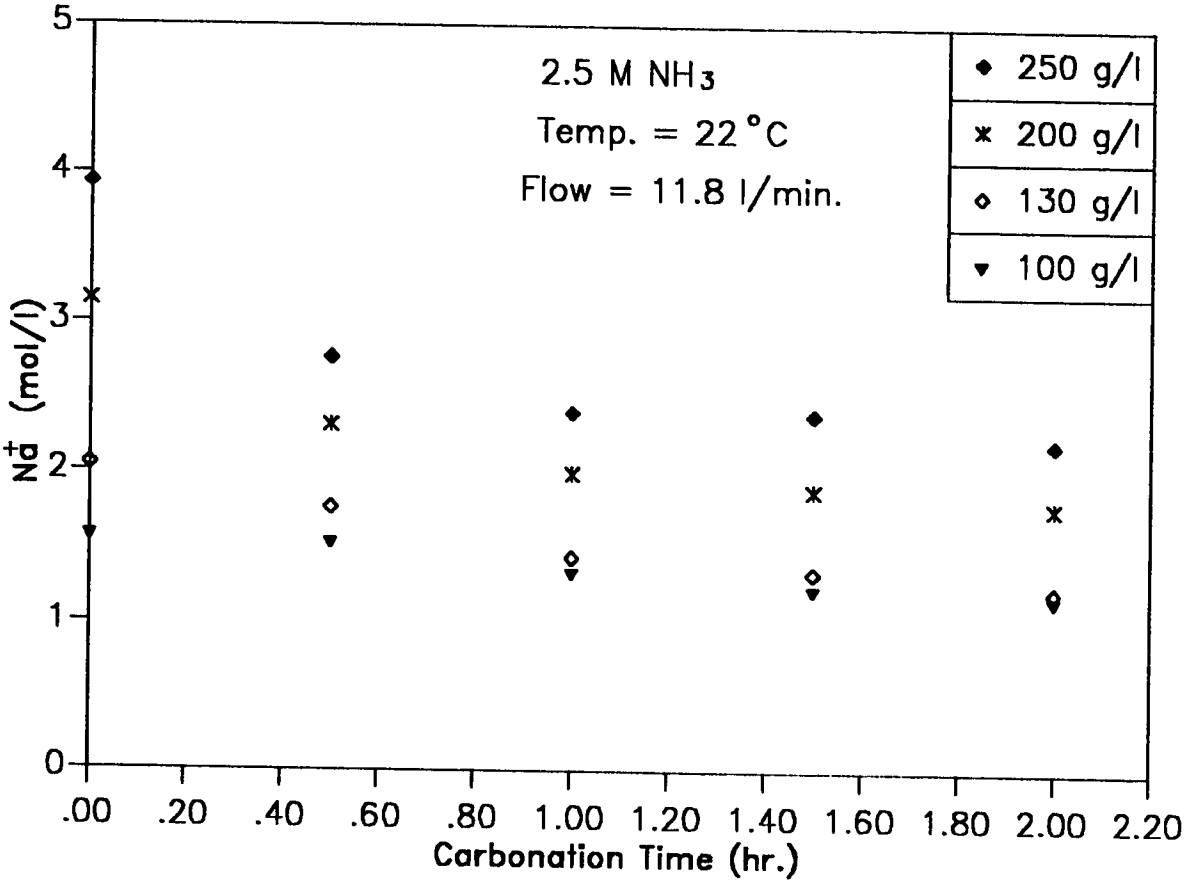

Figure 4.32 Effect of Sabkha Concentration (B.C.)

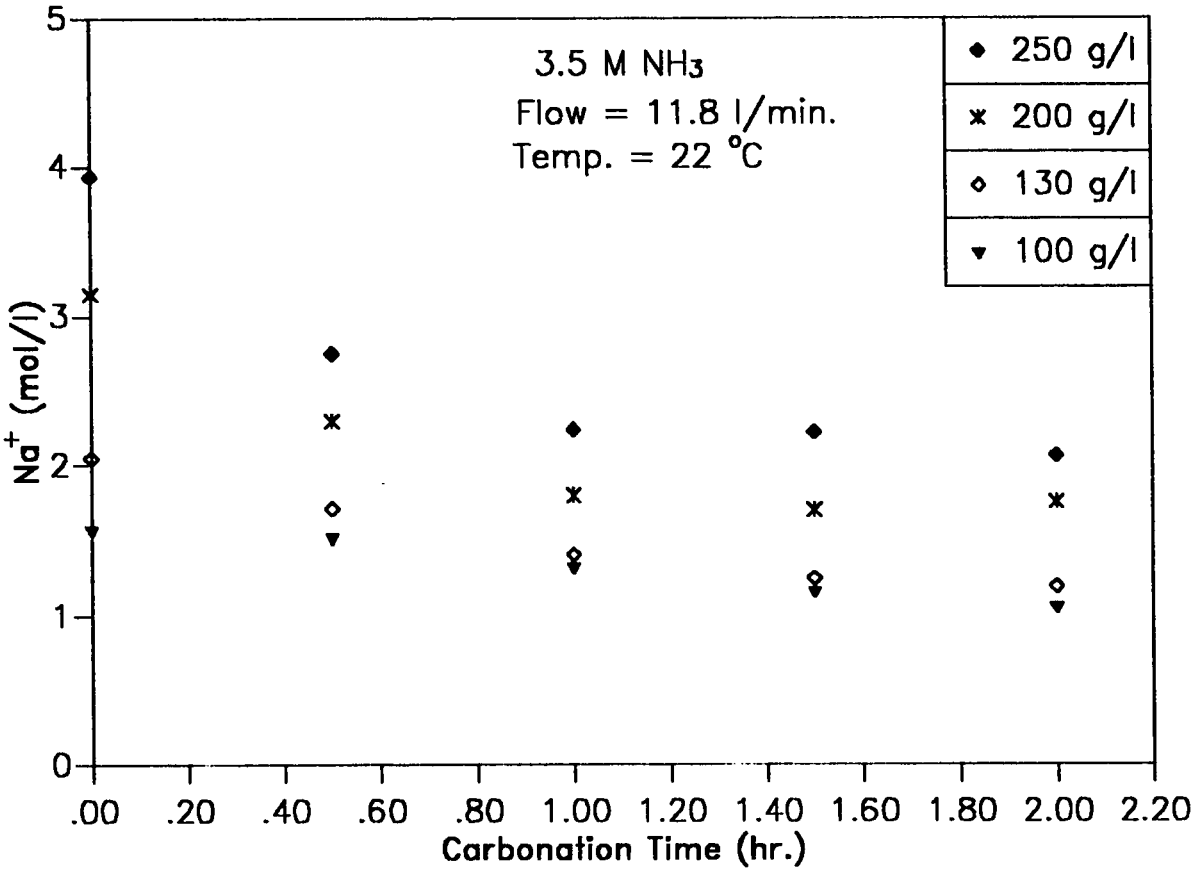

Figure 4.33 Effect of Sabkha Concentration (B.C.)

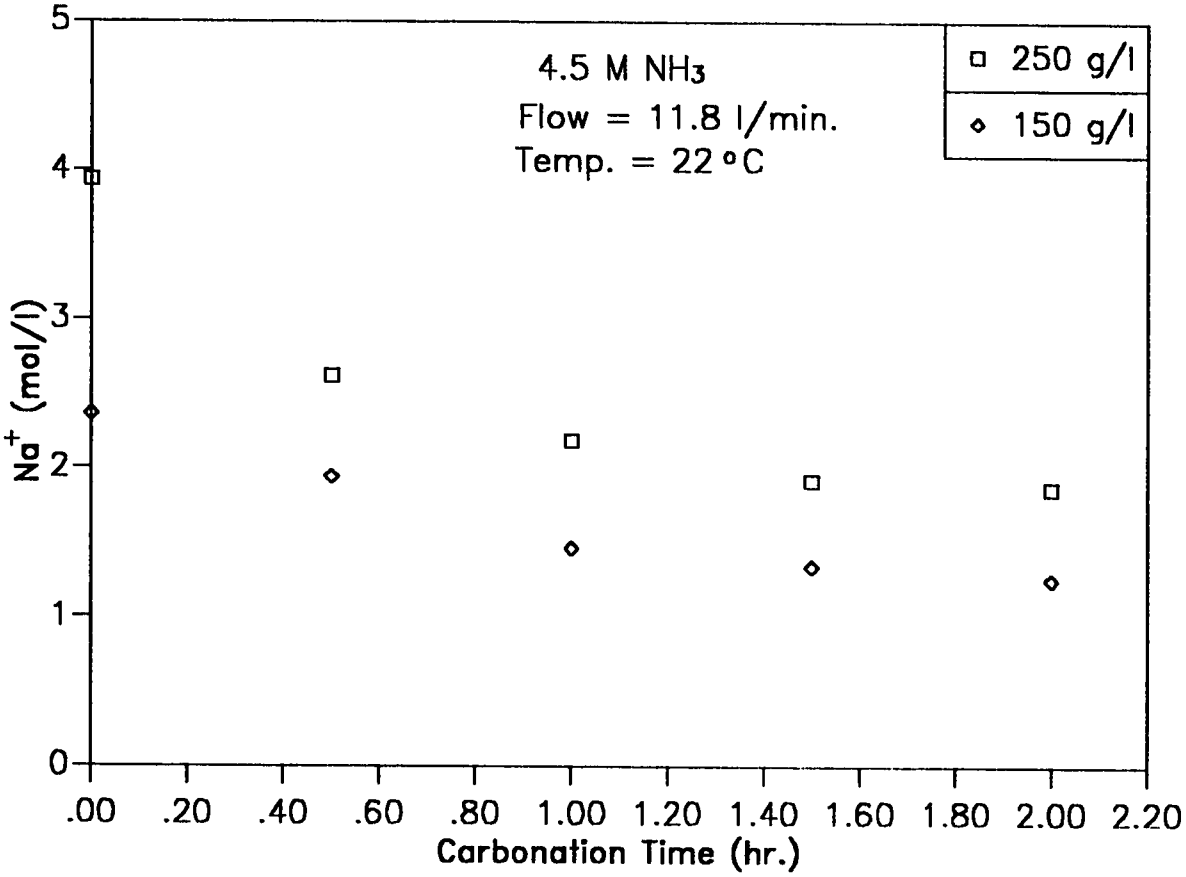

Figure 4.34 Effect of Sabkha Concentration (B.C.)

4.2.6 Initial Sabkha Salt Concentration

Various concentrations of sabkha salt were used in the bubble column to investigate the conversion efficiency. Figure 4.32 is for 2.5 M NH_3 solution with salinity ranging from 1.6 to 3.9 M $NaCl$. The result shows that the conversion of Na^+ increases with the time of carbonation.

For any specified carbonation time the conversion of Na^+ increases with salinity concentration, and therefore the efficiency of the process improves with higher salinity, indicating that there is abundance of NH_4HCO_3 to react with NaCl. Similar trends of result are obtained when higher concentrations of NH_3, 3.5 M and 4.5 M were used.

4.2.7 Initial Ammonia Concentration in the Sabkha

The effect of initial NH_3 concentration was investigated by studying ammoniacal solutions of 2.5 M, 3.5 M and 4.5 M respectively. Figure 4.35 shows the result for 2.5 M NH_3 concentration when sabkha concentration is 250 g/l. The results also indicate that increasing the concentration of initial NH_3 raises the conversion efficiency.

While Figure 4.36 is for 200 g/l sabkha salt. The results of this figure show that, the Na^+ removal increases with higher concentra-

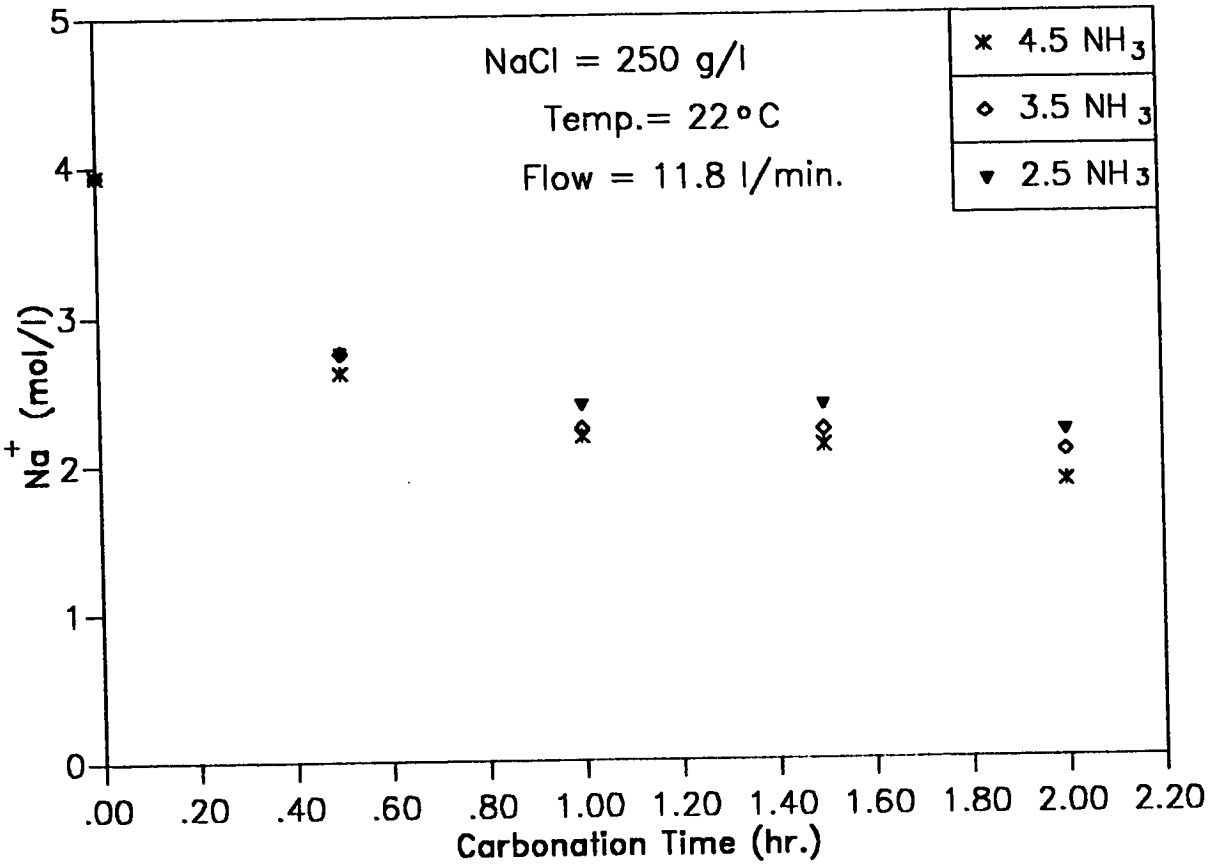

Figure 4.35 Effect of NH_3 Concentration on Sabkha (B.C.)

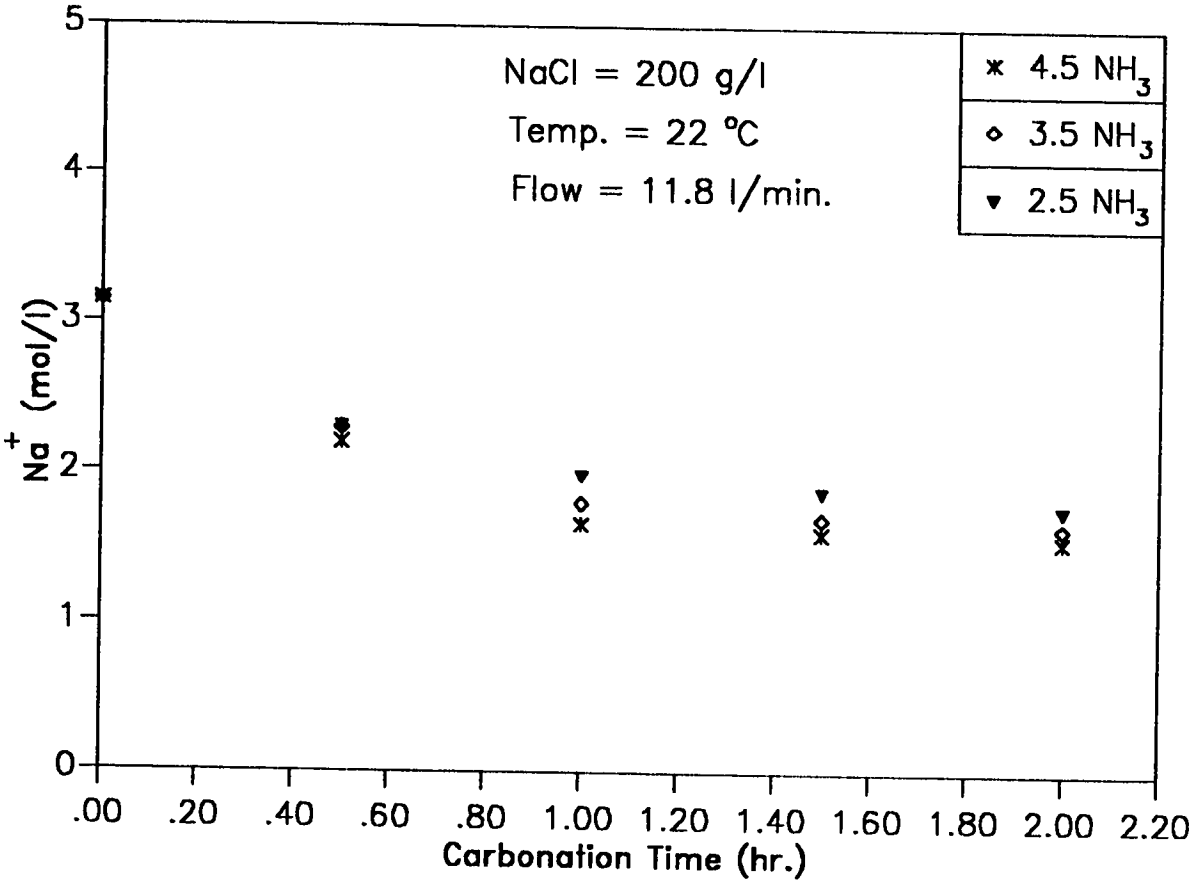

Figure 4.36 Effect of NH_3 Concentration on Sabkha (B.C.)

tion of NH_3. Therefore, conversion efficiency is promoted. Figure 4.37 is for 100 g/l of sabkha salt. The effect of NH_3 in this case, is to enhance the process conversion. Indeed the the concentration of Na^+ decreases with carbonation time and with increase of NH_3 concentration.

4.2.8 Initial Concentration Ratio of $NH_3/NaCl$ in the Sabkha

The effect of $NH_3/NaCl$ ratio of ammoniacal sabkha is shown in Tables 4.9 - 4.11. As noted earlier, there is a value of this ratio which will provide the maximum conversion of an initial Na^+ concentration.

Table 4.9 shows the result when 2.5 M NH_3 solution is used. The percentage conversion is found to increase with a decrease of this ratio from 1.6 to 0.6. It was expected that percentage conversion will diminish as the ratio takes values far from unity. However, in this case, although the ratio drops to 0.6, the conversion in effect assumes higher values. This is probably due to complex nature of sabkha, which somehow lowers the reactivity of NaCl and hence the actual concentration of NaCl available for reaction behaves as if it is less than the experimentally determined values. This results in the increase of the conversion efficiency as the NaCl concentration is increased and the formed NH_4HCO_3 is provided more chance to

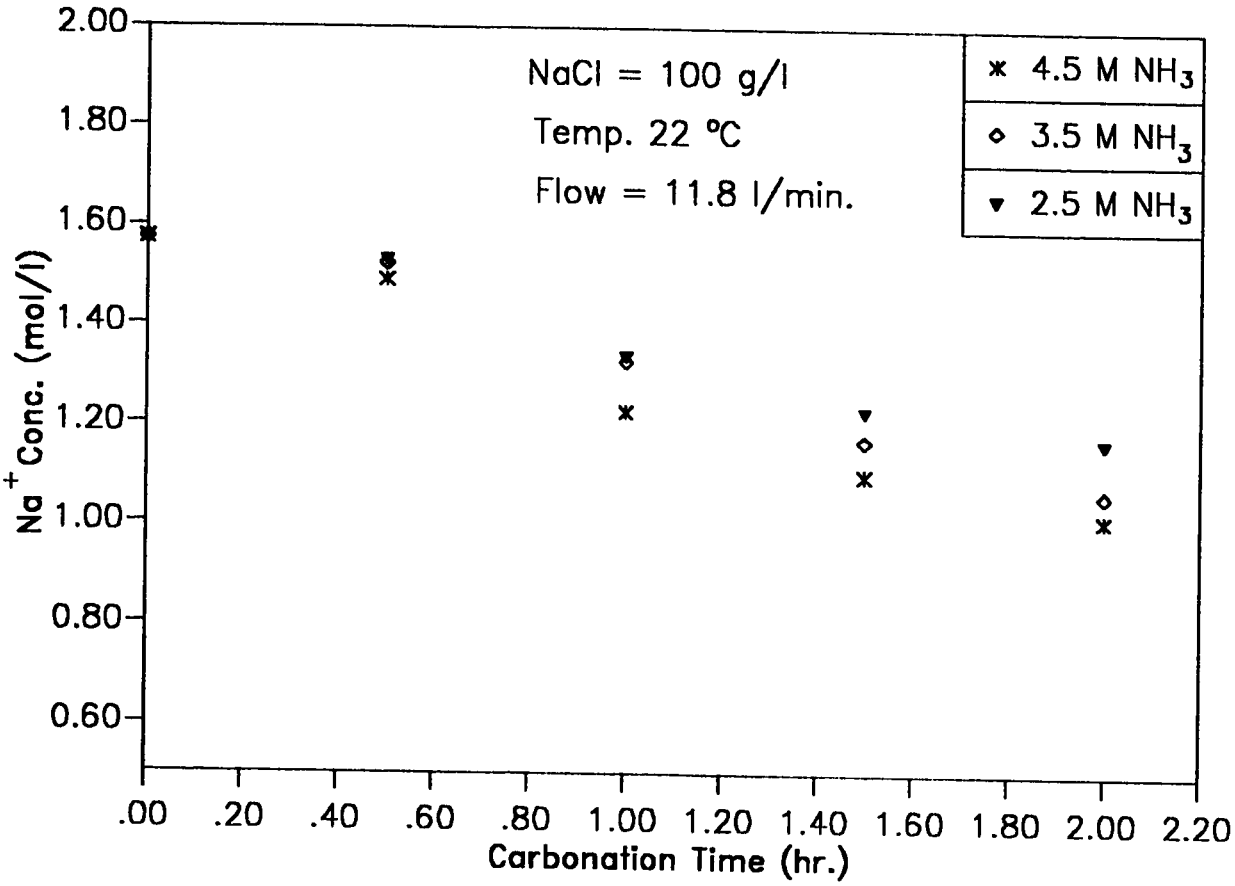

Figure 4.37 Effect of NH_3 Concentration on Sabkha (B.C.)

Table 4-9 Effect of Concentration Ratio of NH_3

Feed: Sabkha Water
Flow: 11.8 li/min
Temperature: 22 °C
Carbonation Time: 2 hr.
Contactor: Bubble Column

NH_3 (M)	NaCl (M)	NH_3/NaCl (ratio)	% Conversion [Na^+]
2.5	1.6	1.6	25.7
2.5	2.0	1.2	40.1
2.5	3.1	0.8	43.5
2.5	3.9	0.6	44.1

Table 4.10 Effect of Concentration Ratio of NH_3/NaCl

Feed: Sabkha Water
Flow: 11.8 li/min
Temperature: 22 °C
Carbonation Time: 2 hr.
Contactor: Bubble Column

NH_3 (M)	NaCl (M)	NH_3/NaCl (ratio)	% Conversion [Na^+]
3.5	1.6	2.2	32.5
3.5	2.0	1.7	41.5
3.5	3.1	1.1	44.2
3.5	3.9	0.9	47.6

Table 4.11 Effect of Concentration Ratio of NH_3/NaCl

Feed: Sabkha Water
Flow: 11.8 l/min
Temperature: 22 °C
Carbonation Time: 2 hr.
Contactor: Bubble Column

NH_3 (M)	NaCl (M)	NH_3/NaCl (ratio)	% Conversion [Na^+]
4.5	1.6	2.8	35.7
4.5	2.4	1.9	46.9
4.5	3.1	1.4	52.4
4.5	3.9	1.1	50.6

react.

Table 4.10 depicts the effect of $NH_3/NaCl$ in the sabkha when NH_3 is 3.5 M. The percentage conversion of Na^+ is found to decrease to 32.5 as the ratio reaches 2.2 and increases to a value of 47.6 as the ratio drops to 0.9.

Table 4.11 shows the effect of $NH_3/NaCl$ in sabkha salt solution when 4.5 M NH_3 is used. The ratio studied ranged between 2.9 to 1.1. It is clear that decreasing the ratio from 2.9 promotes the percentage conversion. This is in accordance with results obtained before.

Therefore, it can be concluded that the ratio of $NH_3/NaCl$ in sabkha salt solution affects the process separation. The percentage conversion generally approaches higher values when the ratio drops below unity.

4.2.9 Reactor Type The performance of the small scale Batch Gas Bubbler (B.G.B) and of the Bubble Column used are found to be different for the same conditions and types of feed. This is shown by the percentage conversions given in Tables 4.1 - 4.11.

The differences are attributed to the following:

a) Design of Gas distributor. In the case of the Bubble Column (B.C), two orifices each of 2.5 mm diameter are used while a

wider mouth of about 10 mm diameter is used in the case of the B.G. Bubbler.

b) The superficial velocities of feed gas are different for the two contactors (1.7 cm/s and 3.2 cm/s), for B.G.B and B.C respectively.

c) The quantitative measurement of CO_2 absorption gives higher values for the case of the B.G. Bubbler as shown in Figure 4.5.

d) The temperature control system is much easier and more efficient in the case of the B.G.Bubbler, since the quantity of solution is only 100 ml compared to 2 litres in the case of the bubble column.

f) The mixing efficencies of the two contactors are different because of the bubble sizes formed and the quantities of the solution involved.

4.3 Hydrodynamics of the Bubble Column

The hydrodynamics of bubble columns are among the important parameters that play an important role in the design and performance of reactors and absorbers. The parameters studied in this work included: the gas holdup, mass transfer coefficient, interfacial area, mixing efficiency and circulation time. These parameters are often termed unadjustable parameters..

4.3.1 Gas Holdup

The concept of the gas holdup was explained in Chapter 2. With a 3.5 inch inside diameter and a height of 72 inch, the column is provided with two orifices at the bottom for gas injection. Each orifice is 2.5 mm diameter. The column is also provided with a liquid level indicator to facilitate the distinction between the dispersion height due to gas flow through the column and the height when there is no gas flow. The values of gas holdup reported are the average of at least three separate runs.

Figures 38-44 show the effect of superficial velocity on the gas holdup. The holdup increases with the increase of the superficial velocity. While Figures 38-41 indicate the effect of the height to diameter ratio on the gas holdup as well, it can be deduced from these results that the value of the gas holdup remains constant if the height of the column reaches 30 cm. Figure 4.38 gives the result of gas holdup as a function of superficial velocity for different heights. For any specific superficial velocity the values of gas holdup are almost similar. Figure 4.39 is similar to Figure 4.40, except that the solution is 10 % NaCl instead of deionized water. The result shows that the value of gas holdup corresponding to the lowest height (30 cm) is slightly higher. Similar trends of results were obtained when solutions of 20 % and 30 % by weight of NaCl solution were used as shown by Figures 4.40 and 4.41, respectively.

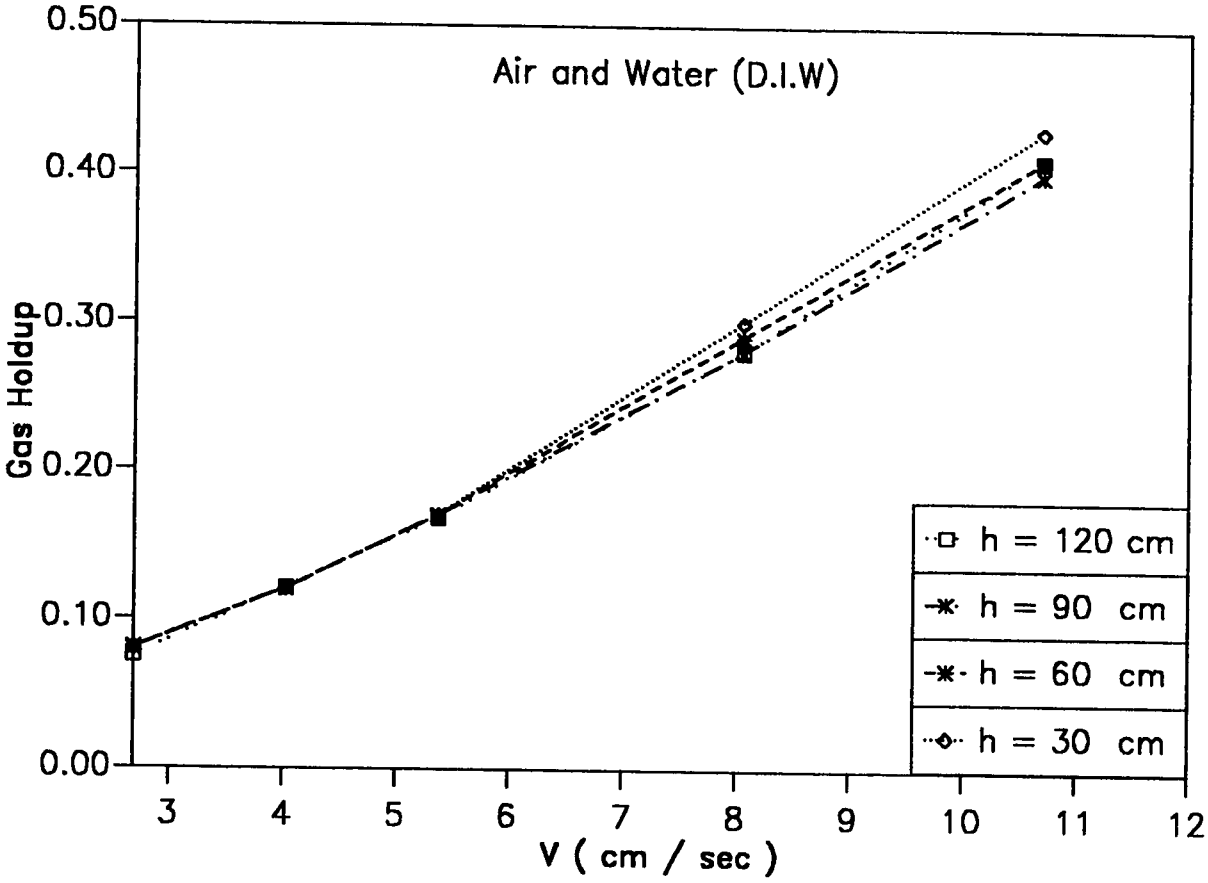

Figure 4.38 Gas Holdup vs Superficial Velocity

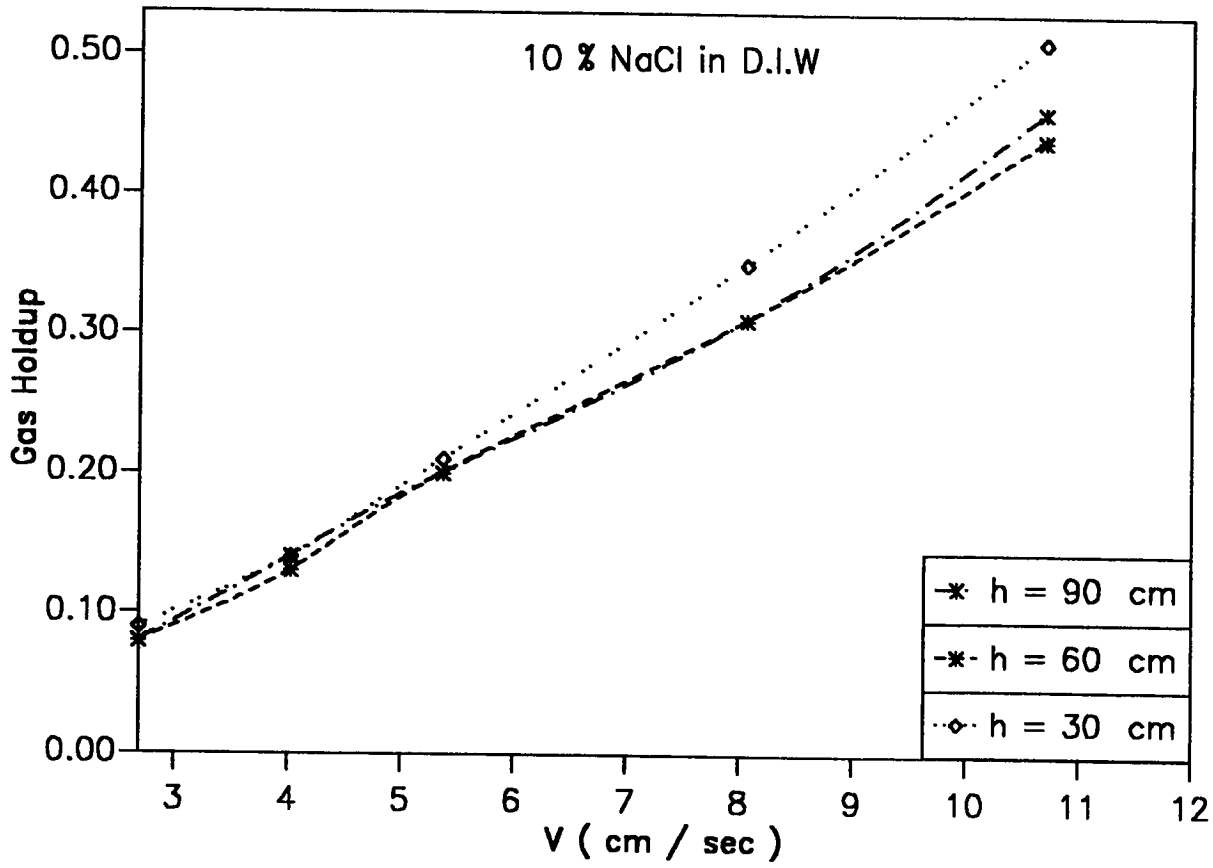

Figure 4.39 Gas Holdup vs Superficial Velocity

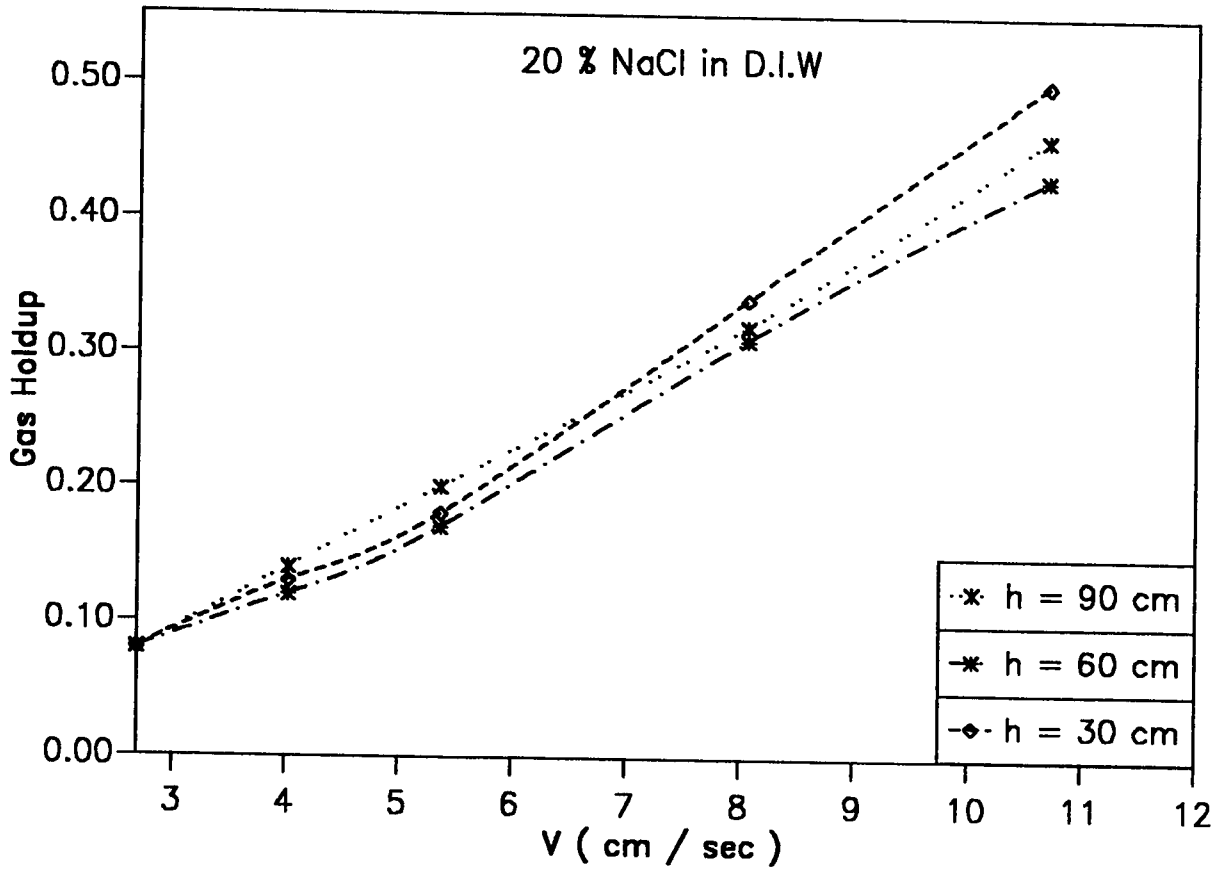

Figure 4.40 Gas Holdup vs Superficial Velocity

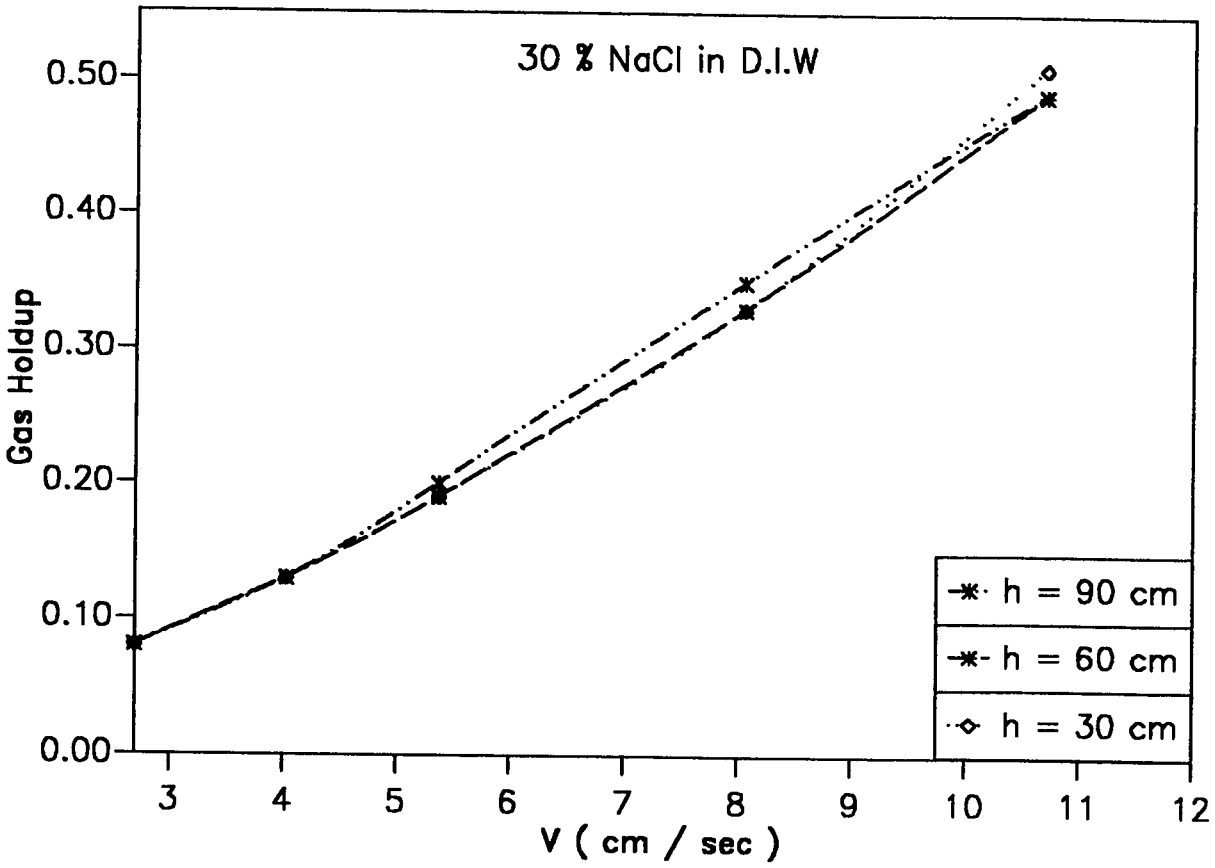

Figure 4.41 Gas Holdup vs Superficial Velocity

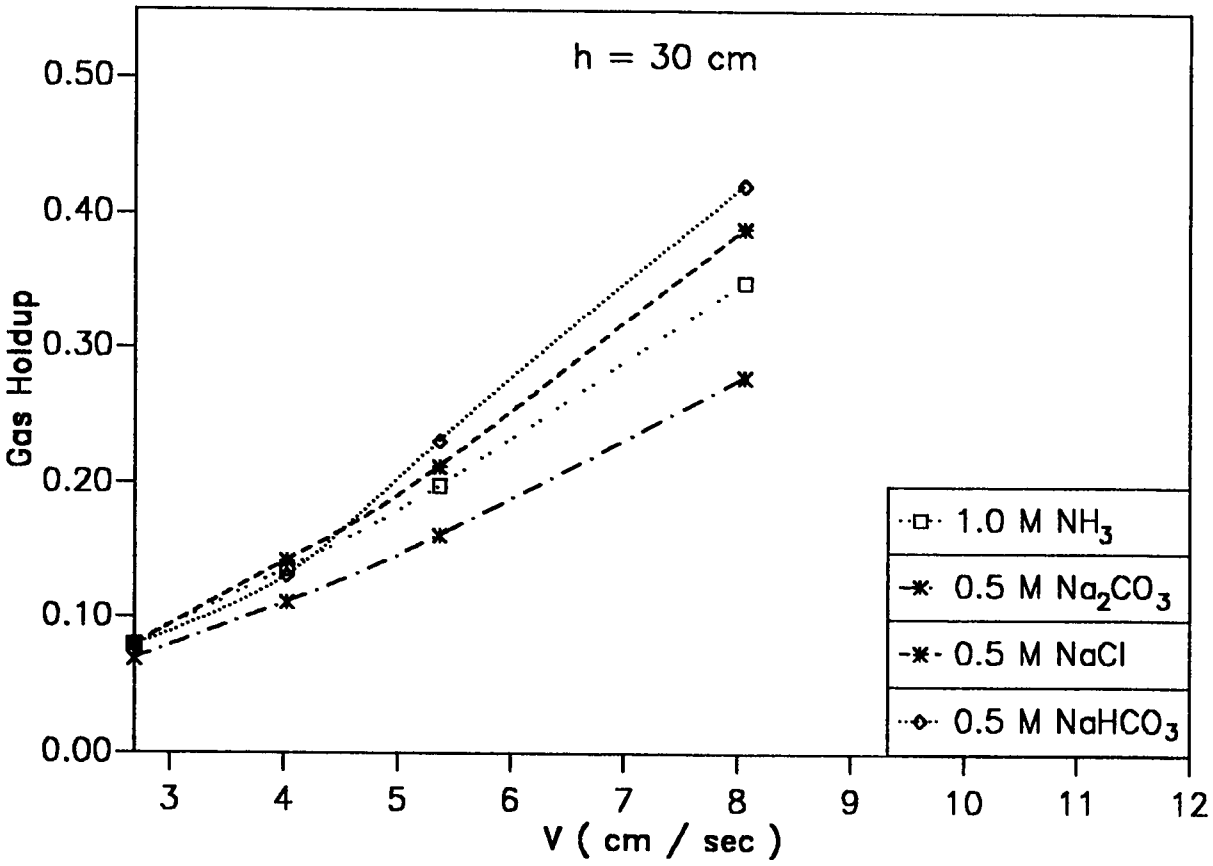

Figure 4.42 Gas Holdup vs Superficial Velocity

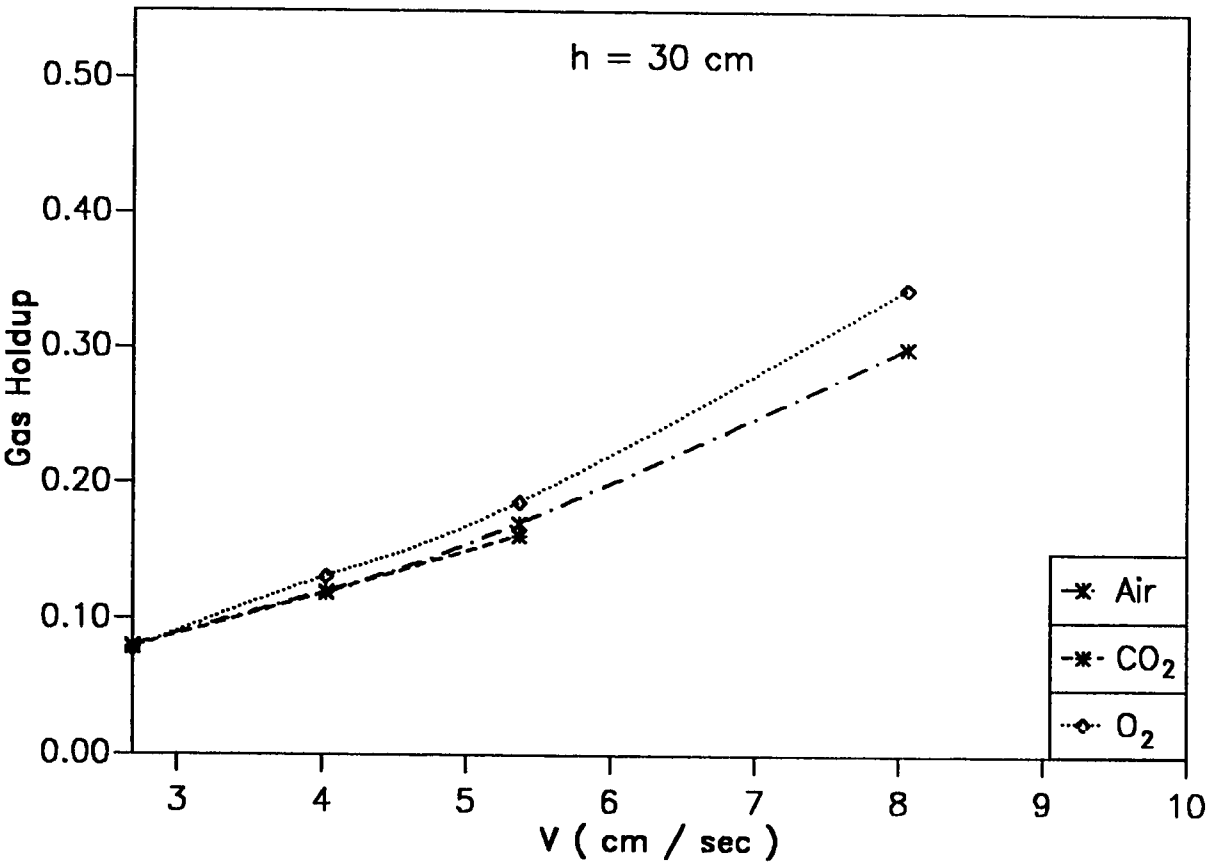

Figure 4.43 Gas Holdup vs Superficial Velocity

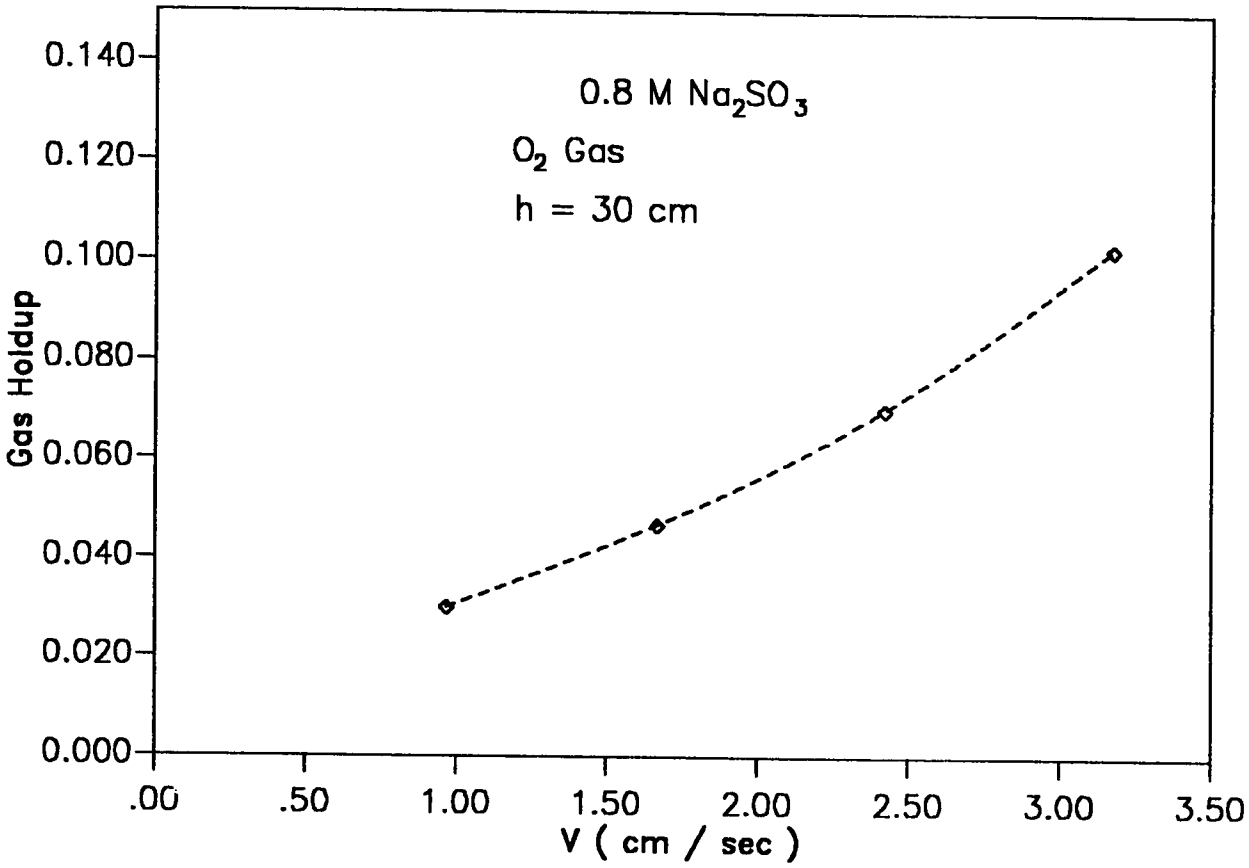

Figure 4.44 Gas Holdup vs Superficial Velocity

The effect of various electrolytes and different types of solution on gas holdup are depicted in Figure 4.42 when aqueous salt of equal molarities were used. The result shows that NaCl solution exhibits a higher value in comparison with $NaHCO_3$ and Na_2CO_3 solutions. Figure 4.43 shows the effect of employing different gas for the measurement of the gas holdup using deionized water. The result shows that values of gas holdup are similar except that with O_2, values are slightly higher.

Figure 4.44 shows the result of the measurement of the gas holdup for 0.8 M sodium sulfite solution and O_2 gas. This system was used for the determination of interfacial area and the mass transfer coefficient. Table B-7 shows the effect of temperature on the gas holdup for different superficial velocities. The result indicates that, for the given temperature interval, the values of gas holdup are identical for each gas flow rate through the column. Therefore, the effect of temperature is negligible for this system at the specified conditions.

4.3.2. Mass Transfer Coefficient

A chemical technique, using the absorption of oxygen into sodium sulfite solutions catalysed by cobalt ions, was used to measure the the gas-liquid interface area "a" and volumetric mass transfer coefficient $K_l a$. The sodium sulfite solution was at an initial concentration

of about 0.8 M and contained roughly $2x10^{5}$ *gmole/l* of cobalt sulphate. Pure O_2 was fed to the bottom of the column after being metered. Operation was batch by batch with respect to the solution. The variations with time of sulfite concentration in the liquid phase was analysed by iodometric titration. Figure 4.45-48 are plots of the sulfite concentration against time. The data points for liquid samples taken at different times fall on single straight lines, indicating that the liquid concentration at a given instant was uniform throughout the vessel within the accuracy of analysis. This fact, shows a high degree of liquid mixing in all directions. Moreover, it indicates that the absorption rate is independent of the concentration of sodium sulfite. The volumetric mass transfer coefficients were determined in the slow chemical regime from the measurement of the rate of absorption (Φ).

$$\Phi = K_L a C^{*}_{O_2} \qquad (4.12)$$

where $C^{*}_{O_2}$ is the solubility of oxygen in the sodium sulfite solution. when the Hatta number was less than unity (Ha < 1). In other words, the volumetric mass transfer coefficient was calculated from this expression:

$$-(1 - \varepsilon_g)\frac{dc}{dt} = 2 K_L a H P \qquad (4.13)$$

where

$\frac{dc}{dt}$ is the slope of the concentration-time plot.

ε_g is the gas holdup.

P is the total pressure and H is the Henry constant.

The Henry's law constant was estimated from the solubility of O_2 in water with correction for the presence of ions by the method of Van Krevelen (1948), on the assumption that the solubility of oxygen in the sodium sulfite solution was equal to that in a sodium sulfate solution of the same normality. The correction of interfacial concentration of oxygen was carried out using the concept elaborated in Appendix A.

4.3.3. Interfacial Area

The interfacial area was determined using chemical technique with the absorption of oxygen into sodium sulfite solutions catalysed by cobalt ions. The interfacial area was determined in the rapid pseudo m-nth order regime from the measurement of the rate of absorption (Φ).

$$\Phi = a C^*_{O_2} \left(\frac{D_{O_2} r}{C^*_{O_2}}\right)^{1/2} \qquad (4.14)$$

Where

D_{O_2} = the diffusion coefficient of oxygen

r = the rate of reaction.

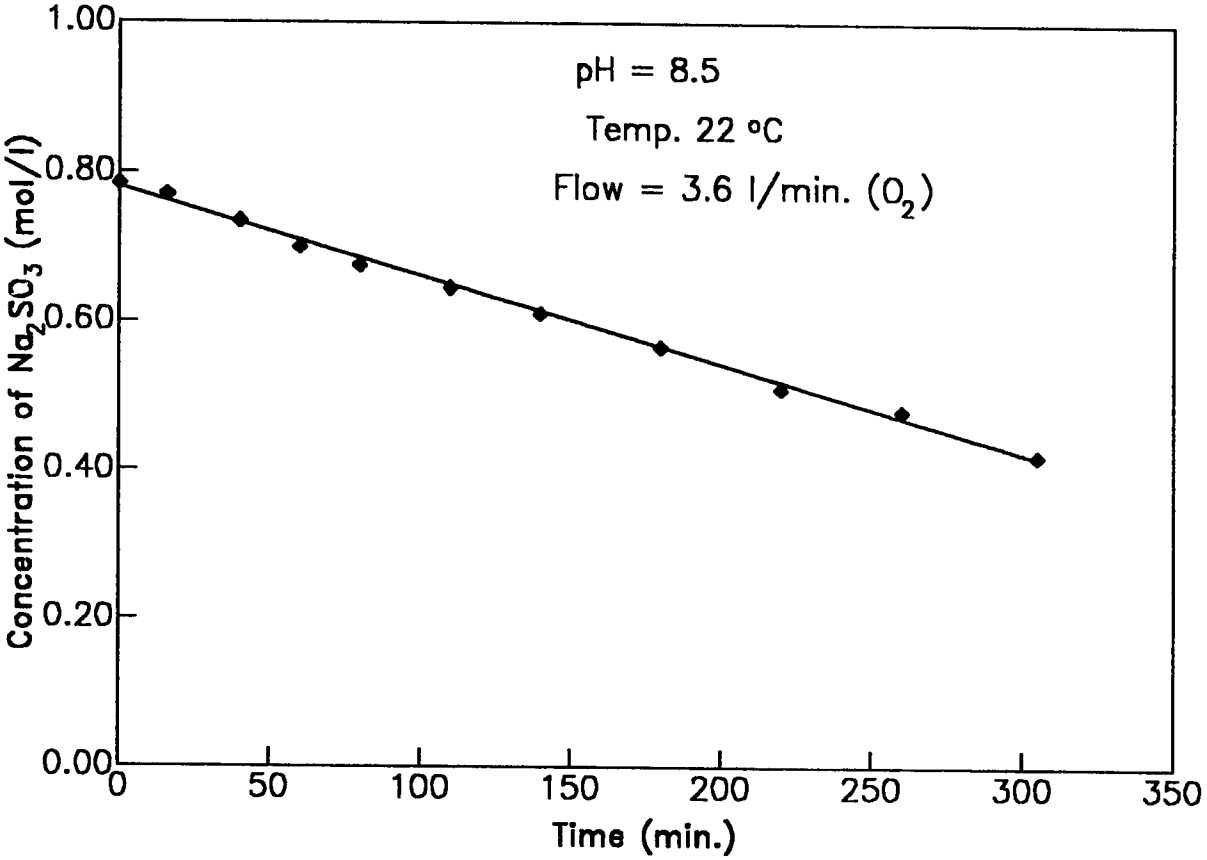

Figure 4.45 Reduction of Na_2SO_3 Conc. With Time

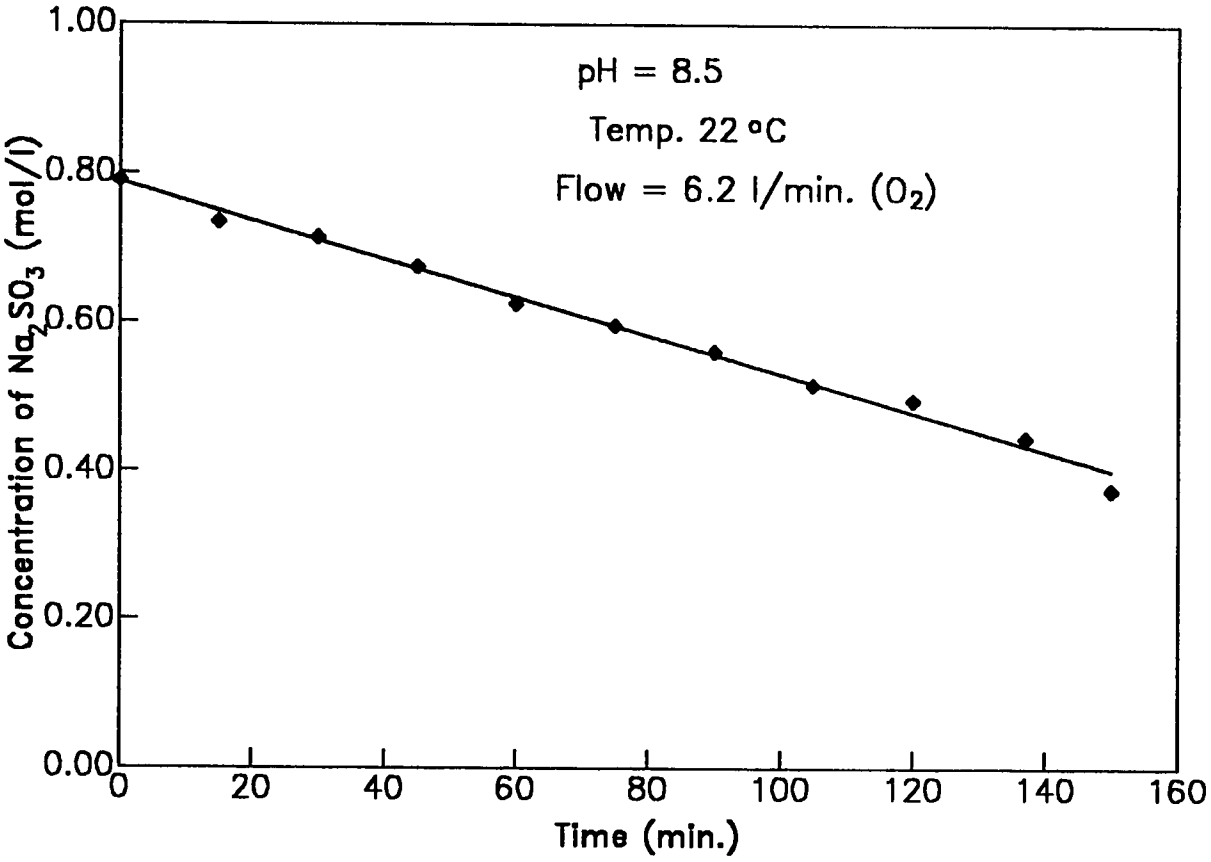

Figure 4.46 Reduction of Na_2SO_3 Concentration With Time

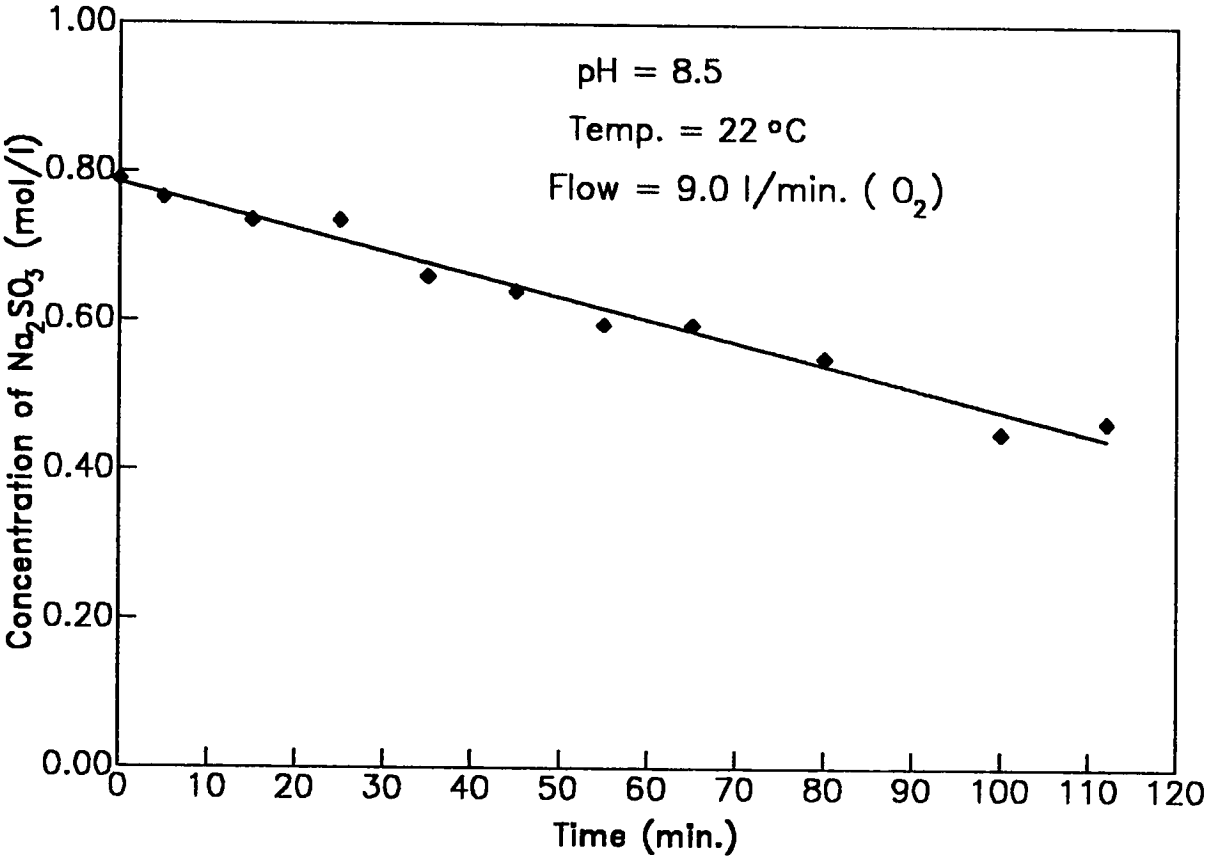

Figure 4.47 Reduction Of Na_2SO_3 Conc. With Time

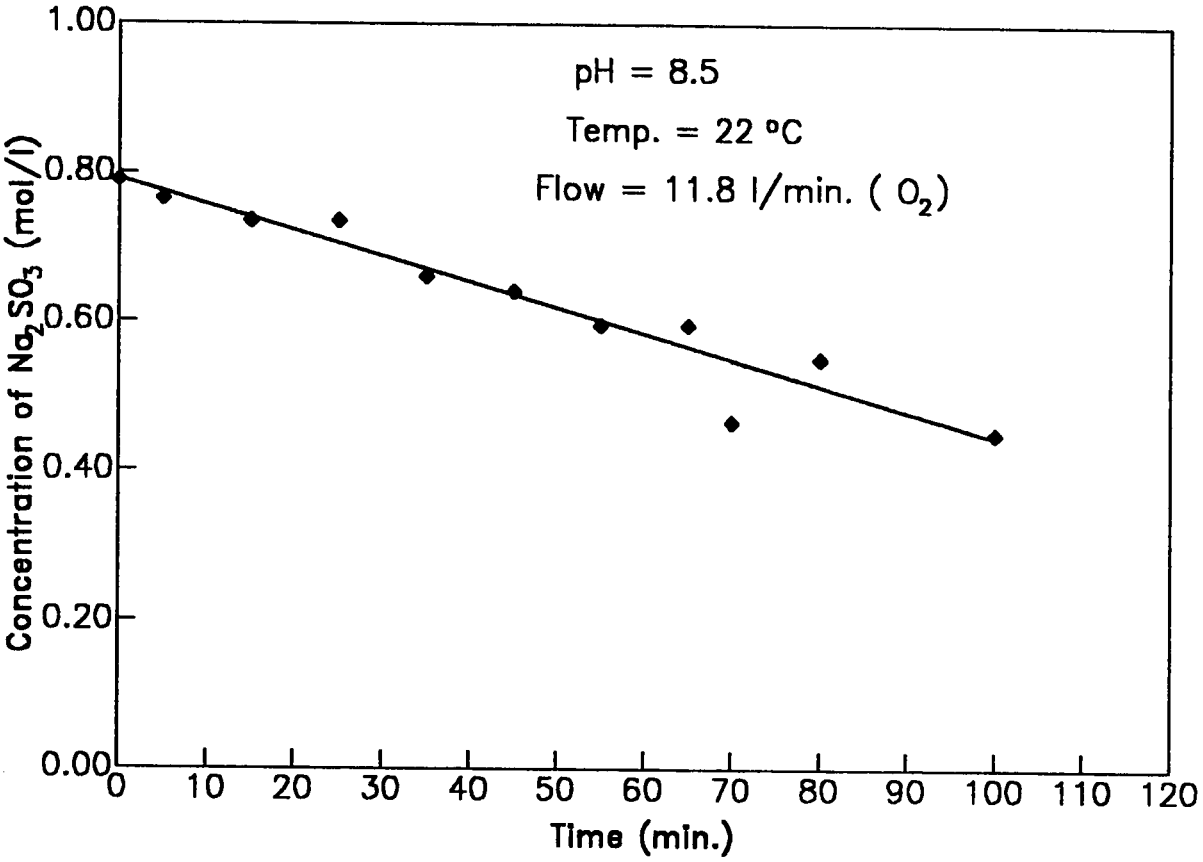

Figure 6.48 Reduction Of Na_2SO_3 Conc. With Time

Provided that

$$3 \leq Ha = \frac{1}{k_L}(D_{O_2}\frac{r}{C^*_{O_2}})^{1/2} < 1 + \frac{D_B}{D_{O_2}}\frac{2C^\circ_B}{C^*_{O_2}} \qquad (4.15)$$

Where

C°_B =Initial concentration of sodium sulfite solution.

D_B = Diffusion coefficient of sodium sulfite solution

Ha = Hatta number.

Absorption rates were measured in solution having a cobalt concentration of $2x10^{-4}$ *gmole/l*. The experimental procedure is similar to that used for the determination the of volumetric transfer coefficient. Figures 49-52 are plots of sulfite concentration against time. The data points fall on straight line showing the absorption rate is independent of the concentration of sodium sulfite. The measurement of the interfacial area was obtained from the absorption rate:

$$a = \frac{-(1-\varepsilon_g)}{2}\frac{dc}{dt}\frac{1}{\sqrt{2/3D_{O_2}K_2C^{3*}_{O_2}}} \qquad (4.16)$$

Where $\frac{dc}{dt}$ is again the slope of concentration-time plot.

K_2 is the reaction rate constant.

Table 4.12 shows the result of the determination of volumetric mass transfer coefficient K_La and interfacial area "a" of the Bubble Column as function of the superficial velocity "V".

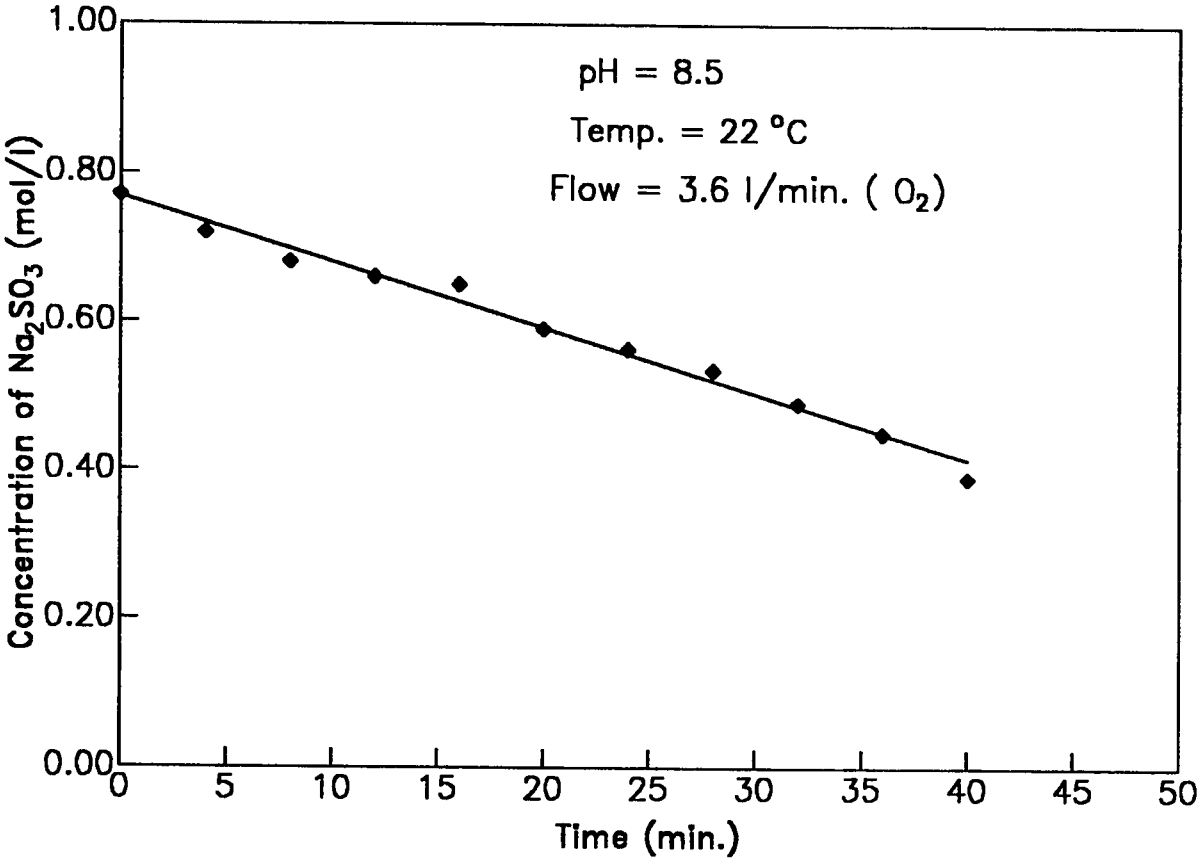

Figure 4.49 Reduction of Na_2SO_3 Conc. With Time

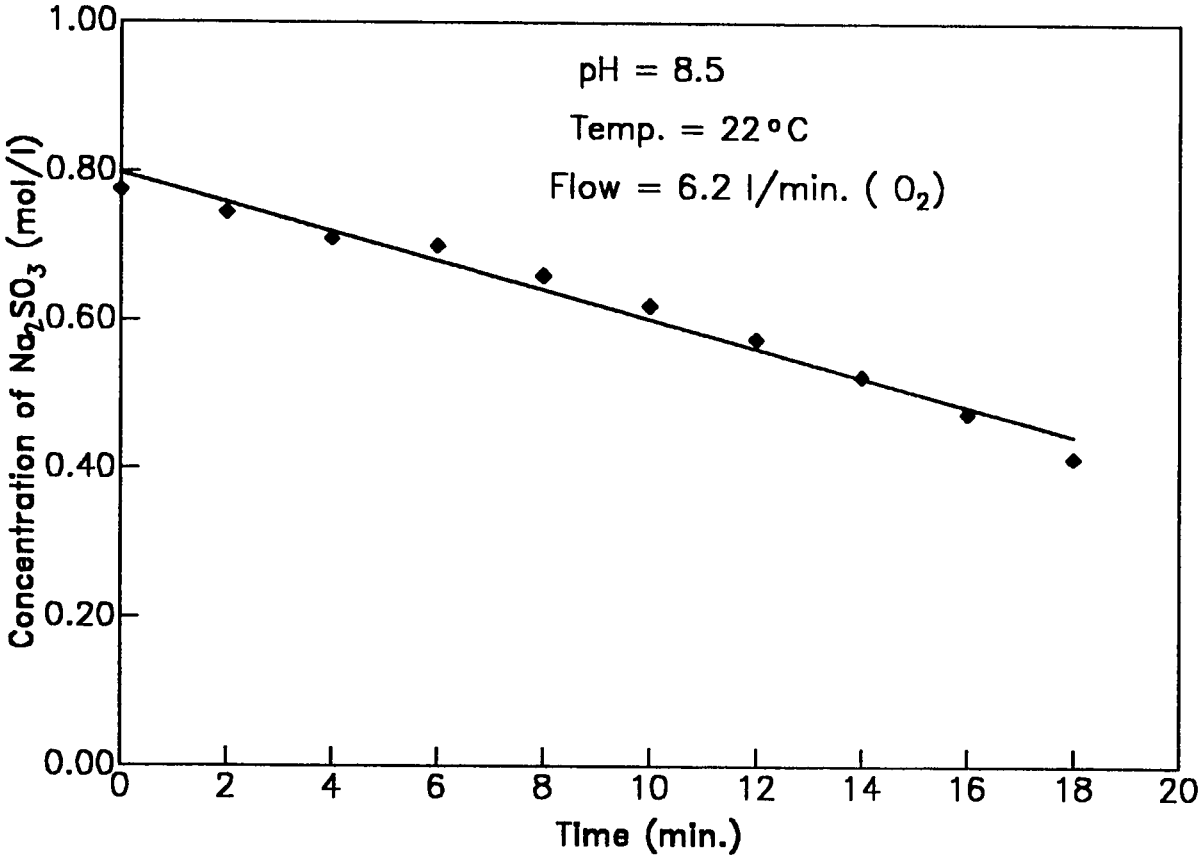

Figure 4.50 Reduction of Na_2SO_3 Conc. With Time

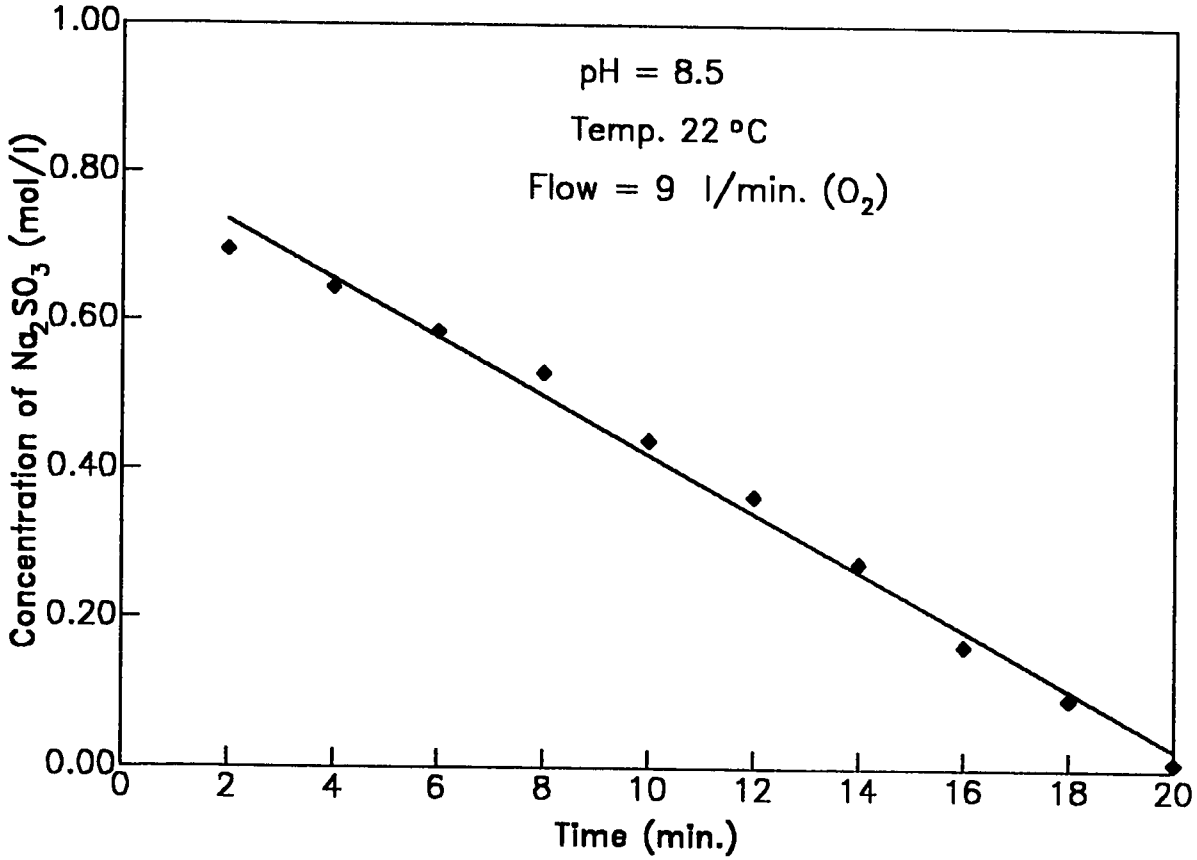

Figure 4.51 Reduction of Na_2SO_3 Conc. With Time

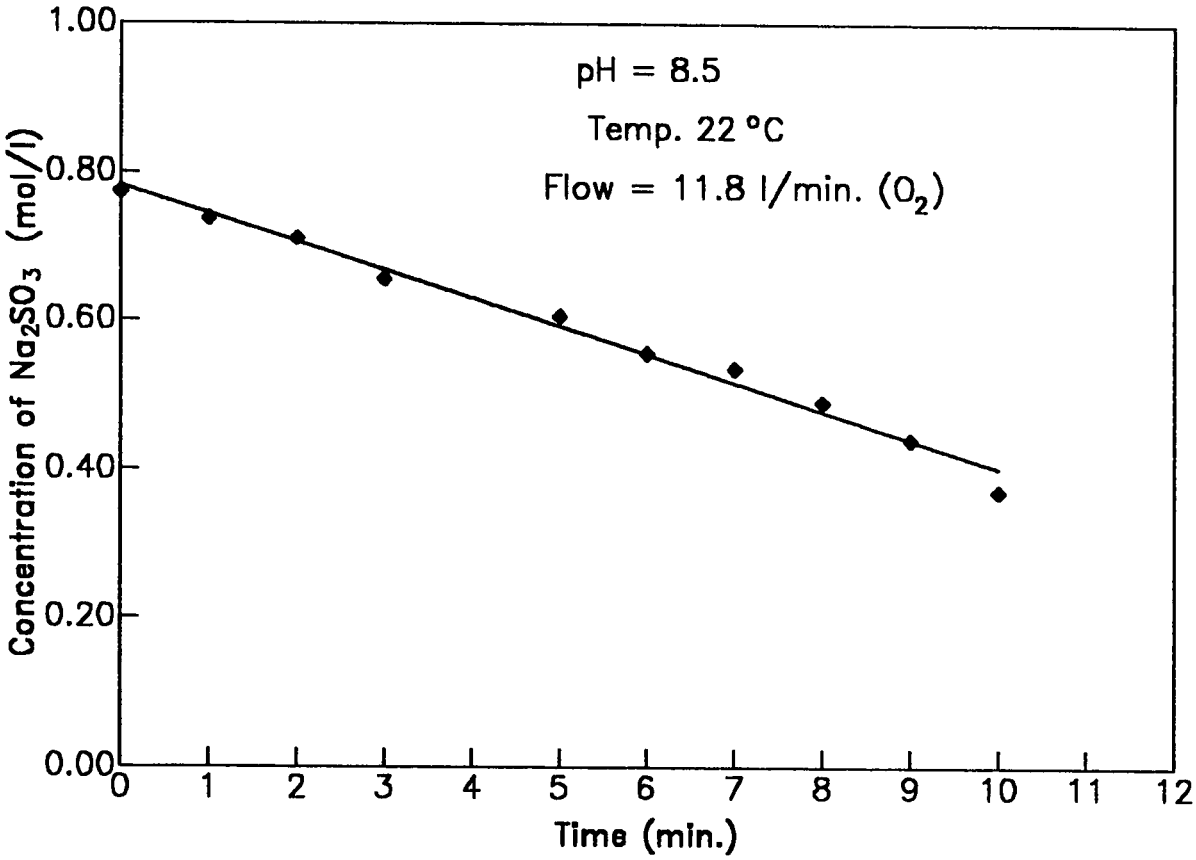

Figure 4.52 Reduction of Na_2SO_3 Conc. With Time

Table 4.12 Values of $K_L a$ and a of the bubble column.

V cm/s	ε_g	$K_L a$ s^{-1}	a cm^{-1}
0.97	0.03	0.02	0.29
1.66	0.05	0.04	0.68
2.40	0.07	0.05	1.19
3.17	0.10	0.11	1.26

The results obtained are in the same range of that of Sharma and Mashelkar (1968), and Keith and Onken (1981). It shows increasing the superficial velocity increases both the volumetric mass transfer coefficient and the interfacial area.

4.3.4 Mixing Efficiency

Experimental analysis was carried out to study the mixing efficiency of a solution. In the process of planning the experiment, the method of the data collection was designed in order not to affect the conclusions that can be drawn from the experiment. The experimental units and the nature of the observations have been decided such that the treatment comparisons be free from systematic errors and that they should be made over a wide range of validity. In these experiments the independent variables to be investigated were mixing Time and circulation time. The order in which the data was collected and

the method of randomization employed suggested both a suitable mathematical model so that a statistical analysis of the data may be performed. Since one factor only is investigated each time, the one-way analysis of variance could be used. In any experiment it has been specifically chosen the mixing time or the circulation time to be the treatment fixed. Tables 4.13, 4.14 and 4.15 provide the mixing time data for both distilled and 10% NaCl solutions and the circulation time experiment. While tables 4.16, 4.17 and 4.18 give the corresponding ANOVA tables.

Table 4-13 Mixing Efficiency of Bubble Column (Mixing Time)

Solution : distilled water
reagents : 0.1N I2
0.1N Na2S2O3
Starch

	Time (Sec.)			
Run #	R=1	R=2	R=3	R=4
1	3.93	2.91	2.29	1.59
2	3.93	2.78	2.71	1.91
3	4.1	3.08	2.49	1.97
4	3.94	2.78	2.53	1.82

Table 4-14 Mixing Efficiency of Bubble Column (Mixing Time)

Solution : 10% NaCl
reagents : 0.1N I2
0.1N Na2S2O3
Starch

	Time (Sec.)			
Run #	R=1	R=2	R=3	R=4
1	5.35	4.51	3.20	2.06
2	5.71	4.27	2.59	2.24
3	5.10	3.45	2.49	1.99
4	4.81	3.74	3.20	1.89

Table 4-15 Mixing Efficiency of Bubble Column (Circulation Time)

	Time (Sec.)			
Run #	R=1	R=2	R=3	R=4
1	20.80	3.09	7.87	4.91
2	5.58	2.98	6.61	2.16
3	8.74	2.13	5.38	4.23
4	8.85	11.99	4.97	4.48
5	22.94	2.56	6.16	6.90
6	5.06	6.48	5.43	6.47
7	10.94	9.88	5.67	4.89
8	9.46	2.42	6.38	3.87
9	13.57	2.95	6.61	3.68

A summary of the ANOVA table for the first experiment which uses distilled water is given below.

Table 4.16 ANOVA for mixing time experiment using distilled water

Source of Variation	Sum of Squares	Degree of Freedom	Mean Square	Fo
Treatment	0.114	3	0.038	
Error	9.863	12	0.822	Fo=0.046
Total	9.977	15		

$F_{0.01,3,12} = 5.95$

Since $F_o < F_{0.01,3,12}$ we conclude that mixing time do not differ and the hypothesis of no difference in mixing time is true.

In the case of 10% NaCl solution, same procedure is adopted in constructing the corresponding ANOVA Table as given Below.

Table 4.17 ANOVA for mixing time experiment using 10% NaCl Solution

Source of Variation	Sum of Squares	Degree of Freedom	Mean Square	Fo
Treatment	0.723	3	0.241	
Error	24.072	12	2.006	Fo=0.120
Total	24.795	15		

$F_{0.01,3,12} = 5.95$

Since $F_o < F_{0.01,3,12}$ we conclude that mixing time do not differ and the hypothesis of no difference in mixing time is true at 99.99% confidence of interval.

The circulation time data are given in Table 4.15 while the corresponding ANOVA table is given in Table 4.18.

In this analysis, same procedure is followed.

Table 4.18 ANOVA for circulation time experiment using distilled water

Source of Variation	Sum of Squares	Degree of Freedom	Mean Square	Fo
Treatment	106.860	3	35.620	
Error	640.73	32	20.002	Fo=1.780
Total	747.59	35		

$F_{0.01,3,32} = 4.36$

Since $F_o < F_{0.01,3,32}$ we conclude that mixing time do not differ and the hypothesis of no difference in mixing time is true at 99.99% confidence of interval.

Chapter V

MODELLING AND CORRELATIONS OF EXPERIMENTAL RESULTS

5.1 Reaction Regimes involved in the Separation Process

The theoretical design of the given process depends primarily on the absorption of carbon dioxide accompanied by chemical reaction in an ammoniated brine solution. This is because the reaction between NaCl and the resultant product "ammonium bicarbonate " of the modified Solvay is a fast ionic reaction:

$$CO_2 + 2\,NH_3 = NH_2COO^- + NH_4^+ \qquad (5.1)$$

$$NH_2COO^- + H_2O = NH_3^+ + HCO_3^- \qquad (5.2)$$

$$NH_4^+ + HCO_3^- + NaCl = NH_4Cl + NaHCO_3 \qquad (5.3)$$

Thus main reaction involved in this process is described as a second order with rate:

$$rate = K_{NH_3}\,|NH_3|\,|CO_2| \qquad (5.4)$$

as reported by Pincet et al., (1956) and Danckwerts and Sharma

(1966). The theoretical evaluation of absorption followed by liquid-phase chemical reaction has received a great deal of attention although the results are not yet routinely useful for design purposes. Early studies of several reaction types were made by Hatta and Van Krevelen and Hoftizer (Danckwerts, 1970). This work has been expanded by more recent investigators to cover reversible reactions, various reaction orders, and reaction rates from very slow to instantaneous. Important contributions have been made by Perry and Pigford (1953), Brian et al. (1961), Gilliland et al. (1958), Brian (1964), Danckwerts and Gillham (1966), Decoursey (1974), Matheron and Sandall (1979), and Olander (1977). The application of the theory to specific gas purification cases has been described by Ouwerkerk (1978).

To establish some useful concepts that pave the way for modeling the experimental results, consider the process of gas absorption of CO_2 component (A) by an aqueous NH_3 component (B) as it takes place in a stirred tank. A pure gas is dispersed into the liquid through an orifice plate and undergoes a second-order reaction with B. A material balance on the reactor is shown below :

Input by Absorption = Output by chemical reaction + Output unabsorbed

$$k_l a V (C_{Ai} - C_A) = Q C_A + V K_2 C_A C_B \qquad (5.5)$$

Where

V = volume of solution;

K_2 = reaction rate constant

Q = Volumetric rate

The following parameters are defined and substituted in Equation (5.5).

$$0 = \frac{V}{Q} \; ; \qquad E = \frac{k_l}{k^{\circ}_l} \tag{5.6}$$

After rearranging, equation 5.5 becomes:

$$C_A = \frac{k^{\circ}_l a\, 0}{1 + K_2 C^{\circ}_B 0 + k_{l_o} a\, 0 E} \tag{5.7}$$

The total rate of solution of A may defined as:

$$R = K_l a V (C_{Ai} - C_A) \quad ; \quad r = \frac{R\rho}{L\, C_{Ai}} \tag{5.8}$$

$$r^{-1} = \frac{1}{k^{\circ}_l a\, 0 E} + \frac{1}{1 + K_2 C_B 0} \tag{5.9}$$

The two terms on the right hand side of equation 5.9 may be thought of representing the resistances to the interfacial mass transfer and to the chemical rate respectively.

Having obtained the expression above with the assumption that the concentration C_B remains the same as C°_B, the following table can be constructed to study the effect of chemical reaction on gas absorption considering the diffusivity of CO_2 to be $D_{CO_2} = 1.8x10^{-5}\ cm^2/s$ and the value of the logarithmic of the reac-

tion constant K_2 varying the range between -8 to +6, i.e $\log K_2 = (-8, -6, -4, -2, 2, 4, 6)$ and with

$$E = (1 + \frac{DK_2 C_B}{(K_l^o)^2})^{1/2} \qquad (5.10)$$

Table 5.1 Value of Parameters in Equation (5.9)

Case	k^o_l (cm/s)	a (cm^{-1})	() (sec)	C^∞_B (mole/l)
A	0.04	1.0	250	2.5
B	0.04	0.1	2500	2.5
C	0.4	0.1	250	2.5
D	0.04	1.0	250	5.0

Equation 5.9 is plotted in Figure 5.1.

Figure 5.1 shows that there are three distinct regimes:

Regime I: where log K_2 is less than -3, the reaction has negligible effect and only physical absorption is taking place.

Regime II: where log K_2 ranges between -3 to 1, the reaction has an appreciable effect.

Regime III: where log K_2 is greater than 1, the reaction occurs rapidly near the interface.

As mentioned before, the basic reaction under investigation which leads to the separation of NaCl from a brine solution involves the absorption of CO_2 in ammmonical brine and is given by :

$$CO_2 + NH_3 = NH_2COO^- + NH_4^+ \qquad (5.11)$$

and is best described as an instantaneous, diffusion-controlled chemical reaction. The effect of chemical reaction in the liquid phase is generally to increase the liquid-film absorption coefficient over that which would be observed with simple physical absorption.

With very slow reactions, however (such as that between carbon dioxide and water), the dissolved molecules apparently migrate well into the body of the liquid before reaction occurs so that the overall mass transfer rate is not appreciably increased by the occurrence of the chemical reaction. In this case, the liquid-film resistance is the

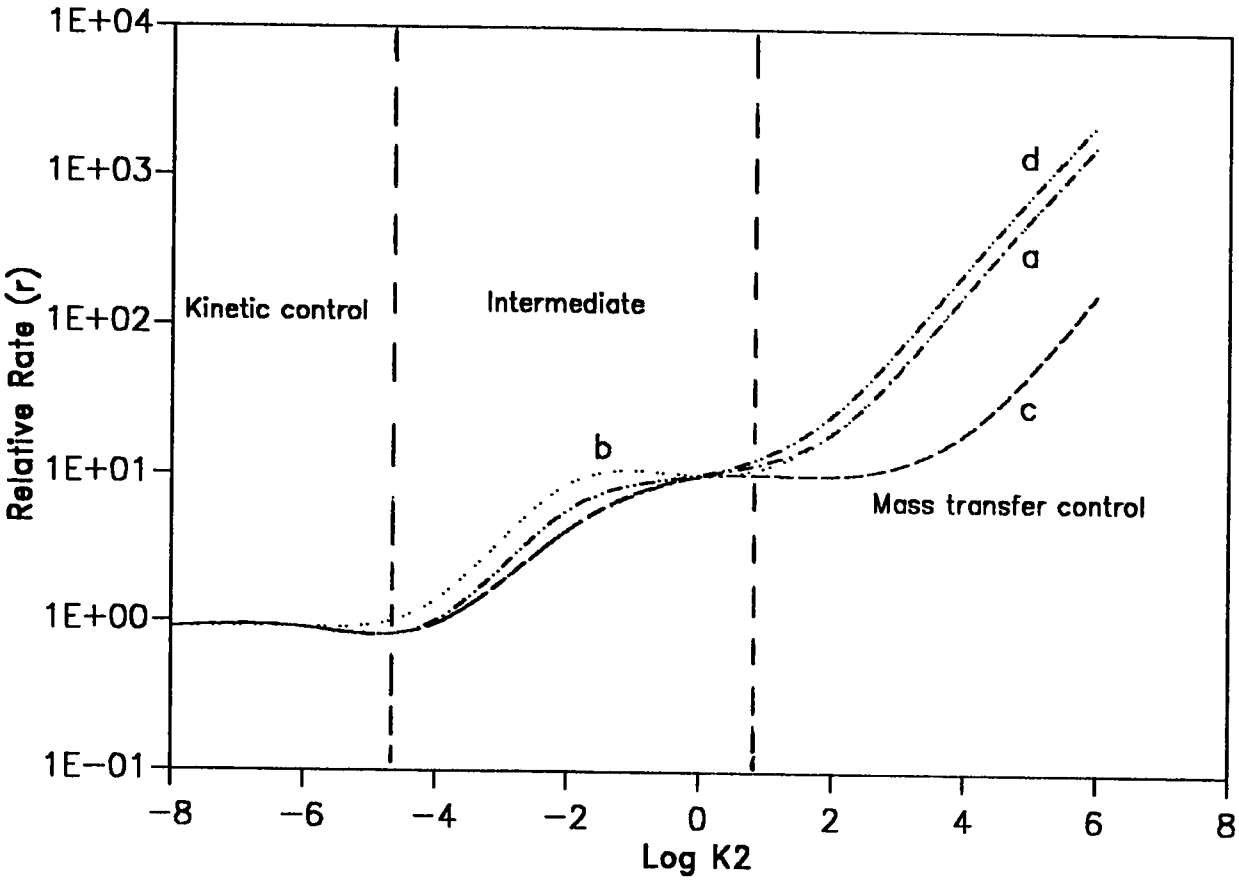

Figure 5.1 Effect of Reactivity on Rate of Absorption

controlling factor, the liquid at interface can be assumed to be in equilibrium with the gas, and the rate of mass transfer is governed by the molecular CO_2 concentration gradient between the interface and the body of the liquid.

At the other extreme are very rapid reactions such as the one we dealing with, where the dissolved molecules migrate only a very short distance before reaction occurs. The location of the reaction zone and the value of absorption coefficient will depend primarily upon the diffusion rate of reactants and reaction products to and from the reaction zone, the concentration of solute at the interface, and the concentration reactant in the body of the liquid. However, since the distance which the solute must diffuse into the liquid is extremely small compared to the distance which it would have to travel for simple physical absorption, a high liquid-film coefficient is observed.

Despite the very fast reaction by which free CO_2 is chemically reacted with NH_3, there is neverless a very appreciable resistance to the passage of carbon dioxide into the solution. Most of the resistance is in the liquid phase. This implies that the reaction must take place at finite rate in an appreciable volume of the liquid rather than on the interface itself. Thus owing to the fact that unless diffusion of carbon dioxide away from the interface occurs, no volume of the liquid is available for the reaction, the two phenomena take place:

a) The faster the diffusion, the deeper is the reaction layer at the interface, while

b) The faster the reaction the thinner is the zone near the interface which has to be supplied with carbon dioxide moles by diffusion.

This explains the fact that both rates of diffusion and reaction have to go hand in hand to produce the right effect on the separation process. Figure 5.2 is a schematic illustration of these phenomena.

Since the effect of chemical reaction is to increase the liquid film coefficient, k_l, over the value it would have in the absence of chemical reaction, k_l^o, a common approach is to utilize the ratio $\frac{k_l}{k_l^o}$, in correlations. This ratio is called enhancement factor, known as E. Both coefficients are affected by the fluid mechanics, but fortunately their ratio, E, has been found to be relatively independent of these factors. It is primarily a function of concentrations, reaction rates, and diffusivities in the liquid phase.

5.2 Modeling

As explained earlier, the controlling phase in the desalination of highly saline waters is the absorption of carbon dioxide by the ammonia solution accompanied by chemical reaction leading to the formation

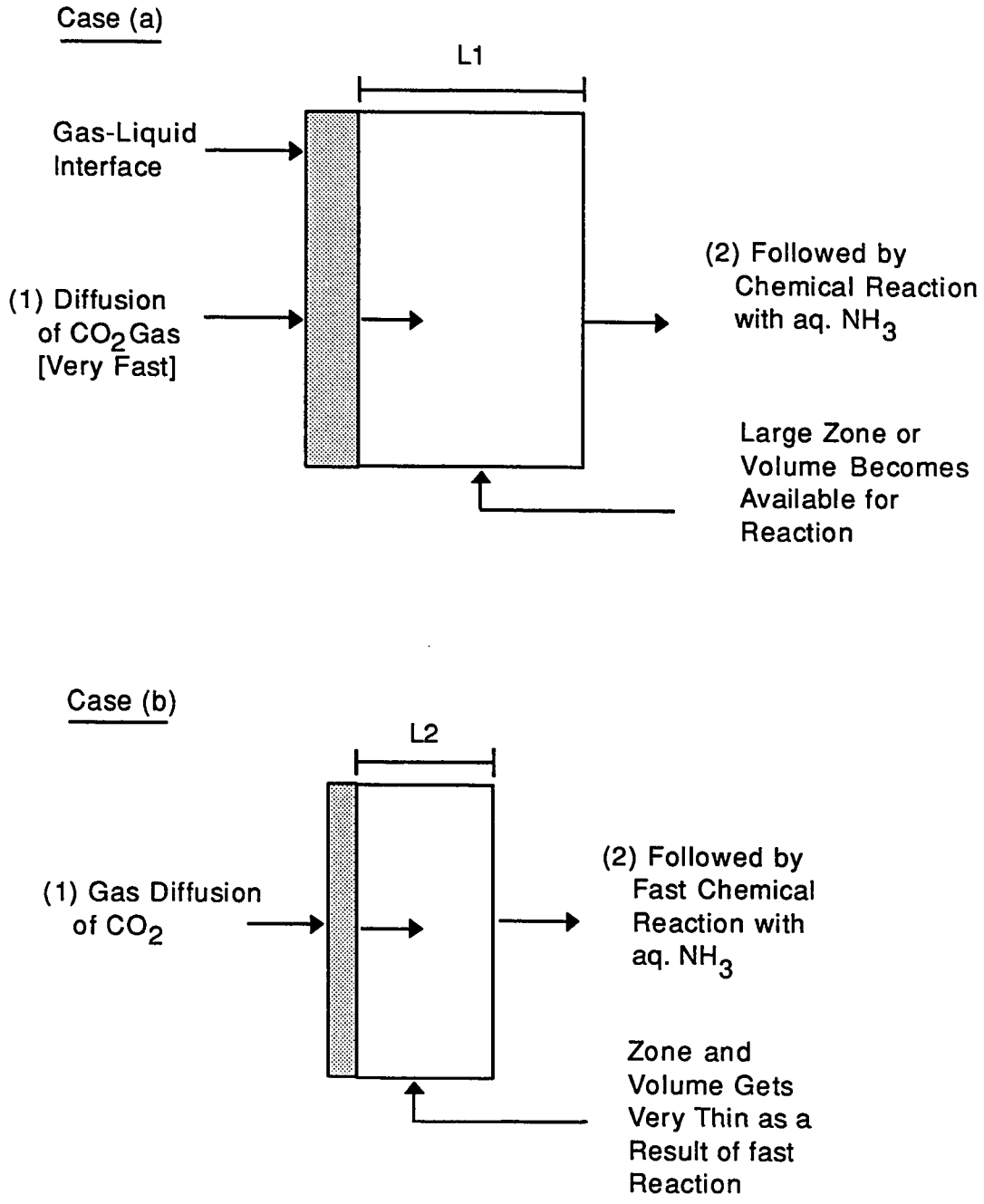

Figure 5.2. Illustration of the Effect of Fast Rates on the Separation process.

of ammonium bicarbonate as compared to the next phase of subsequent formation of sodium bicarbonate $NaHCO_3$. Accordingly, the methodology followed for the theoretical modeling of the separation reactions underlying the separation process will be concerned primarily with this particular phase, and involves the following:

1. The development of the main diffusion equation accompanied by chemical reaction for carbon dioxide in aqueous ammonia solution.

2. Formulation of the relationships that describe the interactions between different species participating in this reaction. This constitutes a set of non linear equations which provides an algorithm to be solved for the dependent parameter, unreacted ammonia(C_B)for a given set of the independent parameters CO_2 absorption and the total NH_3 used in a given run.

3. A graphical plot is carried out next between the absorption rate of CO_2 versus C_B A straight line relationship confirm the proposed equation developed in step 1.

4. Finally values of unreacted ammonia determined experimentally, are to be compared with the theoretical values obtained in step 2 (C_B). This comparison is valid provided that the experimental conditions allow for enough absorption of carbon dioxide to form the ammonium bicarbonate regime.

This modeling will establish a system that provides a method to calculate the conversion efficiency of the separation process. These steps are proposed in the form of block diagram as shown next in Figure 5.3.

5.2.1. The Development of the Diffusion Equation

The types of concentration profiles near the gas-liquid interface in a chemically reacting liquid, bimolecular system represented by

$$C_A + C_B = C_C \tag{5.12}$$

have been well explained by Sherwood,Pigford and Wilke as shown in Figure 5.4

The reaction rate in many such examples can be represented by

$$R = K C_A C_B \tag{5.13}$$

This system could represent very well our separation process in which the absorption of carbon dioxide in ammonia solution to form ammonium carbonates takes place. The process involves simultaneous diffusion and chemical reaction near an interface. To account for the influence of a chemical reaction on the concentration of a diffusing species in the important region near an interface between phases, one must include a reaction rate expression in the unsteady state diffusion equation, to have the following expression

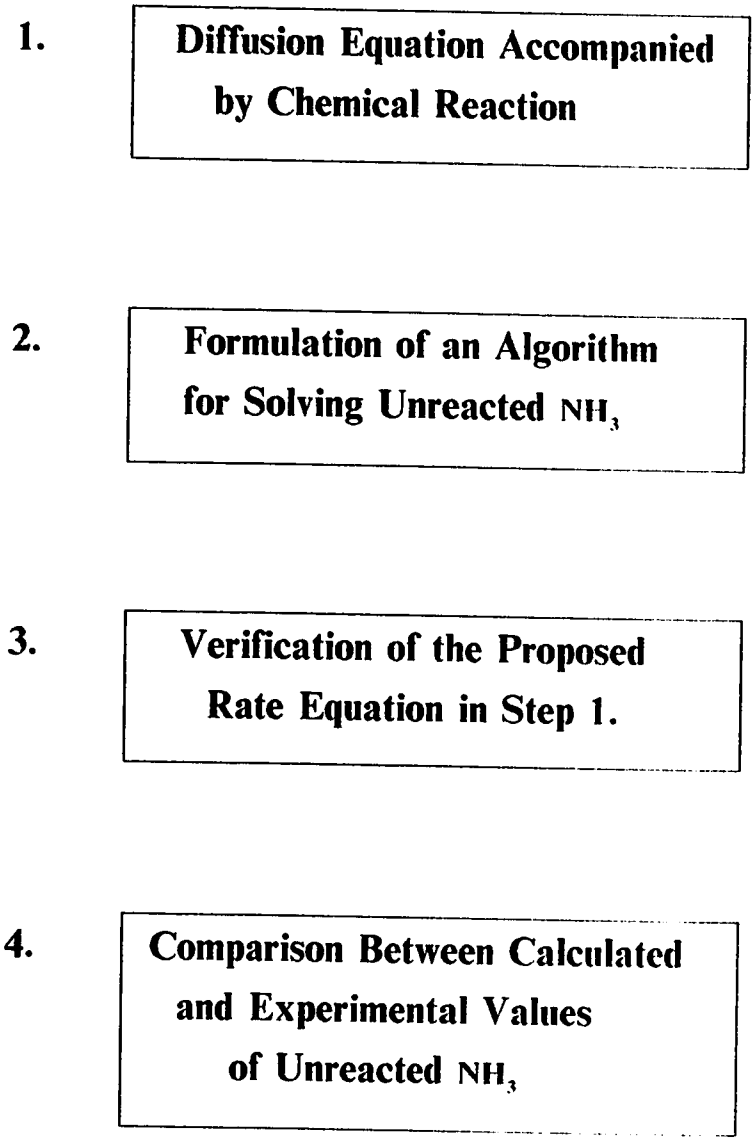

Figure 5.3 Solution Steps for Modeling

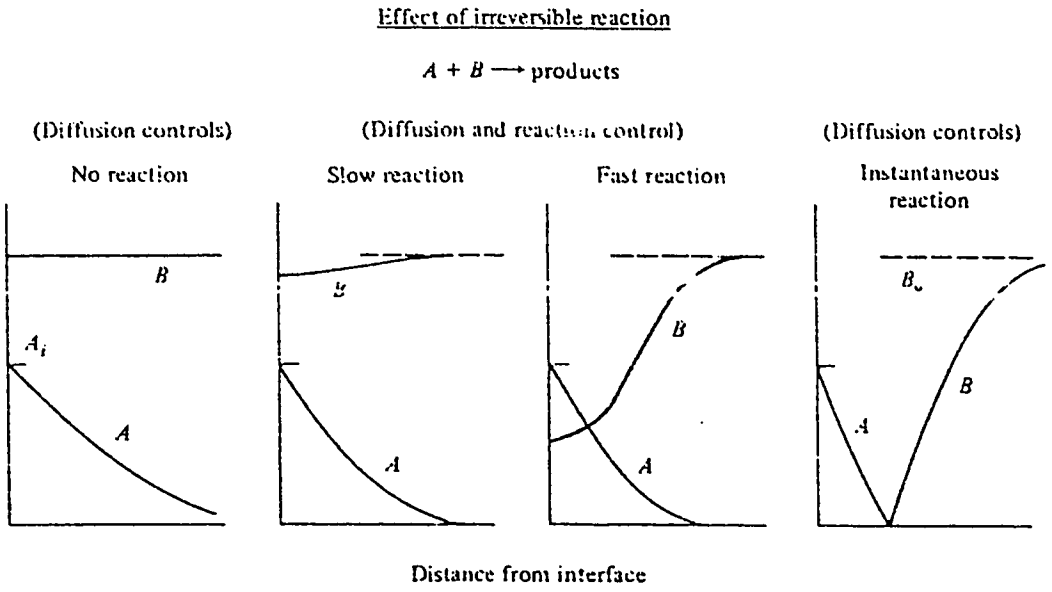

Figure 5.4 Types of Concentration Distribution near an Interface in a Chemically Reactive Liquid (Carberry, 1976).

$$D\frac{\delta^2 C_i}{\delta y^2} = \frac{\delta C_i}{\delta t} + u\frac{\delta C_i}{\delta x} + R_i(c) \qquad (5.14)$$

Where R_i, represent the rate of loss of component i owing to chemical reaction per unit volume of fluid. Obviously, development of the theory of diffusion-affected reactions can take on, as many forms as there are different expressions for R_i and different fluid flow situations. Since the system under study involves two reacting species. Equation (5.14), has to be used twice: once for ammonia and once for carbon dioxide. Many investigators have adopted some simplifications and assumption techniques to solve the above equation. One such approach reported by Cussler (1984), implies that reaction rate K is so large that A and B react immediately and completely upon contact in the solution. Then the product C_A*C_B must be zero every wherein the liquid.

a) C_B being zero near the interface, while C_A is finite:

$$C_A * C_B(=0) = 0 \qquad (5.15)$$

b) C_A being zero deep in solution, while C_B is finite and equal to C_B^o (initial concentration).

$$C_B^o * C_A(=0) = 0 \qquad (5.16)$$

Accordingly a sharp reaction plane is formed in the liquid as shown earlier in Figure 5.4. However, due to the very fast rate of absorp-

tion of A, the plane moves rapidly from its initial position located at the interface into the liquid to a new position, represented by:

$$l = 2.5(\alpha t)^{0.5} \tag{5.17}$$

Where L is the distance from the interface to the reaction plane, and α is constant. Figure 5.5 shows the concentration profiles of reactants near an interface of infinitely fast chemical reaction. Now behind the moving zone, it could be assumed that carbon dioxide absorption is represented by the transient diffusion equation without any reaction term; the same applies to ammonia in the region to the right of the plane. The final expressions obtained when based on the above assumptions, for mass transfer coefficient and the rate equations are give as follows :

$$k_l a = \sqrt{\frac{D_A}{D_B}} \left(\frac{1 + D_B C_B^o}{D_A z C_{Ai}} \right) \frac{\sqrt{4 D_A}}{\pi t_D} \tag{5.18}$$

$$N_A = \sqrt{\frac{D_A}{D_B}} \left(C_{A_i} + \frac{D_B}{D_A} \cdot \frac{C_B^o}{z} \right) k_l^o \tag{5.19}$$

$$N_A = k_l^o C A_i \left(\sqrt{\frac{D_A}{D_B}} + \sqrt{\frac{D_B}{D_A}} \frac{C_B^o}{z C_{Ai}} \right) = k_l^o C_{Ai} F_i \tag{5.20}$$

Where

D_A = diffusivity of CO_2 gas in the ammonia solution

D_B = diffusivity of Ammonia

C_{Ai} = solubility of CO_2 gas in the ammonia solution

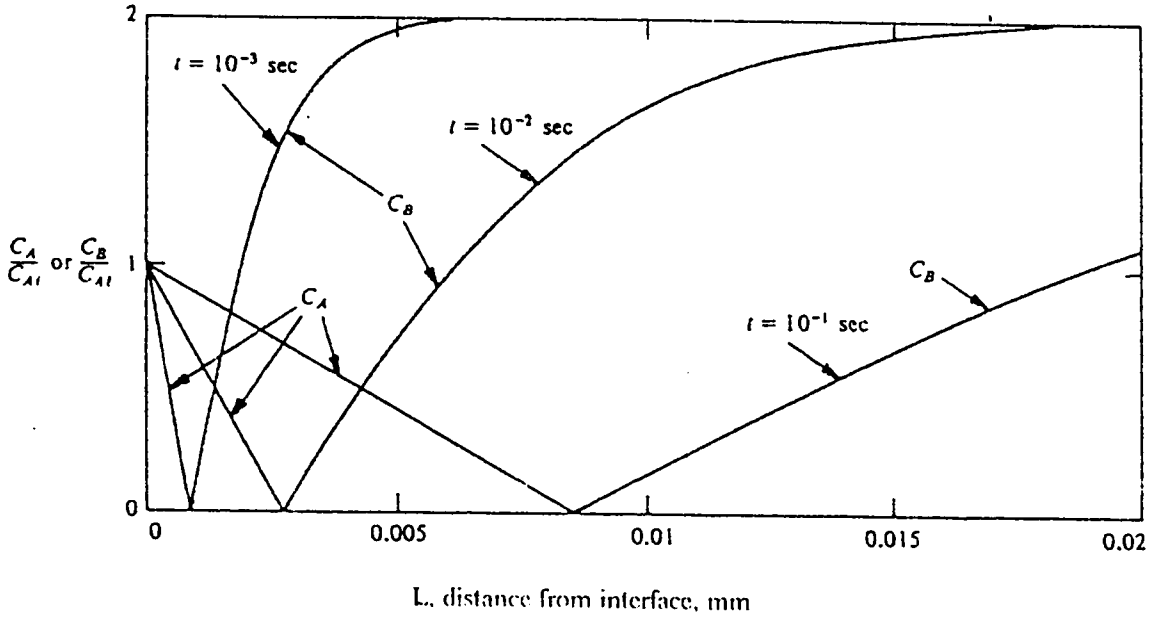

Figure 5.5 Concentration Profile of Reactors near an Interface Infinitely Fast Chemical Reaction (Carberry, 1976).

N_A = Absorption rate of CO_2 gas in the ammonia solution

t_D = diffusion time

z = stoichiometric coefficient of the reaction

k_l^o = liquid film coefficient in the absence of reaction

$k_l a$ = volumetric mass transfer coefficient

5.2.2 Formulation of an Algorithm to solve for C_B

In this step, the set up of the main equilibrium relationships involved in the formation of ammonium bicarbonate and the formulation of a system of non-linear equations are considered. A numerical solution is then carried out using the Newton/Raphson technique to compute the equilibrium compositions of all components involved in the system, mainly, the unreacted ammonia concentration as a function of the rate of carbon dioxide absorption and the initial ammonia concentration.

The main equilibrium relationships are:

$$H_2O = OH^- + H^+ \qquad (5.21)$$

$$H_2CO_3 = HCO_3^- + H^+ \qquad (5.22)$$

$$HCO_3^- = CO_3^{--} + H^+ \qquad (5.23)$$

$$NH_4^+ = NH_3 + H^+ \qquad (5.24)$$

$$NH_2COO^- + H_2O = NH_3 + HCO_3^- \qquad (5.25)$$

A system of eight non-linear equations is then constructed as follows:

$$K_w = |H^+||OH^-| \qquad (5.26)$$

$$K_1 = \frac{|H^+||HCO_3^-|}{|H_2CO_3|} \qquad (5.27)$$

$$K_2 = \frac{|H^+||CO_3^{2-}|}{|HCO_3^-|} \qquad (5.28)$$

$$K_a = \frac{|H^+||NH_3|}{|NH_4^+|} \qquad (5.29)$$

$$K_h = \frac{|NH_3||HCO_3^-|}{|NH_2COO^-|} \qquad (5.30)$$

$$|NH_3|_T = |NH_3| + |NH_4^+| + |NH_2COO^-| \qquad (5.31)$$

$$|CO_2|_T = |HCO_3^-| + |CO_3^{2-}| + |NH_2COO^-| \qquad (5.32)$$

$$|NH_4^+| + |H^+| = |HCO_3^-| + 2|CO_3^{2-}| + |OH^-| + |NH_2COO^-| \qquad (5.33)$$

This system of eight non-linear Equations (5.26- 5.33), has eight unknowns. Equation(5.21) represents the equilibrium dissociation reaction of water, while Equations (5.22 - 5.23) are the first and second equilibrium dissociation reactions of carbonic acid respectively. Equation (5.24) is the equilibrium dissociation reaction of

ammonia in aqueous solution, while Equation (5.25) represents the hydrolysis of ammonium carbamate. Equations (5.31 - 5.32) are the total material balance for ammonia and carbon dioxide respectively, while Equation (5.33) is the electroneutrality or charge balance of all species present in the system. Table 5.2 shows the Jacobian Matrix of the above system of equations. The solution of these equations provide the the concentration of unreacted ammonia, in addition to other equilibrium concentrations. Table 5.3 provides the numerical solution for the case of 6.2 M ammonia solution under the specified carbon dioxide rate. Similar solutions for other conditions are given in Appendix D .

5.2.3 Verification of the Proposed Rate Equation:

Now the verification of the existence of instantaneous regime can be carried out, as the rate of absorption of carbon dioxide was measured experimently.

As proposed earlier, the absorption rate of CO_2 is given by:

$$N_A a = k_l a C_{Ai} E_i \tag{5.34}$$

where E_i, the enhancement factor for instantaneous reaction :

$$E_i = \frac{\sqrt{\frac{D_A}{D_B}}}{z C_{Ai}} + \frac{C_B}{z C_{Ai}} \sqrt{\frac{D_B}{D_A}} \tag{5.35}$$

Hence:

Table 5.2 Jacobian Matrix

$-[OH^-]$	$-[H^+]$	0	0	0	0	0	0	-f1
$-[HCO_3^-]$	0	$-[H^+]$	$10^{-6.382}$	0	0	0	0	-f2
$-[CO_3^{2-}]$	0	$10^{-10.377}$	0	$-[H^+]$	0	0	0	-f3
$-[NH_3]$	0	0	0	0	$-[H^+]$	2.2^{-10}	0	-f4
0	0	$-[NH_3]$	0	0	$-[HCO_3^-]$	0	0.285	-f5
0	0	0	0	0	-1	-1	-1	-f6
0	0	-1	0	-1	0	0	-1	-f7
1	-1	-1	0	-2	0	+1	-1	-f8

Where

f1 = $10^{-14} - [OH^-][H^+]$

f2 = $10^{-6.382}[H_2CO_3] - [HCO_3^-][H^+]$

f3 = $10^{-10.377}[HCO_3] - [CO_3^{2-}][H^+]$

f4 = $2.2^{-10}[H_2NH_2^-] - [H_2NH][H^+]$

f5 = $0.285*[NH_2COO^-] - [NH_3][HCO_3^-]$

f6 = $[NH_3]_T - \{[NH_3] + [NH_4^-] + [H_2NCOO^-]\}$

f7 = $[CO_2]_T - \{[HCO_3^-] + [CO_2^{2-}] + [H_2NCOO^-]\}$

f8 = $[NH_4^-] + [H^+] - \{[OH^-] + [HCO_3^-] + 2[CO_3^{2-}] + [NH_2COO^-]\}$

Table 5.3. Equilibrium Composition of Aqueous Carbonated Ammonia Solution 6.2 M NH_3 , Flow 2 l/min. , Temp. 22 °C

Time (min)	$[CO_2]$ (mole/l)	$[H^-]$ (mole/l)	$[OH^-]$ (mole/l)	$[HCO_3^-]$ (mole/l)	$[H_2CO_3]$ (mole/l)	$[CO_3^-]$ (mole/l)	$[NH_3]$ (mole/l)	$[NH_4^-]$ (mole/l)	$[H_2NCOO^-]$ (mole/l
1	0.05466	4.0394E-12	0.0025	5.2588E-7	5.1192E-12	0.0546	6.0882	0.1118	1.1234E-5
4	0.13292	9.8922E-12	0.01	3.1308E-6	7.4638E-11	0.1329	5.9332	0.2668	6.5178E-5
5	0.15566	1.1661E-11	8.5755E-4	4.3217E-6	1.2145E-10	0.1556	5.8878	0.3121	8.9282E-5
6	0.17654	1.3311E-11	7.5128E-4	5.5943E-6	1.7945E-10	0.1764	5.8462	0.3537	1.1476E-4
7	0.21654	1.6539E-11	6.0463E-4	8.5247E-6	3.3978E-10	0.2164	5.7663	0.4335	1.7248E-4
8	0.23183	1.7798E-11	5.6187E-4	9.8208E-6	4.2123E-10	0.2316	5.7358	0.4640	1.9765E-4
10	0.30804	2.4276E-11	4.1192E-4	1.7794E-5	1.0410E-9	0.3077	5.5835	0.6161	3.4861E-4
20	0.55833	4.8286E-11	2.0710E-4	6.4087E-5	7.4574E-9	0.5571	5.0832	1.1157	0.0011
40	0.95625	9.7953E-11	1.0209E-4	2.2231E-4	5.2479E-8	0.9527	4.2876	1.9090	0.0033
60	1.37291	1.7439E-10	5.7343E-5	5.6728E-4	2.3841E-7	1.3655	3.4547	2.7384	0.0069
80	1.75833	2.8718E-10	3.4821E-5	0.0012	8.2666E-7	1.7459	2.6845	3.5042	0.0113
100	2.06208	4.3479E-10	2.3000E-5	0.0021	2.2189E-6	2.0445	2.0779	4.1066	0.0154
120	2.31375	6.4278E-10	1.5557E-5	0.0035	5.4340E-6	2.2908	1.5760	4.6046	0.0194

$$\frac{N_A a}{C_{Ai}} = k_l a \{ \sqrt{\frac{D_A}{D_B}} + (\sqrt{\frac{D_B}{D_A}} + \frac{1}{z C_{Ai}}) C_B \} \qquad (5.36)$$

If the instantaneous regime prevails, then the plot of the left hand side of the equation versus C_B should give a straight line. For this verification, it is important to know the unreacted ammonia concentration in the bulk. This ammonia concentration was obtained from the solution of non-linear equation considered above. The plots given in Figures 5.6 to 5.8 show the existing instantaneous regime, for different cases of initial ammonia concentration used in the separation process.

5.2.4 Comparison Between Experimental and Theoretical Results

Once the regime of reaction is established, the comparison can be carried out between the values of unreacted ammonia obtained from the results of the analysis of filtrate and precipitates and corresponding values obtained by means of numerical solutions described earlier. The theoretical calculation of unreacted ammonia requires feeding parameters such as the total amount of carbon dioxide absorbed for the specified time of carbonation and the total amount of ammonia fed to the column as shown by Figure 5.9.

Figure 5.9 illustrates the schematic determination of unreacted ammonia by numerical and experimental techniques. This scheme

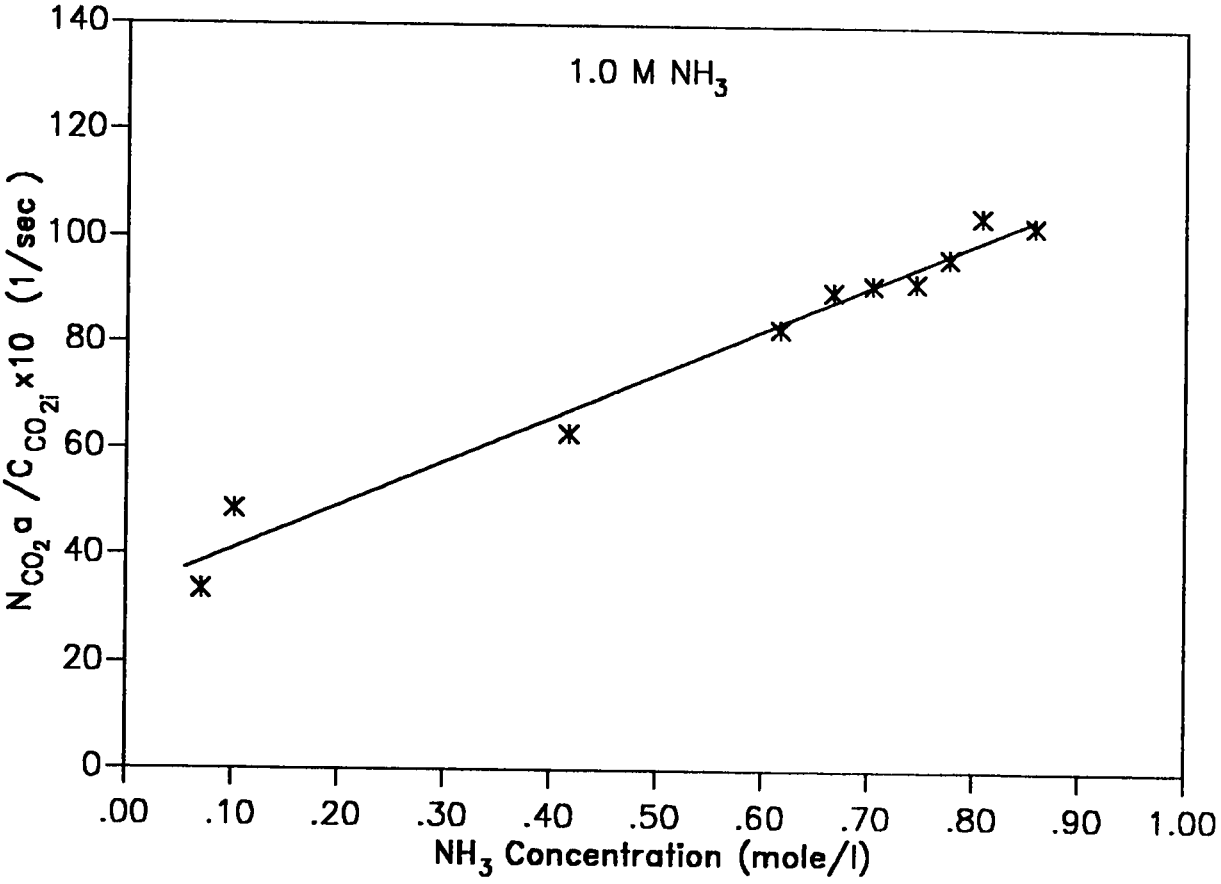

Figure 5.6 Verification of Instantaneous Regime

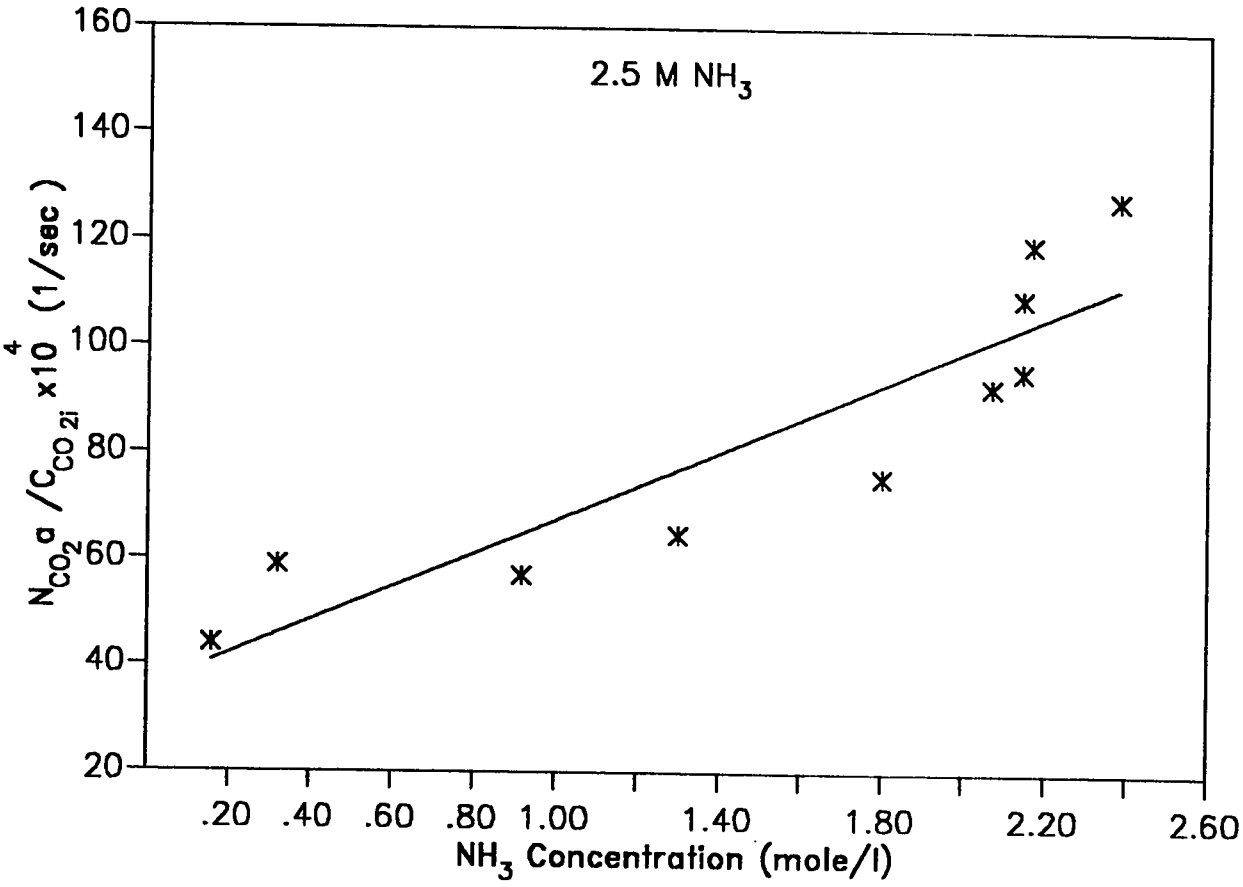

Figure 5.7 Verification of Instantaneous Regime

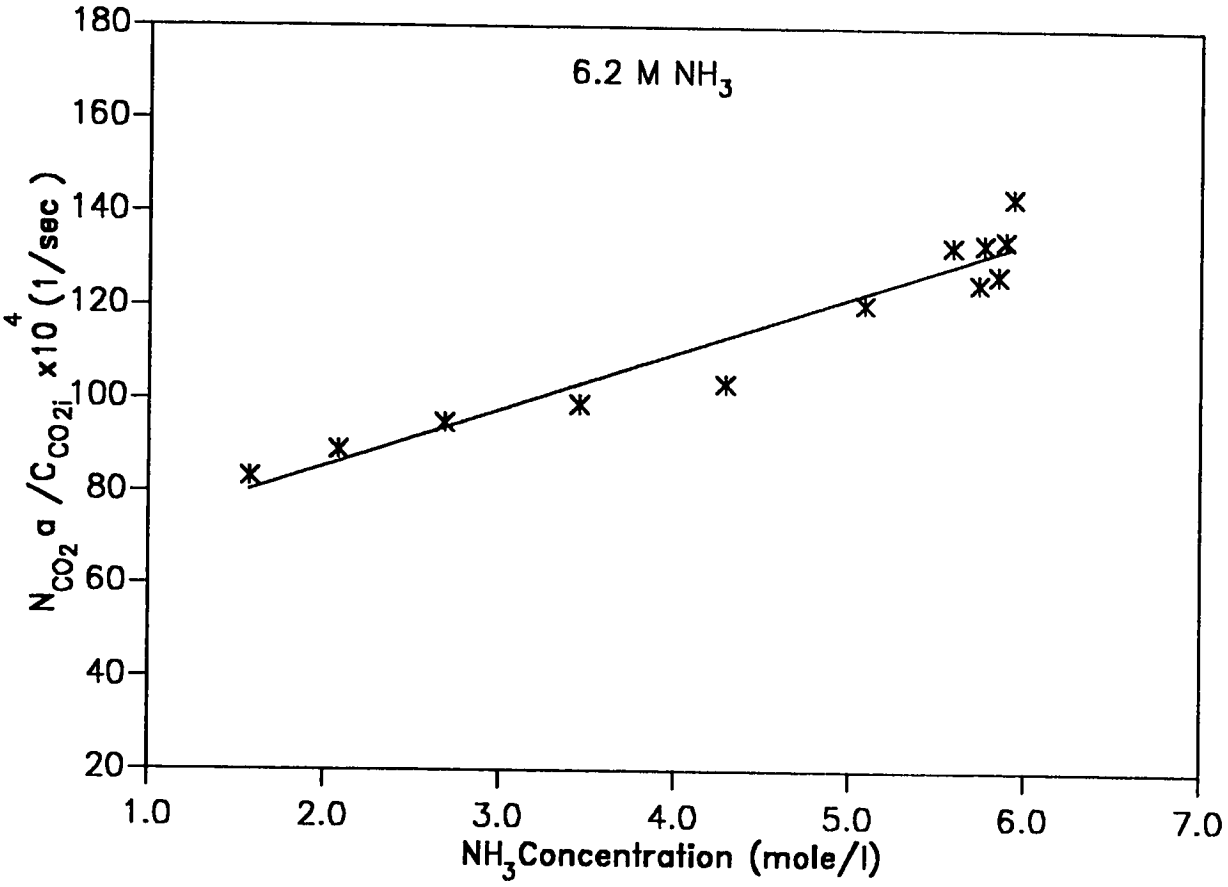

Figure 5.8 Verification of Instantaneous Regime

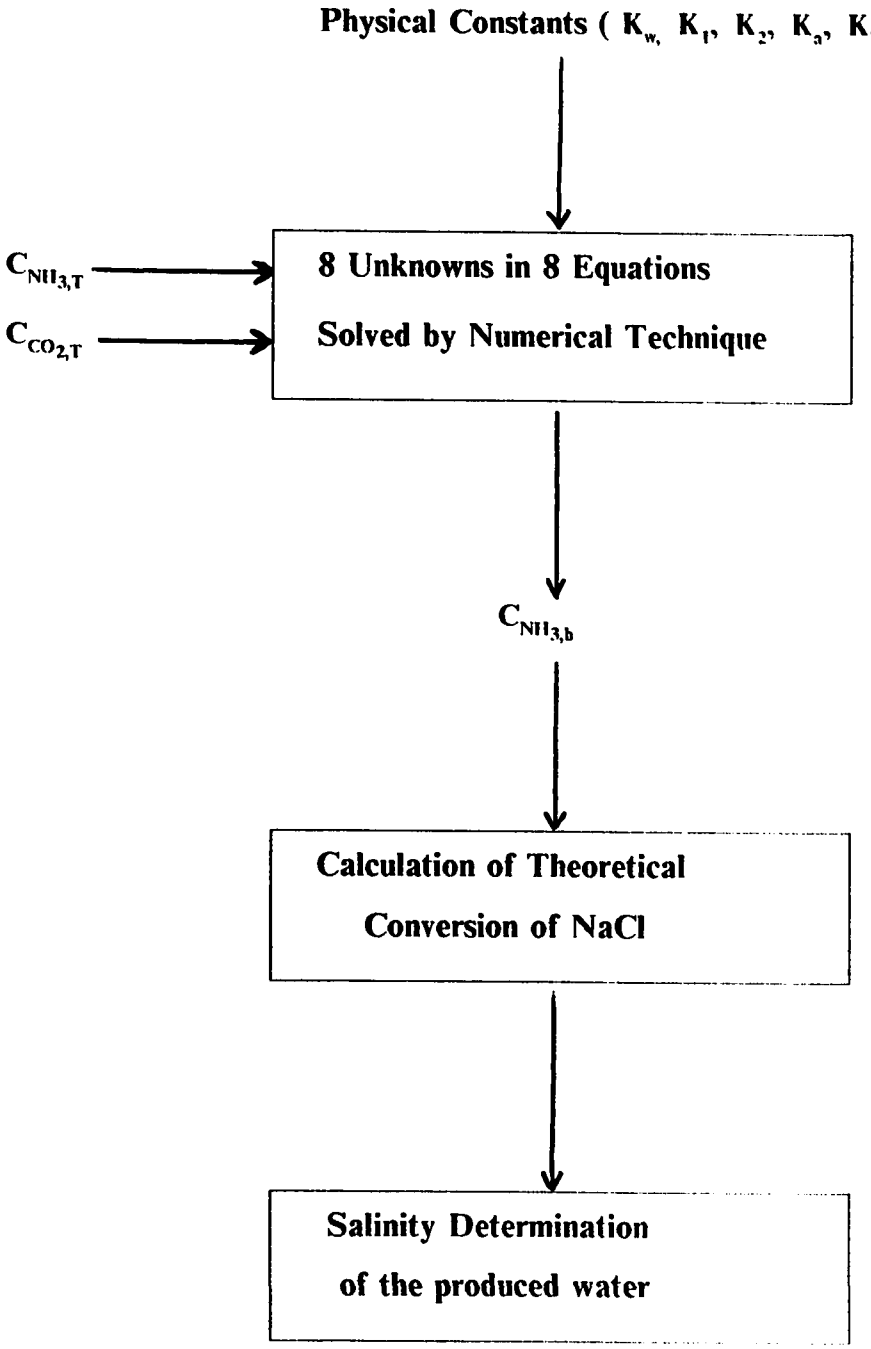

Figure 5.9 Schematic Determination of Unreacted NH_3

provides the theoretical determination of NaCl conversion and hence the salinity computation of the produced water. The values of unreacted ammonia are plotted in Figures 5.10 and 5.11. These curves show a close agreement between experimental and theoretical values.

Absorption Rate of CO_2

Another way of verifying that the system behaves as a diffusion-controlled mass transfer system with an instantaneous reaction regime is to study the rate of absorption of carbon dioxide both experimentally and theoretically. This was made possible by the total carbon analyzer (TOC) machine that measures the experimental absorption rates of CO_2 of different initial ammonia concentrations. The experimental values can be compared to theoretical values of absorption rates of carbon dioxide. In this case, the instantaneous enhancement factor, E_i, may be expressed, according to Danckwerts (1970), as:

$$E_i = \frac{1}{erf(\frac{\sigma}{\sqrt{D_A}})} \tag{5.37}$$

Where σ is defined by

$$e^{\frac{\sigma^2}{D_B}} erfc(\frac{\sigma}{\sqrt{D_B}}) = \frac{C^o_B}{ZC_{Ai}}\sqrt{\frac{D_B}{D_A}}\, e^{\frac{\sigma^2}{D_A}} erfc(\frac{\sigma}{\sqrt{D_A}}) \tag{5.38}$$

Equations (5.37) and (5.38) are solved numerically and the

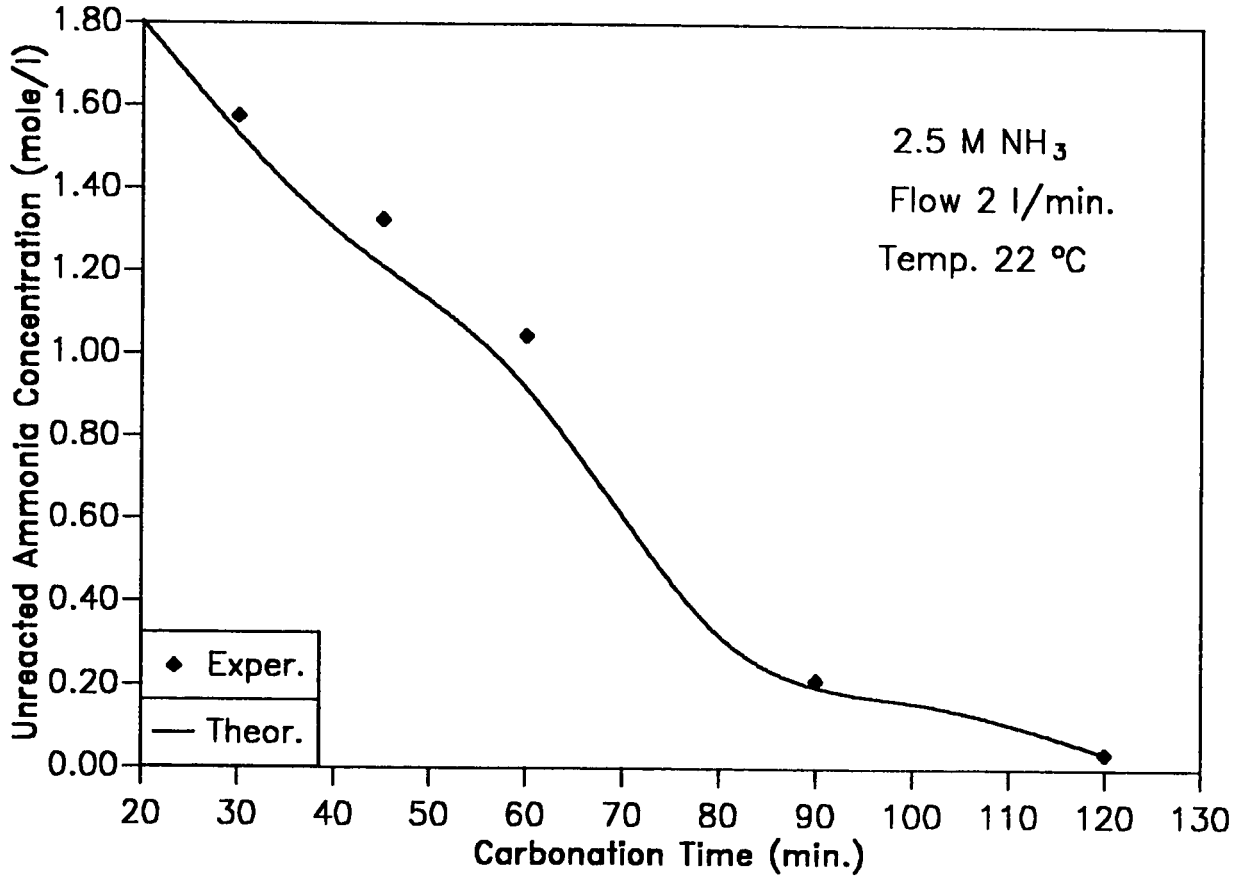

Figure 5.10 Comparison Between Calculated & Experimental Unreacted NH_3

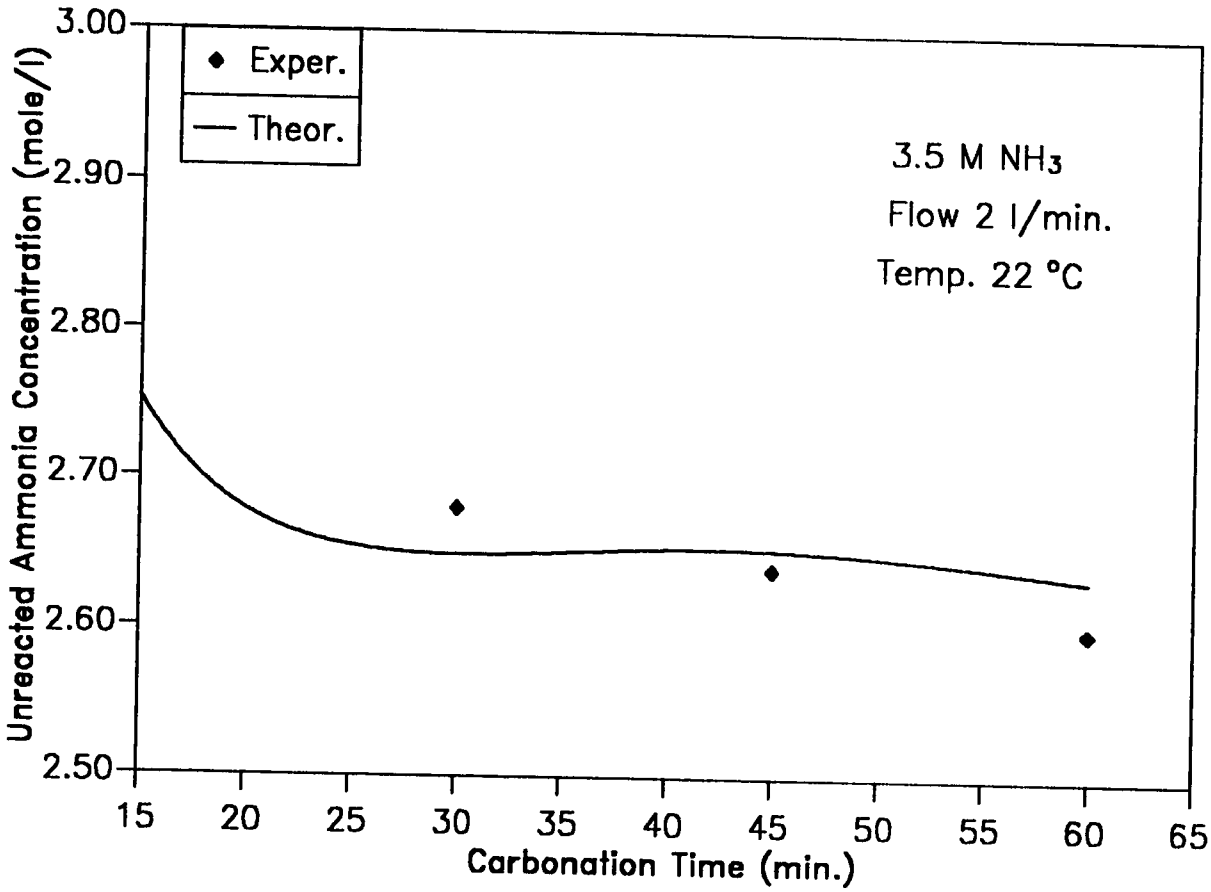

Figure 5.11 Comparison Between Calculated & Experimental unreacted NH_3

theoretical absorption rates of carbon dioxide are computed using Equation (5.39). Steps of this scheme are shown in Figure 5.12.

$$N_A a = = 2\left(\sqrt{\frac{D_A}{t\pi}}\right) a C_{Ai} E_i \qquad (5.39)$$

The results are shown graphically as a plot of the absorption rate of CO_2 against carbonation time. Figures 5.13 - 5.17 give the comparison between experimental and theoretical absorption rates of CO_2. The good agreement between the corresponding experimental and theoretical values again verifies the reaction regime that is responsible in the separation process of the presented system.

5.3 Semibatch Gas-Liquid Reactor Model

$$CO_2 + 2NH_3 \rightarrow \quad \text{Product} \qquad (5.40)$$

Assumptions

1. The gas flow is an ideal plug flow.

2. The liquid in the contactor is assumed to be completely backmixed.

3. The physical properties of the liquid remains unchanged during the operation.

$$E_i = \frac{1}{\operatorname{erf}\left(\frac{\sigma}{\sqrt{D_{CO_2}}}\right)} \tag{5.37}$$

$$e^{\frac{\sigma^2}{D_{NH_3}}} \operatorname{erfc}\left(\frac{\sigma}{\sqrt{D_{NH_3}}}\right) = \frac{C^0_{NH_3}}{ZC_{CO_{2i}}} \left(\frac{D_{NH_3}}{D_{CO_2}}\right) e^{\frac{\sigma^2}{D_{CO_2}}} \operatorname{erfc}\left(\frac{\sigma}{\sqrt{D_{CO_2}}}\right) \tag{5.38}$$

$$N_{CO_2} a = 2\left\{ \left(\frac{D_{CO_2}}{t\pi}\right) \right\} a C_{CO_{2i}} E_i \tag{5.39}$$

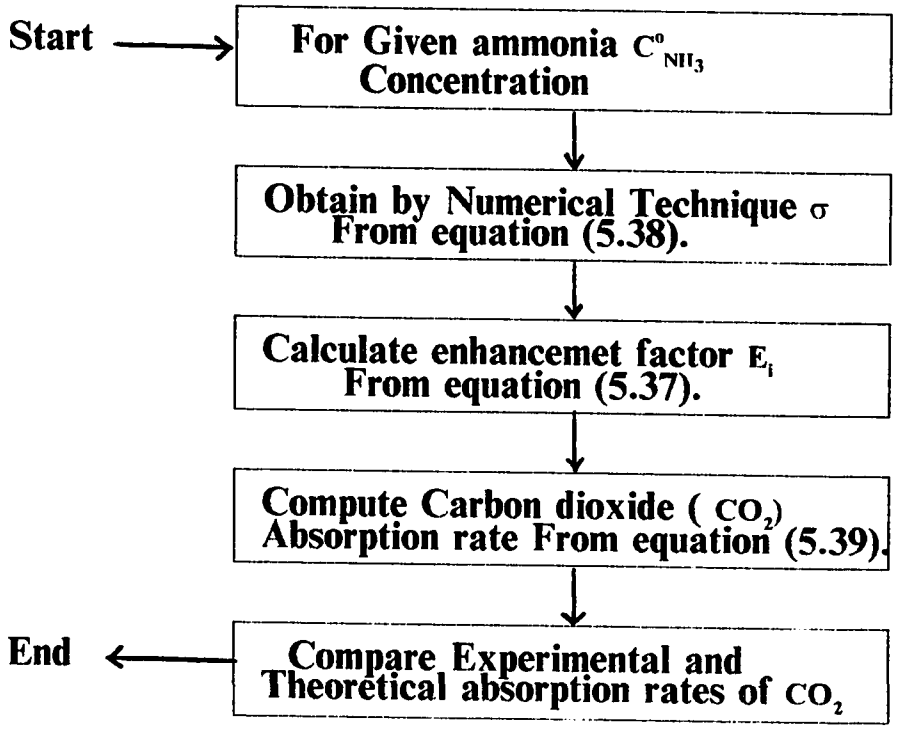

Figure 5.12 Verification of Absorption Regime

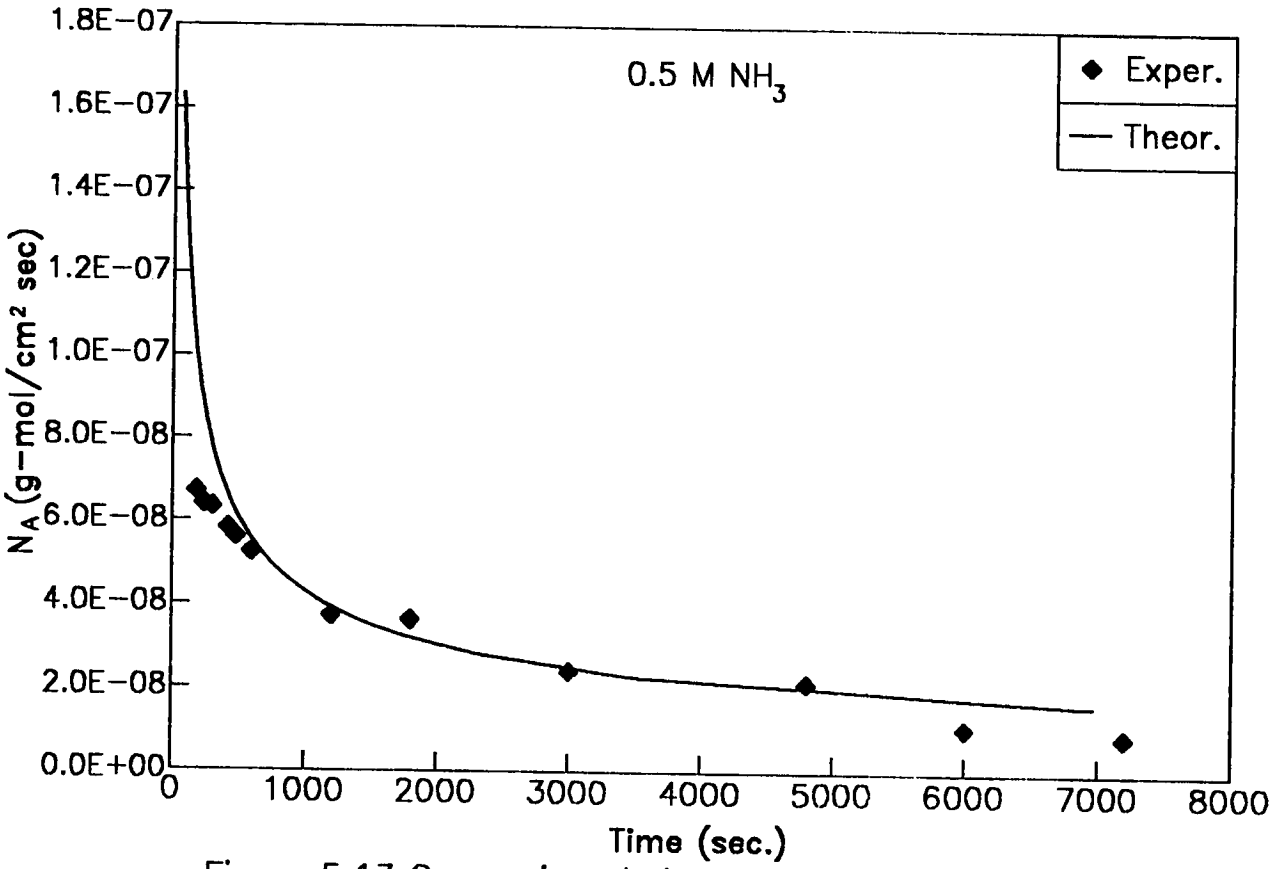

Figure 5.13 Comparison between Measured and Calculated Absorption Rates of CO_2

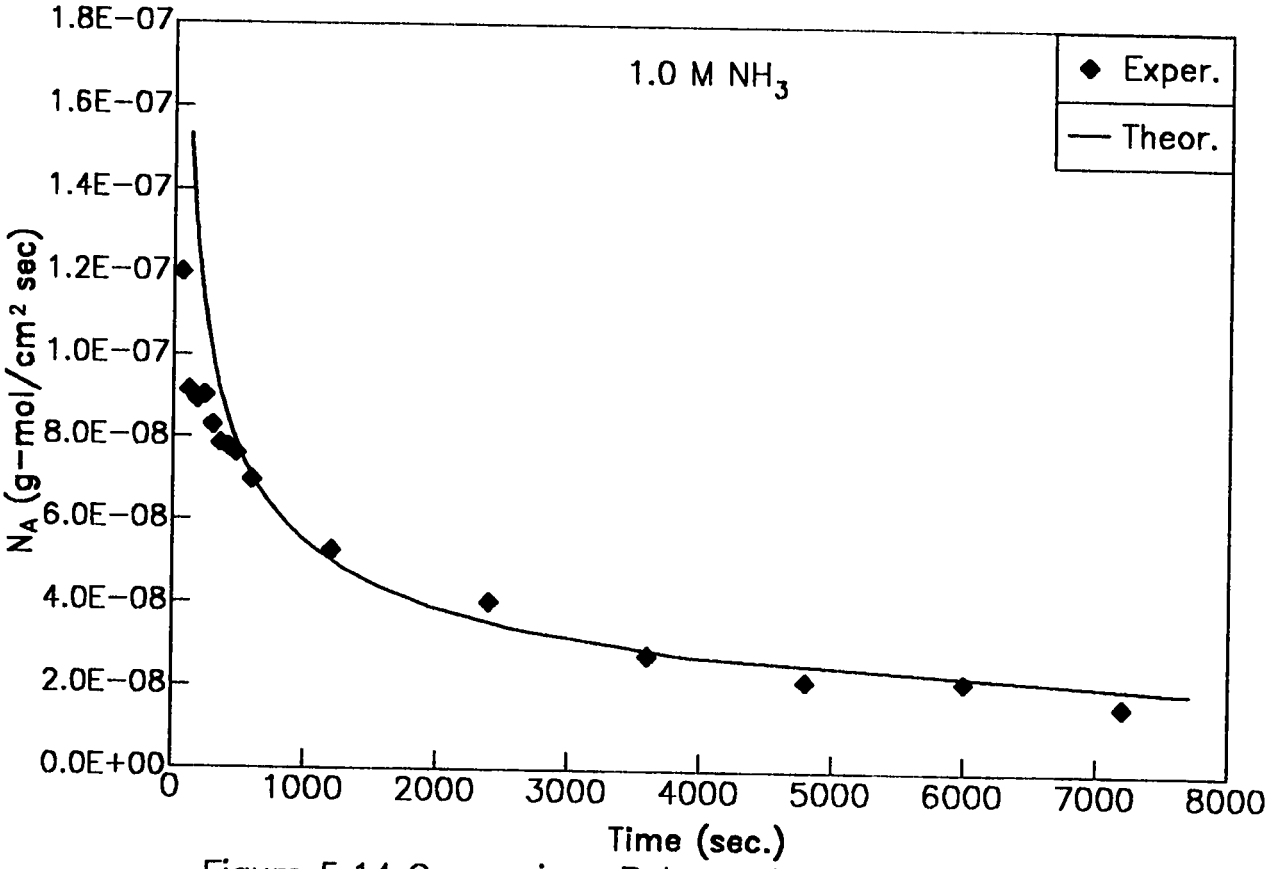

Figure 5.14 Comparison Between Measured and Calculated Absorption Rates of CO_2

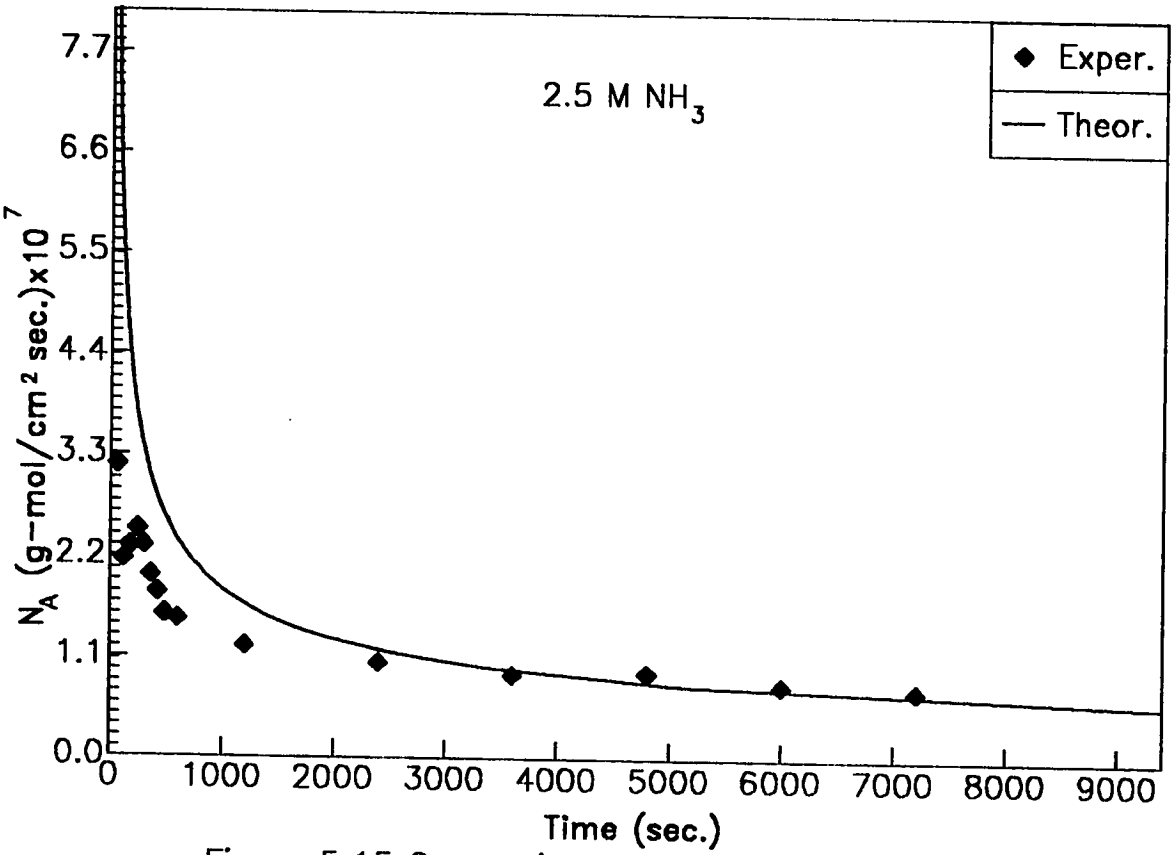

Figure 5.15 Comparison Between Measured and Calculated Absorption Rates of CO_2

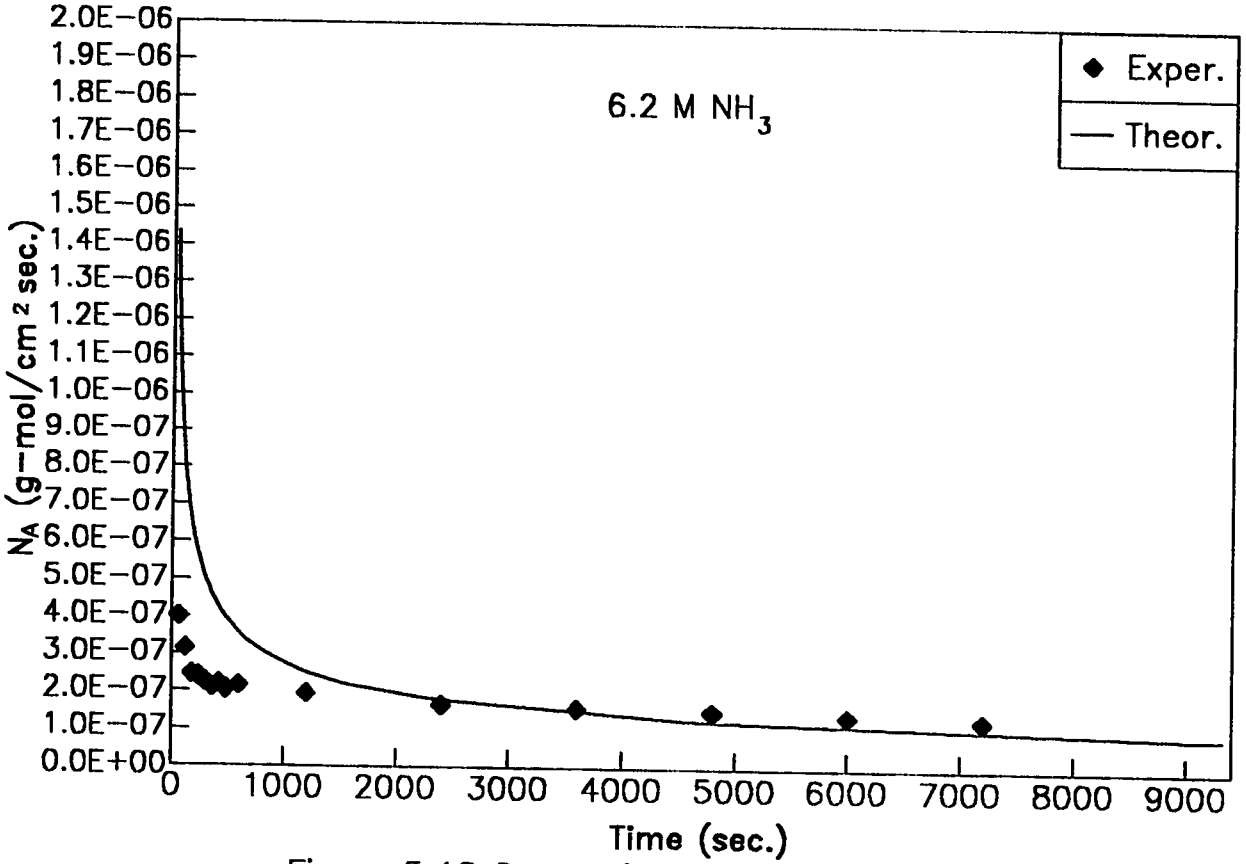

Figure 5.16 Comparison Between Measured and Calculated Absorption Rates of CO_2

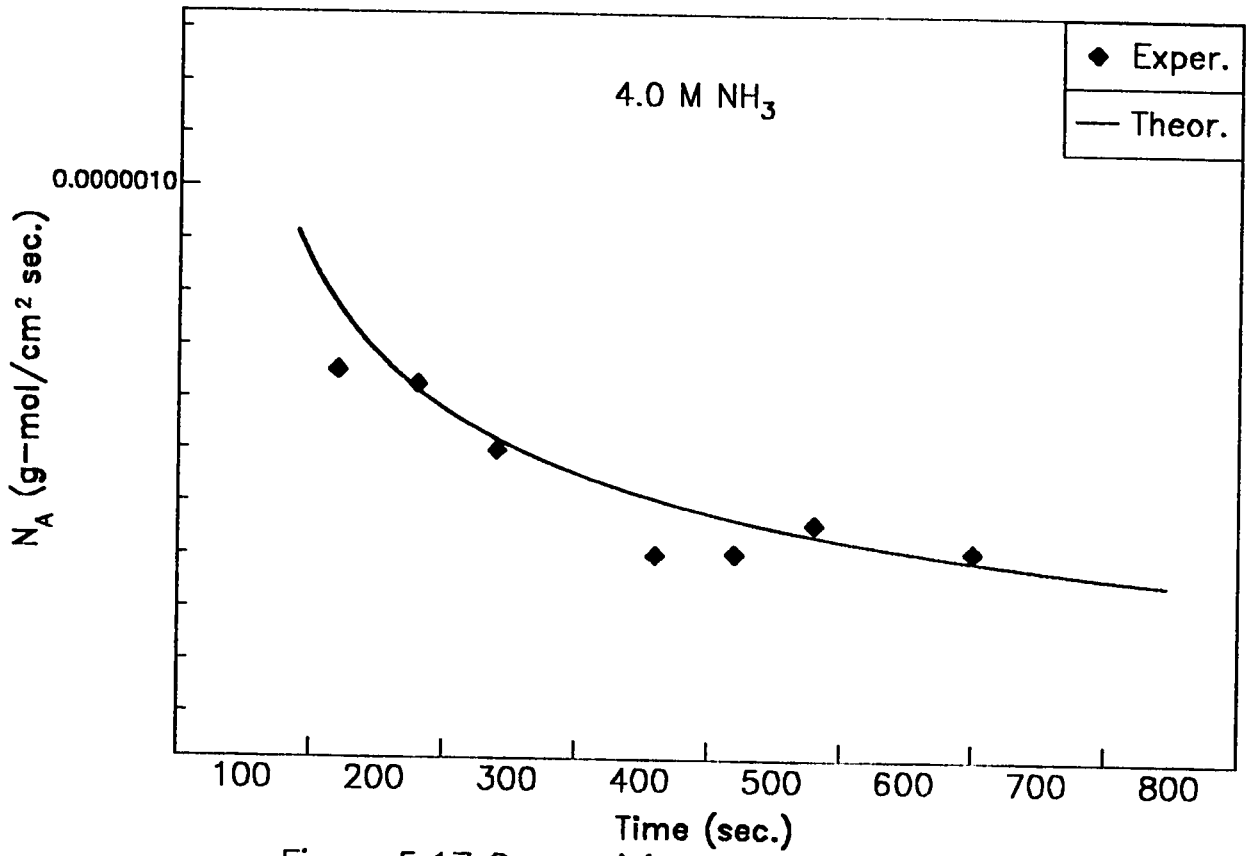

Figure 5.17 Comparision Between Measured and Calculated Absorption Rates of CO_2

4. The gas-film resistance is negligible and therefore not to be taken into consideration.

5. Solubility of CO_2 is assumed constant.

Mass balance for the liquid phase (NH_3):

$$-(1-E_g)\frac{dC_{NH_3}}{dt} = Z R_{CO_2} a = 2 K_L a C_{CO_{2i}} E_i \qquad (5.41)$$

$$-(1-E_g)\frac{dC_{NH_3}}{dt} = 2\{\frac{\sqrt{D_{CO_2}}}{\sqrt{\pi t}}\} a C_{CO_{2i}} E_i \qquad (5.42)$$

$$C_{NH_3} = C^{o}_{NH_3} - \frac{2}{1-E_g} a C_{CO_{2i}} E_i \{\sqrt{(D_{CO_2} t/\pi)}\} \qquad (5.43)$$

Where

E_g = gas holdup

E_i = enhancement factor for instantaneous reaction

t = carbonation time

$C^{o}_{NH_3}$ = initial ammonia concentration

C_{NH_3} = unreacted ammonia concentration

a = interfacial area

$C_{CO_{2i}}$ = solubility of carbon dioxide in the solution

D_{co_2} = carbon dioxide diffusivity

This model provides a theoretical determination of the unreacted ammonia concentration left in the solution after a known period of carbonation time has been carried out. The enhancement factor is assumed to be constant and equal to its value in the instantaneous regime. The interfacial area has to be given .

5.4 Statistical Model

The experimental data can be correlated statistically using regression analysis. For instance, the case of 12 M NH_3 and 3.25 M NaCl separation using the Batch Gas Bubbler may be considered. Since, in this study, it was important to know, the mathematical correlation between carbonation time and Na^+ concentration remaining in the solution, it was necessary that the conditions for efficient operation of the experiment be handled in such a way that the data were capable of providing the desired information from the adopted statistical model. The statistical analysis used serves as a basis for the formulation of a relationship between the physical quantities involved in the experiment. Various statistical models were tested and their accuracy was

checked using the parameters such as the coefficient of determination and the coefficient of variation. The summary of the results is depicted in the Table 5.4.

Table 5.4 Best fit tests of different models

Model type	R^2	Adj. R^2	C.V
Linear	0.95	0.93	16.06
Quadratic	0.98	0.97	11.54
Exponential	0.97	0.96	35.80

First, a linear model was developed which provided a satisfactory representation of the data except at the extreme ends of the carbonation time. Despite the fact that deviations do exit at low and high ranges of carbonation time, however, the linear model gave a coefficient of determination of 0.95. Since in this experiment the regressor variable is the carbonation time only, the goodness of fit for the data can be represented adequately by the coefficient of determination instead of the adjusted one. The coefficient of variation, which is an indication of the precision of the model, for the linear model was found to be 16.06.

Secondly, an exponential model was tested. The exponential model was linearized using appropriate transformation. The model coefficients of variation and determination as given in Table 5.4 show that it is not the best fit model of the data. However, it is better than the linear model described earlier. Finally, a polynomial model of degree 2 was tested. The best fit was achieved using this model as the corresponding values of parametric coefficients are shown in the above table. This model has fitted most of the data except in the initial range of carbonation time. Sodium ion concentration can be expressed as a function of the carbonation time. The model obtained is of the following type:

$$y = ax^2 + bx + c \qquad (5.44)$$

Where

a = 0.282

b = -1.826

c = 3.393

x = Carbonation Time

y = Sodium ion Concentration

The best fit is indicated by the closeness of the coefficient of determination to unity. A typical example is depicted in Figure

5.18 which has a coefficient of determination (R^2) of 0.98 which indicated that 98% of the data is accounted by the regression equation :

$$y = 0.282\,x^2 - 1.826\,x + 3.393 \qquad (5.45)$$

As it can be noticed from the figure, the best fit of the experimental data is represented by a parabolic model.

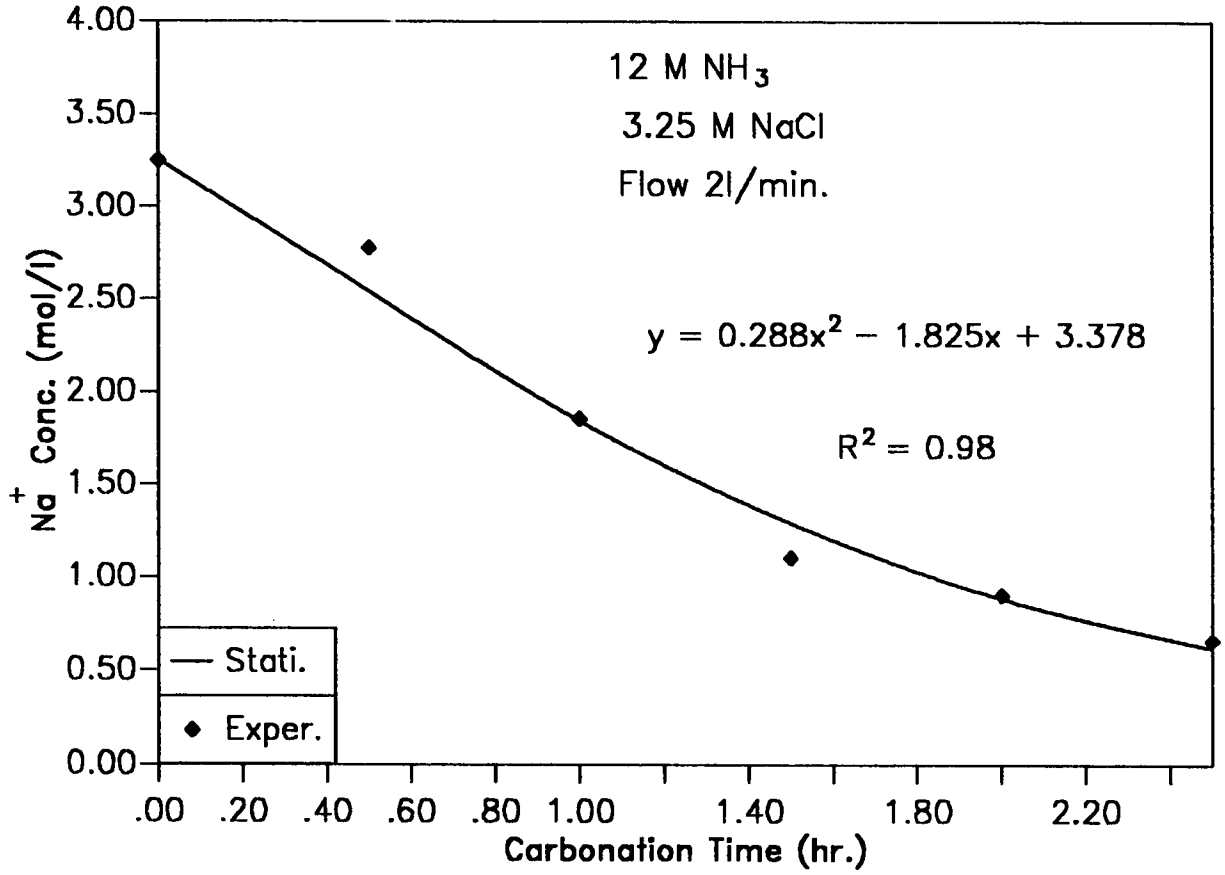

Figure 5.18 Comparison Between Experimental Data and a Statistical Model

Chapter VI

ENERGY REQUIREMENTS

6.1 Introduction

To compare the Solvay process with the other conventional desalination processes in terms of energy requirement, it is necessary to know the amount of free energy of formation involved to various stages of the process. The magnitude and the sign of free energy of formation provide a means of estimating the energy requirement. For a process operating both at constant temperature and constant pressure, the maximum availabe useful work is measured by a decrease of Gibbs free energy of formation.

Dodge (1944) laid down the following rough guide to whether a reaction was thermodynamically promising at a given temperature:

If $\Delta G^o < 0$, then the reaction is promising ,

If $0 < \Delta G^o < 10{,}000$ cal/mol, the reaction is of doubtful promise but warrants further study.

If $\Delta G^o > +\ 10{,}000$ cal/mol, the reaction is very unfavorable and would be feasible only under unusual circumstances.

The simplest way to obtain the free energy change is by algebraic combination of the free energies of formation of the various

substances concerned. Free-energy changes can be obtained by the addition of the values for reactions whose algebraic sum is the reaction in question. The fundamental basis for this is the fact that ΔG^o depends only on initial and final states and not on the intermediate steps by which the final state is reached. The free energy ΔG^o is the difference between the free energies of the products and reactants at their standard state.

$$\Delta G^o = \sum \Delta G^o_{f\,prods} - \sum \Delta G^o_{f\,reactants} \qquad (6.1)$$

The standard free energy of formation of substances not available can be estimated using the method of Krevelin and Chemin (1951). They suggested that ΔG^o might be correlated as a linear function of temperature and that the constants were additive functions of the atomic groups comprising the molecule, which are represented by:

$$\Delta G^o = A + B\,T \qquad (6.2)$$

The free energy of a reaction can be computed using the heat capacity method; which allows the variation of the temperature. If molal heat capacities as function of temperature are known for each species taking part in the reaction and can be expressed by equations of the form :

$$C_p = a + b\,T + C\,T^{-2} \qquad (6.3)$$

Then an analytical expression may be developed for standard heat of reaction as follows:

$$\Delta H^{\circ}_{T} = \Delta H^{\circ}_{298} + \int_{298}^{T} \Delta C_p dt \qquad (6.4)$$

Which leads to:

$$\Delta C_p = \sum_{prod} n C_p - \sum_{reactant} n C_p \qquad (6.5)$$

$$\text{and} \quad \Delta H^{\circ}_{T} = \Delta H_o + \Delta a T + \frac{\Delta b T^2}{2} - \frac{\Delta C}{T} \qquad (6.6)$$

Where,

ΔH°_{T} = the standard heat of reaction at temperature T

ΔH_o = constant.

The constant ΔH_o may be calculated if the standard heat of reaction is known at a single temperature such as 25 $^{\circ}C$. Table 6.3 provides the heat capacities of the interesting species. The standard free energy is related to the standard heat of reaction and the equilibrium constant by the following equations.

$$\Delta G^{\circ} = \Delta H^{\circ} - T\Delta S^{\circ} \qquad (6.7)$$

$$\Delta G^{\circ} = -RT \ln K_{eq} \qquad (6.8)$$

When the effects of temperature on ΔG° are considered using (6.7), the following equation is obtained:

$$\frac{\Delta G^o}{T} = -\int \frac{\Delta H^o}{T^2} dt \qquad (6.9)$$

Now using equations (6.8) and (6.9) gives:

$$\ln K_{eq} = -\frac{\Delta H_o}{RT} - \Delta a \ln T - \frac{\Delta b T^2}{2} - \frac{\Delta C}{2T} - RI T \qquad (6.10)$$

Where I is a constant of integration, which may be evaluated from a knowledge of the equilibrium constant at one temperature. The variation of the standard free energy change with temperature can be obtained by combining equations (6.9) and (6.10)

$$\Delta G^o = -\Delta H_o - \Delta a T \ln T - \frac{\Delta b T^2}{2} - \frac{\Delta C}{2T} - RI T \qquad (6.11)$$

Calculations:

The ΔG^o_{298} of the infeasible chemical reaction leading to the formation of soda ash according to the equation:

$$2NaCl + CaCO_3 = CaCl_2 + Na_2CO_3 \qquad (6.12)$$

may be obtained using values of standard free energy given in the literature:

$$\Delta G^o_{298} = \sum \Delta G^o_{prod} - \sum \Delta G^o_{reactant} \qquad (6.13)$$

= (-195.36 -249.55) - (2 x -91.894 -270.8) = 9678 cal/mol,

which confirms that the reaction as such is endothermic and requires a method of overcoming the positive ΔG as carried out successfully in the classical Solvay process. The free energy changes involved in

the Solvay process are determined using the concept elaborated before. The process consists of a series of reactions which occur approximately at the given temperatures.

Table 6.1. Heat Capacities of inorganic Substances

Compound	Cp (Cal/mol degree)
$CaCo_3$	19.68 + 0.01189T - 30760 T^{-2}
CaO	10.0 + 0.00484T - 108000 T^{-2}
CO_2	10.32 + 0.00274T - 195500 T^{-2}
H_2O	8.22 + 0.0015T - 0.00000134 T^{-2}
$CaCl_2$	19.6 + 0.00386T
$NaCl_2$	10.79 + 0.0042 T
NH_3	6.7 + 0.0063 T
NH_4Cl	9.8 + 0.0368 T
$NaHCO_3$	11.8 + 0.032 T
$Ca(OH)_2$	2.41
Na_2CO_3	29.8

First reaction:

$$CaCO_3 = CaO + CO_2 \quad 1000^{\circ}C \tag{6.14}$$

Step 1: Find ΔH^{o}_{298} and ΔG^{o}_{298}

ΔH^{o}_{298} = (-94.052 - 151.7) - (- 289.5) = 43.748 kcal/mol

ΔG^{o}_{298} = (-94.26 - 144.3) - (- 270.8) = 32.24 kcal/mol

Step 2: Find Δa, Δb, Δc from the heat capacity.

Δa = (10.34 + 10) - (19.68) = 0.66

Δb = (0.00274 + 0.00484) - (0.1189) = -0.00431

Δc = (-195500 -108000) - (-307600) = 4100

Step 3: Find ΔH_{o} from equation (6.6) at T = 298 K

ΔH_{o} = 473748 cal/mol -0.066 * 298 + 0.00431 (298 * 298)/2 + 4100/298 = 43765 cal /mol

Step 4: Find RI from equation (6.11), at T = 298 K

RI = 1/298(-32240 + 43756 - 0.66 * 298 ln(298) + 0.00431 (298 * 298)/2 - 4100/(2 * 298) = 35.5033

Step 5: Find ΔG^{o}_{T} from equation (6.11), at T = 1273 K

ΔG^{o}_{1273} = 43756 -0.66 * 1273 ln(1273) - 0.00431 (1273 * 1273)/2 - 4100/(2 * 1273) - 35.5033 * 1273

ΔG^{o}_{1273} = -10940.108 cal /mol

2nd Reaction:

$$CaO + H_2O = Ca(OH)_2 \quad 100^{\circ}C \qquad (6.15)$$

ΔG°_{373} = - 3770.319 cal /mol

3rd Reaction:

$$Ca(OH)_2 + 2NH_4Cl = CaCl_2 + 2NH_3 + 2H_2O \quad 120^{\circ}C \qquad (6.16)$$

ΔG°_{393} = - 23517.198 cal /mol

4th Reaction:

$$NH_3 + H_2O + CO_2 + NaCl = NaHCO_3 + NH_4Cl \qquad (6.17)$$

ΔG°_{333} = - 1546.898 cal /mol

5th Reaction:

$$2\,NaHCO_3 = Na_2CO_3 + H_2O + CO_2 \quad 200^{\circ}C \qquad (6.18)$$

ΔG°_{473} = - 7140.44 cal /mol

Now the Gibbs free energy for the overall reaction of classical Solvay process is the sum of Gibbs free energy of the reactions (6.14), (6.15),(6.16), (6.17) (carried out for 2 moles of $NaHCO_3$ produced) and (6.18).

ΔG°_{total} = - 48461.753 cal /mol of soda ash.

For the case of the modified Solvay process (as proposed in this

work), the relevant reactions and the free energy determinations are given next. Basically, the proposed process utilizes reactions (6.17) and (6.18) only.

Using equation (6.17), at the operating temperature of 22 $^{\circ}C$, we get:

ΔG^{o}_{295} = - 4755.446 cal /mol

The overall Gibbs free energy of the modified Solvay process is given as follows:-

$\Delta G^{o}_{total} = 2(-4755.446) + (-7140.44)$

ΔG^{o}_{total} = - 16651.232 cal /mol of soda ash, as a final product.

As a desalting technique for converting sodium chloride into sodium bicarbonate only, the process will involve this energy (in accordance with reaction 6.17, for one mole of bicarbonate produced, one mole of NaCl is converted):

ΔG^{o}_{total} = -4755.446 cal / mole of NaCl converted

i.e

ΔG^{o}_{total} = -4755.446 cal/mole x 4.2 J/cal mole/58.45 g = - 341.7 kJ/kg of sodium chloride

In terms of desalted water, one can figure out the Gibbs free energy required for separation per kg of water produced as follows. For saline water of 20 % by weight of salt, such as sabkha resources

, 80 kg of desalted water could be recovered for each 20 kg of salt converted. The energy of separation equivalent to Gibbs free energy can be calculated as follows:

-341.7 kJ/kg * 20/80 = 85.4 kJ/kg of pure water.

This value falls within the range of the common conventional processes as shown in Table 2.4. However, the desalting is applied here to highly saline waters and the rejects from the conventional MSF process can be further treated with this method.

6.2 Power Input

Power input to gas and liquid phases per unit volume of bubble column reactor ($\frac{E}{V_r}$), in a sparged system is the sum of three terms corresponding to the power to overcome the static head, the kinetic power of liquid and gas respectively, to a first approximation (Botton, 1980):

$$\frac{E}{V_r} = \rho_E g (V_l + V_G) + \frac{V^2_{Lo}}{2H_m} \rho_l V_l + \frac{V^2_{Go}}{2H_m} \rho_G V_G \qquad (6.19)$$

Where

V_r = reactor volume

E_g = gas holdup

V_G = gas superficial velocity

ρ_G = gas density

ρ_L = liquid density

$$\rho_E = \rho_g E_g + \rho_l (1-E_g). \qquad (6.20)$$

E = power input

Sample Calculation

V_r = 1860 ml

g = 980 cm/ s^2

E_g = 0.1

V_G = 3.1 cm/s

ρ_G = 1.8294 g/l

ρ_L = 1.1279 g/ml

ρ_E = 10115.2929 g/l

Power = $E = V_r * \rho_E g V_g$ = 0.5737 Watt.

Chapter VII

CONCLUSIONS AND RECOMMENDATIONS

The work carried out during this research involved an experimental investigation of a non-conventional approach to desalination, using a modified classical Solvay Process. Synthetic saline and sabkha waters were used as a feed source for sodium chloride. The work included as well the design of a suitable experimental set-up and the experimental determination of the hydrodynamic parameters of gas liquid bubble column. The experimental data are analysed and the chemical reactions of the separation process are modeled. Finally, computation of free energy of separation of the system and the power input to the column are determined using thermodynamic principles.

7.1 Conclusions

The following conclusions may be drawn based on the experimental findings:

(1) The proposed separation process of Modified Solvay technique can be used for desalting highly saline waters.

(2) The technical feasibility of the modified process in separating NaCl from saline water was established. Indeed removals of

82.2% and 66.7% of sodium ion were found in the cases of the synthetic saline and sabkha waters, respectively, using a batch gas bubbler. The amount of NH_4Cl produced is in exact proportion to the converted NaCl.

(3) The determination of major chemical constituents of sabkha water using atomic absorption spectrometer showed high concentration of NaCl salt, up to 25 % by weight. Sabkha water is a potential feed for this process.

(4) The CO_2 absorption process underlying the separation of NaCl from the brine and its conversion into $NaHCO_3$ and NH_4Cl was shown to be in the instantaneous regime, hence process reactions are diffusion-controlled.

(5) The study of the effect of temperature showed an optimum temperature of separation of 22 $^{\circ}C$. This was indicated by the minimum Na^{+} concentration in the filtrate. At lower temperatures reaction rates were relatively poor, while at higher temperatures the absorption of the solute gas decreases with the increase of the temperature.

(6) An appreciable change of pH is seen in the initial period of process, however, pH values in the range of 8 - 10, were found to be effective and favoring to the formation of bicarbonate of sodium.

(7) The conversion of NaCl was found to be a function of the feed types, such as sabkha and synthetic saline waters, under similar process conditions. This is due to diversity in the concentrations and types of ions present, which brings different rheological properties of the solution that affect the solubility of CO_2 gas in the solution or the consumption of the reactants such as NH_3 by means of side reactions.

(8) The salinity of the brine affects the conversion efficiency in the case of the synthetic saline water. Under the same process conditions the higher the salinity the lower is the conversion of NaCl.

(9) The initial concentration of ammonia is found to affect both solubility and reaction of the absorbed gas, so that it increases the formation of ammonium bicarbonate which then reacts with the NaCl in the brine. Hence its increase generally increases the conversion process.

(10) The initial concentration ratio of NH_3 to NaCl affects the process separation. The percentage conversion assumes higher values when the concentration ratio is around 1.2. The right proportion of feed contributes to the successful utilization of the principal raw materials, such as ammonia and sodium chloride, and eventually brings better achievement in the separation of salt.

(11) For the same initial ammonia concentration, the higher the ammonium chloride formation the higher is the sodium chloride salinity, while for equal sodium chloride salinity, the formation of NH_4Cl increases with the increase of ammonia concentration in the feed.

(12) An experimental set-up for determining the non-adjustable parameters such as gas holdup, interfacial area and mass transfer coefficient was designed. The value of gas holdup remains constant when the height of column reaches 30 cm. However, the gas holdup increases with the increase of the superficial velocity of the gas and it is not affected by the temperature change.

(13) The values of interfacial area and the volumetric mass transfer coefficient were found to increase as the superficial gas velocity increased for the bubbly flow regime and were in accordance with literature values.

(14) The total Gibbs free energy for the conversion of NaCl into $NaHCO_3$ and NH_4Cl is 341.7 kJ per kg of sodium chloride , while the power input to the column is found to be 0.57 Watts.

(15) This research study establishes a relevant data base and basic fundamentals that can permit the rational design of a bubble column for the separation of highly saline waters using the

modified Solvay process. This is particularly applicable to the Kindom of Saudi Arabia, where indigenous sabkha deposits are plentful.

7.2 Recommendations

At the end of this work, the following recommendations are proposed for further investigation of saline water conversion using the experimental data obtained in this research:-

(1) Further investigation of the use of counter and cocurrent continuous bubble columns and stirred tank reactors for the same process.

(2) Use of amines of possible industrial significance for the absorption of carbon dioxide in addition to the ammonia which was used in this study.

(3) Investigation of conversion efficiency under non-isothermal absorption processes and the use of higher pressures.

(4) Use of gas mixtures containing carbon dioxide, rather than the pure carbon dioxide used in this study, to estimate its effect on the conversion that may result from variations of kinetic and the mass transfer properties of process reactions.

(5) Further study on the potential use of sabkha, as a source for useful minerals such as Magnesium, using this process.

(6) Investigation of the effect of different types of gas distributor and various column dimensions on the conversion process.

NOMENCLATURE

A	Solute gas
C_A^*	Interfacial concentration or physical solubility of gas ($\frac{Kmol}{m^3}$)
C_A^o	Concentration of the gas in bulk liquid phase ($\frac{Kmol}{m^3}$)
a	Interfacial area per unit volume, m^{-1}
B	Liquid phase reactant
C_B^o	Concentration of B in the bulk ($\frac{Kmol}{m^3}$)
CA	Chlor-Alkali
cosh	Hyperbolic cosine
C_{Ai}	Interfacial concentration of A, $\frac{Kmol}{l}$
C_B	Liquid phase concentration, $\frac{Kmol}{l}$
C_i	Concentration of ion, $\frac{kg-ion}{l}$
D_A	Diffusion coefficient of component A in solution ($\frac{m^2}{s}$)
D_B	Diffusion coefficient of liquid phase component ($\frac{m^2}{s}$)
D, Dc	Column diameter, m
d_{vs}	Standard mean dispersed-phase diameter, m
d	Diameter of the bubble, m
EDC	Ethylene dichloride
E, E_A	Enhancement factor
E_i	Enhancement factor for instantaneous reactions
erf	error function
erfc	complementary error function (1-erf)

E, E_g	Gas holdup
gc	Gravitational conversion factor Kgm Kg(force) $^{-1}m^{2}$
g	Gravitational Constant, ms^{-2}
Ha	Hatta number
H_d	Dispersion height, m
H_c	Clear liquid height, m
He	Distribution coefficient of Henry's law $(\frac{Kmol}{m^3})$ gas
h_s	Salting out parameter $\frac{l}{kg-ion}$
I_o	Intensity of light $\frac{kg-ion}{l}$
J_a	Mass flux of component A $\frac{Kmol}{m^2 sec}$
I	Ion strength of solution, g−ion/l
i-	Ion specific constant of negative ions $\frac{l}{kg-ion}$
i+	Ion specific constant of positive ions $\frac{l}{kg-ion}$
i_g	Contribution of solute gas to salting out parameter $\frac{l}{kg-ion}$
K	Reaction rate constant Eq. (1.5) , kmol/m-s
K_l	Liquid side physical mass transfer coefficient (m/s)
K_1	First order reaction rate constant (1/s)
K_2	Second order reaction rate constant (l/mol-s)
K_la	Volumetric mass transfer coefficient, 1/s
k^o_l	Liquid film coefficient in the absence of reaction, m/s

M	Hatta number, defined by equation (2.20)
MSF	Multistage flash distillation
N_A	Absorption rate of gas, $(\frac{Kmol}{m^2 s})$
N_2	Ratio defined as $\frac{D_B C_B^o}{ZD_B C_A^*}$
N	Total number of bubbles
P	Pressure or product specie Kg(force)m^{-2}
ppm	Parts per million
Q	Volumetric flow rate of gas $m^3 s-1$
r(x,t)	Rate of reaction per unit volume $(\frac{Kmol}{m^3 s})$
R_A	Rate of mass transfer of component A Eq. (1.5) (s^{-1})
s	Rate of surface renewal, s^{-1}
TDS	Total dissolved solids
tanh	Hyperbolic tangent
t	Time, s
t_D	Diffusion time, s
V_r	Reactor Volume, m^3
V_g, V_s	Superficial gas velocity, m/s
V_{bs}	Bubble rise velocity, m/s
Z, Y	Stoichiometric coefficient or column height, m
Z_i	Valency of ion
ΔG	Change in Gibbs Energy (kJ/kg)

GREEK LETTERS

α	Constant in Equation (5.16)
β	Defined by Equation (2.39)
δ	Film thickness
ε	Gas holdup
φ	reaction modulus defined by Equation (2.49)
Φ	Reaction capacity
Θ	Exposure time, or contact time
Δ	Difference operator
γ	Defined by Equation (2.34)
ρ_l	Density of liquid kg/ m^3
σ	Defined by Equation (5.37)

SUBSCRIPTS AND SUPERSCRIPTS

A	Gas phase component
B	Liquid phase component
bs	Bubble rise
c	Column
D	Diffusion
G, g	Gas
f	Dispersed liquid
i	Instantaneous or ions or interficial
l	liquid phase
o	in the standard state, or bulk concentration
r	Reactor
s	Superficial
vs	Bubble mean
*	interfacial
2	Second order

REFERENCES

Abdel-Aal, H. K., Ba-Lubaid, K. M., A. A. Shaikh, and Al-Harbi, D. K. "Recovery of Mineral Salts and Potable Water from Desalting Plant Effluent by Evaporation". Part II. Proposed Simulation System for Salt Recovery. Separation Science and Technology, 25(4), 437- (1990).

Abdel-Aal, H. K., Ba-Lubaid, K. M., Al-Harbi, D. K., and A. A. Shaikh. "Recovery of Mineral Salts and Potable Water from Desalting Plant Effluent by Evaporation". Part 1. Evaluation of the Physical Properties of Highly Concentrated Brines. Separation Science and Technology, 25(3), 309- (1990).

Abdel-Aal H.K. "Projected Economics of New Magnesium Production Process", Int. J. Hydrogen Energy 7 (5), 429- (1982).

Abdel-Aal H.K. "Separation of Magnesium Chloride from Sodium Chloride in Sea Water by the Dense Phase Technique" , Separation Science and Technology, 24 (7 & 8), 475- (1989).

Abdel-Aal H.K., Stiles G.B. and Holland C.D., "Formation of Interfacial Area at High Rates of Gas Flow Through Submerged Orifices.", J. AIChE., No.1, 12, 174- (1966).

Abraham M. and Sawant S.B. "Hydrodynamics and Mass Transfer Charateristics of Packed Bubble Columns" The Chem. Eng. J. 43, 95- (1990)

Akili, W. and Ahmed, N., "The Sabkhas of Eastern Saudi Arabia: Geotechnical Considerations", First Saudi Engineers Conference, King Abdulaziz University, May, 2, 302- (1983).

Akili, W., "On Sabkha Sands of Eastern Saudi Arabia", Proceedings of Symposeum on Geotechnical Problems in Saudi Arabia, King Saud University, Riyadh, 2, 775- (1991).

Akili, W., and Torrance, J. K., "Geotechnical Characterisrics of Salt-Laden Soils (Sabkha), The Arabian Gulf Coast", Proc. 6th Southeast Asian Conf. on Soil Engg., Taipei, 1- (1980).

Akili, W., and Fletcher, E. H., "Ground Conditions for Housing Foundations in Dhahran Region, Eastern Province, Saudi Arabia", Proc. Int. Conf. Housing Problems in Developing Countries, Dhahran, 2, 533- (1978).

Akili, W., and Torance, J. K., "The Development and Geotechnical Problems of Sabkha, with Preliminary Experiments on the Static Penetration of Cemented Sands", Q. J. Eng. Geol., 14, 59- (1981).

Akita K and Yoshida F. "Gas Holdup and Volumetric Mass Transfer Coefficient in Bubble Columns" Ind. Eng. Chem. Proc. Des.

Dev. 12, 76- (1973).

Akita K. and Yoshida F., "Bubble Size, Interfacial Area , and Liquid Phase Mass Transfer Coefficients in Bubble Columns", Ind. Eng. Chem. Proc. Des. Dev., 13, 84- (1974).

Ali K.M. and Hossain D. "Geotechnical and Geochemical Charateristics of Obhor Sub-Soil" Journal of King Abdulaziz University: earth Science 1, 205- (1988).

Alper E., "Measurement of Effective Interfacial Area in Packed Column Absorber by Chemical Methods.", Trans. Instn. Chem. Engrs. 57, 64- (1979).

Anderson J.L. and Quinn J.A. " The Transition to Slug Flow in Bubble Columns Working at Large Gas and Liquid flowrates" AIChE J. 27, 66- (1981).

Aou Al Heija M.K. and Shehata W.M."Engineering Properties of Al-Lith Sabkha, Saudi Arabia" 5th International IAEG Congress, Buenes Aires, 935- (1986).

Astarita G., "Mass Transfer with Chemical Reaction", Elsevier Amestedam, 24- (1967).

Astarita G., Savage D.W. and Biso A., "Gas Treating with Chemical Solvents.", John Wiley and Sons, Inc. 98- (1983).

Bach H.F. and Pilhofer T."Variation of Gas Holdup in Bubble Col-

umns with Physical Properties of Liquids and Operating Parameters of Columns"Germ. Chem. Eng. 1, 270- (1978).

Bhaga D.B., Pruden B. and Weber M.E., "Gas Holdup in Bubble Column Containing Organic Liquid Mixtures.", Can. J. Chem. Eng. 19, 417- (1971).

Barnea D., Shoham O.and Taitel Y., " Flow Pattern Charaterization in Two Phase by Electric Conductance Probe" of Gas Liquid and Gas Coal Slurry Mixtures in Vertical Tubes" int. J. Multiphase flow, 6, 387- (1980).

Bathurst R.G.C. "Carbonate Sediments and Their Diagenesis" Developments in Sedimentology, Second Enlarged Edition, Elsevier, 658- (1975).

Bojnowski, J. H., and Hanks, D. L. "Low-energy Separation Process." AICHE, 86, No. 10, 67- (1979).

Bojnowski, J. H., "Guidelines for Developing Low Energy Separation Process." AICHE, 2, 1205- (1977).

Botton R., Cosserat D. and Charpentier J.C." Influence of Column Diameter and High Gas Throughputs on the Operation of Bubble Column" Chem. Eng. J. 16, 107- (1978).

Botton R. , Cosserat D., and Charpentier "Mass Tranfer in Bubble Column Operating at High Gas Throughputs" 20, 87- (1980).

Brian P.L.T., Hurley J.F. and Hasseltine E.H., "Penetration Theory for Gas Absorption Accompanied by a Second Order Chemical Reaction.", A.I.ChE.J., No.2, 7, 226-(1961).

Brian P.L.T., "Gas Absorption Accompanied by an Irreversible Reaction of General Order.", A.I.ChE. J., No.1, 10, 5- (1964).

Burckhart R. and Deckwer W.D., "Bubble Size Distribution and Interfacial Areas of Electrolyte Solutions in Bubble Columns", Chem. Eng. Sci. 30, 351- (1975).

Burgess J.M. and Calderbank P.H., "The Measurement of Bubble Parameters in Two Phase Dispersion-I. The Development of an Approved Probe Technique", Chem. Eng. Sci., 30, 743- (1975).

Bush p. "Some Aspects of Diagenetic History of the Sabkha in Abu. Dhabi, Persian Gulf." In Pursen V.H., ed. the Persian Gulf Springer-Verlag, Berlin. 395- (1973).

Bushnak, A. A. "Water Supply Challenge in the Gulf Region." Desalination, 78, 137- (1990).

Calistru C., et al., "Possibilities of Modifying the Solvey Process for Ash Production." Reviste de Chimie, Brucresti, 34, 7, 625- (1983).

Calderbank P.H., Evans F. and Rennie J., "The Mass Transfer Efficiency and Techniques for Measuring Gas-Liquid Interfacial

Areas and Foam densities in Plate Columns", Proc. Int. Symp. Dist. (Instn. Chem. Engrs.) Brighton, 51- (1960).

Calderbank P.H. and Pereira J., "The Prediction of Distillation Plate Efficiency from Froth Properties", Chem. Eng. Sci., 32, 1427- (1977).

Carberry J.J., "Chemical and Catalytic Reaction Engineering" McGraw-Hill Chemical Engineering Series, 256-257 (1976).

Chao R.E., "Thermochemical Water Decomposition Process.", Ind. Engng. Chem., Proc. Res. Dev. 13, 94- (1974).

Comstock C."Magnesium and Magnesium Compound",U.S. Bur. Mines inf. Circ. 8201- (1963).

Cussler E.L., "Diffusion: Mass Transfer in Fluid Systems.", Cambridge University Press, New York, 372- (1984).

Danckwerts P.V., "Gas-Liquid Reactions", Mc Graw-Hill, New York, 53- (1970).

Danckwerts P.V. and Gillham A.J., "The Design of Gas Absorbers I-Methods for Predicting Rates of Absorption With Chemical Reaction in Packed Columns and Tests With 1 1/2 Rashig rings.", Trans. Instn. Chem. Engrs., 44, T42- (1966).

Danckwerts P.V.and Alper E., "Design of Gas Absorbers: Laboratory Point Model of Packed Column Absorber.", Tans. IChem. Eng.,

53, 54- (1975).

Danckwerts P.V., "Significance of Liquid-Film Coefficients in Gas Absorption.", Ind. Eng. Chem., 43, 1460- (1951).

Danckwerts P.V. and Sharma M.M., "The Absorption of CO_2 into Solutions of Alkalis and Amines, with Some notes on Hydrogen Sulphide and Carbonyl Sulphide.", The Chem. Eng. Oct. ce, 244- (1966).

Danckwerts P.V., "Unsteady-State Diffusion or Heat Conduction with Moving Boundary.", Trans. Faraday Soc. 46, 701- (1950).

Danckwerts P.V., "The Reaction of CO_2 with Ethanolamines.", Chem. Eng. Sci. 34, 443- (1979).

Deckwer W.D., "Coal Liquefication Via Indirect Routes., Mass Transfer with Chemical Reactions in Multi-Phase Systems." Proc. of Nato ASI, Turkey (1981).

Deckwer W.D. and Schumpe A., "Effectiveness of Mass Transfer Chemical Reactions in the Homogeneous and Hetrogenous Regimes of Vertical Gas Liquid Flow" ed. Durst, F., Tskilauri and Afgan N.H. Hemisphere Publ. Corp. Washington, dc. 2, 1038- (1979).

Deckwer W.D., Louisi Y., Zaidi A , and Ralek M., "Hydrodynamic Properties of Fischer - Tropsch Slurry Process" Ind. Eng.

Chem. Proc. Des. Dev. 19, 699- (1980a).

De Coursey W.J., "Absorption with Chemical Reaction: Development of New Relation for the Danckwerts Model., " Chem. Engng. Sci., 29, 1867- (1974).

De Groot K., "The Chemistry of Submarine Cement Formation at Dohat Hussain in the Persian Gulf"Sedimentology, 12, 63- (1969).

Dodge B.F., " Chemical Engineering Thermodynamics" 1st ed., Mc Graw - Hill, New York, 489 - (1944).

Doraiswamy L.K. and Sharma M.M., "Heterogenous Reaction: Analysis, Examples and Reactor Design.", Wiley Interscience, New York (1981).

Dunn I.J. and Einsele A., "Oxygen Transfer Cefficients by Dynamic Method.", J. Appl. Chem. Biotech., 25, 707- (1975).

Ellis G.I., "Arabian Salt-Bearing Soil (Sabkha) As an Engineering Material.", TRRL Report LR 523, Crowthorne, Berkshire, 21- (1973).

Erol A.O., "Engineering Geological Considerations in a Salt Dome Region Surrounded by Sabkha Sediments, Saudi Arabia" Engineering Geology, 26, 215- (1989).

Evans G., Schmid V. ,Bush P. and Nelson H., "Stratigraphy and

Geologic History of the Sabkha" Abu.
Dhabi, Sedimentology 12, 145- (1969).

Fair J.R., " Designing Gas - Sparged Reactors" Chem. Eng. 74, 67- (1967).

Faith W.L.; Key D.B. and Clark R.E. "Industrial Chemicals" 4th. edn. wiley, New York, 45- (1975).

Fookes P.G. , French W.J. and Rice S.M.M., "The Influence of Ground and Groundwater Geochemistry on Construction in Middle East"Quarterly Journal of Engineering Geology, London 19, 214- (1986).

Fookes P.G., "Road Geotechnics in Hot Deserts "Journal of the Institution of Highway Engineers, XXIII No.10, 11- (1976).

Fookes P.G., French W.J. and Rice S.M.M., "The Influence of Ground and Groundwater Geochemistry on Construction in the Middle East",Q.J. Eng. Geol., London, 18, 101- (1985).

Ford D.E., Mashalkar R.A. and Ulbrecht J., "Mixing Times in Newtonian and Non-Newtonian Fluids." Proc. Tech. Int. 17, 803- (1972).

Friedman G.M., "Significance of Red Sea in Problem of Evaporites and Basinal Limestone," A.,A.P.G. Bulletin, 56, 1072- (1972)

Forresten R. C., "Production of HCl as by Product of the Solvay

Process." AICHE, 65th Anniversary meeting, New York, 26- (1973).

Ghazali, F. M., Fatani, M. N. and Khan, A. M., "Geotechnical Properties of Sabkha of the Western Region, Suadi Arabia", 2nd Suadi Engineers Conference, University of Petroleum and Minerals, Dhahran, Saudi Arabia, 4, 1945-(1985).

Glennie, K.W., "Desert Sedimentary Environments" Developments in Sedimentology, Elsevier, Amesterdam , 14, 222- (1970).

Godfrey P.B., "Modern Evaporite Deposition and Geochemistry of Coexisting Brines, the Sabkha,Trucial,Arabian Gulf" Journal of Sedimentary Petrology, 39, 70- (1969).

Al-Golaikah, A. M., "Desalination by Saline Water Conversion Corporation of Saudi Arabia." Desalination, 50, 83- (1984).

Gopal J.S. and Sharma M.M., "Mass Transfer Charateristics of Low H/D Bubble Column" Can. J. Chem. Eng. 61, 517- (1983).

Govier G.W. and Aziz K., "The Flow of Complex Mixture in pipes" Van Nostrand Reinhold, New York, 33- (1972).

Guerin P., Carrean P.J., Patterson W.I. and Paris J., "Characterization of Helical Impelars by Circulation Times." Can. J. Chem. Eng. 62, 301- (1984).

Herbrechtsmeier P. and Steiner R., "Realtiver Gasgehalt in Blasen-

saulen-Abstrom Reaktoren" Chem. Ing-tech. 52, 468- (1980).

Higbie R., "The Rate of Absorption of a Pure Gas into Still Liquid During Short Periods of Exposure.", Trans. A.I.ChE. J., 31, 365- (1935).

Hikita H., Asai S., Tanigawa K., Segawa K. and Kitao M., "Gas Holdup in Bubble Column " Chem. Eng. J. 20, 59- (1980).

Hikita H. and Asai S., "Gas Absorption with (M,N)th Order Irreversible Chemical Reaction.", Int. Chem., 4, 332- (1964).

Hills J.H., "The Operation of a Bubble Column at High Throughputs I . Gas Holdup Measurements" Chem. Eng. J. 12, 89- (1976).

Hills J.H., "Radial Non Uniformity of Velocity and Voidage in Bubble Column" Trans. Inst Chem. Engrs. 52, 1- (1974).

Hines D.A., "The Large Scale Pressure Cycle Fermenter Configuration)", Proc.1st Eur. Congr. Biotechn. CH-Interlaken, Dechema Monographs, Verlag Chemie, Weinheim, 82, 55- (1978).

Hodgson I.F., Caronna S. and Abu-taleb M.G., "Geotechnical Aspects of a Development Project for the Coastal Town of Jizan, "Second Symposium on Geotechnical Problems in Saudi Arabia, Riyadh, May 164- (1989).

Hou T.P., "The Manufacture of Soda ", 2nd. ed. ; New York Van Nostrand Reinhold, 40- (1991).

Hsu K.J.and Schneider J., "Progress Report on Dolomitezation - Hydrology of Abu Dhabi Sabkha, Arabia Gulf" In: Purser, B.H. (Editor), The Persian Gulf, Springer-Verlag, 409- (1973).

Hsu H.K. and Siegenthaler, C., "Preliminary Experiments on Hydrodaynamic Movement Induced by Evaporation and their Bearing on the Dolomite Problem", Sedimentology, 12, 11- (1969).

Illing L.V., Wells A.J. and Taylor, J.C.M., "Penecontemporary Dolomite in the Persian Gulf" In: Dolomitization and Limestone Diagenesis, Sepm. Spe. Pub. 13, 38- (1965).

Iqbal H.K. and Sayed I. H., "Engineering Properties of Sabkha Soils in the Benghazi Plain Construction Problems", Engg. Geol., 17, 175- (1981).

Javdani K. Schwalbe S. and Fischer J., "Multiphase flow of Gas Liquid and Gas Coal Slurry Mixtures in Vertical Tubes" Argonne National Laboratory Report , ANL-76, Argonne, 116- (1977).

Johnson H., Kamal M.R., Pierson G.O. and Ramsay J.B., "Sabkhas of Eastern Saudi Arabia,"In: Al sayyari S.S. and Zolt J.G. (Ed.), Quarternary Period in Saudi Arabia, Springer-Verlag, Austria 84- (1978).

Joosten G.E.H. and Danckwerts P.V., "Chemical Reaction and Effective Interfacial Areas in Gas Absorption.", Chem. Eng. Sci., 28,

453- (1973).

Joshi J.B., "Axial Mixing in Multiphase Contactors A Unified Approach " Trans inst Chem. Eng. 58, 155- (1980).

Joshi J.B. and Sharma M.M., " Mass Transfer Charateristics of Horizental Sparged" Trans inst. Chem. Engrs. 54, 42- (1976).

Kato Y., Nishiwaki A., Kago T. FuKuda and Tanaka S., " Gas Holdup and Overall Volumetric Absorption Coefficient in Bubble Columns with Suspended Solid Particles: Absorption Rates of Oxygen by an Aqueous Solution of Sodium Sulfite" Int. Chem. Eng. 13, 582- (1973).

Kastannoka F., "The effect of Column Diameter on the Hydrodynamic Parameters of a Bubble Column with a Plate as a Gas Distributor" Coll. Czch. Chem. Commun. 42, 1494- (1977).

Kawagoe K.T., Inoue K., Nakao K. and Otake T., "Flow Pattern and Gas Holdup Conditions in Gas Sparged Contactors" Int. Chem.Eng. 16, 176- (1976).

Keitel G. and Onker U., "Errors in the Determination of Mass Transfer in Gas-Liquid Dispersions.", Chem. Eng. Sci., No.12, 36, 1927- (1981).

Kettan M.A. and Abdel-Aal H.K., "Production of Magnesium Chloride from Brines Using Solar Energy", in Pro ceedings of 4th

International Symposium on Fresh Water from the Sea, 2, 509- (1973).

Kinsman D.J.J., "Modes of Formation, Sedimenttary Association, and Diagnostic Features of Shallow - Water and Supratidal Evaporites" The American Association of Petroleum Geologists Bulletin (AAPG), 53, 830- (1969).

Kobel H.E., Borchers and Langemann and Martins J., "Warmeubergan an Blasensaulen-II. Messungen an Vicosen Suspensionen.", Chem. Ing. Tech., 32, 84- (1960).

Koide T., Morooka S., Ueyama K., Matsuura A., Yamashita F., Iwamoto S., Kato Y., Inoue H., SHigeta M., Suzuki S. and Akehata T., "Behaviour of Bubbles in Large Scale Bubble Columns.", Chem. Eng. Japan., 12, 98- (1979).

Landau J., Gomaa H.G. and Al Taweel A.M., "Comparison of Methods for Measuring Interfacial Area in Gas-Liquid Dispersion.", Can. J. Chem. Eng., 55, 13- (1977a).

Levich V.G., " Physico Chemical Hydrodynamics " Prentice - Hall, Englewood Cliff, NJ, 12- (1962).

Linek V. and Vacek V., "Chemical Engineering Use of Catalyzed Sulfite Oxidation Kinetics for the Determination of Mass Transfer Charateristics of Gas-Liquid Contactors.", Chem. Eng. Sci., 36, 1747- (1981).

Lockett M. and Kirk P., "Ideal Bubbly Flow and Actual Flow in Bubble Columns" Trans inst. Chem. Engrs. 53, 267- (1975).

McDnough J.A., Tomme W.J. and Holland C.D., "Formation of Interfacial Area in Immiscible Liquids by Orifice Mixers.", A.I.ChE.J., 6, 615- (1958).

Mashelkar R.A., "Bubble Columns.", Br. Chem. Eng., 15, 1293 - (1970).

Mashelkar R.A. and Sharma M.M., "Mass Transfer in Bubble and Packed Columns.", Trans. inst. Chem. Engrs., 48, T162- (1970).

Matheron E.R. and Sandall O.C., "Effective Interfacial Area Detrmination by Gas Absorption Accompanied by Second Order Irreversible Chemical Reaction.", A.I.ChE. No.2 , 25, 332- (1979).

May D. and Rudd D.F., "Development of Solvay Clusters of Chemical Reactions.", Chem. Engng. SCi. 31, 59- (1976).

Miller D.N., "Gas Holdup and Pressure Drop in Bubble Column Reactors" Ind. Eng. Chem. Process Des Dev. 19, 37- (1980).

Miyata T. "Soda Ash Production in Japan and a New Asahi Process" Chem. Ind. No.4, 21 feb. 142- (1983).

Miyauchi and Shyu C.N., " Flow of Fluids in Gas Liquid Columns" Kagaku Kogaku, 34, 958- (1970).

Al-Mutaz, I. S., and Wagialla, K. M., "Techno-Economic Feasibility of Extracting Minerals from Desalination Brines.", Elsevier Science Publishers B.V., No.3, 69, 297- (1988).

El-Naggar Z.R., "Foundation Problems in Sabkhah Deposits" Short Course on Foundation Engineering For Practicing Engineer, KFUPM, Dhahran, April 9-13, SD1- (1988).

Novak R. and Schuster W.; U.S. Pat. 3466196, 9 sept. 3- (1969).

Olander D.R., "Simultaneous Mass Transfer and Equilibrium Chemical Reaction.", A.I.chE. J., 6, 233- (1960).

Oshinowo T. and Charles, M.E., "Vertical Two Phase Flow - Part I Flow Pattern Correlations " Can. J. chem. Eng. 52, 25- (1974).

Ouwerkerk C., "Design For Selective Hydrogen Sulfide Absorption.", Hydrocarbon Process, 57, 89- (1978).

Oyevaar M.O., Bosr and Westerterp K.R., "Interfacial Area and Gas Holdups in Gas Liquid Contactors at Elavated Pressure from o.1 to 8 Mpa" Chem Eng. Sci. 46, 1271- (1991).

Patil V.K and Sharma M.M., "Solid-Liquid Mass Transfer Coefficient in Bubble Columns up to 1 m Diameter, Chem. Eng. Res. Des, 61, 23- (1983).

Patterson R.J. and Kinsman D.J.J., "Hydrologic Frame Work of Sabkha Along the Arabian Gulf",the American Association of Petro-

leum Geologists Bulletin, No.8, 65, 23- (1981).

Pearson J.R.A., "Diffusion of One Substance into a Semi- Infinite Medium Containig Another with Second order Reaction.", Appl. Sci. Res. AXI., 321- (1963).

Peter, I., "Ammonia Absorption in Soda Production." Reviste de Chimie, Brucresti, No.10, 22, 601- (1971).

Peter, I., "Modernization of Alkali Industries." Chemical Age of India, No.10, 39, 607- (1988).

Pilhofer, Th., and Miller, H.D., "Photoelektrische Me Bmethode Zur Bestimmung der Grobenverteilung Mitteldisperser Tropfen in Einem Nicht Mischbaren Flussigen Zweistoff-System.", Chem. Eng. Tech. 44, 295- (1972).

Pinsent B.R.W., Pearson L. and Roughton F.J.W., "The Kinetics of Combination of Carbon Dioxide with Ammonia.", Trans. Faraday Soc, 52, 1594- (1956).

Purser B.H. and Sibold E., "The Principal Environmental Factors Influencing Holocene Sedimentation and Diagenesis in the Persian Gulf.", (Ed.), The Persian Gulf, Spriner-Verlag, Berlin, 1- (1973).

Quiker G. and Deckwer W.D., "Gasehalt und Phasengrenzflache in Begasten Kohlenwassertoffen.", Chem. Ing. Tech., 53, 474- (1981a).

Reid R.C. and Sherwood T.K.,"The Properties of Gases and Liquids; their Estimation and Correlation", 2nd. Ed., Mc Graw - Hill, New York, 332- (1966).

Reith T. and Beek W.J., "The Oxidation of Aqueous Sodium Sulphite Solutions.", Chem. Eng. Sci., 28, 1331- (1973).

Renfro, A.R., " Genesis of Evaporite-Associated Stratiform Metalliferous Deposits - A Sabkha Process" Economic Geology, 69, 33- (1974).

Resmisk W., "Process Analysis and Design for Chemical Hydrodaynamic Movement Induced by Evaporation and their Bearing Engineers." New York, McGrow Hill, 67- (1981).

Richards G.M., Ratcliff G.A. and Danckwerts P.V., "Kinetics of CO_2 Absorption-III. First Order Reaction in a Packed Column.", Chem. Eng. Sci., 19, 325- (1964).

Rodionow A.I. and Patzelt H. and Wiss Z., "Ein Beitrag Zur Hydrodynamik Ablaufbarer Siebboden.", Techn. Hochsch. Lewna-Merseburg, 11, 435- (1969).

Rudd D.F., "Accessible Designs in Solvay Cluster Synthesis.", Chem. Engng. Sci. 31, 701- (1976).

Sahay B.N. and Sharma M.M., "Absorption in Packed Bubble Columns " Chem. Eng. Sci. 28, 2245- (1973).

Schugerl K., Luke J. and Oels U., "Bubble Column Bioreactors", Adv. Biochem. Eng., ed., Ghose T.K., Fiechter A. and Blakeborogh N., 7, 1- (1977).

Schugerl,K., Luke J., Lehmann I. and Wagner F., " Application of Tower Bioreactors in cell Mass Production " Adv. Biochem. Eng. 8, 63- (1978).

Schumpe A., Serpeemn Y., and Deckwer W.D., "Effective Use of Bubble Column Reactors" Ger. Chem. Eng. 2, 234- (1979).

Schumpe A., "Die chemische Bestimmung von phasengren- Zflachen in Blasensaulen bi uneinheitlichen Blasengroben " Dr. Thesis, Universitat Hanover (1981).

Schumpe A.and Grund A., " The Gas Disengagement Technique for Studing Gas Holdup Structure in Bubble Columns". Can. J. Chem. Eng. 64, 891- (1986).

Scott L.S., Hayes W.B. and Holland C.D., "The Formation of Interfacial Area in Immiscible Liquids by Orifice Mixers.", A.I.ChE.J., 4, 346- (1958).

Senhal A.P., Tames G.D. and Dragomir B.B., " Holdup and interfacial Area Measurements Using Dynamic Gas Disengagement" AIChE, 35, 931- (1989).

Seizawa I., Kataoke A.I. and Michiyoshi I., "Turbulence Structure of Air-Water Flow ", Int.J. Multiphase Flow, 2, 221- (1975).

Shah Y.T., Kelkar B.G., Godbole S.P. and Deckwer W.D., "Design Parameters Estimation for Bubble Column Reactors " AIChE J. 28, 353- (1982).

Shah Y.T, Stiegel G.J., and Sharma M.M., " Backmixing in Gas-Liquid Reactors" AIchE J. 24, 364- (1978).

Sharma M.M. and Mashelkar R.A, "Absorption With Reaction in Bubble Columns.", (Instn. Chem. Engrs. London), I. Chem. E. Symp. Ser. No. 28, 10- (1968).

Sharma M.M. and Danckwerts P.V., "Chemical Methods of Measuring Interfacial Area and Mass Transfer Coefficients in Two Phase Systems.", Br. Chem. Eng., 15, 522 - (1970).

Shearman D.J., "Origin of Marine Evaporites by Diagenesis "Transactions of Institution of Mining and Metallurgy 75, B208- (1966).

Sherwood.T.K., Pigford R.L. and Wilke C.R., "Mass Transfer.", Mc Graw-Hill Co., New York, 300- (1975). 75, B303- (1966).

Shreve R.N., "Chemical Process Industries", 5nd. ed. Mc Graw - Hill, 224- (1984).

Shulman H.L. and Molstad M.C., "Gas Bubble Columns for Gas-Liquid Contacting.", Ind. Eng. Chem. 42, 1058- (1950).

Silver R.S., "Technological and Environmental Aspects of Desalina-

tion." Desalination, 42, 1- (1982).

Smith C.L., "Brines of Wadi as Sirhan _ Kingdom of Saudi Arabia, U.S. Department of the Interior, Geologic Survey, Saudi Arabian Mission No. Tr1 28- (1980).

Sridharan K. and Sharma M.M., "New System and Methods for the Measurement of Effective Interfacial Area and Mass Transfer Coefficients in Gas-Liquid Contactors.", Chem. Eng. Sci., 3, 767 - (1976).

Sriram K. and Mann R., "Dynamic Gas Disengagement: A New Technique for Assessing the Behavior of Bubble Columns.", Chem. Eng. Sci., 32, 571- (1977).

Stipho A.S., "Some Engineering Properties of Stabilized Soils " Engineering Geology, 26, 181- (1989).

Suachelli. V., "Fertilizer Nitrogen its Chemistry and Nitrogen." Reinhold Publishing Corporation, NEw York, 237- (1964).

Tallmadge et al., "Minerals from Sea Salt", Ind. Engng. Chem. No.7, 56, 44- (1964).

Tallbenblatt, S.A., "Middle East Water Problems: A Challenge for the 1980's." Desalination, 40, 7- (1982).

Taylor J.C.M. and Illing L.V., "Holocene Intertidal Calcium Carbonate Cementation, Qatar, Persian Gulf" Sedimentology, 12, 69-

(1969).

Todtenhaupt E.K., "Blasengrobenverteilung in techischen Begasung-Sapparaten.", Chem. Eng. Tech., 43, 336- (1971).

Towell G.D., Strand C.P. and Ackerman G.H., "Mixing and Mass Transfer in Large Diameter Bubble Columns.", Chem. E., Symp. Ser., A.I.Ch.E.-Inst., No.10, 97- (1965).

Trambouze P., Van Landeghem H. and Wauquier J.P. "Chemical Reactors: Design -Engineering - Operation.", Imprimerie Nouvelle, 45800 Saint -Jean -de Braye, 193-201(1981).

Van Krevelen D.W. and Hoftizer P.J., "Kinetics of Simultaneous Absorption and Chemical Reaction.", Chem. Eng. Prog. 44, 529- (1948).

Van Krevelen D.W. and Chermin H.A.G., "Estimation of free energies", Che Eng. Sci., 1, 66- (1951).

Vemeer D.J. and Krishna R., "Hydrodynamics and Mass tranfer in Bubble Columns Operating in the Churn Turbulent Regime.", Ind. Eng. Chem. Proc. Dev., 20, 475- (1981).

Vermulen Th., Williams G.M. and Langlois E., "Interfacial Area in Liquid-Liquid and Gas-Liquid agitation.", Chem. Eng. Prog., 51, 85- (1955).

Wallis G.B., "One Dimensional Two Phase Flow " Mc Graw - Hill, New

York, 45- (1969).

Westerterp K.R., Van Dierendonck L.L. and De Kraa J.A., "Interfacial Area in agitated Gas-Liquid Contactors.", Chem. Eng. Sci., 18, 157- (1963).

Weiland P., Sick R. and Onker U., "Determination of Volumetric Mass Transfer Coefficients in Gas -liquid Dispersion by the Oxidation of Hydrazine " Ger. Chem. Eng. 4, 379- (1981).

Wood G.V. and Wolf M.J., "Sabkha Cycles in the Arab/Darb Formation of the Trucial Coast of Arabia" Sedimentology, 12, 165- (1969).

Yamashita F., Mori Y. and Fujita S., " Size Size Distribution of Bubbles in a Column-Comparison between the Two Point Electric Probe Method and the Photographic Mehtod.", J. Chem. Eng. Japan, 12, 5- (1979).

Ying D.H., Givens E.N. and Weimer R.F., " Gas holdup in Gas-Liquid and Gas-Liquid Solid Flow Reactors " Ind. Eng. Chem. Process Des. Dev. 19, 635- (1980a).

Yoshida F. and Yoshiaru M., "Gas Absorption in Agitated Gas-Liquid Contactors: Interfacial Area, Gas Holdup, Liquid Phase Mass Transfer Coefficient and Reaction Factor.", Ind. Eng. Chem. Proc. Dev., 2, 263- (1963).

Yoshida F. and Akita K., "Performance of Gas Bubble Columns :

Volumetric Liquid Phase Mass Transfer Coefficient and Gas Holdup" AIChE J. 11, 9- (1965).

Zlokarnik M., " Advance Biochemical Engineering", Springer - Verlag, Berlin -Heidelberg - New York 8, 133- (1978).

Appendix A

PHYSICAL PROPERTIES

Solubility of Oxygen in Electrolyte Solutions

When considering the absorption of gas that reacts with the solvent, it is generally important to get the solubility of unreacted gas. The solubility cannot be determined by conventional methods. However, in electrolytic solutions the solubility can be estimated using the Van Krevelen and Hoftijzer method (1948). This relates the solubility in solution to that in water at equal temperatures

$$Log(\frac{He}{He_w}) = h_s I \qquad \text{(A-1)}$$

Where He and He_w the values of Henry constant for the solution and water respectively, and I is the ionic strength of the solution often expressed as:

$$I = 1/2 \sum C_i Z_i^2 \qquad \text{(A-2)}$$

Where Z_i the valency of ions and C_i their concentration. The h_s is the salting-out parameter and is given as

$$h_s = i + i_+ + i_g \qquad \text{(A-3)}$$

The parameter h_s is the sum of the contributions of different species present in the solution such as negative and positive ions and dissolved gases. Table A-1 gives the ionic specific constants for salting-out constants for negative and positive ions, while Table A-2 gives the corresponding values for dissolved gas species.

The solubility of O_2 in mixed electrolyte solutions may be computed (Danckwerts and Gillham, 1966).

Table A-1 Values of i_+ and i_- for different ions (Danckwerts, 1970)

l/g i_+ ion		l/g i_- ion	
H^+	0.000	OH^-	0.066
Na^+	0.091	Cl^-	0.021
K^+	0.074	NO_3^-	-0.001
NH_4^+	0.028	SO_4^{--}	-0.022
Mg^{++}	0.051	Br^-	0.012
Zn^{++}	0.048	CO_3^{--}	0.021
Ca^{++}	0.053	I^-	0.005

Table A-2 Values of i_g (l/g ion) for different gases at 25° C (Danckwerts, 1970)

gases	i_g
H_2	-0.002
O_2	0.022
CO_2	-0.019
N_2O	0.000
H_2S	-0.033
NH_3	-0.054
C_2H_2	-0.009
SO_2	-0.103

Table A-3. Values of Salting-out parameter (Hikita et al., 1978)

Temperature oC	$h_{sF}(Na_2SO_3)$ l/g ion
15	0.122
17	0.119
20	0.115
25	0.108
30	0.101
35	0.094
40	0.087
45	0.080
50	0.073

Table A-4. Physical Properties of NaCl Solutions

Temperature of fluid = 22 °C

Sample type	Density g/ml	Viscosity cp	S.Tension g/ s^2
D.I. Water	1.0033	0.8621	70.4
NaCl 10%	1.0692	1.1083	64.5
NaCl 20%	1.1280	1.3037	70.8
NaCl 30%	1.1800	1.6978	74.3

Table A-5. Densities of Aqueous Sodium Chloride (Perry, 1973)

%	0°C	10°C	25°C	40°C	60°C	80°C	100°C
1	1.0075	1.0071	1.0041	0.9991	0.9900	0.9785	0.9651
2	1.0151	1.0144	1.0111	1.0059	0.9967	0.9825	0.9719
4	1.0304	1.0292	1.0253	1.0198	1.0103	0.9988	0.9855
8	1.0612	1.0591	1.0541	1.0480	1.0381	1.0264	1.0134
12	1.0924	1.0895	1.0836	1.0770	1.0667	1.0549	1.0420
16	1.1242	1.1206	1.1140	1.1069	1.0962	1.0842	1.0713
20	1.1566	1.1525	1.1453	1.1377	1.1268	1.1146	1.1017
24	1.1900	1.1856	1.1778	1.1697	1.1584	1.1463	1.1331
26	1.2071	1.2025	1.1944	1.1861	1.1747	1.1626	1.1492

Table A-6. Plant Intake Water Analysis (Al-Khobar Desalination Plant)

Parameter	Value
pH	8.05
Appearance	clear
Turbidity	1.0 NTU
Conductivity	69.3 ms/cm
Total Dissolved Solids	50583 ppm
Total Hardness as CaCO3	9256 ppm
Total Alkalinity as CaCO3	127 ppm
Sodium	16100 ppm
Potassium	590 ppm
Calcium	470 ppm
Magnesium	1963 ppm
Copper	0.006 ppm
Iron	0.007 ppm
Chlorides	28000 ppm
Sulfates	3700 ppm

Table A-7. Blow Down Analysis (Al-Khobar Desalination Plant)

Parameter	Value
pH	8.40
Conductivity	8.9 ms/cm
Chlorides as Cl	36.96 g/kg
Total Alkalinity	168 ppm as CaCO3
Copper	0.106 ppm
Iron	0.022 ppm
Sodium	19400 ppm
Potassium	1100 ppm
Magnesium	2000 ppm
Calcium	500 ppm

Table A-8. Volumetric Oxygen Transfer Coefficients K_La from Literature (Keitel and Onker, 1981)

Reactor Type Dimensions	Specific Power Input $[kW/m^3]$	U_{SG} $[cm/s]$	System	K_La $[s^{-1}]$
ST 3.0 m^3	0.6 - 1.0	0.6 - 0.25	I	0.055 - 0.065
4.6 m^3	0.75 - 0.9	1.24 - 0.85	I	0.028 - 0.032
BC/PP H = 4.0 m	-	1.0 - 2.0	I	0.03 - 0.06
d = 0.14 m	-	1.0 - 2.0	II	0.035 - 0.105
H = 4.0 m	-	1.0 - 2.0	I	0.03 - 0.05
d = 0.15 m	-	1.0 - 2.0	II	0.035 - 0.07
BC/S H = 4.0 m	-	2.0	I	0.04
d = 0.14 m	-	2.0	II	0.05
H = 7.23 m	-	2.0	I	0.016
d = 0.20 m	-	2.0	II	0.022

ST = stirred tank,

BC/PP = bubble column with porous plate,

BC/S = bubble column with sieve,

System I = air/water; System II = air/water + salt,

H = height, $[m]$, d = diameter $[m]$,

U_{SG} = superficial gas velocity.

Appendix B

HYDRODYNAMIC MEASUREMENT DATA

Table B-1: Raw Data For Gas Holdup

Column Height = 180 cm
Utility = Air and Water (D.I.W)
Temperature of fluid = 22 °C

V (l/min.)	h = 30cm $\Delta h(cm)$	h = 60cm $\Delta h(cm)$	h = 90cm $\Delta h(cm)$	h = 120cm $\Delta h(cm)$
10	2.4 2.3 2.2	4.7 4.7 4.6	6.8 6.9 6.7	9.0 9.0 9.1
Avg	2.3	4.7	6.8	9.0
15	3.5 3.7 3.8	7.4 7.0 7.5	11.0 10.8 10.7	14.2 14.7 14.7
Avg	2.7	7.3	10.8	14.5
20	5.2 4.9 5.2	10.1 9.8 10.0	15.8 15.0 15.5	20.4 20.2 19.7
Avg	5.1	9.9	15.4	20.1
30	8.9 9.2 9.0	17.3 17.5 17.0	25.6 25.8 25.1	33.6 33.3 33.8
Avg	9.0	17.3	25.5	33.6
40	12.8 13.0 13.3	24.0 25.5 23.7	35.7 36.5 35.6	49.3 49.4 48.9
Avg	13.0	24.4	35.9	49.2

Table B-2: Raw Data For Gas Holdup

Column Height = 180 cm
Utility = Air and 10% NaCl Solution
Temperature of fluid = 22 °C

V (l/min.)	h = 30cm $\Delta h(cm)$	h = 60cm $\Delta h(cm)$	h = 90cm $\Delta h(cm)$	h = 120cm $\Delta h(cm)$
10	2.6 2.5 2.7	4.8 4.7 4.8	7.2 7.2 7.5	9.7 9.6 9.7
Avg	2.6	4.7	7.3	9.7
15	4.4 4.3 4.2	7.7 7.6 7.8	12.2 12.2 12.6	16.07 15.9 16.2
Avg	4.3	7.7	12.3	16.1
20	6.4 6.2 6.4	11.6 11.9 11.8	18.5 18.2 18.3	22.6 22.6 22.7
Avg	6.3	11.8	18.3	22.6
30	10.7 10.6 10.4	18.7 18.5 18.4	27.9 27.8 27.8	39.5 38.8 38.8
Avg	10.6	18.5	27.8	39.0
40	15.3 15.2 13.3	26.6 27.2 23.7	41.1 40.7 35.6	
Avg	15.3	26.5	41.3	

Table B-3: Raw Data For Gas Holdup

Column Height = 180 cm
Utility = Air and 20% NaCl Solution
Temperature of fluid = 22 °C

V (l/min.)	h = 30cm $\Delta h(cm)$	h = 60cm $\Delta h(cm)$	h = 90cm $\Delta h(cm)$	h = 120cm $\Delta h(cm)$
10	2.3 2.5 2.5	4.5 4.8 4.5	7.5 7.3 7.4	9.1 9.2 9.0
Avg	2.4	4.6	7.4	9.1
15	3.8 4.0 3.8	7.2 6.9 7.2	13.1 12.8 12.6	15.1 15.0 15.3
Avg	3.9	7.1	12.8	15.1
20	5.7 5.2 5.4	10.0 10.3 10.1	18.1 18.2 18.3	21.8 22.4 22.6
Avg	5.4	10.1	18.2	22.3
30	11.0 11.5 11.5	18.7 18.7 18.8	29.4 28.3 29.0	38.7 38.2 38.9
Avg	11.3	18.7	28.9	38.9
40	15.4 16.0 13.3	25.5 26.4 23.7	41.5 41.0 35.6	
Avg	15.6	25.8	41.2	

Table B-4: Raw Data For Gas Holdup

Column Height = 180 cm
Utility = Air and 30% NaCl Solution
Temperature of fluid = 22 °C

V (l/min.)	h = 30cm $\Delta h(cm)$	h = 60cm $\Delta h(cm)$	h = 90cm $\Delta h(cm)$	h = 120cm $\Delta h(cm)$
10	2.5 2.3 2.3	4.4 4.6 4.7	7.2 7.1 7.2	9.6 9.4 9.4
Avg	2.4	4.6	7.2	9.5
15	3.8 3.9 3.8	7.6 7.8 7.2	11.9 12.0 12.0	15.0 15.2 15.2
Avg	3.8	7.5	11.9	15.2
20	5.8 5.6 5.6	11.6 11.0 10.7	18.1 18.2 18.4	22.1 22.5 22.1
Avg	5.7	11.1	18.2	22.2
30	9.8 9.8 9.7	19.7 20.0 18.9	29.2 29.5 29.4	38.8 38.1 38.2
Avg	9.8	19.5	29.4	38.4
40	15.2 15.3 15.3	29.7 29.5 29.8	44.5 43.3 43.3	
Avg	15.3	29.5	43.7	

Table B-5: Raw Data For Gas Holdup

Column Height = 30 cm
Utility = CO_2 % O sub 2 and D.I.Water
Temperature of fluid = 22 °C

V (l/min.)	O_2 $\Delta h(cm)$	CO_2 $\Delta h(cm)$
10	2.4 2.1 2.5	2.4 2.4 2.3
Avg	2.3	2.4
15	3.9 4.0 3.9	3.3 3.6 3.8
Avg	3.9	3.6
20	5.5 5.8 5.4	4.9 4.7 4.9
Avg	5.6	4.8
30	10.0 10.4 10.6	
Avg	10.3	

Table B-6: Raw Data For Gas Holdup

Column Height = 30 cm
Utility = $NaHCO_3$ %NaCl%;%Na sub 2 CO sub 3 %;%NH sub 3
Temperature of fluid = 22 °C

V (l/min.)	$NaHCO_3$ 0.5M $\Delta h(cm)$	NaCl 0.5M $\Delta h(cm)$	$NaCO_3$ 0.5M $\Delta h(cm)$	NH_3 1.0M $\Delta h(cm)$
10	2.3 2.4 2.4	2.3 2.4 2.4	2.1 2.2 1.9	2.3 2.5 2.4
Avg	2.4	2.4	2.1	2.4
15	3.9 4.2 3.7	4.2 4.0 4.6	3.4 3.3 3.3	4.0 4.2 4.0
Avg	3.9	4.3	3.3	4.1
20	6.8 7.0 7.0	6.4 6.3 6.4	4.8 5.0 4.7	5.5 6.0 6.3
Avg	6.9	6.4	4.8	5.9
30	12.7 12.5 12.7	11.5 12.0 11.5	8.2 8.4 8.4	10.1 10.5 10.8
Avg	12.6	11.7	8.3	10.5

Table B-7: Raw Data For Gas Holdup at Various Temperatures.

Column Height = 30 cm
Utility = Air and Water (D.I.W)
Temperature of fluid = (10-40) °C

V (l/min.)	t = 10 °C	t = 20 °C	t = 30 °C	t = 40 °C
0	0	0	0	0
7.5	0.061	0.061	0.060	0.060
10	0.083	0.083	0.083	0.082
15	0.122	0.122	0.122	0.122

Table B-8: Data For Volumetric Mass Transfer Coefficient

pH = 8.5
Column Height = 30 cm
Flow of O_2 = 3.6 l/min.
Temperature = 22 °C

Time (min)	$Na_2S_2O_3$ (ml)	Na_2SO_3 (M)
0.0	9.30	0.78
16.0	9.60	0.77
40.0	10.3	0.73
60.0	11.00	0.70
80.0	12.50	0.67
110.0	12.10	0.64
140.0	12.80	0.61
180.0	13.70	0.56
220.0	14.80	0.51
260.0	15.40	0.48
305.0	16.60	0.42

Table B-9: Data For Volumetric Mass Transfer Coefficient

pH = 8.5
Column Height = 30 cm
Flow of O_2 = 6.2 l/min
Temperature = 22 °C

Time (min)	$Na_2S_2O_3$ (ml)	Na_2SO_3 (M)
0.0	9.20	0.79
15.0	10.30	0.73
30.0	10.70	0.71
45.0	11.50	0.67
60.0	12.50	0.62
75.0	13.10	0.59
90.0	13.80	0.56
105.0	14.70	0.51
120.0	15.10	0.49
137.0	16.10	0.44
150.0	17.50	0.37

Table B-10: Data For Volumetric Mass Transfer Coefficient

pH = 8.5
Column Height = 30 cm
Flow of O_2 = 9 l/min.
Temperature = 22 °C

Time (min)	$Na_2S_2O_3$ (ml)	Na_2SO_3 (M)
0.0	9.20	0.79
5.0	9.70	0.76
15.0	10.3	0.73
25.0	10.30	0.73
35.0	11.80	0.66
45.0	12.20	0.64
55.0	13.10	0.59
65.0	13.10	0.59
80.0	14.00	0.55
100.0	16.00	0.45
112.0	15.70	0.46

Table B-11: Data For Volumetric Mass Transfer Coefficient

pH = 8.5
Column Height = 30 cm
Flow of O_2 = 11.8
Temperature = 22 °C

Time (min)	$Na_2S_2O_3$ (ml)	Na_2SO_3 (M)
0.0	9.50	0.77
10.0	10.80	0.71
20.0	12.5	0.62
30.0	13.90	0.55
40.0	15.30	0.48
50.0	16.80	0.41
60.0	19.20	0.29
70.0	21.00	0.20

Table B-12: Data For Interfacial Area Measurement

pH = 8.5
Column Height = 30 cm
Flow of O_2 = 3.6 l/min.
Temperature = 22 °C

Time (min)	$Na_2S_2O_3$ (ml)	Na_2SO_3 (M)
0.0	9.60	0.77
4.0	10.60	0.72
8.0	11.4	0.68
12.0	11.80	0.66
16.0	12.00	0.65
20.0	13.20	0.59
24.0	13.75	0.56
28.0	14.30	0.53
32.0	15.20	0.49
36.0	16.00	0.45
40.0	17.20	0.39

Table B-13 : Data For Interfacial Area Measurement

pH = 8.5
Column Height = 30 cm
Flow of O_2 = 6.2 l/min.
Temperature = 22 °C

Time (min)	$Na_2S_2O_3$ (ml)	Na_2SO_3 (M)
0.0	9.50	0.77
2.0	10.10	0.74
4.0	10.80	0.71
6.0	11.00	0.70
8.0	11.80	0.66
10.0	12.60	0.62
12.0	13.50	0.57
14.0	14.50	0.52
16.0	15.50	0.47
18.0	16.70	0.41
20.0	17.70	

Table B-14: Data For Interfacial Area Measurement

pH = 8.5
Column Height = 30 cm
Flow of O_2 = 9.0 l/min.
Temperature = 22 °C

Time (min)	$Na_2S_2O_3$ (ml)	Na_2SO_3 (M)
2.0	11.10	0.69
4.0	12.10	0.65
6.0	13.30	0.58
8.0	14.40	0.53
10.0	16.20	0.44
12.0	17.70	0.36
14.0	19.50	0.27
16.0	21.70	0.16
18.0	23.10	0.09
20.0	24.8	0.01
22.0	25.00	

Table B-15: Data For Interfacial Area Measurement

pH = 8.5
Column Height = 30 cm
Flow of O_2 = 11.8 l/min.
Temperature = 22 °C

Time (min)	$Na_2S_2O_3$ (ml)	Na_2SO_3 (M)
0.0	9.54	0.77
1.0	10.26	0.74
2.0	10.80	0.71
3.0	11.90	0.65
5.0	12.90	0.60
6.0	13.90	0.55
7.0	14.30	0.53
8.0	15.20	0.49
9.0	16.20	0.44
10.0	17.6	0.37

Appendix C

FILTRATE AND PRECIPITATE ANALYSIS OF SABKHA SAMPLES

Table C-1. Filtrate Analysis (Batch Gas Bubbler) 25 g/100ml Sabkha, 4.5 M NH_3, Flow 2 l/min., Temp. $22°C$.

Time hr.	Filt. Weight g	Filt. Conc. mg/l	Filt. Density g/ml	% CO_3^2	% HCO_3	% Cl	NH_4Cl g
0.33	1123517	83200	1.2033	12.01	-	13.53	0.3764
0.50	112.2300	63800	1.1856	11.2	-	13.66	0.6113
0.75	107.4051	65400	1.1753	11.05	0.59	13.87	0.8728
1.00	96.2440	57000	1.1658	8.78	1.037	14.25	1.2662
1.50	89.306	53400	1.1600	4.72	4.19	14.53	0.4972
2.00	96.1451	41200	1.1482	3.06	5.0	13.75	1.9883
2.50	91.0229	39000	1.1389	1.91	5.46	13.65	1.5854

Table C-2. Filtrate Analysis (Batch Gas bubbler) 25 g/100ml Sabkha, 2.5 M NH_3, Flow 2 l/min., Temp. $22°C$.

Time hr.	Filt. Weight g	Filt. Conc. mg/l	Filt. Density g/ml	% CO_3^2	% HCO_3	% Cl	NH_4Cl g
0.33	119.7531	91200	1.1835	4.84	-	12.76	0.2509
0.50	117.6354	80400	1.1794	5.02	-	12.82	0.2909
0.75	115.7653	73000	1.1704	4.75	-	12.96	0.5731
1.00	107.7194	65800	1.1665	2.65	1.80	12.42	0.9194
1.50	107.0667	61200	1.1587	1.89	1.35	12.71	1.1811
2.00	105.4171	58800	1.1526	0.77	2.54	12.45	1.5383
2.50	104.4731	54400	1.1533	0.57	2.11	13.09	1.3545

Table C-3. Filtrate Analysis (Batch Gas bubbler) 25 g/100ml Sabkha, 3.5 M NH_3, Flow 2 l/min., Temp. $22°C$.

Time hr.	Filt. Weight g	Filt. Conc. mg/l	Filt. Density g/ml	% CO_3^2	% HCO_3	% Cl	NH_4Cl g
0.33	119.0819	88800	1.1936	10.83	1.17	13.80	0.2176
0.50	118.6675	79000	1.1932	10.83	0.58	13.62	0.2681
0.75	111.4818	66800	1.1780	7.89	0.89	13.50	0.6360
1.00	106.2391	62600	1.1703	6.8	1.19	13.52	0.8175
1.50	101.0004	46600	1.1511	3.08	2.74	13.52	1.6501
2.00	97.5915	38600	1.1456	1.93	3.06	13.11	1.0158
2.50	96.3720	41200	1.1439	0.98	4.26	12.80	1.7601

Table C-4. Filtrate Analysis (Batch Gas Bubbler) 25 g/100ml Sabkha, 7.5 M NH_3, Flow 2 l/min., Temp. $22°C$.

Time hr.	Filt. Weight g	Filt. Conc. mg/l	Filt. Density g/ml	% CO_3^2	% HCO_3	% Cl	NH_4Cl g
0.33	121.7125	82400	1.2088	20.66	-	15.78	0.4561
0.50	117.9608	72000	1.2076	18.01	-	15.73	0.8160
0.75	110.0013	62800	1.1965	16.97	-	15.74	1.1195
1.00	98.1165	52100	1.1911	19.52	-	15.42	1.2008
1.50	88.9713	42000	1.1816	16.61	-	15.60	1.3216
2.00	84.7828	35600	1.1674	11.44	-	16.33	1.9496
2.50	79.7648	30000	1.1585	6.3	4.24	15.27	2.933

Table C-5. Precipitate Analysis (Batch Gas Bubbler) 25 g/100ml Sabkha, 4.5 M NH_3, Flow 2 l/min., Temp. $22°C$.

Time hr.	ppt. weight g	ppt. conc. mg/g	% CO_3	% HCO_3	% Cl
0.33	0.9575	284	83.30	2.18	11.32
0.50	3.8685	367	79.70	-	11.65
0.75	6.4113	387	86.86	-	11.19
1.00	12.9219	389	77.56	-	11.58
1.50	10.3663	388	87.5	-	11.45
2.00	12.7031	405	86.2	-	11.60
2.50	14.5620	407	83.37	-	11.55

Table C-6. Precipitate Analysis (Batch Gas Bubbler) 25 g/100ml Sabkha, 2.5 M NH_3, Flow 2 l/min., Temp. $22°C$.

Time hr.	ppt. weight g	ppt. conc. mg/g	% CO_3	% HCO_3	% Cl
0.33	0.3742	37	92.65	-	13.11
0.50	2.6246	362	89.80	-	13.45
0.75	4.2266	389	85.05	-	12.98
1.00	6.4158	398	82.13	-	13.19
1.50	7.7265	409	80.64	-	13.85
2.00	8.2403	420	79.32	-	14.01
2.50	8.4748	401	60.98	2.9	13.23

Table C-7. Precipitate Analysis (Bacth Gas Bubbler) 25 g/100ml Sabkha, 3.5 M NH_3, Flow 2 l/min., Temp. 22°C.

Time hr.	ppt. weight g	ppt. conc. mg/g	% CO_3	% HCO_3	% Cl
0.33	0.3845	31	84.37	-	10.45
0.50	2.6296	355	75.65	-	9.87
0.75	6.0054	393	91.0	-	10.67
1.00	7.3413	402	85.35	-	10.16
1.50	11.0197	405	88.72	0.92	10.25
2.00	12.6096	399	79.74	2.13	10.53
2.50	12.4454	407	84.28	3.14	11.21

Table C-8. Precipitate Analysis (Batch Gas Bubbler) 25 g/100ml Sabkha, 7.5 M NH_3, Flow 2 l/min., Temp. 22°C.

Time hr.	ppt. weight g	ppt. conc. mg/g	% CO_3	% HCO_3	% Cl
0.33	1.5895	300	91.36	-	11.00
0.50	4.0031	384	92.45	3.33	11.97
0.75	7.3800	400	64.38	21.36	12.00
1.00	11.4664	338	41.44	45.16	11.32
1.50	14.2508	343	54.88	18.52	11.73
2.00	15.6759	370	62.89	22.65	12.34
2.50	16.3624	361	62.62	23.89	11.98

Table C-9. Filtrate Analysis (Bubble Column) Vol. 1.5 l - 2.5 M NH_3, Flow 11.8 l/min., Temp. 22°C. carbonation time 1/2 hr.

Sabkha g/l	Filt. Weight g	Filt. Conc. g/ml	Filt. Density mg/l	% CO_3^2	% HCO_3	% Cl	NH_4Cl g
100	1097.246	37600	1.1256	15.45	4.59	5.75	1.2150
130	1120.001	40600	1.1388	7.72	3.06	7.74	2.2760
200	1073.024	53200	1.1485	5.74	1.67	10.31	5.4780
250	1080.837	63600	1.1619	4.71	1.34	12.36	6.9310

Table C-10 Filtrate Analysis (Bubble Column) Vol. 1.5 l - 2.5 M NH_3, Flow 11.8 l/min., Temp. $22°C$. carbonation time 1 hr.

Sabkha g/l	Filt. Weight g	Filt. Conc. g/ml	Filt. Density mg/l	% CO_3^2	% HCO_3	% Cl	NH_4Cl g
100	1097.316	30800	1.1267	5.81	6.15	5.58	2.2690
130	1076.006	31400	1.1247	5.44	3.69	7.22	6.4780
200	1080.687	45800	1.1422	4.05	2.59	10.30	6.8050
250	1067.593	55200	1.1464	2.84	2.10	12.39	11.4870

Table C-11 Filtrate Analysis (Bubble Column) Vol. 1.5 l - 2.5 M NH_3, Flow 11.8 l/min., Temp. 22°C. carbonation time 1 1/2 hr.

Sabkha g/l	Filt. Weight g	Filt. Conc. g/ml	Filt. Density mg/l	% CO_3^2	% HCO_3	% Cl	NH_4Cl g
100	1085.713	27600	1.1250	4.39	7.86	5.59	3.0490
130	1082.410	30800	1.1323	4.29	5.56	7.75	6.2780
200	1062.490	43400	1.1372	2.88	3.96	10.24	9.4210
250	1064.205	55000	1.1480	1.91	3.03	12.34	12.0590

Table C-12 Filtrate Analysis (Bubble Column) Vol. 1.5 l - 2.5 M NH_3, Flow 11.8 l/min., Temp. 22°C. carbonation time 2 hr.

Sabkha g/l	Filt. Weight g	Filt. Conc. g/ml	Filt. Density mg/l	% CO_3^2	% HCO_3	% Cl	NH_4Cl g
100	1093.792	29200	1.1223	4.65	7.86	5.64	2.8040
130	1078.618	32800	1.1272	3.12	6.80	7.44	6.9170
200	1043.483	43000	1.1367	2.32	3.98	10.27	9.6250
250	1051.943	56200	1.1537	1.14	3.62	12.17	13.6290

Table C-13 Filtrate Analysis (Bubble Column) Vol. 1.5 l - 3.5 M NH_3, Flow 11.8 l/min., Temp. 22°C. carbonation time 1/2 hr.

Sabkha g/l	Filt. Weight g	Filt. Conc. g/ml	Filt. Density mg/l	% CO_3^2	% HCO_3	% Cl	NH_4Cl g
100	1125.395	34800	1.1362	13.32	5.64	6.80	0.6950
130	1114.253	39400	1.1402	10.89	3.94	7.40	1.3870
200	1012.076	52800	1.1561	10.00	---	10.46	4.6190
250	965.219	64200	1.1686	7.73	---	12.80	6.7640

Table C-14 Filtrate Analysis (Bubble Column) Vol. 1.5 l - 3.5 M NH_3, Flow 11.8 l/min., Temp. 22°C. carbonation time 1 hr.

Sabkha g/l	Filt. Weight g	Filt. Conc. g/ml	Filt. Density mg/l	% CO_3^2	% HCO_3	% Cl	NH_4Cl g
100	1104.703	28200	1.1423	9.55	6.73	6.36	2.1290
130	1075.894	32400	1.1492	7.85	6.46	7.91	4.615
200	1026.104	41400	1.1422	7.85	6.47	10.36	6.4210
250	998.448	51400	1.1546	5.67	1.50	12.89	11.8750

Table C-15 Filtrate Analysis (Bubble Column) Vol. 1.5 l - 3.5 M NH_3, Flow 11.8 l/min., Temp. $22°C$. carbonation time 1 1/2 hr.

Sabkha g/l	Filt. Weight g	Filt. Conc. g/ml	Filt. Density mg/l	% CO_3^2	% HCO_3	% Cl	NH_4Cl g
100	1078.794	25000	1.1136	10.16	4.94	6.39	3.7050
130	1057.906	28800	1.1346	6.74	7.48	7.86	6.8850
200	1033.295	39200	1.1402	6.73	1.85	10.55	8.9620
250	1031.590	52200	1.1539	4.95	2.11	12.60	14.6760

Table C-16 Filtrate Analysis (Bubble Column) Vol. 1.5 l - 3.5 M NH_3, Flow 11.8 l/min., Temp. 22°C. carbonation time 2 hr.

Sabkha g/l	Filt. Weight g	Filt. Conc. g/ml	Filt. Density mg/l	% CO_3^2	% HCO_3	% Cl	NH_4Cl g
100	1072.481	25800	1.1257	9.61	2.86	6.29	2.9350
130	1074.883	29200	1.1334	5.98	5.91	7.88	4.6900
200	1030.063	40400	1.1459	4.42	3.20	10.55	7.3020
250	1045.623	53800	1.1509	3.44	2.47	12.60	11.9320

Table C-17 Filtrate Analysis (Bubble Column) Vol. 1.5 l - 4.5 M NH_3, Flow 11.8 l/min., Temp. $22^{\circ}C$. carbonation time 1/2 hr.

Sabkha g/l	Filt. Weight g	Filt. Conc. g/ml	Filt. Density mg/l	% CO_3^2	% HCO_3	% Cl	NH_4Cl g
100	1125.372	35000	1.1562	16.00	4.32	7.43	0.5330
150	1095.612	44600	1.1585	15.21	1.87	9.50	5.3070
200	1025.334	50600	1.1609	13.10	1.04	11.37	5.1530
250	1067.820	60200	1.1774	11.66	0.69	13.09	6.1400

Table C-18 Filtrate Analysis (Bubble Column) Vol. 1.5 l - 4.5 M NH_3, Flow 11.8 l/min., Temp. 22°C. carbonation time 1 hr.

Sabkha g/l	Filt. Weight g	Filt. Conc. g/ml	Filt. Density mg/l	% CO_3^2	% HCO_3	% Cl	NH_4Cl g
100	1108.614	37000	1.1439	17.20	0.48	6.48	0.4540
150	966.969	33600	1.1501	11.85	3.13	9.47	2.6680
200	980.310	38200	1.1600	9.85	0.89	11.45	7.6770
250	944.688	50200	1.1612	8.29	1.13	12.87	16.2050

Table C-19 Filtrate Analysis (Bubble Column) Vol. 1.5 l - 4.5 M NH_3, Flow 11.8 l/min., Temp. 22°C. carbonation time 1 1/2 hr.

Sabkha g/l	Filt. Weight g	Filt. Conc. g/ml	Filt. Density mg/l	% CO_3^2	% HCO_3	% Cl	NH_4Cl g
100	1097.872	28200	1.1193	9.67	5.49	6.57	2.1330
150	1038.156	30800	1.1394	7.79	4.65	8.87	6.4570
200	1023.980	38600	1.1424	5.74	4.40	10.72	11.9190
250	1019.294	48600	1.1425	6.25	0.85	12.76	16.5490

Table C-20 Filtrate Analysis (Bubble Column) Vol. 1.5 l - 4.5 M NH_3, Flow 11.8 l/min., Temp. $22°C$. carbonation time 2 hr.

Sabkha g/l	Filt. Weight g	Filt. Conc. g/ml	Filt. Density mg/l	% CO_3^2	% HCO_3	% Cl	NH_4Cl g
100	1061.666	28200	1.1383	8.76	6.73	6.67	4.0980
150	1015.842	28800	1.1437	6.75	7.61	8.74	7.090
200	1026.688	39600	1.1445	3.95	4.41	10.44	10.5310
250	1025.740	47800	1.1518	3.42	3.82	12.79	17.1200

Table C-21 Precipitate Analysis (Bubble Column) 2.5 M NH_3, Flow 11.8 l/min., Temp. 22°C. carbonation time 1/2 hr.

Sabkha g/l	ppt. weight g	ppt. conc. mg/g	% CO_3	% HCO_3	% Cl
100	3.3960	44.0000	67.98	-	5.12
130	19.3920	263.0000	32.50	62.39	8.45
200	63.7550	314.0000	44.19	36.51	11.39
250	83.3110	319.0000	37.72	38.45	11.75

Table C-22. Precipitate Analysis (Bubble Column) 2.5 M NH_3, Flow 11.8 l/min., Temp. 22°C. carbonation time 1 hr.

Sabkha g/l	ppt. weight g	ppt. conc. mg/g	% CO_3	% HCO_3	% Cl
100	17.519	350	81.66	14.80	5.06
130	40.817	360	79.28	13.34	8.60
200	69.268	359	68.86	22.03	11.11
250	97.23	335	49.62	34.81	11.89

Table C-23. Precipitate Analysis (Bubble Column) 2.5 M NH_3, Flow 11.8 l/min., Temp. 22°C. carbonation time 1 1/2 hr.

Sabkha g/l	ppt. weight g	ppt. conc. mg/g	% CO_3	% HCO_3	% Cl
100	21.51	353	82.04	14.12	4.98
130	52.795	281	26.54	69.87	7.85
200	894.23	301	34.67	62.68	11.00
250	115.425	289	26.53	62.48	12.11

Table C-24. Precipitate Analysis (Bubble Column) 2.5 M NH_3, Flow 11.8 l/min., Temp. 22°C. carbonation time 2 hr.

Sabkha g/l	ppt. weight g	ppt. conc. mg/g	% CO_3	% HCO_3	% Cl
100	22.984	289	37.41	60.15	4.01
130	49.576	307	42.48	54.29	6.35
200	97.623	289	27.61	52.50	10.91
250	117.423	298	29.50	57.57	11.75

Table C-25. Precipitate Analysis (Bubble Column) 3.5 M NH_3, Flow 11.8 l/min., Temp. 22°C. carbonation time 1/2 hr.

Sabkha g/l	ppt. weight g	ppt. conc. mg/g	% CO_3	% HCO_3	% Cl
100	2.924	303	75.82	-	5.10
130	27.869	282	41.95	52.12	7.45
200	88.344	302	20.71	58.81	10.44
250	112.566	315	23.82	34.11	11.78

Table C-26. Precipitate Analysis (Bubble Column) 3.5 M NH_3, Flow 11.8 l/min., Temp. 22°C. carbonation time 1 hr.

Sabkha g/l	ppt. weight g	ppt. conc. mg/g	% CO_3	% HCO_3	% Cl
100	18.930	375	94.60	-	4.92
130	41.253	370	86.78	8.18	8.47
200	85.514	368	72.12	14.43	10.21
250	118.278	344	56.26	26.35	11.55

Table C-27. Precipitate Analysis (Bubble Column) 3.5 M NH_3, Flow 11.8 l/min., Temp. 22°C. carbonation time 1 1/2 hr.

Sabkha g/l	ppt. weight g	ppt. conc. mg/g	% CO_3	% HCO_3	% Cl
100	26.415	361	95.47	-	4.35
130	47.655	375	35.59	6.60	9.12
200	100.184	375	81.90	6.10	11.10
250	141.675	292	22.57	64.48	11.45

Table C-28. Precipitate Analysis (Bubble Column) 3.5 M NH_3, Flow 11.8 l/min., Temp. 22°C. carbonation time 2 hr.

Sabkha g/l	ppt. weight g	ppt. conc. mg/g	% CO_3	% HCO_3	% Cl
100	26.637	365	88.60	2.42	5.10
130	52.243	318	43.78	55.19	7.23
200	96.919	323	44.94	43.89	10.21
250	132.415	301	31.17	54.37	11.67

Table C-29. Precipitate Analysis (Bubble Column) 4.5 M NH_3, Flow 11.8 l/min., Temp. 22°C carbonation time 1/2 hr.

Sabkha g/l	ppt. weight g	ppt. conc. mg/g	% CO_3	% HCO_3	% Cl
100	3.387	30	60.60	-	12.97
150	34.271	332	59.52	28.67	12.65
200	80.942	302	24.19	59.84	11.69
250	102.868	290	22.44	62.44	10.96

Table C-30. Precipitate Analysis (Bubble Column) 4.5 M NH_3, Flow 11.8 l/min., Temp. 22°C. carbonation time 1 hr.

Sabkha g/l	ppt. weight g	ppt. conc. mg/g	% CO_3	% HCO_3	% Cl
100	2.7494	34	8.54	-	13.23
150	90.066	300	16.91	70.50	12.81
200	126.280	300	21.26	58.67	11.14
250	176.235	292	8.35	42.37	10.96

Table C-31. Precipitate Analysis (Bubble Column) 4.5 M NH_3, Flow 11.8 l/min., Temp. 22°C. carbonation time 1 1/2 hr.

Sabkha g/l	ppt. weight g	ppt. conc. mg/g	% CO_3	% HCO_3	% Cl
100	25.393	285	36.14	59.62	12.78
150	77.842	298	31.15	56.70	12.35
200	116.875	284	23.20	64.70	11.34
250	144.506	286	26.72	99.0	10.65

Table C-32. Precipitate Analysis (Bubble Column II) 4.5 M NH_3, Flow 11.8 l/min., Temp. 22° carbonation time 2 hr.

Sabkha g/l	ppt. weight g	ppt. conc. mg/g	% CO_3	% HCO_3	% Cl
100	38.576	239	15.71	73.55	13.23
150	90.020	281	23.65	66.73	12.21
200	115.402	282	20.22	66.78	11.2
250	158.963	276	17.54	71.63	10.65

Appendix D

EQUILIBRIUM CONCENTRATIONS OF UNREACTED AMMONIA

Table D-1. Equilibrium Composition of Aqueous Carbonated Ammonia Solution 1.0M NH_3. Flow 2 l/min. . Temp. 22°C

Time (min)	$[CO_2]$ (mole/l)	$[H^-]$ (mole/l)	$[OH^-]$ (mole/l)	$[HCO_3^-]$ (mole/l)	$[H_2CO_3]$ (mole/l)	$[CO_3^-]$ (mole/l)	$[NH_3]$ (mole/l)	$[NH_4^-]$ (mole/l)	$[H_2NCOO^-]$ (mole/l
1	0.0316	1.5380E-11	6.6499E-4	1.1340E-6	4.1098E-11	0.0317	0.9360	0.0640	3.7245E-6
3	0.7125	3.6633E-11	2.7298E-4	6.2156E-6	5.4874E-10	0.0712	0.8572	0.1427	1.8690E-5
4	0.0966	5.2733E-11	1.8964E-4	1.2130E-5	1.5415E-9	0.0966	0.8066	0.1933	3.4330E-5
5	0.1166	6.3295E-11	1.5799E-4	1.6828E-5	2.5669E-9	0.1116	0.7765	0.2234	4.5850E-5
6	0.1275	7.5328E-11	1.3275E-4	2.2866E-5	4.1509E-9	0.1274	0.7449	0.2551	5.9763E-5
7	0.1479	9.2420E-11	1.0820E-4	3.2539E-5	7.2472E-9	0.1478	0.7041	0.2958	8.0390E-5
8	0.1666	1.0998E-10	9.0923E-5	4.3629E-5	1.1564E-8	0.1665	0.6666	0.3333	1.0205E-4
10	0.1918	1.3671E-10	7.3149E-5	6.2355E-5	2.0543E-8	0.1915	0.6167	0.3832	1.3492E-4
20	0.2917	3.0759E-10	3.2511E-5	2.1334E-4	1.5814E-7	0.2911	0.4169	0.582 8	3.1204E-4
40	0.4500	1.9341E-9	5.1704E-6	0.0021	9.6043E-6	0.4472	0.1021	0.8972	7. 3786E-4
60	0.4660	2.8694E-9	3.4850E-6	0.0032	2.1841E-5	0.4621	0.0712	0.9281	7. 8857E-4
80	0.4917	8.2054E-9	1.2187E-6	0.0094	1.8608E-4	0.4814	0.0261	0.9730	8.6141E-4

Table D-2. Equilibrium Composition of Aqueous Carbonated Ammonia Solution 2.5M NH_3, Flow 2 l/min. . Temp. 22°C

Time (min)	$[CO_2]$ (mole/l)	$[H^-]$ (mole/l)	$[OH^-]$ (mole/l)	$[HCO_3^-]$ (mole/l)	$[H_2CO_3]$ (mole/l)	$[CO_3^-]$ (mole/l)	$[NH_3]$ (mole/l)	$[NH_4^-]$ (mole/l)	$[H_2NCOO^-]$ (mole/l
2	0.0592	1.1016E-11	9.0776E-4	1.5522E-6	4.1208E-11	0.0591	2.3808	0.1192	1.2967E-5
3	0.0950	1.8148E-11	5.5101E-4	4.1057E-6	1.7957E-10	0.0950	2.3095	0.1905	3.3277E-5
4	0.1375	2.7224E-11	3.6732E-4	8.9126E-6	5.8474E-10	0.1374	2.2246	0.2753	6.9570E-5
5	0.16041	3.2413E-11	3.0852E-4	1.2378E-5	9.6692E-10	0.1603	2.1789	0.321	9.4635E-5
6	0.1660	3.3713E-11	2.9662E-4	1.3323E-5	1.0824E-9	0.1659	2.1677	0.3322	1.0134E-4
7	0.17708	3.6329E-11	2.7526E-4	1.5315E-5	1.3408E-9	0.1769	2.1456	0.3543	1.1529E-4
8	0.17708	3.6329E-11	2.7526E-4	1.5315E-5	1.3408E-9	0.1769	2.1456	0.3543	1.1529E-4
10	0.2146	4.5600E-11	2.1930E-4	2.3290E-5	2.5594E-9	0.2144	2.0706	0.4292	1.6921E-4
20	0.3500	8.5508E-11	1.1695-4	7.1192-5	1.467E-8	0.3495	1.8	0.6996	4.4962E-4
40	0.6000	2.0278E-10	4.9316E-5	2.8907E-4	1.4126E-7	0.5984	1.3002	1.1984	0.0013
60	0.7916	3.7892E-10	2.6391E-5	7.1186E-4	6.5004E-7	0.7886	0.9175	1.5802	0.0023
80	1.0916	1.4923E-9	6.701E-6	0.0039	1.3852E-5	1.0834	0.3206	2.175	0.0043
100	1.1750	3.2335E-9	3.0926E-6	0.0089	6.9696E-5	1.1611	0.1589	2.3361	0.0050

Table D-3. Equilibrium Composition of Aqueous Carbonated Ammonia Solution 3.5M NH_3, Flow 2 l/min. , Temp. 22°C

Time (min)	$[CO_2]$ (mole/l)	$[H^-]$ (mole/l)	$[OH^-]$ (mole/l)	$[HCO_3^-]$ (mole/l)	$[H_2CO_3]$ (mole/l)	$[CO_3^-]$ (mole/l)	$[NH_3]$ (mole/l)	$[NH_4^-]$ (mole/l)	$[H_2NCOO^-]$ (mole/l
3	0.0842	1.1448E-11	8.7349E-4	2.2946E-6	6.3306E-11	0.0841	3.2508	0.1692	2.6173E-5
4	0.1000	1.3715E-11	7.2914E-4	3.2660E-6	1.0795E-10	0.1000	3.2193	0.2007	3.6891E-5
5	0.1150	1.5905E-11	6.2874E-4	4.3554E-6	1.6694E-10	0.1149	3.1894	0.2306	4.874E-5
6	0.1350	1.8892E-11	5.2932E-4	6.0727E-6	2.7648E-10	0.1349	3.1495	0.2705	6.7108E-5
8	0.1833	2.6435E-11	3.7829E-4	1.1535E-5	7.3483E-10	0.1832	3.0530	0.3668	1.2357E-4
10	0.2500	3.7675E-11	2.6543E-4	2.2416E-5	2.0353E-9	0.2497	2.9198	0.5000	2.2965E-4
20	0.3708	6.0884E-11	1.6425E-4	5.3702E-5	7.8795E-9	0.3702	2.6783	0.7412	5.0466E-4
40	0.3833	6.3527E-11	1.5741E-4	5.7918E-5	8.8670E-9	0.3827	2.6533	0.7662	5.3921E-4
60	0.3910	6.8127E-11	1.5231E-4	5.2836E-5	9.4562E-9	0.3901	2.6345	0.7819	5.6422E-4

Table D-4. Equilibrium Composition of Aqueous Carbonated Ammonia Solution 4.0M NH_3. Flow 2 l/min. . Temp. 22°C

Time (min)	$[CO_2]$ (mole/l)	$[H^-]$ (mole/l)	$[OH^-]$ (mole/l)	$[HCO_3^-]$ (mole/l)	$[H_2CO_3]$ (mole/l)	$[CO_3^-]$ (mole/l)	$[NH_3]$ (mole/l)	$[NH_4^-]$ (mole/l)	$[H_2NCOO^-]$ (mole/l
1	0.10362	1.2069E-11	8.2855E-4	2.9781E-6	8.6622E-11	0.1036	3.7919	0.2080	3.9624E-5
2	0.1073	1.2516E-11	7.9897E-4	3.1974E-6	9.6444E-11	0.1072	3.7846	0.2153	4.2460E-5
3	0.1509	1.7985E-11	5.5601E-4	6.4621E-6	2.8009E-10	0.1508	3.6976	0.3023	8.3840E-5
4	0.1668	2.0047E-11	4.9882E-4	7.9624E-6	3.8468E-10	0.1667	3.6658	0.3340	1.0242E-4
6	0.1696	2.0407E-11	4.9002E-4	8.2388E-6	4.0519E-10	0.1695	3.6604	0.3395	1.0581E-4
7	0.2004	2.4523E-11	4.0770E-4	1.1701E-5	6.9155E-10	0.2003	3.5987	0.4011	1.4776E-4
8	0.2625	3.3242E-11	3.0083E-4	2.0766E-5	1.6636E-9	0.2622	3.4747	0.5250	2.5318E-4
10	0.29330	3.7805E-11	2.6451E-4	2.6385E-5	2.4039E-9	0.2930	3.4132	0.5865	3.1598E-4

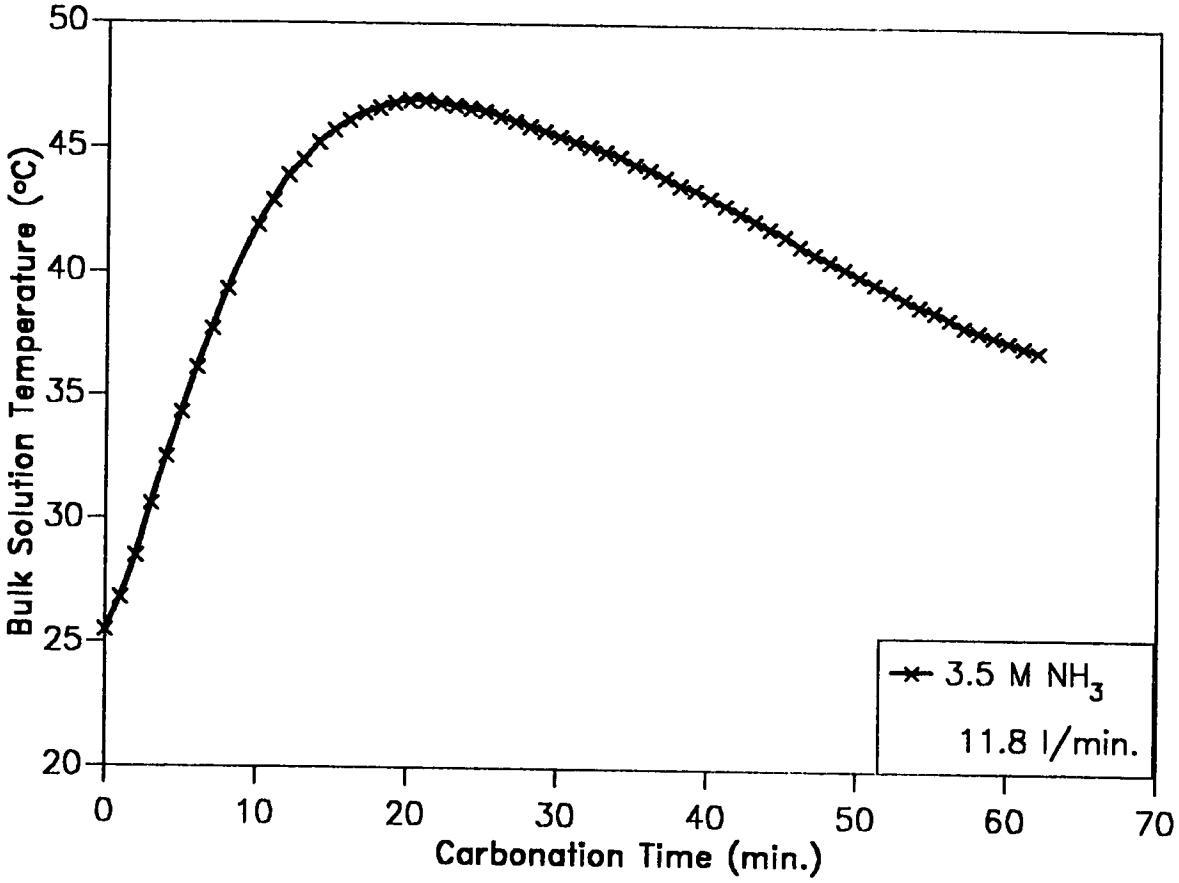

Figure D–5 Temperature–Time Profile

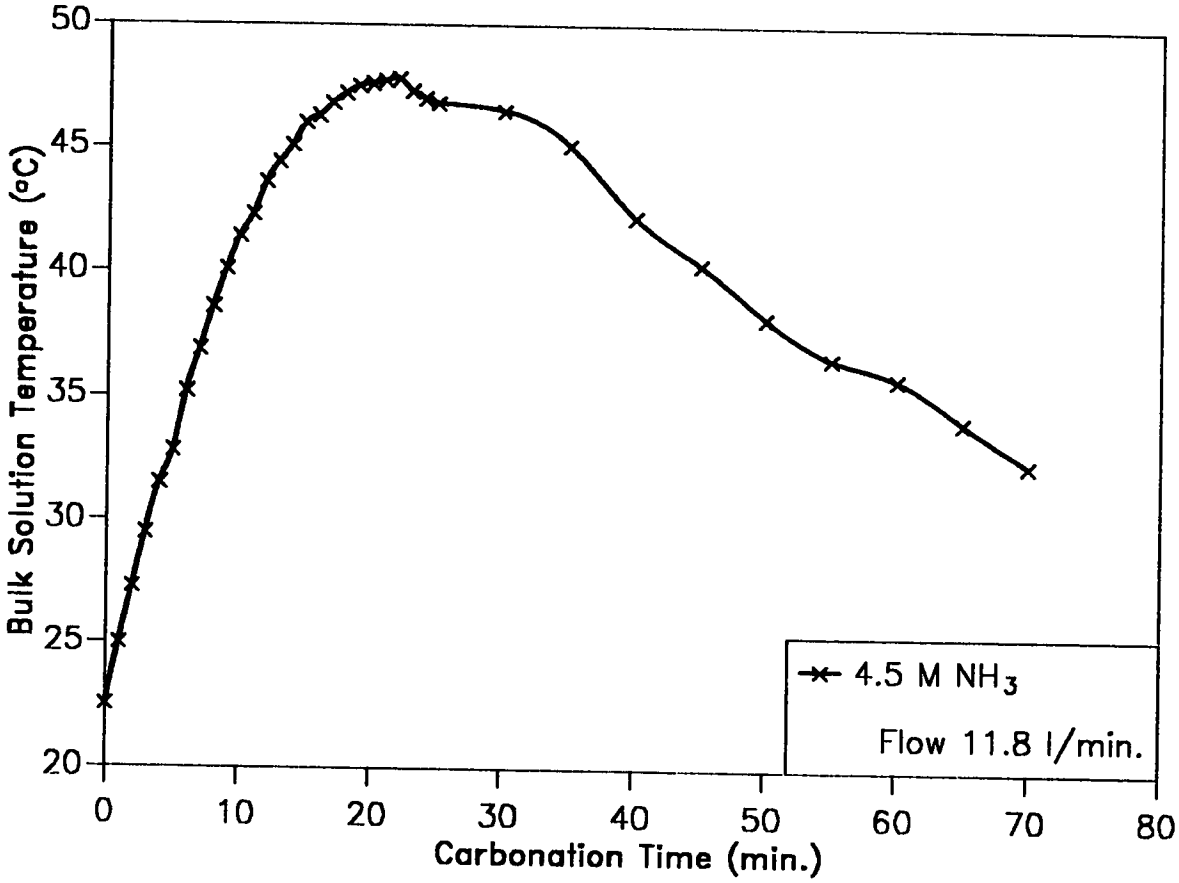

Figure D–6 Temperature–Time Profile

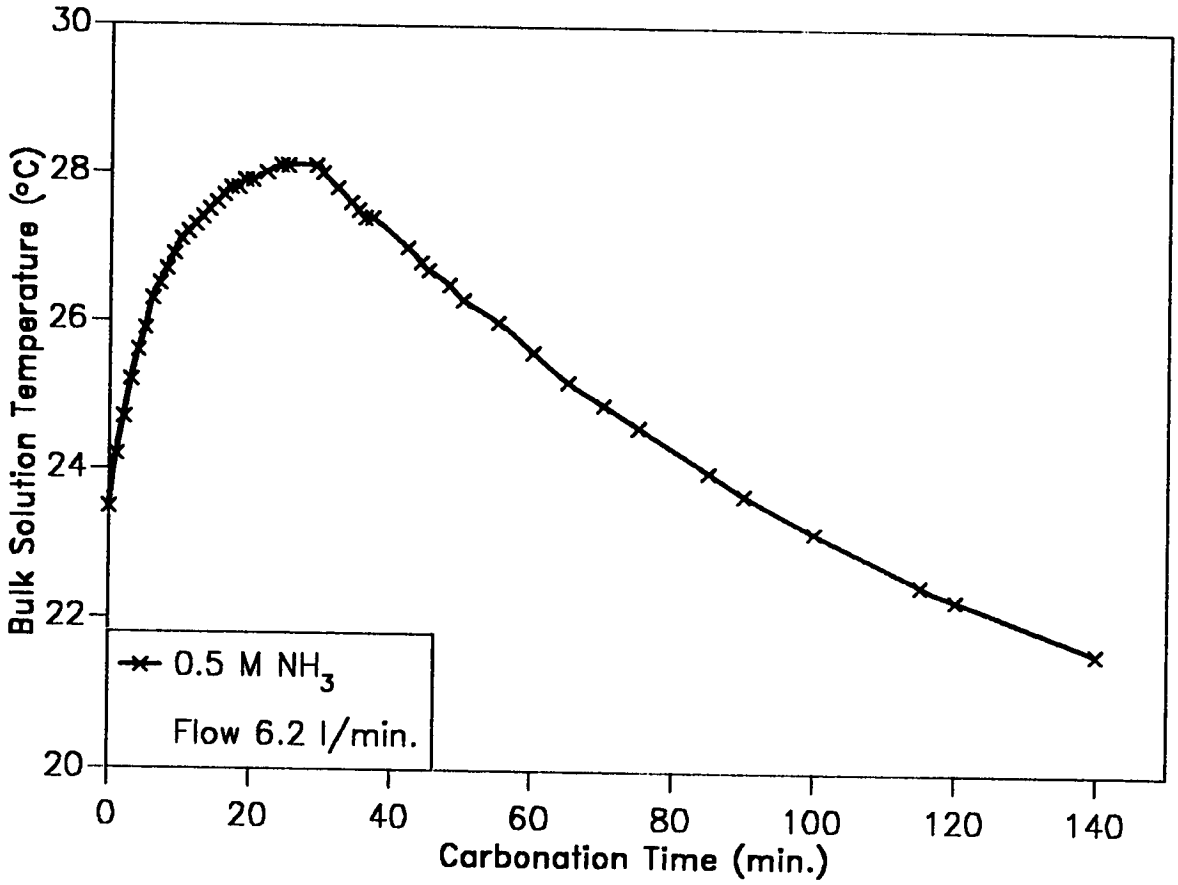

Figure D–7 Temperature–Time Profile

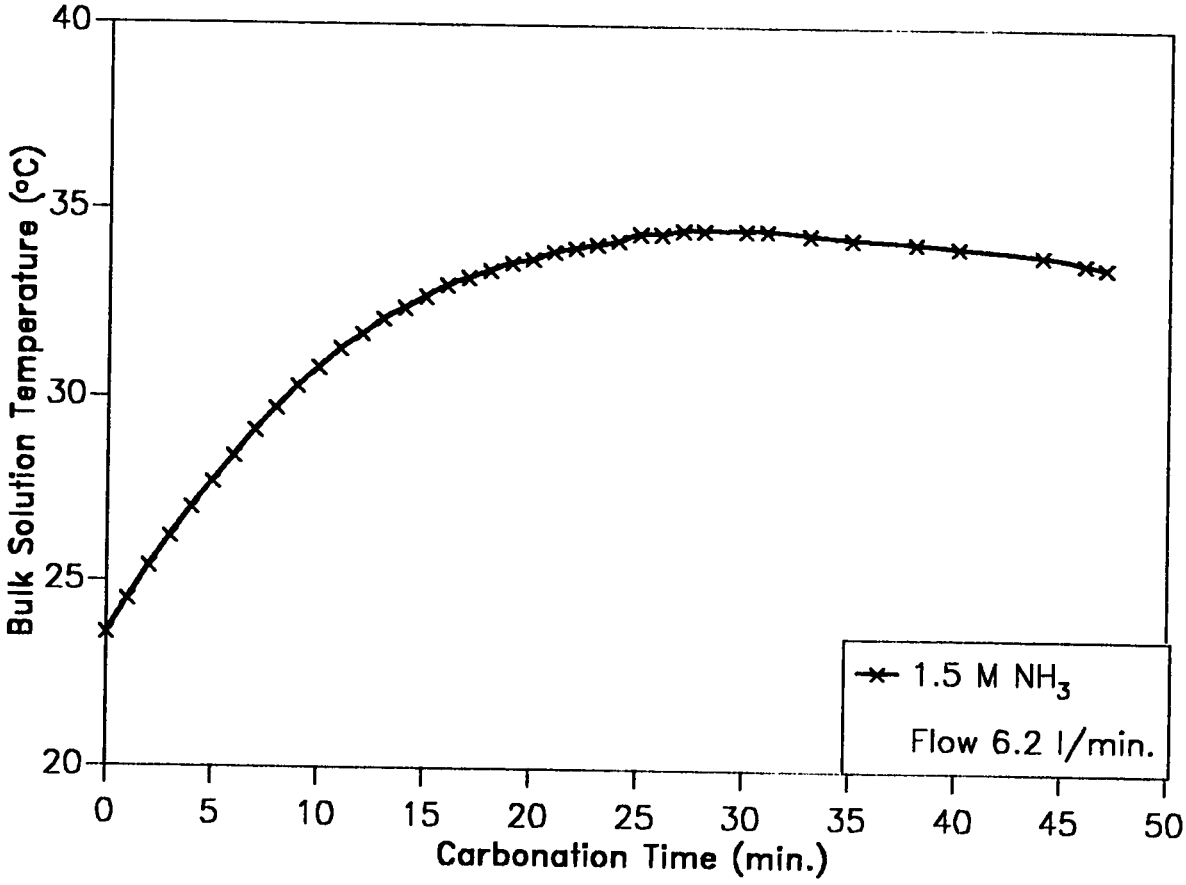

Figure D–8 Temperature–Time Profile

Appendix E

RAW DATA

Table E-1: Raw Data " Batch Gas Bubbler "

Feed: Synthetic Saline Water

Flow: 2 l/min.

Temperature: 22°C

Run #	NH_3 M	Time of CO_2 (*hr*)	Weight of Salt (g/100ml)
1	2.5	0.5	25
2	2.5	1.0	25
3	2.5	1.5	25
4	2.5	2.0	25
5	2.5	2.5	25
6	2.5	0.5	30
7	2.5	1.0	30
8	2.5	1.5	30
9	2.5	2.0	30
10	2.5	2.5	30
11	3.5	0.5	25
12	3.5	1.0	25
13	3.5	1.5	25
14	3.5	2.0	25
15	3.5	2.5	25
16	3.5	1.0	30
17	3.5	1.5	30
18	3.5	2.0	30
19	3.5	2.5	30

Table E-2: Raw Data " Batch Gas Bubbler "

Feed: Synthetic Saline Water

Flow: 3 l/min.

Temperature: 22°C

Run #	NH_3 M	Time of CO_2 (*hr*)	Weight of Salt (g/100ml)
1	4.5	0.5	25
2	4.5	1.0	25
3	4.5	1.5	25
4	4.5	2.0	25
5	4.5	2.5	25
6	7.5	0.5	22
7	7.5	1.0	22
8	7.5	1.5	22
9	7.5	2.0	22
10	12.0	0.5	19
11	12.0	1.0	19
12	12.0	1.5	19
13	12.0	2.0	19
14	12.0	2.5	19

Table E-3: Raw Data " Batch Gas Bubbler "

Feed: Sabkha Water

Flow: 2 l/min.

Temperature: 22°C

Run #	NH_3 M	Time of CO_2 (hr)	Weight of Salt (g/100ml)
1	2.0	0.33	25
2	2.0	0.5	25
3	2.0	0.75	25
4	2.0	1.0	25
5	2.0	1.5	25
6	2.0	2.0	25
7	2.0	2.5	25
8	3.5	0.33	25
9	3.5	0.5	25
10	3.5	0.75	25
11	3.5	1.0	25
12	3.5	1.5	25
13	3.5	2.0	25
14	3.5	2.5	25
15	4.5	0.33	25
16	4.5	0.5	25
17	4.5	0.75	25
18	4.5	1.0	25
19	4.5	1.5	25
20	4.5	2.0	25
21	4.5	0.5	25
22	7.5	0.33	25
23	7.5	0.5	25
24	7.5	0.75	25
25	7.5	1.0	25
26	7.5	1.5	25
27	7.5	2.0	25
28	7.5	2.5	25

Table E-4: Raw Data " Bubble Column "

Feed: Synthetic Saline Water

Flow: 11.8 l/min.

Temperature: 22°C

Run #	NH_3 M	Time of CO_2 (*hr*)	Weight of Salt (g/100ml)
1	2.5	1.0	13
2	2.5	2.0	11
3	2.5	2.5	10
4	2.5	2.5	13
5	2.5	2.5	20
6	2.5	2.5	25
7	3.5	1.0	18
8	3.5	1.5	18
9	3.5	1.5	25
10	3.5	1.5	15
11	3.5	1.5	20
12	4.5	1.0	18
13	4.5	1.0	20
14	4.5	1.0	23
15	4.5	0.5	23
16	4.5	1.0	25
17	1.5	2.0	20
18	1.5	3.0	20
19	1.5	3.0	25
20	1.5	2.0	30
21	1.5	2.5	20

Table E-5: Raw Data " Bubble Column "

Feed: Sabkha Water

Flow: 11.8 l/min.

Temperature: 22 °C

Run #	NH_3 M	Time of CO_2 (*hr*)	Weight of Salt (g/100ml)
1	2.5	0.5	10
2	2.5	0.5	13
3	2.5	0.5	20
4	2.5	0.5	25
5	2.5	1.0	10
6	2.5	1.0	13
7	2.5	1.0	20
8	2.5	1.0	25
9	2.5	0.5	10
10	2.5	0.5	13
11	2.5	0.5	20
12	2.5	0.5	25
13	2.5	2.0	10
14	2.5	2.0	13
15	2.5	2.0	20
16	2.5	2.0	25
17	3.5	0.5	10
18	3.5	0.5	13
19	3.5	0.5	20
20	3.5	1.0	25
21	3.5	1.0	10
22	3.5	1.0	13
23	3.5	1.0	20
24	3.5	1.0	25
25	3.5	1/2.0	10
26	3.5	1/2.0	13

Table E-6: Raw Data " Bubble Column "

Feed: Sabkha Water

Flow: 11.8 l/min.

Temperature: 22°C

Run #	NH_3 M	Time of CO_2 (*hr*)	Weight of Salt (g/100ml)
27	3.5	0.5	20
28	3.5	0.5	25
29	3.5	2.0	10
30	3.5	2.0	13
31	3.5	2.0	20
32	3.5	2.0	25
33	4.5	0.5	10
34	4.5	0.5	15
35	4.5	0.5	20
36	4.5	0.5	25
37	4.5	1.0	10
38	4.5	1.0	15
39	4.5	1.0	20
40	4.5	1.0	25
41	4.5	0.5	10
42	4.5	0.5	15
43	4.5	0.5	20
44	4.5	0.5	25
45	4.5	2.0	10
46	4.5	2.0	15
47	4.5	2.0	20
48	4.5	2.0	25

Unreacted NH_3

It has been shown the utility of total balance of NH_3 in the process of determination of unreacted NH_3 by the numerical technique.

$$(NH_3)_{total} = (NH_3)_{unreacted} + (NH_4^{\dagger}) + (H_2NCOO^{-})$$

However, the concentration of the carbamate ion cannot be determined but luckily, as given in appedix-E, it has negligible value and may be taken as zero. Therefore, the experimental determination of unreacted ammonia depends on the determination of ammonium chloride.

$$(NH_3)_{unreacted} = (NH_3)_{total} - (NH_4^{\dagger})$$

The determination of ammonium chloride in the filtrate is carried out gravimetrically in the following way:

pipette 10ml of the filtrate into evaporating dish, evaporate just to dryness over a steam bath, and dry to a constant weight in an electric oven at 105 oC. Weigh the contents of the dish. Ignite the contents over a low gentle flame until all NH_4Cl fumes disappear. Cool and weigh again. The difference is NH_4Cl.

Once the $NH_4^{\dagger}$ concentration is found, its subtraction from the initial NH_3 concentration will provide the required unreacted NH_3 concentration

Appendix F

COMPUTER PROGRAMS

PROGRAM 1

COMPUTER PROGRAM FOR CALCULATING EQUILIBRIUM COMPOSITIONS OF NH_3 AND OTHER IONS, IN A SYSTEM OF EIGHT NON-LINEAR EQUATIONS.

```
C .....
C          NEWTON RAPHSON METHOD
C .....
IMPLICIT REAL *8(A-H, O-Z)
      EXTERNAL FCN, FCNB, DFCNB
      DIMENSION XOLD(21), XINC(21), A(21, 21)
C    THE EQUATIONS ARE DEFINED IN TERMS OF LETTERS
```

$A = (H^{+})$
$B = (OH^{-})$
$C = (HCO_3^{-})$
$D = (H_2CO_3)$
$E = (CO_3^{--})$
$F = (NH_3)$
$G = (NH_4^{+})$
$H = (H_2NCOO^{-})$

```
    1 READ (5,*)ITMAX, IPRINT, N, EPS1, EPS2
      COUNT = COUNT+1
      IF(ITMAX.LT.0) STOP
C .....
C    PLEASE SPECIFY THE INITIAL ESTIMATES
C .....
      READ (5,*)(XOLD(I), I=1, N)
      DO 2, I = 1, N
      XOLD(I) = COUNT+I*.001
    2 CONTINUE
C .....
C    WRITE(8,*)'GIVE ME THE TOTAL CONC.OF NH3 & CO2
C .....
C    READ (8,*) TT1 ,TT2
```

```
      TT1 = 0.05
      TT2 = 0.02
C.....
C   NEWTON RAPHSON ITERATION STARTS
C.....
      DO 9 ITER = 1, ITMAX
C     ------- CALL ON CALCN TO SET UP THE MATRIX
C.....
      CALL CALCN (XOLD, A, 21)
C.....
C     WRITE(6,1000)((A(I, J), J=1, 9), I=1, 8)
C     WRITE (8,*) 'CALC IS PERFECT'
C     WRITE(6,*)'ITER', ITER
        DETER=SIMUL(N, A, XINC, EPS1, 0, 21)
C     WRITE(6, 900)ITER
C     WRITE(6,1000)((A(I,J), J=1, 9), I=1, 8)
        IF( DETER.NE.0) GO TO 3
C.....
      WRITE(8,*)'MATRIX IS ILL CONDITIONED OR SINGULAR'
C.....
      GO TO 1
C.....
C   CHECK FOR CONVERGENCE AND UPDATE XOLD VALUES
C.....
    3 ITCON=1
C     WRITE(8,*)ITER, (XINC(I), I=1, N)
C     WRITE(8,*)ITER, (XOLD(I), I=1, N)
        DO 5 I=1,N
        IF(DABS(XINC(I)).GT.EPS2)  ITCON=0
    5 XOLD(I)=XOLD(I)+XINC(I)
C     DO 111 I=1, N
C     IF(XOLD(I) .LT. 0) XOLD(I) =0.
  111 CONTINUE
      WRITE(6,500)ITER, (XOLD(I), I=1, N)
      WRITE(8,500)ITER, (XOLD(I), I=1, N)
      IF(ITCON.EQ.0) GO TO 9
C     WRITE(6,500)ITER, (XOLD(I), I=1, N)
      GO TO 1
    9 CONTINUE
      WRITE(6,400)
```

```
C     GO TO 1
  400 FORMAT('NO CONVERGENCE ')
  500 FORMAT(2X,'ITER', I3//4E16.3/4E16.3//)
C     +'XOLD(3)', E12.3, 3X,'XOLD(4)', E12.3/
C     +'XOLD(5)', E12.3, 3X,'XOLD(6)', E12.3, 3X,'XOLD(7)', E12.3, 3X,
C     +'XOLD(8)', E12.3/)
  900 FORMAT(1X, I2/)
 1000 FORMAT(1X, 9E10.3/)
C
      END
C
C.....
C     SUBROUTINE CALCN: FOR OBTAINING THE JACOBIAN
c                 MATRIX
C.....
C
      SUBROUTINE CALCN(DXOLD, A, NRC)
C.....
      IMPLICIT REAL*8(A-H, O-Z)
      REAL*8 A, DXOLD, XOLD, LAM
      DIMENSION XOLD(20), DXOLD(NRC), A(NRC, NRC)
C     DATA P/20./
C.....
C .....SHIFT ELEMENTS OF DXOLD TO XOLD AND CLEAR
C                   A ARRAY
C.....
      DO 1 I=1, 8
      XOLD(I)=DXOLD(I)
      DO 1 J=1, 9
    1 A(I,J)=0.0
C.....
C .....COMPUTE NON ZERO ELEMENTS OF A .....
C.....
      A(1,1)=XOLD(2)
      A(1,2)=XOLD(1)
      A(1,9)=1E-14 -(XOLD(1)*XOLD(2))
      A(2,1)=XOLD(3)
      A(2,3)=XOLD(1)
      A(2,4)=-4.1495E-7
      A(2,9)=4.14954E-7*XOLD(4)-(XOLD(1)*XOLD(3))
      A(3,1)=XOLD(5)
      A(3,3)=-4.1976E-11
      A(3,5)=XOLD(1)
      A(3,9)=4.1976E-11*XOLD(3)-(XOLD(1)*XOLD(5))
```

```
      A(4,1)=XOLD(6)
      A(4,6)=XOLD(1)
      A(4,7)=-2.2E-10*XOLD(7)
      A(4,9)=2.2E-10*XOLD(7) -(XOLD(1)*XOLD(6))
      A(5,3)=XOLD(6)
      A(5,6)=XOLD(3)
      A(5,8)=-0.285*XOLD(8)
      A(5,9)=0.285*XOLD(8) -(XOLD(6)*XOLD(3))
      A(6,6)=-1.
      A(6,7)=-1.
      A(6,8)=-1.
      A(6,9)=-TT1+XOLD(6)+XOLD(7)+XOLD(8)
      A(7,3)=-1.
      A(7,5)=-1.
      A(7,8)=-1.
      A(7,9)=-TT2+XOLD(3)+XOLD(5)+XOLD(8)
      A(8,1)=1
      A(8,2)=-1.
      A(8,3)=-1.
      A(8,5)=-2.
      A(8,7)=1
      A(8,8)=-1
      A(8,9)=XOLD(8)+2*XOLD(5)+XOLD(3)+XOLD(2)-XOLD(1)-XOLD(7)
      RETURN
      END

C.....
C     FUNCTION SIMUL COMPUTES THE INVERSE OF THE
C     N BY N MATRIX IN PLACE AND ALSO COMPUTES THE
C     N SOLUTIONS CORRESPONDING TO THE SET OF LINEAR
C     EQUATIONS.THESE ARE PLACED IN THE 'X'MATRIX.

C.....
      IMPLICIT REAL*8(A-H, O-Z)
      REAL*8 A, X, EPS, SIMUL
      DIMENSION IROW(50), JCOL(50), JORD(50), Y(50),
      A(NRC, NRC), X(N)
      MAX=N
      IF(INDIC.GE.0)MAX=N+1

C..... IS N LARGER THAN 50 .....

      IF(N.LE.50)GO TO 5
      PRINT 200
      SIMUL=0.0
      RETURN

C..... BEGIN ELIMINATION PROCEDURE .....
```

```
    5 DETER=1.0
      DO 18 K=1, N
      KM1=K-1

C..... SEARCH FOR THE PIVOT ELEMENT .....

      PIVOT=0.0
      DO 11 I=1, N
      DO 11 J=1, N

C ..... SCAN ROW AND JCOL ARRAYS FOR INVALID PIVOT

C                    SUBSCRIPTS
      IF(K.EQ.1)GO TO 9
      DO 8 ISCAN=1, KM1
      DO 8 JSCAN=1, KM1
      IF(I.EQ.IROW(ISCAN))GO TO 11
      IF(J.EQ.JCOL(JSCAN))GO TO 11
  8   CONTINUE
  9   IF(DABS(A(I,J)).LE.DABS(PIVOT))GO TO 11
      PIVOT=A(I,J)
      IROW(K)=I
      JCOL(K)=J
  11  CONTINUE

C..... INSURE THAT SELECTED PIVOT IS LARGER THAN EPS .....

      IF(DABS(PIVOT).GT.EPS)GO TO 13
      SIMUL=0.0
      RETURN

C.....UPDATE THE DETERMINANT VALUE .....

  13  IROWK=IROW(K) C
      JCOLK=JCOL(K)
      DETER=DETER*PIVOT

C.....NORMALIZE PIVOT ROW ELEMENTS .....

      DO 14 J=1,MAX
  14  A(IROWK,J)=A(IROWK,J)/PIVOT

C..... CARRY OUT INVERSE AND ELIMINATION AND DEVELOP

C                    INVERSE
      A(IROWK,JCOLK)=1.0/PIVOT
      DO 18 I=1,N
      AIJCK=A(I,JCOLK)
      IF(I.EQ.IROWK)GO TO 18
      A(I,JCOLK)=-AIJCK/PIVOT
```

```
      DO 17 J=1,MAX
   17 IF(J.NE.JCOLK)A(I,J)=A(I,J)-AIJCK*A(IROWK,J)
   18 CONTINUE

C..... ORDER SOLUTION VALUES(IF ANY) AND CREATE JORD

C                    ARRAY
      DO 20 I=1,N
      IROWI=IROW(I)
      JCOLI=JCOL(I)
      JORD(IROWI)=JCOLI
   20 IF(INDIC.GE.0)X(JCOLI)=A(IROWI,MAX)

C.....ADJUST SIGN OF DETERMINANT.....

      INTCH=0
      NM1=N-1
      DO 22 I=1,NM1
      IP1=I+1
      DO 22 J=IP1,N
      IF(JORD(J).GE.JORD(I))GO TO 22
      JTEMP=JORD(J)
      JORD(J)=JORD(I)
      JORD(I)=JTEMP
      INTCH=INTCH+1
   22 CONTINUE
      IF(INTCH/2*2.NE.INTCH)DETER=-DETER

C.....IF INDIC IS POSITIVE RETURN WITH RESULTS .....

      IF(INDIC.LE.0)GO TO 26
      SIMUL=DETER
      RETURN
C..... IF INDIC IS -VE OR ZERO, UNSCRAMMBLE THE INVERSE.....

C.....FIRST BY ROWS .....

   26 DO 28 J=1,N
      DO 27 I=1,N
      IROWI=IROW(I)
      JCOLI=JCOL(I)
   27 Y(JCOLI)=A(IROWI,J)
      DO 28 I=1,N
   28 A(I,J)=Y(I)

C.....THEN BY COLUMNS .....

      DO 30 I=1,N
      DO 29 J=1,N
      IROWJ=IROW(J)
```

```
      JCOLJ = JCOL(J)
   29 Y(IROWJ) = A(I,JCOLJ)
      DO 30 J = 1,N
   30 A(I,J) = Y(J)

C.....RETURN FOR INDIC NEGATIVE OR ZERO .....

      SIMUL = DETER
      RETURN

C.....FORMAT FOR OUTPUT STATEMENT .....

  200 FORMAT(1X,' TOO BIG' )
      END
C. ..........................................................................

      FUNCTION FCN(X)
C. ..........................................................................

      FCN = 1.0 + .1419526*X
      RETURN
      END
C. ..........................................................................

      FUNCTION FCNB(X)
C. ..........................................................................

      FCNB = 271.3627*X*X-9.419608*X
      RETURN
      END
C. ..........................................................................

      FUNCTION DFCNB(X)
C. ..........................................................................

      DFCNB = 542.725*X-9.419608
      RETURN
      END
```

PROGRAM 2

COMPUTER PROGRAM FOR CALCULATING THE ABSORPTION RATE OF CARBON DiOXIDE IN AMMONIA SOLUTION.

```
C .....
C       ABSORPTION RATE CALCULATION
C .....

C       DIMENSION X(500),Y1(500),Y2(500),Y3(500),Y4(500)
C       OPEN(UNIT=10,FILE = 'FIG4B1 DATA',STATUS='UNKNOWN')
C       OPEN(UNIT=11,FILE = 'N8A1 DATA',STATUS='UNKNOWN')
C       DOUBLE PRECISION S1,S2,S3,S4,S5,S6,S7,S8
C       PRINT *, 'EXECUTION BEGINS . . '

C .....
C       INPUT DATA
C .....

          PI = 3.14159
          TOL = 1.E-3
          DA = 1.90E-5
          CAI = 4.E-5
          CB = 3.5E-3
          Z  = 2.
          DB = 1.64E-5
          SIGMA = 4.E-3
          K = 1


   10     S1 = CB/(Z*CAI)
          S2 = SQRT(DB/DA)
          S3 = EXP(SIGMA*SIGMA/DA)
          S4 = EXP(SIGMA*SIGMA/DB)
          S51=SIGMA/SQRT(DA)
          S52=ERF(S51)
          S5 = S52
          S61=SIGMA/SQRT(DB)
          S62=ERF(S61)
          S6 = 1- S62
          S7=S4*S6
          S8=S1*S2*S3*S5
C       PRINT *, '   '
C       PRINT *, 'S62  =', S62
C       PRINT *, 'S5   =', S5
C       PRINT *, 'S6   =', S6
C       PRINT *, '   '
C       PRINT *, 'S7   =', S7
C       PRINT *, 'S8   =', S8
C       PRINT *, 'DEL  =', ABS(S8-S7)
```

```
C       PRINT *, '    '
C.....
            IF (ABS(S7-S8) .LT. TOL) GOTO 15
C.....

            IF ((S7-S8) .GT. 0) THEN
            SIGMA = SIGMA + 0.05*SIGMA
               ELSE
                  SIGMA = SIGMA - 0.05*SIGMA
            ENDIF

            IF (K .GT. 400) STOP
            K = K + 1
            GOTO 10
C.....
C       DETERMINATION OF ENHANCEMENT FACTOR
C.....

 15     EI = 1/S5

            PRINT *, 'EI = ',EI
            DO 20 I = 10, 120, 10
C.....
C       COMPUTATION OF ABSORPTION RATE
C.....

            ANA=2*EI*CAI*SQRT(DA/(I*PI))
            PRINT*, 'I=',I,'          ANA =', ANA
 20     CONTINUE
            STOP
            END
```